Feasibility Study for a New Assay for NF-κB and DNA-Supported Catalysis

INAUGURALDISSERTATION

zur Erlangung des Doktorgrades
der Fakultät für Chemie, Pharmazie und Geowissenschaften
der Albert-Ludwigs-Universität Freiburg

vorgelegt von

Dominik Altevogt
aus Münster

2009

Vorsitzender des Promotionsausschusses:	Prof. Dr. Rolf Schubert
Referent:	Prof. Dr. Willi Bannwarth
Korreferent:	Prof. Dr. Irmgard Merfort
Datum der Promotion:	09. Juli 2009

Für meine Familie

Die Neugier steht immer an erster Stelle eines Problems, das gelöst werden will.
Galileo Galilei (1564-1642)

Acknowledgements

First of all, I would like to express my sincere gratitude to Prof. Dr. Willi Bannwarth for his outstanding supervision, for his great confidence in my skills and for the thereby granted freedom of research, as well as for many valuable advices and inspiring discussions.

My special appreciation goes to my parents Gisela Altevogt and Dr. Rudolf Altevogt, my sister Julia Pifer and my girlfriend Andrea Kienzler who always supported me during the course of my studies. Without their loving help and encouragement this thesis would not have been possible.

I also wish to express my cordial thanks to Prof. Dr. Irmgard. Merfort, Dr. Andrea Hrenn and Dr. Claudia Kern from the Pharmaceutical Institute of the Albert-Ludwigs-Universität Freiburg for the constructive collaboration as well as for providing valuable suggestions that improved the quality of this study. Additionally I want to thank Prof. Dr. Irmgard Merfort for her expert opinion on my thesis.

For support during fluorescence measurements my gratitude goes to Prof. Dr. Peter Gräber and Roland Bienert from the Institute of Physical Chemistry of the Albert-Ludwigs-Universität Freiburg.

Special thanks are also due to Prof. Dr. Clemens Richert, Dr. Carolin Ahlborn and Katja Imhof at the University of Stuttgart (formerly University of Karlsruhe) for recording and interpreting thermal denaturing curves of oligonucleotides.

I am very grateful to Dr. Alexander Müller, Dr. Lilia Clima, Dr. Matthew Uzagare, Luigi Rumi, Rolf Kramer, Hartmut Rapp, Andrea Kienzler, Eva Hensle, Sandra Barudio and Claudia Stork for numerous academic discussions, all their inspiring ideas and useful suggestions.

To all members of our research group I would like to extend my thanks for the pleasant and friendly working environment.

I am deeply indebted to Andrea Kienzler, Hartmut Rapp and Eva Hensle for the time comsuming proofreading of this thesis.

Special gratitude goes to our analytical department: I wish to thank Dr. J. Wörth and C. Warth for MS measurements; Dr. M. Keller, M. Schonhardt and F. Reinbold for NMR-measurements; and E. Hickl for elemental analyses.

Common Abbreviations

A	Acceptor
Å	Ångström ($1.00 \cdot 10^{-10}$ m)
A_{260}	Absorption at 260 nm
aromat.	Aromatic NMR Signal
bfDNA	Backfolding DNA
BMT	5-Benzylmercaptotetrazole
BSA	Bovine Serum Albumin
CH	Cyclohexane
CI	Chemical Ionization
CPG	Controlled Pore Glass
D	Donor
d	Doublet or Days
dA	2'-Deoxy Adenosine
dA^{bz}	5'-DMT-2'dAdenosine (6-*N*-benzoyl)-β-cyanoethyl-phosphoramidite
dC	2'-Deoxy Cytidine
DCA	Dichloroacetic Acid
dC^{bz}	5'-DMT-2'-dCytidine (4-*N*-benzoyl)-β-cyanoethyl-phosphoramidite
dd	Doublet of Doublet
ddd	Doublet of Doublet of Doublet
dG	2'-Deoxy Guanosine
dG^{ib}	5'-DMT-2'-dGuanosine-(2-*N*-isobutylat)-β-cyanoethyl-phosphoramidite
DiDc	Poly-deoxyinosinyl-deoxycytidylic-acid
DMF	*N,N*-Dimethylformamide
DMSO	Dimethylsulfoxide
DMT	Dimethoxytrityl
DNA	Deoxyribonucleic Acid
Dr.	Doctor (Academic title, Doctor (gen.: doctoris) means teacher in Latin)
dsDNA	Double-stranded DNA
dt	Doublet of Triplet
DTT	Dithiothreitol
Δ	Refluxed
δ	Chemical Shift
e.V.	Electron Volt
EDTA	Ethylenediaminetetraacetic Acid
EI	Electron Impact Ionization
EMSA	Electrophoretic Mobility Shift Assay
equiv.	Equivalents
ESI	Electron Spray Ionization
EtOAc	Ethyl Acetate
F	Fractions
FRET	Fluorescence Resonance Energy Transfer
h	Hour
HEPES	4-(2-Hydroxyethyl)-1-piperazineethanesulfonic Acid
HPLC	High Pressure Liquid Chromatography

HV	High Vacuum
Hz	Hertz
IKK	Inhibitor κB Kinase
iNOS	Inducible Nitric Oxide Synthase
IκB	Inhibitor κB
J	Coupling Constant
K	Kelvin
kV	Kilo Volt
L	Linker
Lit.	Literature
m	Multiplet
m/z	Mass/ Charge
m_{br}	Brought Multiplet
MHz	Megahertz
min	Minutes
MLCT	Metal to Ligand Charge Transfer
MMT	Monomethoxytrityl
Mp	Melting Point
mw	Molecular Weight
NF-κB	Nuclear Faktor κB
NMR	Nuclear Magnetic Resonance
OD	Optical Density
Oligo	Oligonucleotide
Ox	Oxidation
PAGE	Polyacrylamide Gelelectrophoresis
PMSF	Phenylmethylsulfonylfluoride
ppm	Parts Per Million
Pur	Purine
Pyr	Pyrimidine
RNA	Ribonucleic Acid
rt	Room Temperature (20°C)
s	Singlet
ssDNA	Single-Stranded DNA
T	Thymidine
t	Triplet
TBE	Buffer of Tris Base, Boric Acid, EDTA
TEAA	Triethylammonium Acetate
TEMED	*N,N,N,N*- Tetramethylethylenediamine
TFA	Trifluoroacetic acid
TLC	Thin Layer Chromatography
TNF-α	Tumornekrose Factor α
TRIS	Tris(hydroxymethyl)aminomethane
UV	Ultra Violet
V	Volt
VIS	Visual

Table of Contents

I. Introduction

In 1962 James Dewey Watson (Fig. 1), Francis Harry Compton Crick (Fig. 2) and Maurice Hugh Frederick Wilkins were awarded the Nobel prize in medicine "for their discoveries concerning the molecular structure of nucleic acids and its significance for information transfer in living material". The revelation of the DNA structure by Watson and Crick in 1953[1] also triggered the desire to create DNA synthetically; a task which's accomplishment is, at least from a chemist's perspective, as important as the discovery of the helical structure of DNA itself, because it gave rise to modern biotechnology.[2, 3]

The first breakthrough on the long road towards this endeavor was achieved a couple of years after Watson and Crick's discovery with the first synthesis of a dinucleotide by Michelson and Todd (Fig. 3) in 1955.[4] The key step in their work was the activation of a 3'-hydrogen-phosphoate by *N*-chlorosuccinimide. Their achievement was closely followed by another approach. In 1957 Hall *et al.* succeeded in synthesizing a dinucleotide via a dinucleoside hydrogen phosphate which could be oxidized to the natural phosphodiester.[5] These two fundamental methods became the basis for the phosphotriester and the H-phosphonate strategy of oligonucleotide synthesis (Scheme 1 a, b).[6, 7]

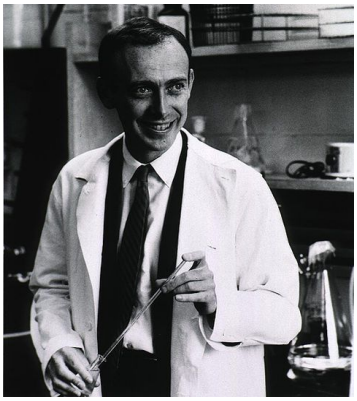

Fig. 1: J. D. Watson.

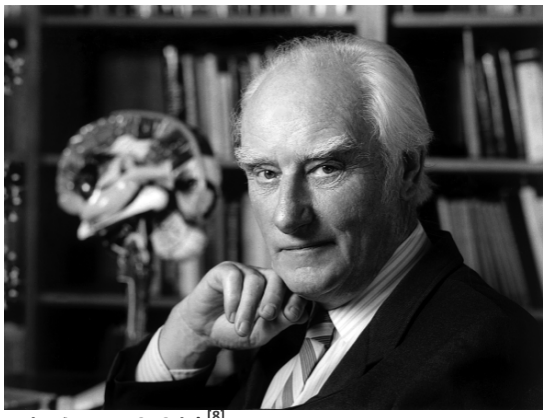

Fig. 2: F. H. C. Crick[8]

The usefulness of short oligonucleotides as an analytical tool in the deciphering of the genetic code was recognized and impressively demonstrated by Khorana and colleagues in 1968 – 1972.[9, 10] During this task they accomplished the synthesis of short, defined oligonucleotide sequences. The synthesis strategy established by them is known as the phosphodiester approach and has been used for many years (Scheme 1 c).[11, 12] It involved the condensation of the free 3'-hydroxyl group of a 5'-protected nucleoside with the 5'-phosphate group of a 3'-protected nucleoside. Two orthogonal protecting groups were used, an acid-labile trityl group for the 5'-hydroxyl function and an base-labile acetyl group for the 3'-hydroxyl function.

In 1975 a new methology was developed by Letsinger and his group, the phosphite triester method (Scheme 1 d).[13, 14] Here a 5'-protected nucleoside is reacted with a cyanoethoxy-phosphate monoester to form a phosphodiester intermediate. To this intermediate a nucleoside with a free 5'-hydroxyl group is coupled yielding a phosphotriester. Among all techniques for the chemical synthesis of oligonucleotides, this approach is still the most commonly used. However, the success of this technique is not only due to its high efficiency, it is also caused by the still ongoing progress in this field.[15, 16] One example for such improvements is the development of deoxyribonucleoside phosphoramidites as stable intermediates by Beaucage and Caruthers in 1981.[17]

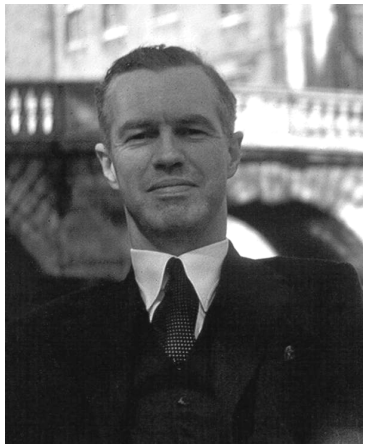

Fig. 3: Sir A. R. Todd

Together with the synthesis of oligonucleotides on solid-support it made automated DNA synthesis possible.[18, 19] This ultimately led to a manifold of modified oligonucleotides, which nowadays are ubiquitous tools in the rapidly growing field of biotechnology.[20, 21]

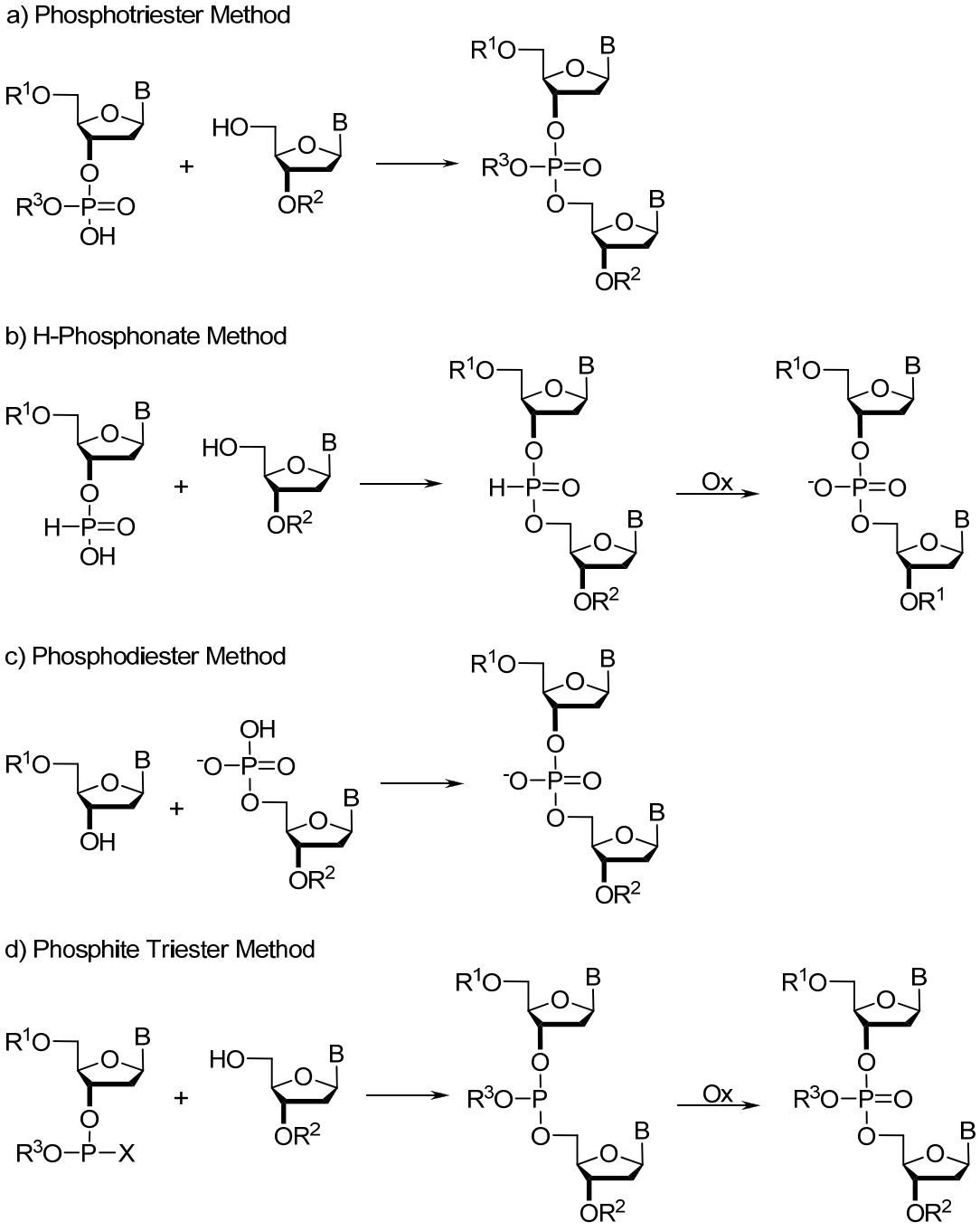

Scheme 1: Methods for the Chemical Synthesis of DNA.
R^1: 5'-Hydroxyl protecting group; R^2: 3'-Hydroxyl protecting group; R^3: Phosphoester protecting group; X: Cyanoethoxy.

Numerous phosphoramidite derivatives for the modification of oligonucleotides are known today.[22] They can be divided up into non-nucleosidic and nucleosidic phosphoramidites. The latter are usually bearing modifications either at the nucleobase, the phosphate backbone or the sugar unit. These artificial DNA building blocks enabled the incorporation of fluorescent, intercalating, crosslinking, lipophilic, fluorophilic, alkylating and DNA cleaving agents into oligonucleotides. Some of these modifications are targeted on improving the synthesis and purification of DNA itself. An example for such a phosphoramidite derivate is a building block bearing long perfluoroalkyl chains,

which was inserted at the 5'-end of a synthetic DNA in order to purify the oligonucleotide from turncated sequences by means of fluorous-fluorous interactions (Fig. 4).[23] Other phosphoramidite derivates, like the hexaethylene glycol phosphoramidite **1** (Fig. 5), aim at increasing the stability of double-stranded DNA by covalently linking the two complementary strands to each other.[24, 25] Modifications, especially of the phosphodiester linkage, can improve nuclease resistance and membrane permeation of natural oligonucleotides making them interesting for therapeutical application.[26, 27] Actually, the majority of synthetic biopolymers is used as diagnostic devices and therapeutic agents. Short oligonucleotides are for instance utilized in the antisense approach where they block the expression of specific genes by binding with the complimentary sequence of mRNA.[28-30] Others are used as molecular probes to gain a better understanding of molecular interactions between nucleic acids and proteins. For this application fluorescent or radioactive markers are of great importance.

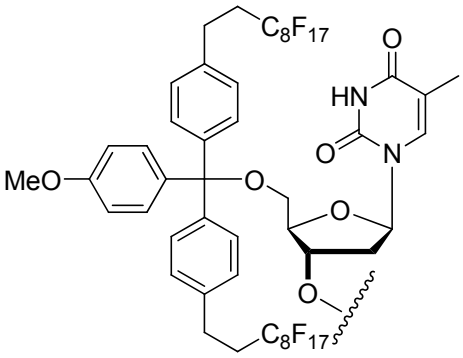

Fig. 4: Fluorous Trityl Protected Thymidine.

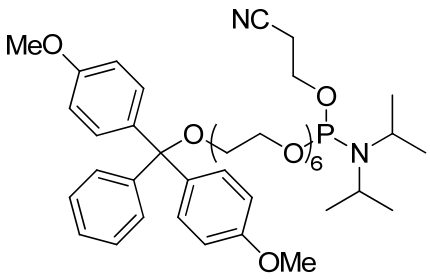

Fig. 5: Hexaethylene Glycol Building Block **1**.

Quite recently also the interest of organic chemists in modified oligonucleotides was sparked.[31] This was triggered by the idea to take advantage of the desirable natural properties of DNA, like its water solubility, its poly-anionic nature and its well defined structure. Other bio-molecules like enzymes had long ago found their way into organic reactions mainly as catalysts. The concept of using modified DNA for this purpose however is fairly new.

The focus of the here presented work lies on two applications from this wide-spread field of modified oligonucleotides: First, fluorescence labeled oligonucleotides and their application as molecular probes for DNA binding proteins will be discussed. The second part of this thesis then highlights oligonucleotides bearing bidentate ligands for DNA-supported catalysis.

Both principles will be addressed in detail after a short presentation of solid phase DNA synthesis in general.

1. Solid-Phase DNA Synthesis

Originally, the concept of insoluble solid supports for the synthesis of linear biopolymers was established by Merrifield for peptide synthesis.[32-34] This principle was then transferred to the synthesis of oligonucleotides.[2] The primary benefit of solid-phase chemistry is the effortless separation of immobilized products from undesired by-products and reactants by means of filtration and washing, giving the possibility to use high excesses of reagents and thereby driving the reaction further to completion. Because the mass of the solid support is usually 10 – 100 times that of the attached compound the method is ideal for the handling of small quantities. Another aspect is the easy automation of solid supported reactions. This is especially true for the synthesis of linear biopolymers where steps are repeated for every prolongation cycle. Such a prolongation cycle for the solid-phase DNA synthesis is outlined in Scheme 2.

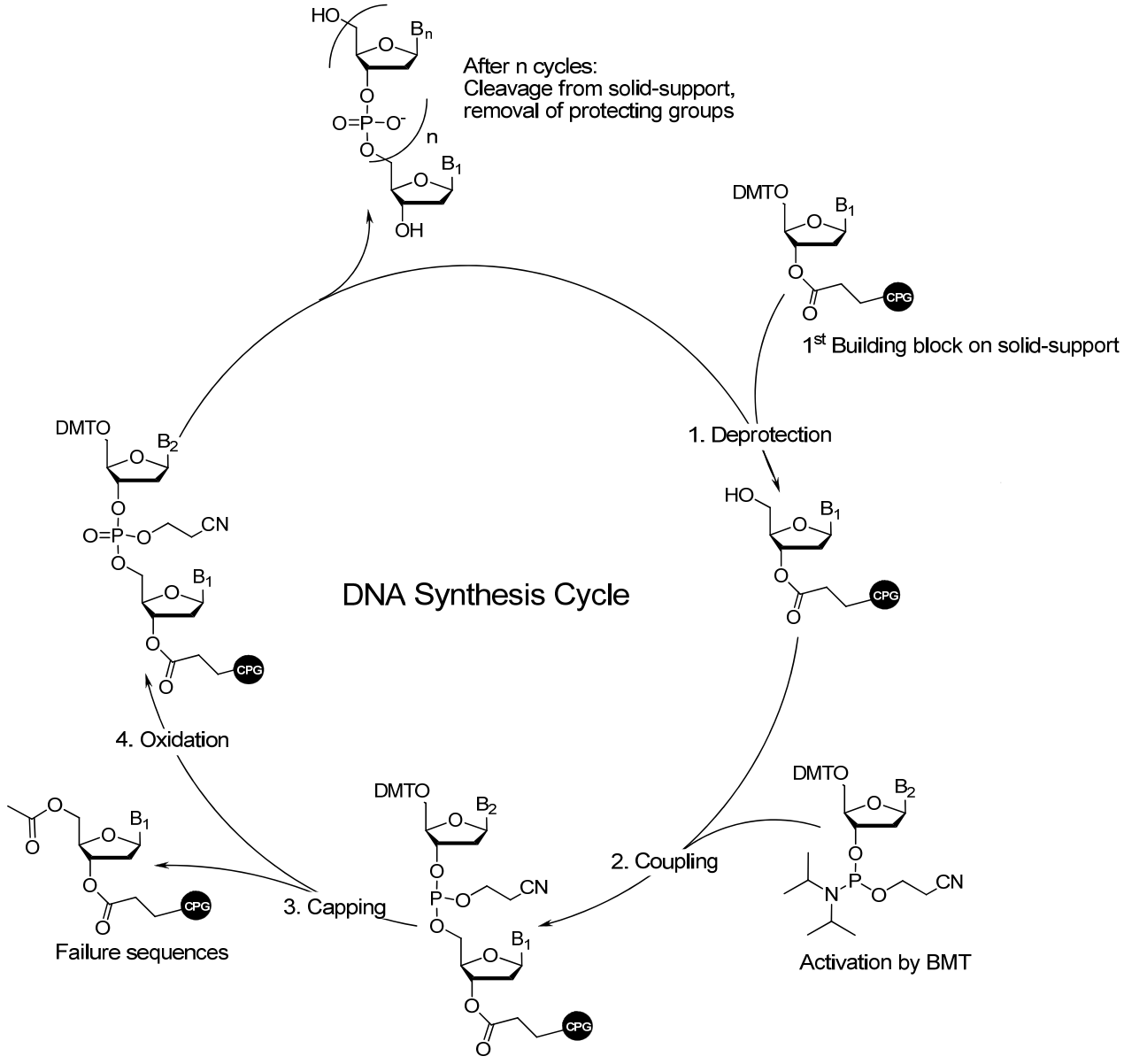

Scheme 2: DNA Synthesis Cycle.

B: Any nucleobase, CPG: Solid support on basis of controlled pore glass, BMT: 5-Benzylmercaptotetrazole.

Contrary to DNA synthesis in nature, artificial DNA synthesis starts at the 3'-end and progresses towards the 5'-end of the oligonucleotide. The first nucleoside is coupled to a solid-support via a long alkyl-chain. Nowadays mainly controlled pore glass (CPG) is used for this purpose.[35] All standard phosphoramidites bound to CPG are commercially available. In the first step the building block is deprotected exposing a free 5'-hydroxyl group, to which the next nucleotide in form of a phosphoramidite is coupled. Usually 5-Benzylmercaptotetrazole (BMT) is employed as an activating agent. The high efficiency of the coupling step is further increased by using a high excess of the phosphoramidite, which drives the reaction to more than 99% conversion. After only a few minutes the coupling reaction is completed and the reagents are washed off. At this stage any sequences that did not react with the phosphoramidite, so called failure sequences, are capped. Capping is achieved by acetylation of the remaining free 5'-hydroxyl functions. After another washing step the new phosphor diester linkage between the nucleosides is oxidized from P(III) to P(V) by the addition of a iodine/collidine/water solution. Yet another washing step completes the cycle which is then repeated for as many times as needed to assemble the desired sequence. Once the synthesis is finished it takes just one further step to cleave the oligonucleotide from the solid support and at the same time remove all remaining protecting groups. The deprotection and cleavage is accomplished by treating the solid supported oligonucleotide with an aqueous solution of ammonia.

1.1. Protecting Groups

For the DNA synthesis cycle to work and to prevent any side reactions during the coupling step an elaborated system of orthogonal protecting groups is needed. It is essential, that the 5'-hydroxyl functionality is exclusively accessible to the substrate while all other nucleophilic centers like the 3'-hydroxyl, the exocyclic amino groups of the nucleobases adenine, guanine and cytosine and the phosphate group remain protected. Therefore, a sophisticated strategy was developed, in which the 5'-hydroxyl group is protected with an acid-labile protecting group, whereas the remaining functionalities are protected with base-labile protecting groups, making it possible to deprotect the 5'-position orthogonally.

The protecting group of choice for the 5'-position is 4,4'-dimethoxy-trityl (DMT), which can be introduced regio-selectively at the desired position (Fig. 6) and is easily cleaved under mild acidic conditions (3% dichloroacetic acid). Another feature of the DMT group is the intensive orange color of the cleavage product. With an absorption maximum of 495 nm it is used to photometrically quantify the efficiency of the previous coupling step.

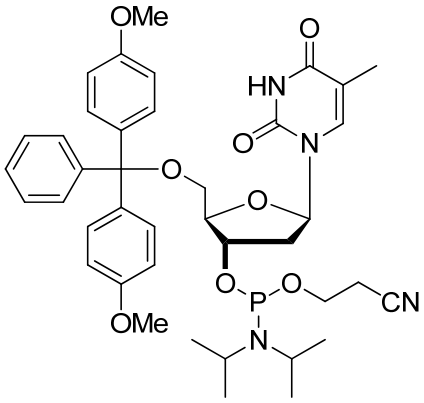

Fig. 6. DMT-Protected Phosphoramidite of Thymidine.

In order to prevent the elongation of the oligonucleotide chain towards the wrong direction, the 3'-hydroxyl end gets protected as ester. The ester bond is stable towards all conditions, which occur during the synthesis cycle and can also be used to couple the 3'-end of the oligonucleotide to the solid-support. The protecting groups of the exocyclic amino functions of the nucelobases, as well as the phosphate group are designed in a similar way, allowing these groups to remain protected during the synthesis cycle. Therefore, the amino functions are transformed into the corresponding amides (Fig. 7) while the phosphate group is protected as ester.

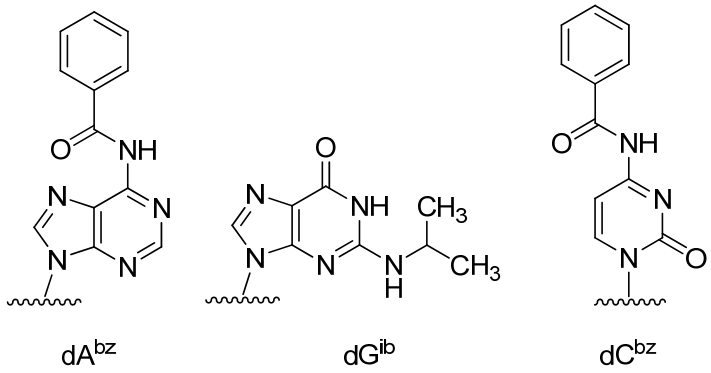

Fig. 7: Protecting Groups for the Exocyclic Amino Functions.
dA^{bz}: 5'-DMT-2'-deoxy-adenosine (6-*N*-benzoyl)-β-cyanoethyl-phosphoramidite, dC^{bz}: 5'-DMT-2'-deoxy cytidine (4-*N*-benzoyl)-β-cyanoethyl-phosphoramidite, dG^{ib}: 5´-DMT-2'-deoxy-guanosine-(2-*N*-isobutylat)-β-cyanoethyl-phosphoramidite, dT: 5´-DMT-thymidine-β-cyanoethyl-phosphoramidite.

1.2. Modified Oligonucleotides

The phosphoramidite approach is not only used for the insertion of natural occurring nucleosides, as mentioned previously, also unnatural nucleosides are frequently inserted into DNA. The primary use of these artificial building blocks is the introduction of new and desired features into DNA which otherwise would not be available. A great advantage of using phosphoramidite building blocks for the introduction of modifications into synthetic oligonucleotides over modifying natural oligonucleotides is the controlled environment. In the synthesis process of a so called modified oligonucleotide all parameters like the base sequence, the length of the oligonucleotide and even the position of the modification within the sequence can be designed at will. The scope of this approach is almost only limited by the imagination of the synthetic chemist. A couple of things

however have to be paid attention to. Naturally, it is of great importance that these phosphoramidites are stable against all conditions used during the synthesis of oligonucleotides.[2] Therefore intensive tests especially regarding the deprotection conditions (dichloroacidic acid and concentrated ammonia) should be carried out. New building blocks should also be screened towards their effect on the stability of single stranded oligonucleotide as well as double-stranded DNA.

Two different approaches for the introduction of such modifications can be followed, the *pre*-synthetic and the *post*-synthetic approach.[36] In the *pre*-synthetic strategy the unnatural building block is synthesized in its entire form prior to its insertion into the oligonucleotide. It is then transformed into the corresponding phosphoramidite and as such used in DNA synthesis. This is obviously the most straight forward approach and usually yields in the best results. For some modifications however this method is not feasible, because of stability issues towards the conditions during DNA synthesis, a poor coupling efficiency of the phosphoramidite or functional groups which are not compatible with the whole process. In these cases a *post*-synthetic strategy is favorable. Instead of coupling the modification in its entity, a phosphoramidite derivate bearing a protected functional group, e.g. an aliphatic amine, is introduced into the oligonucleotide (Fig. 8). Subsequently the desired modification is selectively coupled to this new functional group. Whether this coupling step can be done on solid support or in solution depends strongly on the protecting group used for masking of the new functional group.

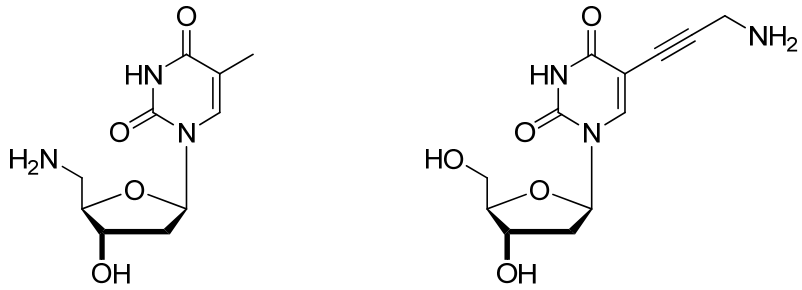

Fig. 8: Artificial DNA Building Blocks for the Post-Synthetic Introduction of Modifications.

The application of modified synthetic DNA and modified natural DNA will be explained exemplary in the following two chapters.

2. Fluorescence Resonance Energy Transfer in DNA

2.1. Theoretical Background

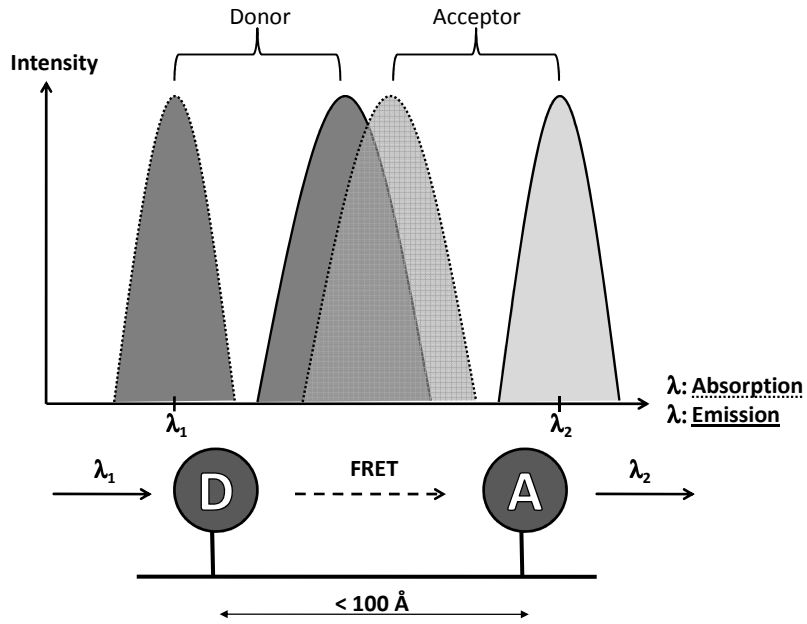

Fig. 9: Basic Principle of FRET.
D: FRET donor, A: FRET acceptor; dotted lines are absorption spectra; full lines are emission spectra.

Fluorescence Resonance Energy Transfer (FRET) is defined as the non-radiative transmission of energy between two fluorophores, the donor fluorophore and the acceptor fluorophore, by means of dipole-dipole interactions. This process was first described by Förster in 1946 and is a variation of the Förster resonance energy.[37, 38] For the non-radiative energy transfers to occur a couple of criteria, regarding the spectral overlap, the orientation and the distance between donor and acceptor, have to be met (Fig. 9).[39, 40] It is essential that the donor emission overlaps well with the acceptor absorption. Quantum physically this means that the energy levels of donor and acceptor between which the energy transfer takes place have to be equivalent. Another factor is the orientation of the two chromophores towards each other. The vibrational levels of donor and acceptor have to be aligned in parallel. In solution this is not an issue, because the molecules can rotate freely. In case donor and acceptor are covalently bound to the same molecule, the issue however has to be addressed. For an efficient FRET also the distance between donor and acceptor can be no larger than ~100 Å. The molecular processes on which FRET is based can best be explained with the help of a Jablonski diagram of the quantum energy levels of a donor and an acceptor pair (Fig. 10).

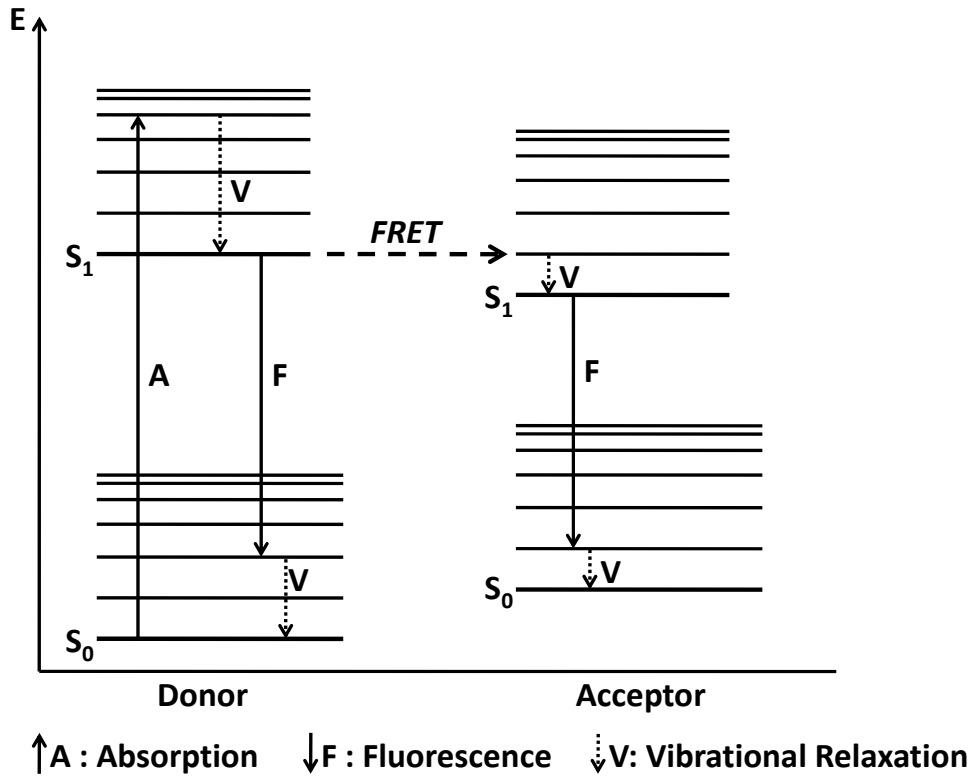

Fig. 10: Jablonski Diagramm.
E: Energy, S_0: Singlet ground state, S_1: First excited singlet state.

Through the absorption of energy in form of radiation a donor can get excited from its singlet ground state S_0 to a higher singlet state. Several excited singlet states are possible. However vibrational relaxation to the first excited state S_1 is fast. From this level the relaxation to the ground state can be achieved through multiple radiative and non-radiative ways. A radiative pathway for the relaxation is the spontaneous emission of light, called fluorescence. The energy of the fluorescence is lower than the *pre*viously absorbed energy, hence a shift to longer wavelength is observed. Relaxation without the emission of light is possible through internal conversion, during which the energy is released in form of heat.

Another possibility for the donor to reach its energetic ground state after excitation is FRET. In this case the energy from the excited state S_1 is transferred to an energetically equal level of a nearby acceptor molecule. The emission free mechanism of the energy transmission is based on dipole-dipole interactions between the excited donor and the acceptor in its ground state. Both donor and acceptor are here interpreted as oscillating dipoles with the same resonance energy. The excited acceptor itself can now either relax to its ground state through fluorescence or by internal conversion. In the second case the acceptor is often referred to as quencher.

As already pointed out, the efficiency of the energy transfer depends on several factors. The effect of those factors on the efficiency has been described by the Förster equation.

$$E = \frac{1}{1 + (r/R_0)^6}$$

Equation 1: Förster Equation.
E: Efficiency, *r*: Donor and acceptor separation distance, R_0: Förster radius.

In the equation, the relative orientation of the chromophores towards each other and their spectral overlap is described by the Förster radius R_0. The Förster radius R_0 is defined as the distance between donor and acceptor at which the FRET efficiency is 50%. For a given donor and acceptor pair the Förster radius is constant in a particular solvent. The Förster equation also stresses the high sensitivity of FRET systems towards changes in the distance *r* between donor and acceptor. They affect the efficiency of the FRET to the 6^{th} power. This distance dependency has an operative range of 20 to 100 Å, making FRET a useful molecular ruler for monitoring biochemical and cellular processes.

2.2. Spectroscopic Methods

Multiple methods for the spectroscopic detection and quantification of FRET are available. The first step however is always the excitation of the donor which is either achieved by a steady state light beam with adequate wavelength or with a light pulse.[41]

In the first case the success of the energy transfer can then be seen either by the fluorescence of the acceptor or by the donor's loss of fluorescence. Fig. 11 depicts a typical emission spectrum of a FRET donor-acceptor pair, in which the emission intensity of the donor was normalized. FRET efficiency can then be evaluated by the intensity of acceptor emission.

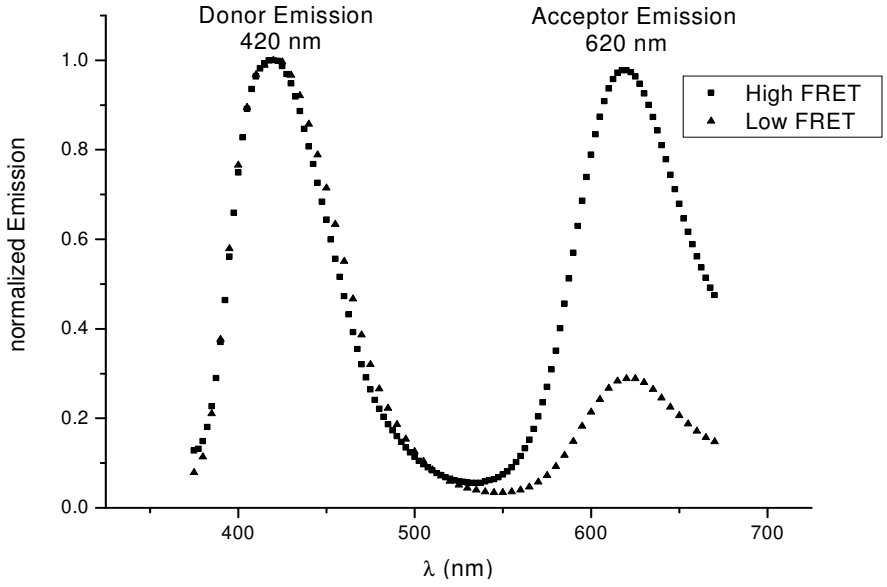

Fig. 11: FRET Emission Spectrum.

The second excitation approach is used in so called time resolved FRET measurements (Fig. 12). In these experiments the decay of the acceptor emission after the light pulse (t_1) is recorded. Depending on the nature of the acceptors the decay can be quite long-lived (microseconds), longer than the one of background emission (nanoseconds). Because of this the acceptor fluorescence can be measured after the decay of the background fluorescence (t_2–t_3) resulting in an extremely sensitive FRET.

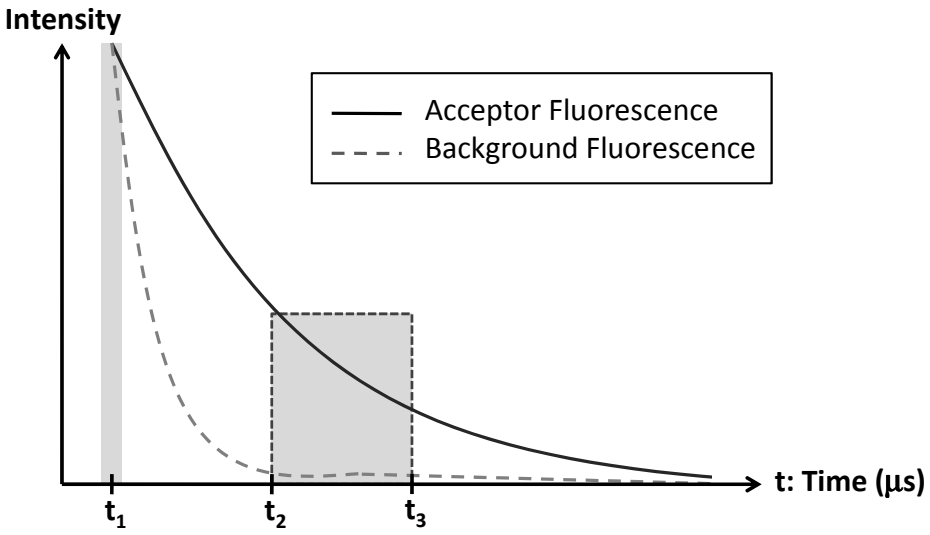

Fig. 12: Spectrum of a Time Resolved FRET.

Even more insights into molecular dynamics are promised by single molecule FRET (smFRET). Single molecule FRET has the potential to enable us to follow processes that previously could not be monitored, because they used to be hidden in an averaged fluorescence of many molecules. By looking at a discrete donor and acceptor pair it is feasible that dynamics like the folding of proteins can be resolved.[42-44]

2.3. FRET Dyes

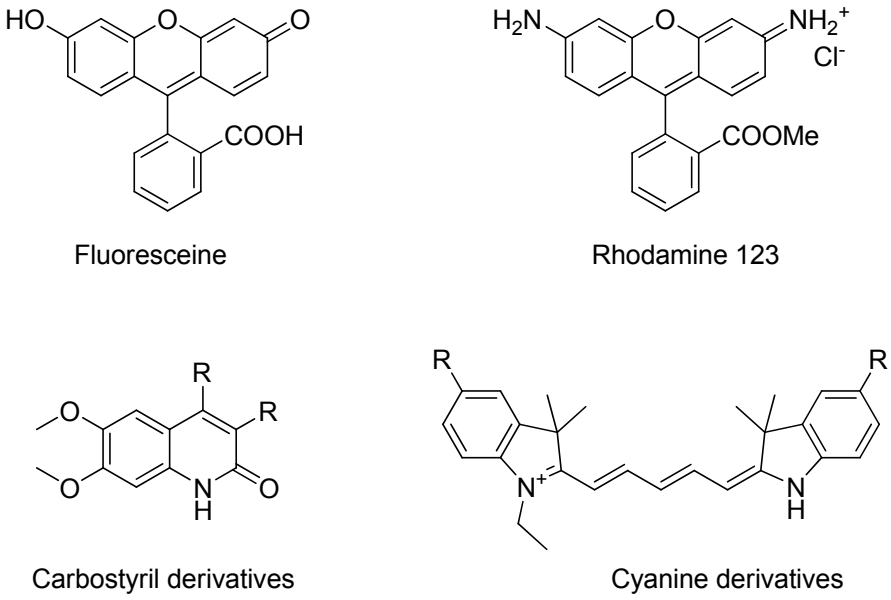

Fig. 13: Typical Organic FRET Dyes.

The traditional domain of FRET dyes is that of organic dyes which have the key advantage of being fairly cheap and well understood.[41] They possess large conjugated π-electron systems as chromophore unit and their fluorescence properties are easily adjusted through auxochrome groups. Today, fluoresceine, rhodamine, carbostyril and cyanine derivates are the most common

among organic dyes used for FRET.[45, 46] They are favored because of their great chemical and thermal stability. Whole libraries of these dyes with various absorption and emission properties are commercially available an, example being the family of Alexa dyes or the Atto dye series.[47-49] However, a broad absorption and emission band with only a small stoke shift is characteristically for them.

Another class of FRET dyes is that of luminescent lanthanide ions.[50] They enjoy growing popularity because of their relative long emission lifetime. This feature is as mentioned essential for time resolved measurements. Among the lanthanide ions Eu^{3+}, Gd^{3+} and Tb^{3+} possess the best emissive properties. The energy gap between their ground state and their first excited state is the largest, which minimizes potential non-radiative deactivation pathways. Gd^{3+} however is not very suitable for biological processes, because its emission is in the UV range and interferes with many organic compounds.[50, 51] Lanthanide ions have a relatively low extinction coefficient so that direct excitation usually does not lead to high luminescence. Indirect excitation is therefore often used. This process, which is called sensitization, uses ligands to transfer energy to the lanthanide ion.[52, 53] These ligands are either themselves chromophores or have chromophores attached to them (Fig. 14). In the first step the chromophore unit is excited which is then followed by the transfers of energy onto an excited state of the metal ion. This ligand to metal energy transfer can either happen from the ligand's singlet or from its triplet state. Because of its longer lifetime the latter is more likely to happen.

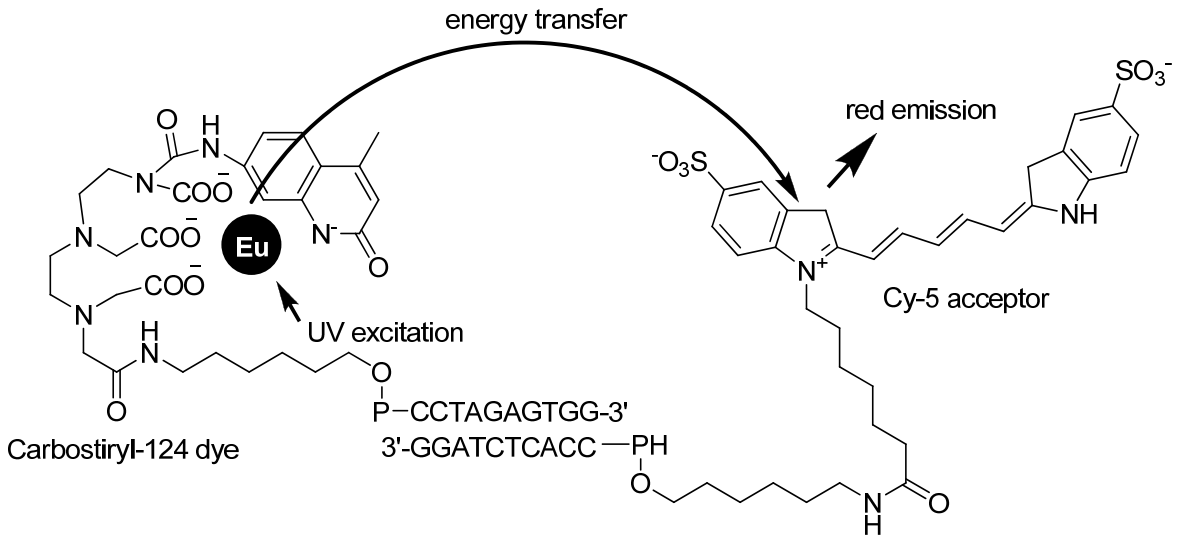

Fig. 14: Example for the Application of Lanthanide Ions as FRET Dyes.[50]
Hybridization sensor: The FRET donor, a carbostiryl sensitized Eu-lanthanide is attached to a single stranded oligonucleotide, while the FRET acceptor is bound to the complementary sequence. Hybridization brings both FRET dyes in close proximity resulting in FRET.

One drawback of lanthanide complexes is their low thermodynamic stability, which leads to dissociation of the complex in low concentration. Good chelating ligands or even cryptates have to be used to prevent this.[54] To overcome the metal leaching other classes of long-lifetime dyes are therefore investigated. A very promising group is the one of charge transfer complexes of transition metals.[55] The excitation of metal to ligand charge transfer complexes (MLCT) results in a transfer of electrons from a MO with metal like character to a MO with ligand like character. Formally it can be seen as the oxidation of the metal and the reduction of one of the ligands (Scheme 3).

$$[Ru^{II}(phen)_3]^{2+} \xrightarrow{h\nu} [Ru^{III}(phen)_2(phen^-)]^{2+}$$

Scheme 3: Oxidation of the Metal and Reduction of the Ligand in MLCT Complexes.

Charge transfers unlike d-d electron transfers in complexes are quantum-mechanically allowed. The result is a highly intense absorption band, the so called charge transfer band. A wide variety of fluorescent MLCTs are known. Of these, especially the bathophenanthroline-ruthenium(II) complexes show desirable properties.[56, 57]

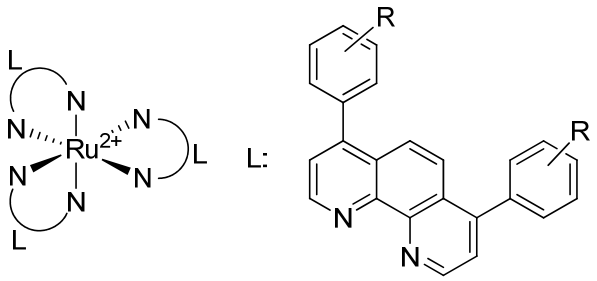

Fig. 15: Bathophenanthroline-Ruthenium(II) Complexes.

Such bathophenanthroline-ruthenium(II) complexes are not only thermodynamically very stable and therefore do not dissociate at low concentrations, they are also chemically inert. Their strong and long-lasting fluorescence (t_{em} = 1-10 µs) after excitation with light pulses of short duration allows for a detection by time-resolved measurements. These complexes are accessible in a synthetically straight forward manner. One phenanthroline unit can be modified with an alkyle linker arm and a terminal carboxy group to allow the coupling of these complexes to bio-molecules via stable amide bonds.[58, 59] Their application in oligonucleotides as well as peptides has been reported in literature.[60, 61] The strong fluorescence of the charge transfer complex leads to a very low detection limit of 10^{-18} mol in 100 µl, which is in the range of radioactive ^{32}P labeling.[56]

2.4. Selected Applications of FRET in DNA

a. Detection of Nucleic Acid Hybridization

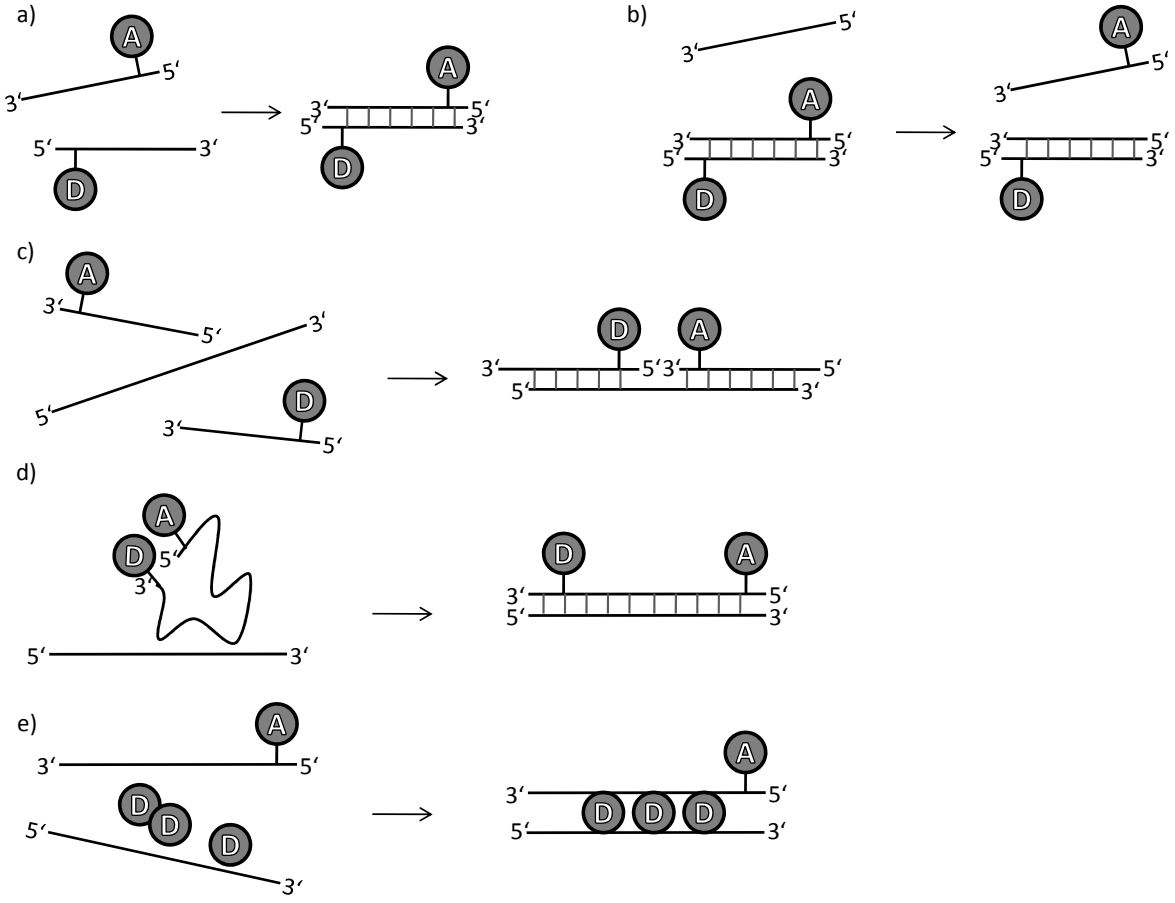

Fig. 16: Exemplary FRET Systems for the Detection of DNA or RNA Hybridization.

The detection of nucleic acid hybridization in general is an essential necessity in the field of molecular biology, genetics or even forensics. Different techniques, most of which are using FRET, have been established.[62-64] A couple of methods are depicted in Fig. 16. The underlying principle is always the same. Hybridization of the probe with a specific oligonucleotide sequence leads to a change in distance between FRET donor and acceptor. The difference of these methods lies in the position of the chromophores within the oligonucleotides. For example, donor and acceptor can be attached to complementary strands (Fig. 16 a and b). Hybridization of such labeled oligonucleotides creates a FRET system. The presence of an unlabeled oligonucleotide with the same or higher affinity is detected by the dissociation of the FRET system. Just the opposite is true for the next approach. Here, the two probes, each carrying only one of the FRET chromophores, are not complementary to each other. Only hybridization of both probes to the same sequence brings donor and acceptor close to each other, establishing the FRET system (Fig. 16 c). It is also possible to attach donor and acceptor to opposite ends of the same oligonucleotide. In such a single-stranded probe a FRET can occur due to its flexibility, whereas the rigid structure of a double helix keeps donor and acceptor further apart (Fig. 16 d). In the last example only one of the FRET dyes is covalently coupled to an oligonucleotide. The formation of double-stranded DNA is in this case detected by the ability of the other dye to intercalate into a double helix (Fig. 16 e).

b. Molecular Beacon

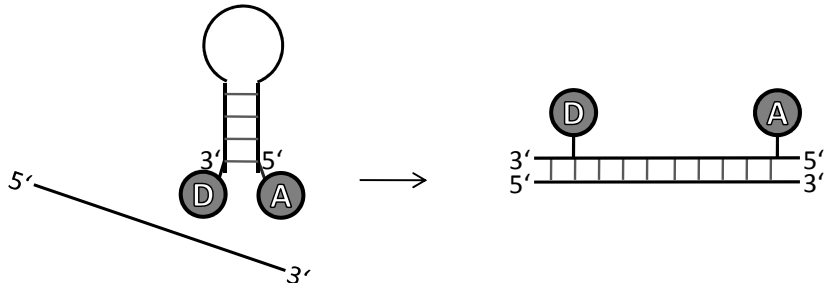

Fig. 17: Molecular Beacon.

Molecular beacons are used for the sequence specific detection of oligonucleotides (Fig. 17).[65-68] The probe itself is a single-stranded oligonucleotide with the FRET donor and acceptor at opposite ends. The characteristic feature of a molecular beacon is the self-complementary sequence at its 3’- and 5’-end. This causes the probe to form a hairpin structure in which donor and acceptor are in close proximity, thus creating a FRET system. The middle part of the molecular beacon resembles the complementary sequence towards which it is sensitive. When probed against such a DNA sequence the hairpin structure unfolds. Thereby the distance between donor and acceptor is increased and the FRET is no longer possible. This can then either be detected by the increase of donor emission or the decrease of acceptor emission.

c. Real-Time PCR Assays

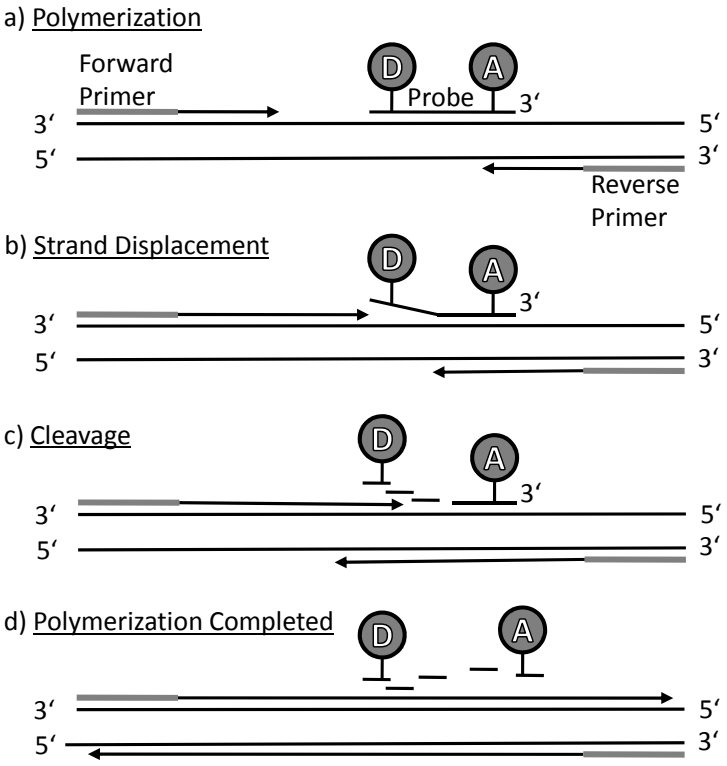

Fig. 18: TaqMan Assay.

One technique to monitor and quantify polymerase chain reaction (PCR) cycles in real time is the TaqMan assay (Fig. 18).[69] The probe in this assay is a short single-stranded oligonucleotide bearing a working FRET system. In the first step of PCR the probe binds sequence-specifically to the dehybridized DNA strand. At this stage the FRET system is still intact and the donor emission is suppressed by the acceptor. During the elongation of the complementary DNA strand by a TaqMan polymerase, the probe will be dismantled by the 5'-3' exonuclease activity of the polymerase. This process destroys the FRET system and the emission of the donor is no longer quenched by the acceptor.

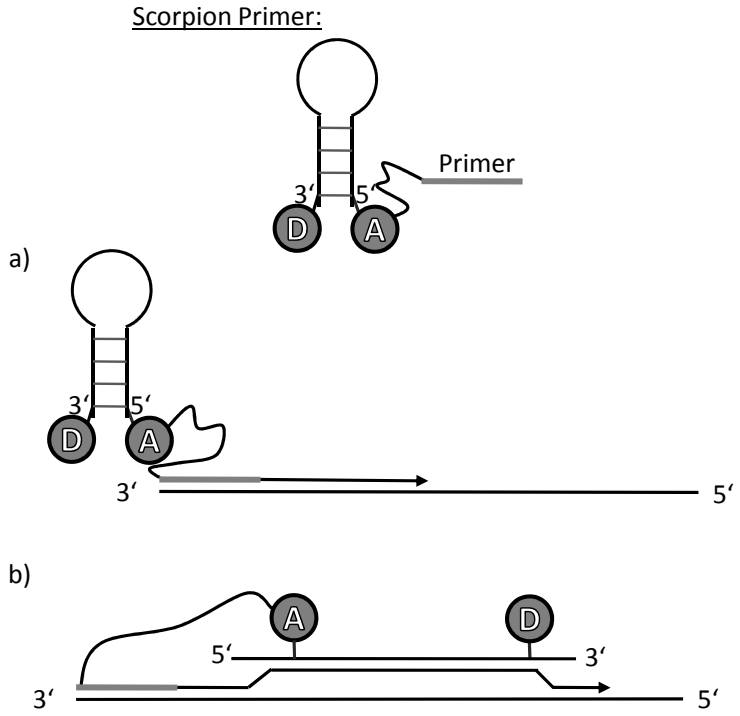

Fig. 19: Scorpion Assay.

Another way to follow PCR by FRET is the Scorpion Assay (Fig. 19).[70] The probe in this case is a complex oligonucleotide, essentially consisting out of a molecular beacon with a PCR primer attached to it. It is called the scorpion primer. The hairpin structure of the scorpion primer is chosen in such a fashion that it can hybridize to the newly formed complementary sequence during the elongation process of PCR. This step effectively increases the distance between the two FRET chromophores and restores the fluorescence of the donor.

d. Automated DNA Sequencing

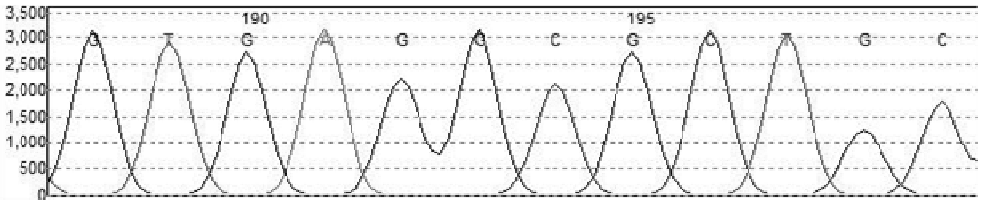

Fig. 20: DNA Sequencing.

A lot of effort is being put into genome sequencing (Fig. 20).[71] New methods for faster and more efficient automated DNA sequences are being proposed. Especially the sequencing of single molecules promises to take genomics into the next level. One of these anticipated methods is the FRET-based sequencing approach by VisiGen.[72] The sequencing is carried out with nucleotides bearing a FRET acceptor at the gamma phosphate. For each of the four nucleotides a different colored acceptor entity is used. The FRET donor is coupled to the polymerase. When the polymerase incorporates a nucleotide, donor and acceptor will come into proximity causing a FRET signal. The color of the signal indicates which nucleotide is being incorporated. After each step the phosphate containing the acceptor is released, so that no additional steps are needed before the next nucleotide is coupled. In the future, DNA sequences can so be read by following the polymerase in real time.

3. 1st Objective of this Thesis

In this thesis we had yet another application of FRET in mind. In an interdisciplinary cooperation with the group of Prof. Dr. Irmgard Merfort of the Pharmaceutical Institute at the University of Freiburg, we were striving for a novel assay for the DNA transcription factor NF-κB based on FRET. This assay was envisaged to consist out of a DNA triple helix as depicted in Scheme 4. The triple helix is composed of a backfolding DNA labeled with the FRET donor and a third oligonucleotide labeled with the FRET acceptor. The acceptor oligonucleotide is attached to the backfolding DNA via Hoogsteen pairing. In this arrangement donor and acceptor entity are in close proximity and a FRET signal can be detected. Upon the addition of transcription factor NF-κB, it replaces the acceptor oligonucleotide by binding specifically to the backfolding DNA. Thereby the distance between donor and acceptor increases and thus can be detected by the decrease of the FRET signal.

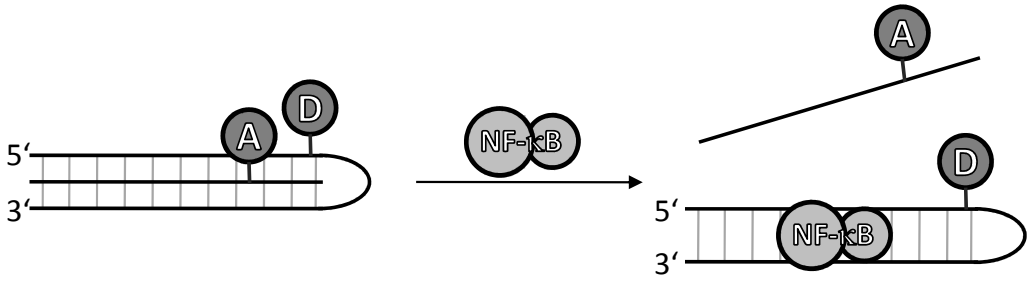

Scheme 4: Principle of the Triple Helix Assay.

The foundation of this work had already been laid during my diploma thesis where an oligonucleotide sequence suitable for the desired purpose had been found. This sequence which was derived from parts of the inducible nitric oxide synthase (iNOS) in mice incorporated all the desired features, the binding sequence for NF-κB, as well as a long homopyrimdine stretch, which is essential for Hoogsteen interactions (Fig. 21). During the diploma thesis several DNA triple helices were synthesized containing this sequence. In order to increase the stability of the double helix, the two iNOS-derived strands were connected via a hexaethylene glycol spacer to form a backfolding DNA which allows for optimal hybridization[22] and also leads to an increase of the stability of the triple helix at the same time.[23] Extensive research on the stability of these triple helices and their binding properties towards NF-κB had been performed.

Fig. 21: Interesting Stretch of the iNOS Sequence.
Bold: NF-κB recognition sequence, Italic: Homopyrimidine sequence.

Based on the obtained results the focus in this thesis laid on establishing the FRET system for the assay. The first goal was to incorporate a FRET donor and acceptor into the most promising DNA triple helix. For this purpose the corresponding oligonucleotide sequences had to be modified with appropriate coupling sites. Since the effect of the dyes on the stability of the triple helix was

unknown, different positions for the FRET dye pair had to be evaluated. After coupling of the dyes the oligonucleotides therefore had to be tested for their FRET properties as well as their binding abilities towards NF-κB.

Successful candidates for the desired assay then finally were subjected to a feasibility study. Here their behavior towards NF-κB and the effect on the FRET was tested.

4. DNA-Supported Catalysis

The classical field of catalytically active biomolecules is that of enzymes. Enzymes play a vital role in almost all cellular processes, but also outside of the realm of biochemistry they have become well established. Enzymes have a long history in industrial chemistry and have been employed as catalysts in various organic reactions.[73, 74] Typical organic reactions of enzymes are the hydrolysis of carboxylic acid esters,[75, 76] phosphate esters,[77, 78] amides,[79] nitriles[80] or epoxides with hydrolase enzymes and the oxidation[81] and reduction[82] of oxidoreductase enzymes. Also C-C coupling reactions are possible, for example with the help of aldolase enzymes.[83]
However, enzymes are not the only natural biomolecules with the ability to catalyse reactions. Already in 1967 it was thought possible that RNA might also function as catalysts.[84, 85] This idea was based on the discovery that RNA can form complex secondary structures similar to those of enzymes. In the 1980s T. R. Cech and S. Altman reported the first catalytic RNA.[86-88] For their work they were awarded the Nobel Prize in chemistry in 1989. The term ribozyme for RNA with enzyme like properties was coined by K. Kruger *et al*. in 1982.[89] Since then ribozymes have become the focus in explanations of a prebiotic world, the hypothetical 'RNA world'.[90] Yet, the scope of naturally occurring ribozymes is very limited. Only hydrolysis and transesterification reaction at internucleotide phosphodiester bonds are known so far. This limitation holds not true for artificial ribozymes, as a vast variety of RNA with new binding properties and catalytic properties have been reported. Most of these artificial ribozymes come from combinatorial nucleic acid libraries and were optimized for their task by direct evolution. [91]

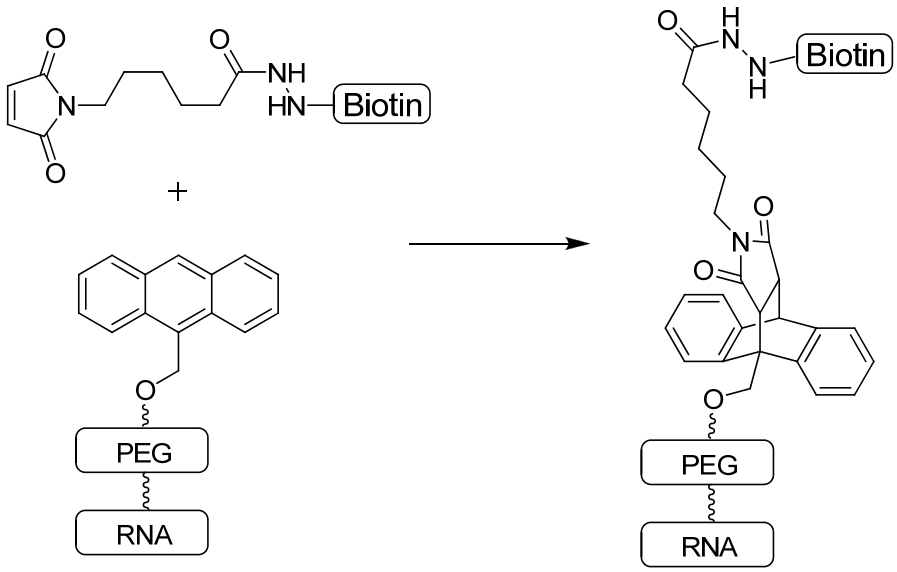

Scheme 5: Diels Alder Reaction Catalyzed by Ribozymes.
Diels-Alder reaction between dienophile biotin maleimide and diene anthracene which is covalently coupled to the RNA by poly(ethylene glycol) (PEG).

One example for this approach is the RNA-catalyzed formation of C-C bonds by Diels-Alder reactions (Scheme 5).[92] The diene anthracene was coupled covalently to RNAs of a combinatorial library (2 x 10^{14} species, 120 randomized positions). This library was screened against the biotin-labeled dienophile maleimide. Successful Diels-Alder reactions resulted in biotinylated RNAs, which were then amplified and subjected to further selection and amplification cycles. After 10 rounds several RNAs were identified, which accelerated the Diels-Alder reaction up to 18,500 fold. Most of these contained a similar motif, which was found to be responsible for the catalytic activity (Fig. 22).

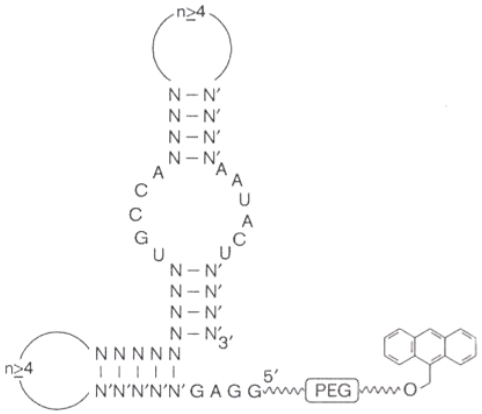

Fig. 22: Typical Motif of Catalytically Active Ribozyme.[91]
N: any nucleotide; N', nucleotide which is complementary to the Watson-Crick base paired N; PEG poly(ethylene glycol).

Other reactions catalyzed by ribozymes include ester hydrolysis reactions, alkylations, acylations and amide bond formations.

Besides RNA also DNA sequences have been researched for catalytical properties.[31, 93] The field of DNA catalysis however is fairly young and the range of reactions is very limited. Natural DNA is not known at all to possess any catalytical properties. A reason for that might be the lack of variety in secondary structure for DNA compared to RNA. Instead, DNA prefers the double helical structure, which shields potential catalytic sides. Nevertheless, the first artificial deoxyribozyme was described in 1994.[94] Since that time some applications of artificial deoxyribozymes have been reported, most of which are either RNA cleavages or RNA ligations.[95, 96]

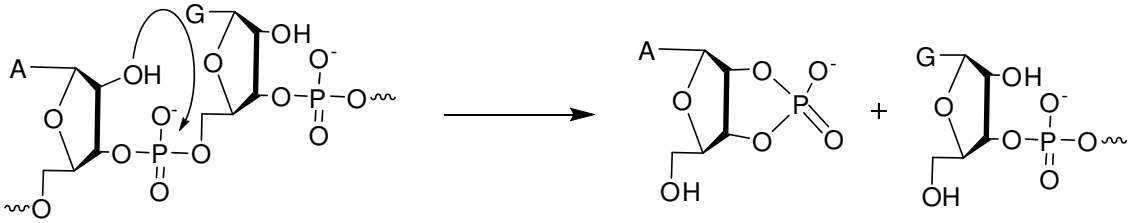

Scheme 6: Deoxyribozyme Catalyzed RNA Cleavage.

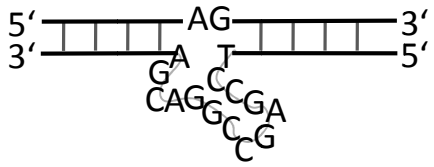

Fig. 23: RNA-Deoxyribozyme 8-17 Duplex.

The site-specific cleavage of RNA is for example possible with deoxribozyme 8-17 (Fig. 23).[97, 98] It targets A-G dinucleotide junctions within RNA and promotes their cleavage in the presence of Mg^{2+} (Scheme 6). An interesting application of such deoxyribozymes as analytical tool was published by Lu *et al*.[99] Their deoxyribozyme 39E selectively cleaves RNA only in the presence of UO_2^{2+}. In combination with a FRET system this dependency was used as sensor for uranium (Scheme 7). In this arrangement the RNA strand was labeled with both FRET dyes (donor and quencher) and the deoxyribozyme was labeled with a second FRET quencher. The use of two quenchers allowed keeping background fluorescence at a minimum, which resulted in an extremely low detection limit of 45 pM beeing far below the toxic UO_2^{2+} level in drinking water, which is 130 nM.

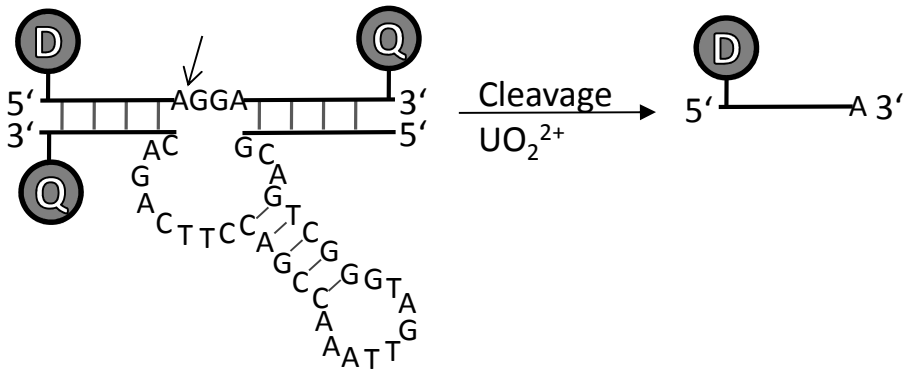

Scheme 7: UO_2^{2+} Senstive FRET Assay.

An example for RNA ligating deoxyribosomes comes from S. K. Silverman *et al*.[100, 101] By means of directed evolution they obtained deoxyribozymes that were tolerant on the RNA sequences and yielded a high 3'-5' ligation selectivity. The new bond was formed by a nucleophilic attack of the 3'-hydroxy group at a 5'-triphosphate (Scheme 8).

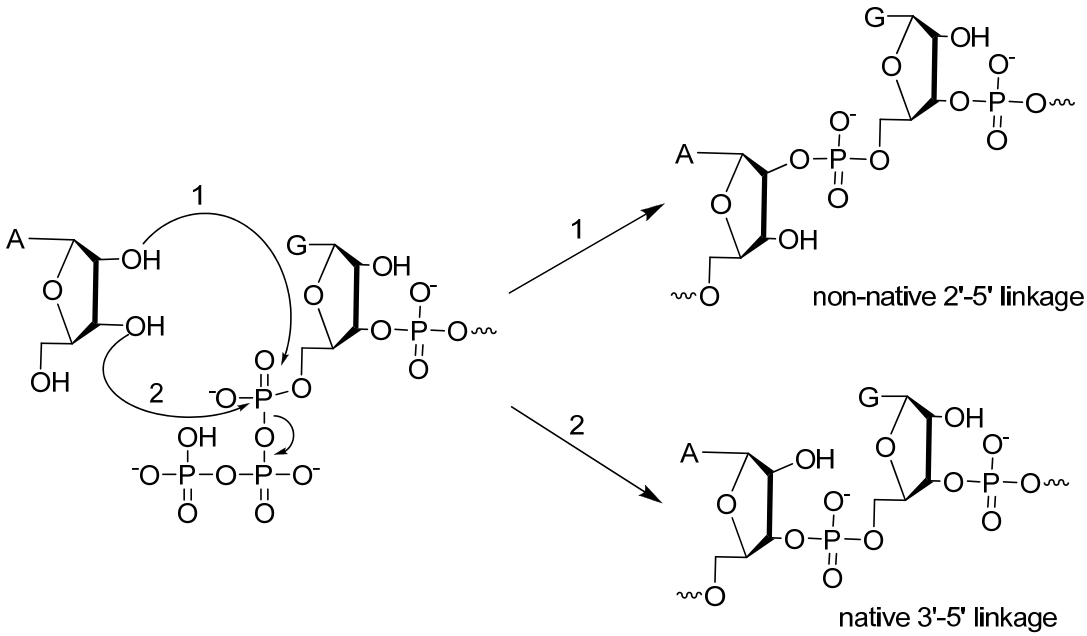

Scheme 8: RNA Ligation.

Even though a lot of progress in the area of ribozymes and deoxyribozymes was made in recent years, these biomolecular catalysts fall short compared to enzymes. One reason for the greater diversity of enzymes could be the larger number of building blocks which compose the sequence. Enzymes can choose from a pool of 20 natural amino acids whereas RNA and DNA each have only four different nucleic acids available. Another advantage of enzymes is their capability to efficiently produce optically active molecules under very mild conditions. This ability is due to the chirality of the amino acids. Nevertheless, side chains of enzymes also allow only for a limited range of reactions, notably hydrolytic ones. The majority of transformations are dependent on co-factors or co-enzymes. Whereas the tertiary structure of the protein is responsible for the discrimination of optical isomers, the latter are responsible for the actual catalytic reaction.

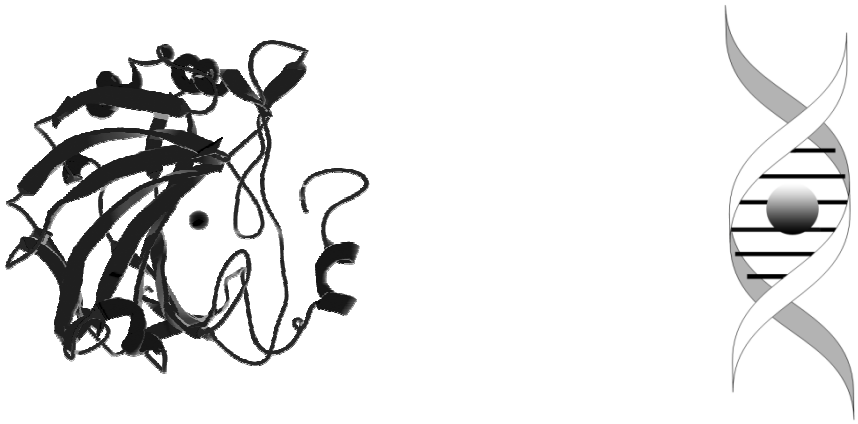

Fig. 24: Structure of Enzyme with Cofactor in the Middle (left) and Envisaged DNA-Catalyst Complex (right).

A new kind of DNA-supported catalysts without the limitations of classic deoxyribozymes might be possible with a similar arrangement (Fig. 24). In such a scenario the helical environment of DNA might induce enantioselective discrimination, while a catalyst could act close to it. First examples for the induction of enantioselectivity by DNA were reported by the group of Feringa.[102] For this purpose Cu^{2+}-complexes of different bidentate intercalators were introduced as catalytic centers into natural double-stranded DNA. These DNA-supported catalysts were then evaluated in Diels-Alder reactions (Scheme 9).

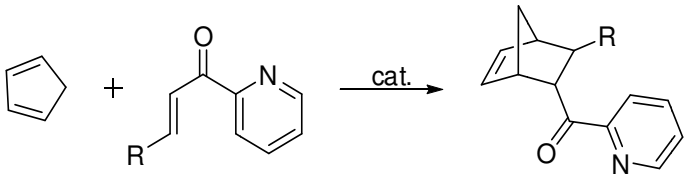

Scheme 9: Diels Alder Reaction.
R: 4-MeO-Ph, Ph and *t*-Bu.

In the first ligand generation the metal binding moiety was coupled to the intercalation unit via a linker molecule (Fig. 25).[102] The Cu^{2+}-complexes of these ligands were then tested together with salmon testes or calf thymus DNA. The results obtained with these catalysts depended strongly on the nature of the metal binding site as well as the length of the linker. With some catalysts good enantioselectivities were achieved. Since the ligands themselves were not able to discriminate enantiomers, Feringa reasoned that observed enantioselectivities were caused by the chirality of the right handed helical structure of DNA. The fact that enantioselectivity increased with decreasing length of linker supported this view. Best results were obtained with a linker length of n = 2.

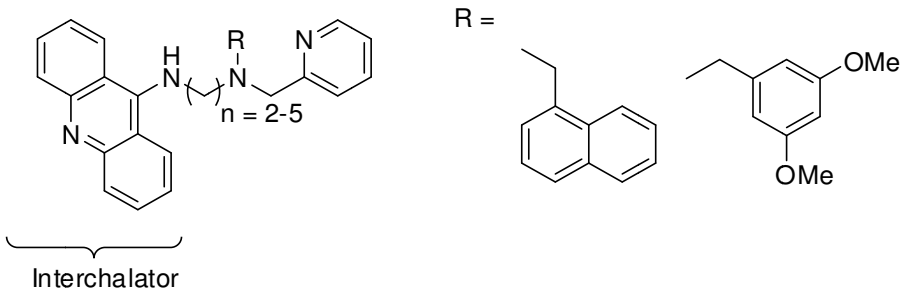

Fig. 25: First Generation Ligands for the DNA-Supported Catalysis.

Even better enantioselectivities were accomplished with the second ligand generation (Fig. 26).[103] The linker entity in these ligands was avoided by directly combining the metal binding site with the interchalating unit. The corresponding Cu^{2+} complexes together with salmon testes DNA gave rise to enantioselectivities of up to >99% in Diels Alder reactions. Best results were obtained with the Cu^{2+} complex of 4,4'-dimethyl-2,2'-bipyridine (dmbipy). Not for all ligands the actual binding mode to DNA is known. Besides intercalation also groove binding or a combination of both is possible. However in the test reactions it became apparent, that moderate DNA-binding strength was advantageous. Possibly, the extra flexibility improves the interactions between catalyst and substrate.

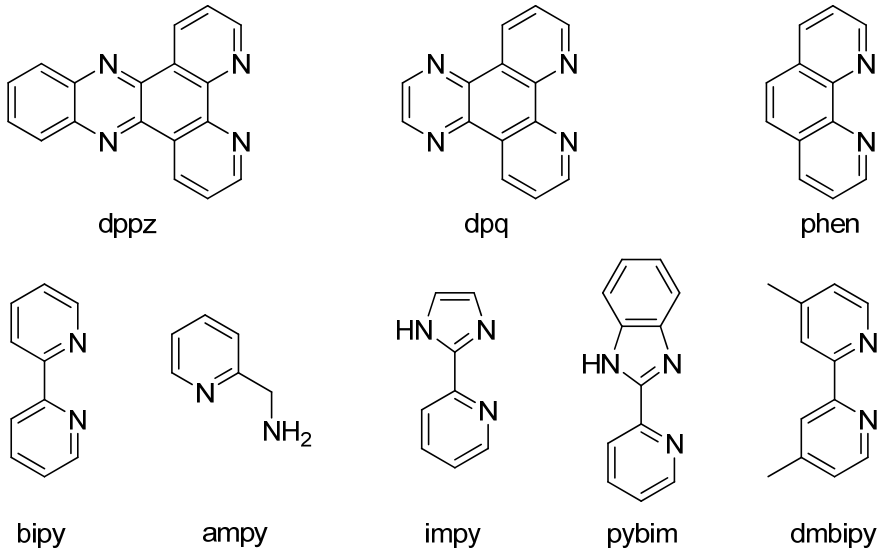

Fig. 26: Second Generation Ligands for the DNA-Supported Catalysis.
dppz: dipyrido-[3,2-a:2',3'-c]-phenazine; dpq: dipyrido [3,2-d:2',3'-f] quinoxaline; phen: 1,10-phenanthroline; bipy: 2,2'-bipyridyl, ampy: 2-aminomethyl-pyridine, impy: 2-(2-pyridyl)imidazole, pybim: 2-(2-pyridyl)benzimidazole; dmbipy,: 4,4'-(bismethyl)-2,2'-bipyridyl.

Kinetic studies of the Diels Alder reactions revealed that the DNA not only has the function of a chiral scaffold but also has a rate accelerating effect on the reaction.[104] The magnitude of the rate acceleration as well as the enantioselectivity seems to be dependent on the base sequence of the DNA. These results imply that instead of the overall helical structure rather the microenvironment of the catalytic site is essential for the outcome of the catalysis. The helical structure is however needed to give the catalyst its necessary rigidity.

The second generation of ligands also proved to be very effective in the DNA-supported catalysis of other reactions. One example is the catalytic Michael addition in water (Scheme 10).[105] In this reaction α,β-unsaturated 2-acylimidazole was used as Michael acceptor and nitromethan or dimethylmalonate as the nucleophile. Again high enantioselectivities of up to 99% ee were obtained. Another example for is the enantioselective C-F bond formation (Scheme 11).[106] Here the catalyst was used to perform the electrophoretic fluorination reactions of β-ketoesters with Selectfluor® as fluorine source. The enantioselectivity of these reactions was however moderate. A maximum of 74% ee was achieved. Just recently also the enantioselective Friedel-Crafts reaction was added to the scope of DNA-supported catalysts.[107] The use of water as solvent makes this reaction interesting, because traditionally it is carried out under anhydrous conditions. Especially

the asymmetric Friedel-Crafts reaction so far only tolerated small quantities of water. By using DNA-supported catalysts however selectivities of up to 93% ee were obtained (Scheme 12).

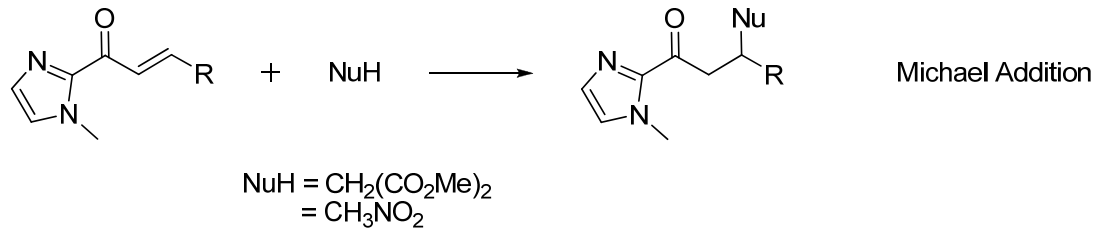

Scheme 10: Michael Addition.

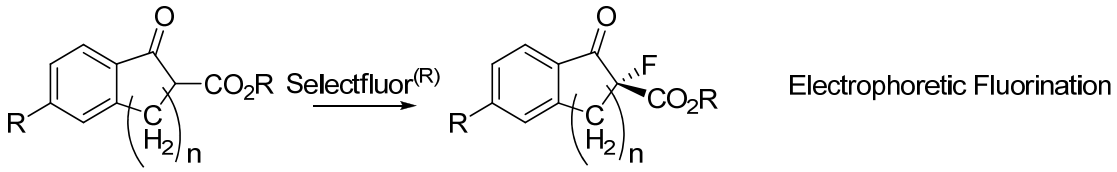

Scheme 11: Electrophoretic Fluorination.

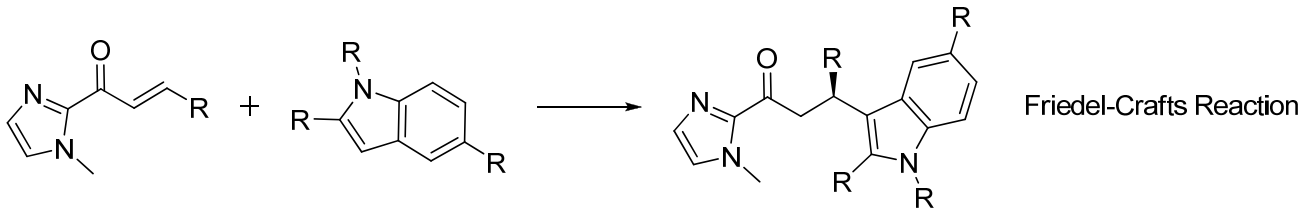

Scheme 12: Friedel-Crafts Reaction.

Until now it is not known whether the catalytic mechanism is the same for all these reactions. It is also not evident whether the quite different substrates in all these reactions favor the same microenvironment to coordinate to DNA. Contradicting this notion is the fact that Diels-Alder reactions, Michael additions, Friedel-Crafts reactions and electrophilic fluorination reactions involve structurally very different transition states. In the absence of kinetic studies for all reactions except Diels-Alder one can only guess. In order to gain a better understanding in the process involved with DNA supported catalysis further studies are needed.

One problem keeping us from gaining a better insight view into the mechanism of DNA-supported catalysis is the method by which the ligands interact with the DNA. From a combinatorial perspective the usage of DNA intercalators as ligands is a wonderful tactic. It makes screening many different ligands fairly easy and in this case ultimately led to remarkable enantioselectivities. The drawback is that no defined catalytic species is generated in this process. Furthermore it is rather probable that many different catalytic species are formed and present during the synthesis, since these ligands can be incorporated randomly into DNA. A well defined catalyst is therefore essential in order to gain a better understanding of DNA-supported catalysis.

5. 2nd Objective of this Thesis

Intrigued by the recent advances in DNA-supported catalysis the intention of this thesis was also the establishment of a new straight forward approach towards DNA-supported catalysis that would allow further investigations of the catalytic mechanism.

A promising way to achieve the outlined goal is the covalent attachment of ligands to double-stranded DNA. This would not only make it possible to pinpoint the location of the catalytic site within DNA, it should also be feasible to identify the local chiral environment of the catalysts or even to change it at will.

In this thesis we therefore focused on two strategies to attach ligands on synthetic DNA. Both plans involved modifying the nucleobase position in a double-stranded DNA, forcing the catalytic center deep inside the DNA double helix. The first route was to completely replace a nucleobase with a bidentate ligand, the second to attach bidentate ligands to existing nucleobases.

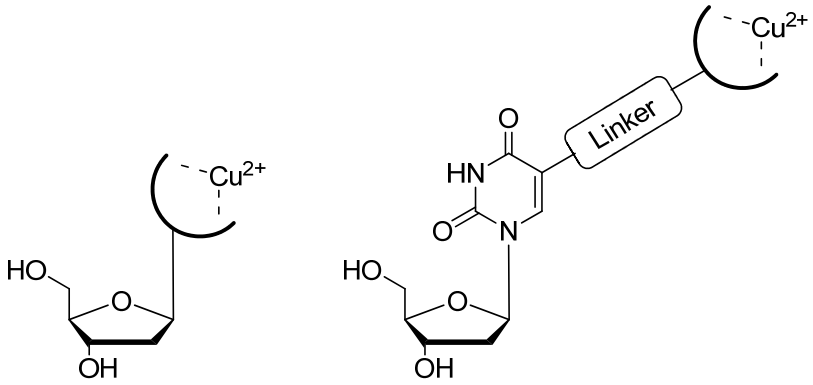

Fig. 27: Possible Binding-Sites for Positioning Bidentate Ligands in the Major Groove of DNA.

The initial step therefore was the synthesis of artificial nucleosides with the desired properties mentioned above. After thorough testing, these nucleosides then had to be transformed into the corresponding phosphoramidites. Their compatibility with state of the art automated DNA synthesis had to be investigated and synthetic DNA strands including these modifications had to be synthesized. Finally the application of the modified oligonucleotides as support for catalysts had to be evaluated.

II. Results and Discussion

1. A New FRET-Based Assay for the Detection of NF-κB

1.1. Introduction

A well researched class of transcription factors is the family of nuclear factor κB (NF-κB). NF-κB is a dimeric protein, which can be composed out of five different monomers, known to exist in mammals: Rel (also known as c-Rel), p65 (also known as RelA or NF-κB3), RelB, p50 (also known as NF-κB1) and p52 (also known as NF-κB2).[108] The most common one is the p50/p65 heterodimer. Usually NF-κB heterodimers are retained in the cytoplasma of resting cells by specific inhibitors, the IκBs.[109] These inhibitors prevent the transport of the protein into the nucleus and thereby DNA binding. Cleavage of the inhibitor IκB from NF-κB results in the activation of the dimers. This process is started by the stimulation of cells with inflammatory messengers like the cytokines TNF-α, IL-1β, viral or bacterial pathogens, which results in the release of the specific IκB kinase IKK. IKK promotes the phosphorylation-induced ubiquitination of IκB proteins. Thus marked IκB is then degraded by the 26S proteasome.[110] The now liberated NF-κB dimers are transported from the cytoplasma to the nucleus (Fig. 28), where they bind to specific DNA sequences with a 5'-GGRNYYYCC-3' motif (*R* can be any purine, *Y* any pyrimidine and *N* any nucleobase).[111]

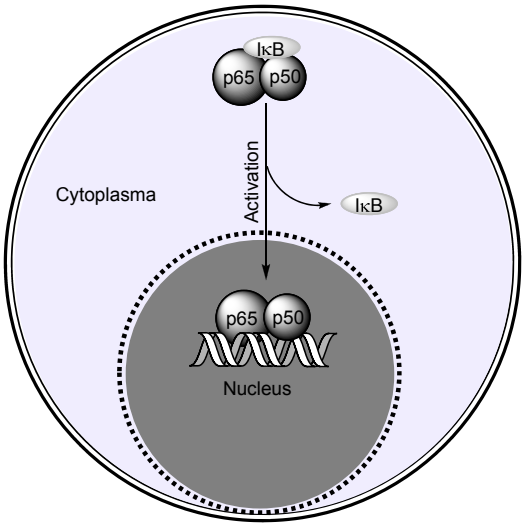

Fig. 28: Transfer of Activated NF-κB from Cell Cytoplasma into the Nucleus.
IκB: Inhibitor of NF-κB, p65/p50: NF-κB heterodimer.

NF-κB participates in transcription of more than 300 genes, including those encoding cytokines, adhesion molecules, acute phase proteins, regulators of apoptosis and inducible effector enzymes.[112] It is imminent, that NF-κB plays an essential role in the innate and adaptive human immune system. Hence, an abnormal activation or regulation of this protein leads to various diseases including those, related to inflammation and enhanced cellular proliferation.[112-116]

Therefore NF-κB has become a primary target for the pharmaceutical industry.[117-121] High expectations are put into future drugs which target NF-κB activation. A very promising approach is the inhibition of IKK, ultimately preventing the cleavage of IκB.[109, 122] A unsolved challenge however remains the target-selective inhibition of the transcription factor. An overall inhibition

would inevitably cause severe side effects, because of NF-κB's pivotal role in so many biological processes.[123] There are good reasons to believe that the key to the solution of this problem lies in the complexity of NF-κB's activation process. Prerequisite is of course a detailed understanding of the functions and mechanisms of NF-κB. Hence there is a need for robust techniques allowing for the rapid, cheap and quantitative detection of NF-κB DNA-binding activities.

The most common way to detect DNA binding proteins is by gel shift assays[124, 125] or DNA footprint assays.[126, 127] Both methodologies rely on a size based separation of DNA sequences in electrophoretic gels. These assays are very sensitive, but rather time consuming. Furthermore, quantifications are difficult and radioactive material is needed.

Another assay is the commercially available TransAM™ kit by Active Motif: It is based upon ELISA, the enzyme-linked immunosorbent assay. This procedure does not need radioactive labels; instead it utilizes specific antibodies to which enzymes are coupled. These enzymes catalyze a color reaction, which is then detected. The downside to this method is its high price accounted to the expensive antibodies. A similar DNA binding assay based upon a modified ELISA was established by Renard *et al*. It was used to study the NF-κB-dependent gene expression using either luciferase or β-galactosidase as reporters.[128, 129]

A new approach to the detection of transcription factors, based on an exonuclease III protection assay combined with a FRET system, was recently published by Jinke Wang *et al*.[37, 130-133] Successful binding of the protein to DNA protects the oligonucleotide from digestion by the exonuclease ExoIII. The FRET system on the DNA remains intact. In absence of a DNA binding protein, the oligonucleotide however will be cleaved by the exonuclease, thereby destroying the FRET system. In a similar assay the activated NF-κB was detected by FRET following the digestion by a restriction endonuclease.[134] The potential of these FRET assays lies in their compatibility with high-throughput screening techniques. However, their success is limited by the stability of the DNA-protein complex, which have a short half life time, as well as by the need for specific restriction enzymes.

A sensitive assay, based solely on interactions between DNA and protein without the necessity for other additives is therefore desirable.

1.2. Strategy

Double helical DNA not only has the ability to undergo sequence specific interactions with proteins; its major groove is also known to bind to short single stranded oligonucleotides, thereby forming a triple helix.[135] Especially homopyrimidine sequences are prone to do this, as they can undergo Hoogsteen pairing (Fig. 29).

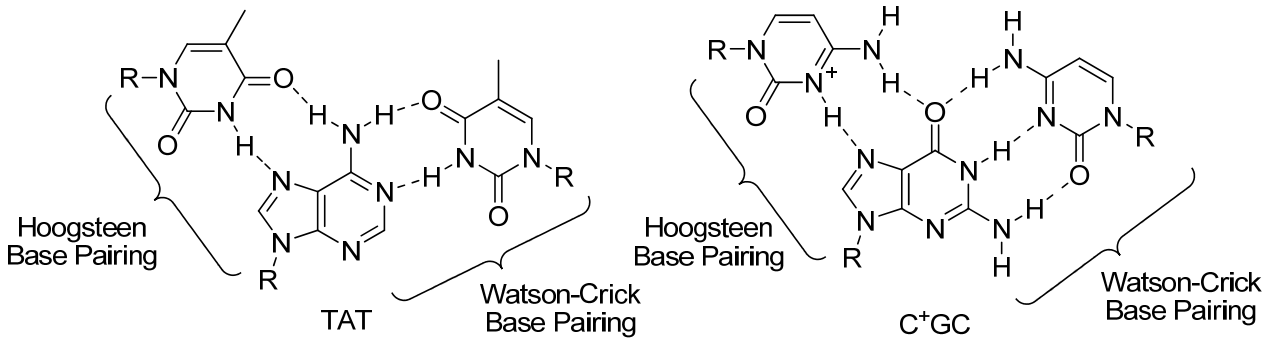

Fig. 29: Hoogsteen Base Triade TAT and C^+GC.

DNA duplexes which incorporated both properties, the binding of proteins and of short oligonucleotide sequences, were established by us in the past (Fig. 30).[136] The most successful one was backfolding DNA **2**. Its sequence was derived from parts of the iNOS mouse gene and comprised two specific binding motifs: One for the transcription factor NF-κb and the other one for a 14mere homopyrimidine oligonucleotide.

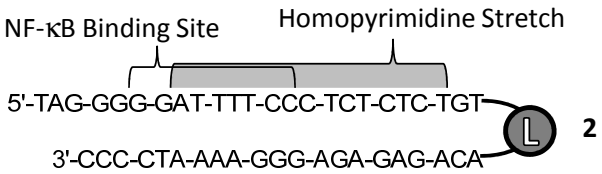

Fig. 30: Backfolding DNA Duplex with Overlapping Bindings Sites for NF-κB and a 14mer Homopyrimidine Oligonucleotide.
L: Hexaethylene glycol linker.

Both features had been intensively evaluated: The affinity of NF-κB towards this double helix had been proven in electrophoretic mobility shift assays (EMSA) and the binding of short oligonucleotides via Hoogsteen pairing had been demonstrated by recording the corresponding melting curves (Thermal Hybridization Studies on page 137). An interesting aspect of this molecule is the overlap of both binding site, which prevents the simultaneous coupling of the two molecules to the DNA.

In the work at hand we envisaged an assay for the detection of the heterodimer NF-κB which exploits this feature. Its principle, as depicted in Scheme 13, is based on FRET. A backfolding DNA sequence containing the double-stranded binding site for NF-κB and the homopyrimidine sequence for the triple helix formation is equipped with a FRET donor, whereas the third oligonucleotide involved in Hoogsteen pairing to said backfolding DNA carries a FRET acceptor. In this triple helical arrangement, donor and acceptor chromophores are in close proximity which should yield in an

intense FRET. Binding of NF-κB will replace the third oligonucleotide strand resulting in a decreased FRET.

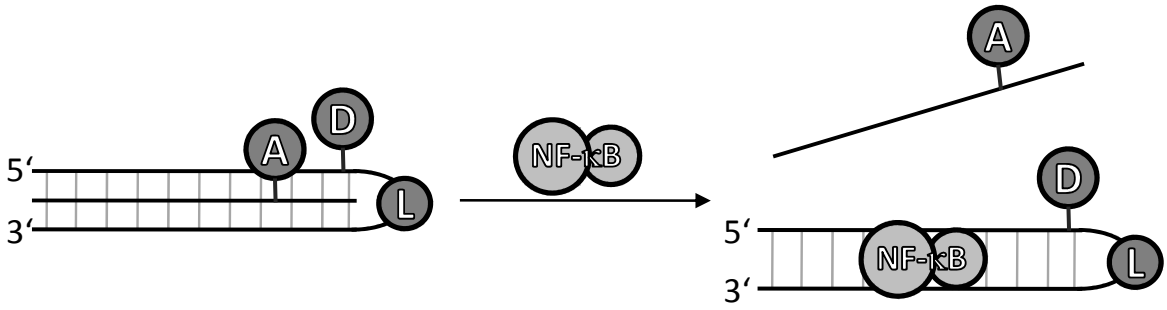

Scheme 13: Principle of FRET-Based Assay for NF-κB.

D: FRET-donor, A: FRET-acceptor, L: Hexaethylene glycol spacer, NF-κB: p65/p50 heterodimer.

1.3. FRET Dyes

A suitable FRET donor and acceptor pair that is well established in a our group is the carbostyril derivative **3** and the Ru(II)-bathophenanthroline complex **4** (Fig. 32).[58] FRET systems consisting of both dyes were successfully implemented in peptides as well as in DNA.[65, 137] Both dyes exhibit excellent thermodynamic stability and chemical inertness. Their spectral properties make them an almost perfect FRET match (Fig. 31). The donor **3** has a strong absorption maximum at 368 nm. Its emission maximum at 435 nm overlaps well with the MLCT absorption band of the Ru(II)-complex **4** at 400-500 nm. The strong red emission of the acceptor **4** can be observed at 618 nm. A very important property of the Ru(II)-complex **4** is its absorption minimum at the excitation wavelength of the donor **3**. This minimizes the probability of exciting the acceptor **4** directly during the excitation of the donor **3**.

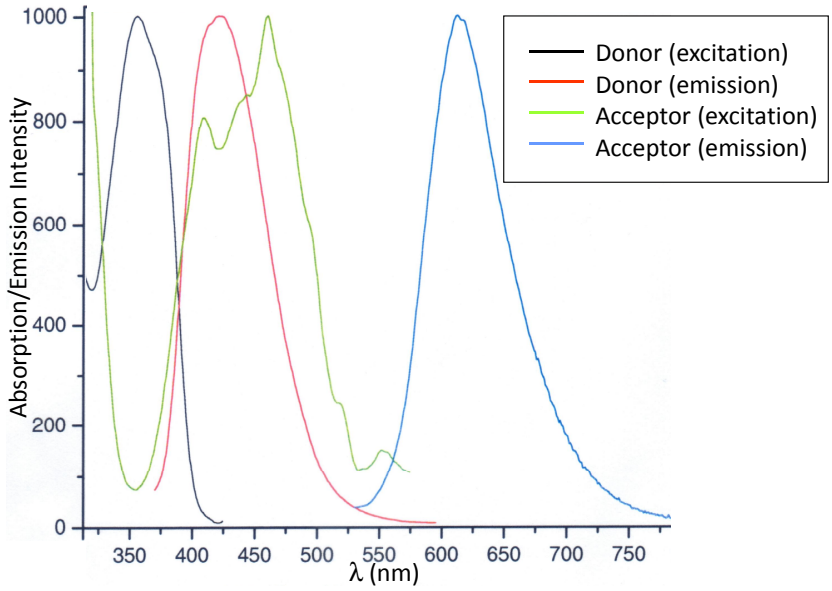

Fig. 31: Absorption and Emission Spectra of Donor 3 and Acceptor 4.

Both, donor **3** and acceptor **4** are equipped with a carboxyl group at the end of a long alkyl/aryl linker chain. This carboxyl functionality is used for the covalent attachment via amide bonds to target molecules bearing an amino group. The long chain between the target molecule and the chromophore allows the chromophore to maintain a certain degree of rotational freedom.

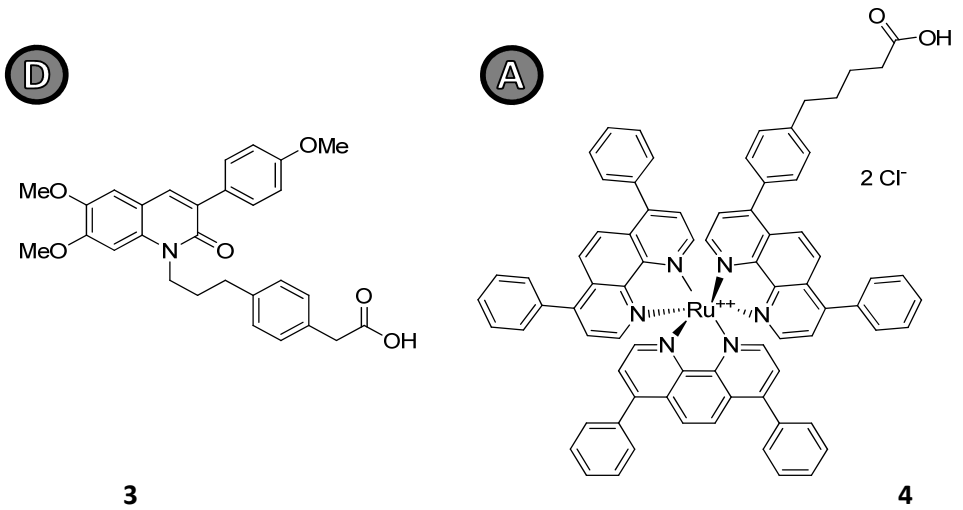

3 **4**

Fig. 32: Envisaged Dyes of the FRET System.

The synthesis of the donor chromophore was performed by Dr. Lilia Clima following previously published protocols.[138] For the sake of completeness the synthesis routes for both dyes will be discussed shortly in the following two chapters.

a. Synthesis of Donor 3

In the first step of the synthesis route (Scheme 14) the two commercially available compounds 3,4-dimethoxybenzamine (**6**) and 2-(4-methoxyphenyl)acetic acid (**7**) were coupled in the presence of the activation reagent TBTU.[139] The resulting amide **5** was exposed to Vilsmeier Haack conditions ($POCl_3$, DMF) upon which it cyclized quantitatively to the quinoline **8**.[140] Hydrolysis under acidic conditions completed the chromophor unit **9**, to which a linker chain bearing a carboxy function was added in three further steps. The *N*-allylation of compound **9** afforded compound **10** in 83% yield. This reaction was performed under microwave radiation at 120°C and 200 W in just 15 minutes.[141] In the next step the carboxy group was introduced via a Heck coupling of **10** with 4-bromophenylacetic acid. The Heck coupling proceeded smoothly with almost quantitative yield. In order to obtain highest flexibility the double bond of the linker chain was reduced by H_2 over palladium on charcoal. This resulted in the desired donor molecule **3**. For the coupling to DNA the carboxylic acid was activated with TSTU in the final step.

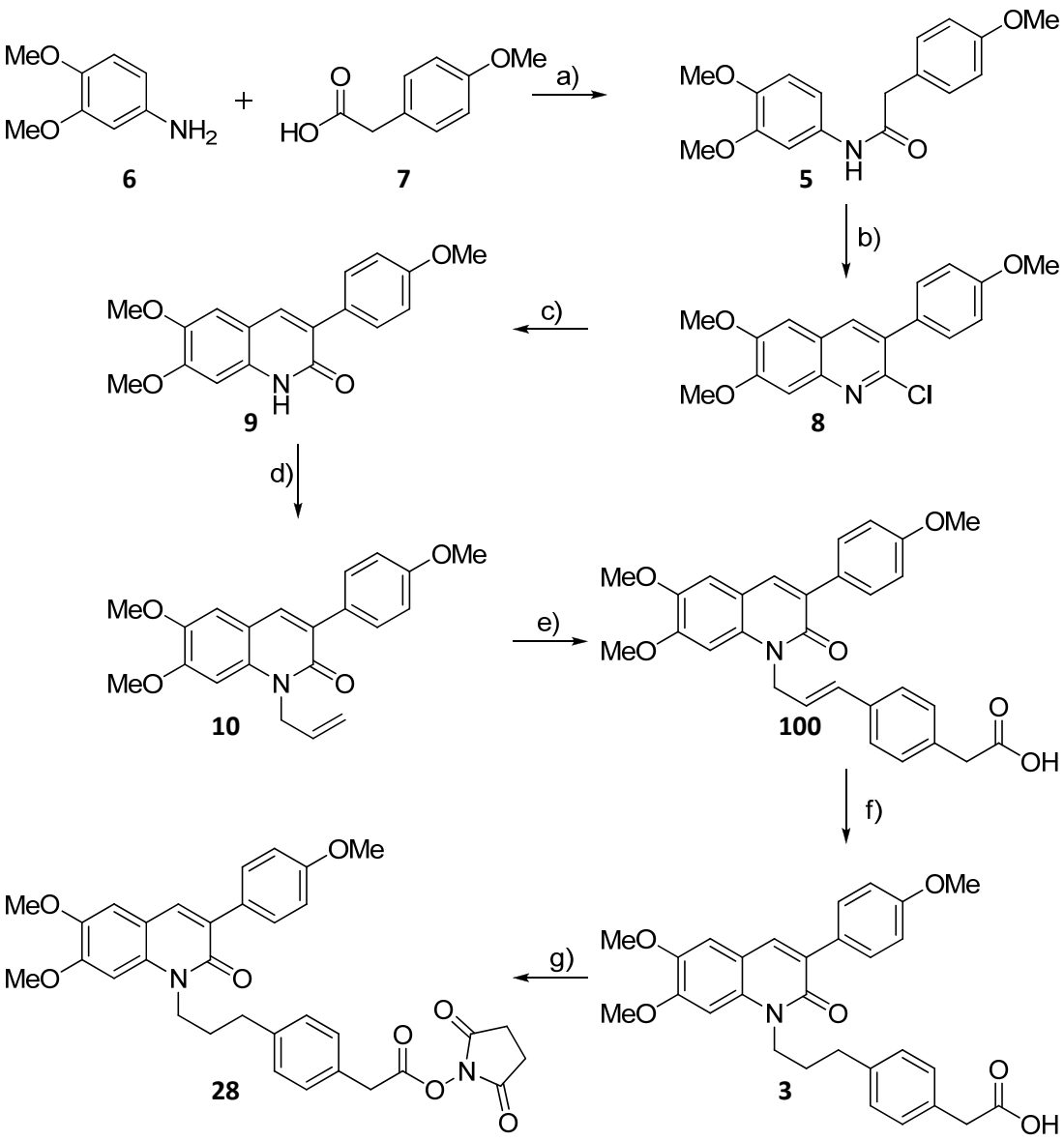

Scheme 14: Synthesis Route for the Donor.

a) TBTU (1.2 equiv.), DIPEA (2.4 equiv.), rt, over night, 83%*; b) (i) 0°C, $POCl_3$ (3.5 equiv.), DMF (3.5 equiv.), rt, 90 min; (ii) 0°C, **5** in toluene, rt, 30 min; (iii) reflux, 4 h, quant; c) AcOH/H_2O, reflux, 20 h., 80%*; d) (i) –78°C, KHMDS (1.2 equiv.) in toluene, 1.5 h, rt, 30 min; (ii) allylbromide (3 equiv.), microwave (200 W) 120°C, 15 min, 85%*; e) 4-bromophenylacetic acid (1.5 equiv.), 5 mol%* $Pd(OAc)_2$, 15 mol%* PPh_3, Cs_2CO_3 (3 equiv.), H_2O, DMF, 90°C, 21 h, 99%*; f) H_2 (1 atm.), 10 mol%* Pd/C, CH_2Cl_2/MeOH (1.5:1), over night, quant; g) TSTU (1.5 equiv.), DIPEA (2.7 equiv.), DMF, 93%*. *Synthesis was carried out by Dr. Lilia Clima.[141]

b. Synthesis of Acceptor 4

For the synthesis of the Ru(II)-bathophenanthroline complex **4** a bathophenanthroline ligand bearing a linker chain with a carboxy function had to be prepared (Scheme 15).[142, 143] The key steps in this synthesis route were two Skraup reactions. The first one proceeded between 2-nitroaniline (**11**) and β-chloropropiophenone (**12**), yielding the aromatic quinoline **13**. The nitro group was then reduced with H_2 over palladium on charcoal to the corresponding amine **14**. This compound underwent the second Skraup reaction with the Friedel-Crafts product **15**, which was obtained from phenylvalerianic acid (**16**) after esterification with methanol. The second Skraup reaction

resulted in a mixture of the methylester **17** and the free carboxylic acid **18**. However since the carboxylic acid **18** was the desired product the crude mixture could be saponified to complete the conversion.

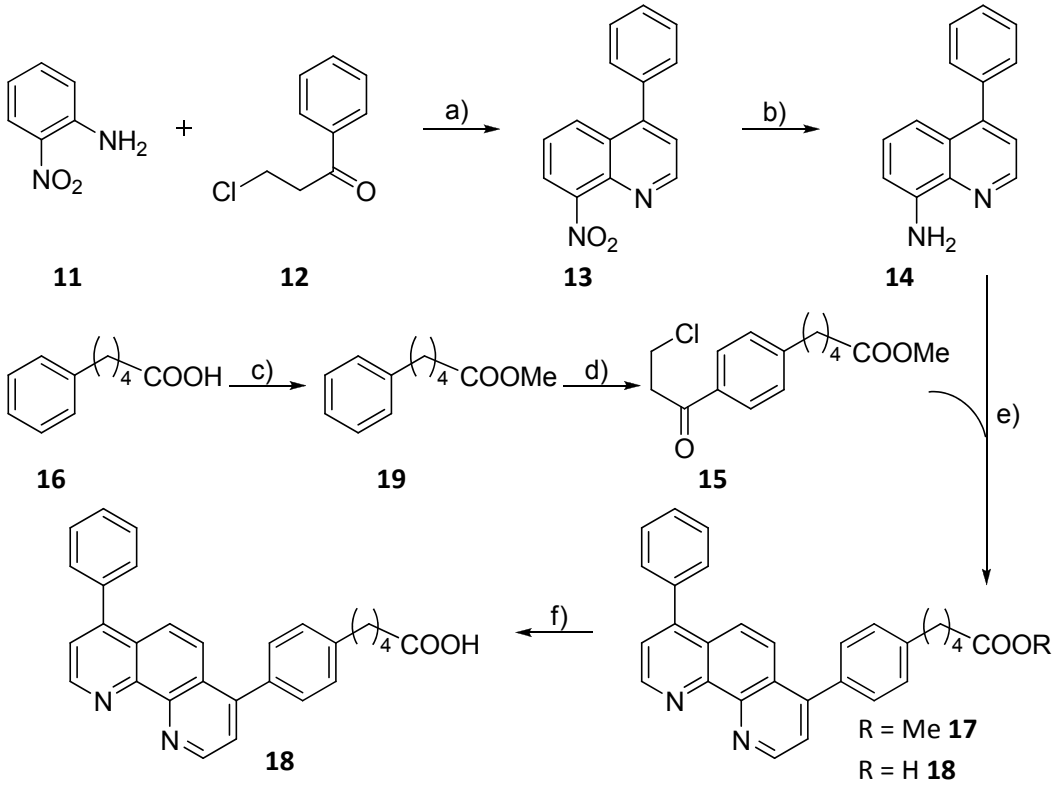

Scheme 15: Synthesis Route for Bathophenanthroline Ligand 18 with Attached Carboxyl Function.

a) (i) **11**, H_3PO_4 (85%*), $As_2O_5{\cdot}(H_2O)$ (1.2 equiv.), 100°C; (ii) **12** (1.4 equiv.), 130°C, 2h, 80%*. b) H_2 (1 atm.), 10 mol% Pd/C, MeOH/toluene, 95%*. c) MeOH, conc. H_2SO_4, reflux, 2 h, 93%*. d) (i) 3-chloropropionyl chloride (1.1 equiv.), $AlCl_3$, CH_2Cl_2, 0°C; (ii) **19**, rt, 1 h, quant. e) (i) **14**, H_3PO_4 (85%*), $As_2O_5{\cdot}(H_2O)$ (1.2 equiv.) 110°C; (ii) **15** (1.4 equiv.), 130°C, 1.5 h; f) NaOH, EtOH/H_2O, 68%* (over 2 steps). *Synthesis was carried out by Dr. Lilia Clima.[141]

The Ru(II)-complex **4** was then synthesized in two further steps (Scheme 16).[144] In the first step $RuCl_3$ (**20**) was refluxed in the presence of two equivalents of 4,7-diphenyl-1,10-phenanthroline (dpp). Although the ligand was added stoichiometrically the formation of $Ru(II)(dpp)_3$ was still favored. To prevent the coordination of a third dpp-ligand in the coordinationsphere of Ru(II) an excess of LiCl was added to the reaction. This increased the concentration of Cl^- as alternative ligand and made it possible to afford the desired $Ru(II)(dpp)_2Cl_2$ (**21**) in 42% yield. The complexation of ligand **18** was achieved in a protic solvent mixture of MeOH and H_2O resulting in the desired acceptor molecule **4**. In the final step the carboxyl group was activated with TSTU for the coupling of the acceptor **22** to DNA.

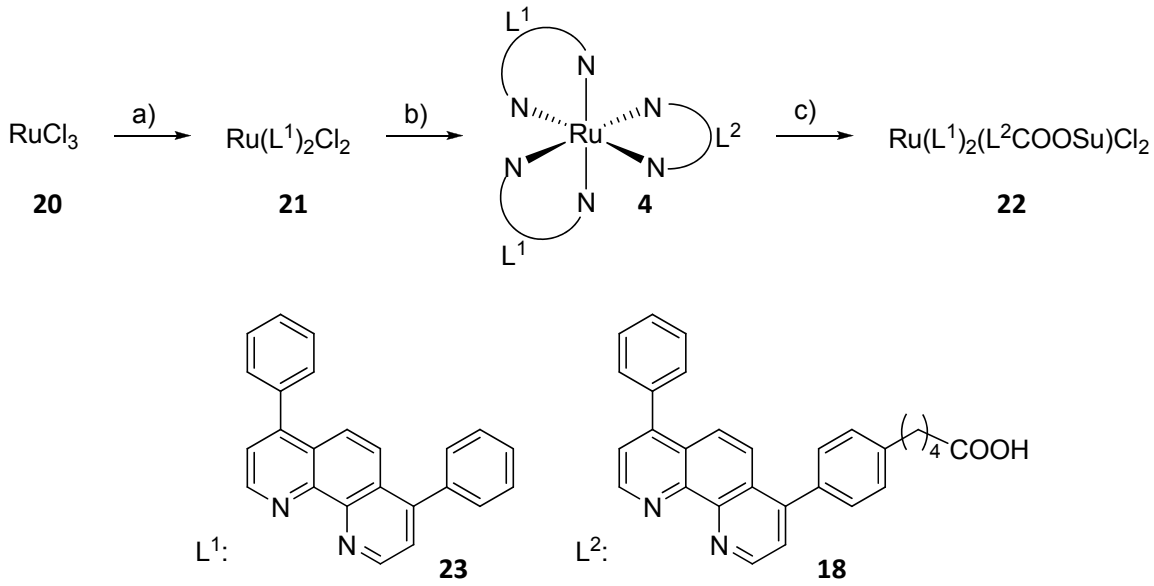

Scheme 16: Synthesis Route for Acceptor 22.

a) **23** (2.0 equiv.), LiCl (10 equiv.), DMF, 160°C, 4.5 h, 42%*. b) **18** (1.5 equiv.) H_2O/MeOH, reflux, 3h, 95%*. c) TSTU (1.5 equiv.), DIPEA (2.7 equiv.), DMF, rt, 3.5 h, 84%*. Synthesis was carried out by Dr. Lilia Clima.[141]

1.4. Synthesis of Artificial DNA Building Blocks

The outlined triple helix system included three unique positions which are not common in natural oligonucleotides. These positions are the two binding sites for the FRET chromophores and the linker unit which interlinks the two complementary strands. For the introduction of these special sites into our oligonucleotides several non-natural DNA building blocks had to be synthesized.

a. Hexaethylene Glycol Linker 1

The stability of short double-stranded oligonucleotides can be increased by fusing the two complementary strands to each other. For this purpose hexaethylene glycol has proven to be the ideal linker molecule.[24] Its length allows for a perfect backfolding of the complementary strands so that the two nucleosides adjacent to hexaethylene glycol can undergo base pairing. Due to the high solubility of hexaethylene glycol in water the natural properties of DNA are not affected by its introduction. In order to use hexaethylene glycol in DNA synthesis, it has to be converted into a suitable building block.[145] Therefore the two hydroxyl functions at opposit ends of the molecules have to be discriminated. One of them has to resemble the 5'-end the other the 3'-end of a nucleoside. Consequently, the pseudo 5'-hydroxyl has to be protected with a trityl-group, whereas the 3'-hydroxyl group has to be transferred into the phosphoramidite.

Such a building block (**1**) is compatible with current DNA synthesis protocols and can be inserted during the oligonucleotide synthesis.

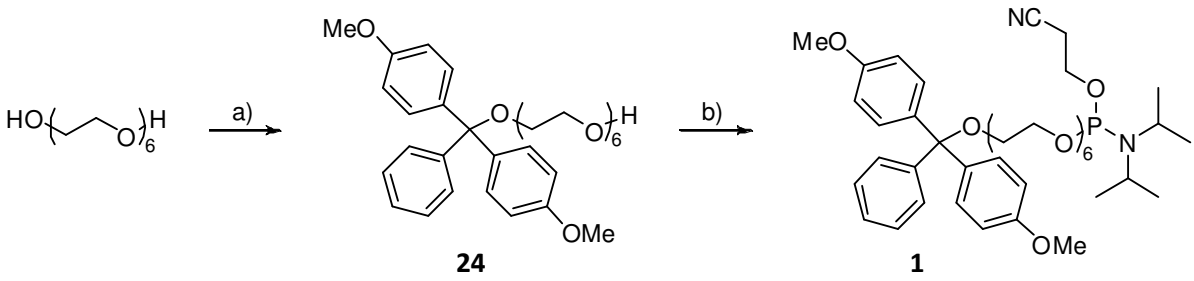

Scheme 17: Synthesis of the HEG-Phosphoramidite.

a) DMT-Cl (0.2 equiv.), pyridine, rt, over night, 41%; b) CH_2Cl_2, diisopropylammonium tetrazolide (0.75 equiv.), $(i\text{-}Pr_2N)_2\text{-}POCH_2CH_2CN$, (2.2 equiv.), rt, 18 h, 92%.

The first step towards building block **1** was the selective mono tritylation of hexaethylene glycol. The reagent of choice for this reaction was dimethoxy-trityl chloride (DMT-Cl). DMT-Cl is highly reactive and easily hydrolyzed: the hydrolyzed product is easily dtectable by its red color. To prevent the hydrolysis of the DMT-chloride, the reaction itself had to be run under anhydrous conditions. Hexaethylene glycol, which is highly hygroscopic, therefore had to be dried thoroughly prior to the reaction with DMT-Cl. An efficient method to remove traces of water is the azeotropic coevaporation. For this the compound is dissolved in a solvent like pyridine or acetonitrile, which is known to form an azeotropic mixture with water. The water is then coevaporated together with the solvent. By repeating this step several times the anhydrous compound is obtained. In our case pyridine was chosen for the azeotropic coevaporation since it was also the solvent for the reaction. During the process of drying, it was beneficial to use a special adapter, which facilitated the exclusion of air and humidity while working with a rotary evaporator (Fig. 33).[146]

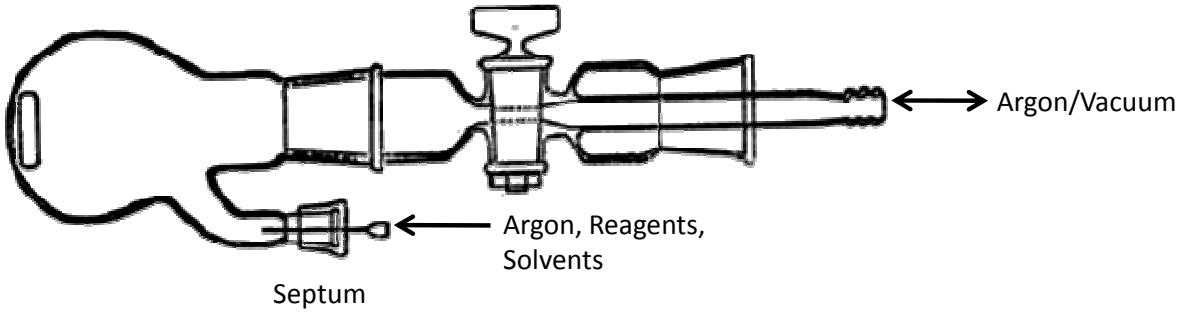

Fig. 33: Adapter for the Evaporation of Solvents under Absolute Conditions.

In order to circumvent bis-tritylation of the diole a 5-fold excess of hexaethylene glycol was used for the reaction. The desired compound **24** was then obtained in 40% yield. Unreacted hexaethylene glycol was re-isolated after column chromatography.

For the phosphorylation of the remaining hydroxyl function in the second step of the synthesis (2-cyanoethoxy)-bis-(*N,N*-diisopropylamino)phosphine (**25**) was used. This reagent was favored over the more reactive chloro(2-cyanoethoxy)-(*N,N*-diisopropylamino)phosphine (**26**) since it is easier to store and also led to excellent yields.[147-149] Its synthesis starting from PCl_3 is shown in Scheme 18.[150-152]

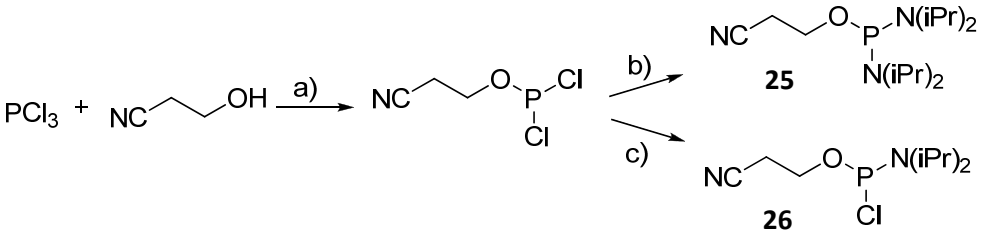

Scheme 18: Synthesis Route for the Phosphinylation Agents 25 and 26 via Dichloro(2-cyanoethoxy)phosphine.
a) , b) HN(*i*-Pr)$_2$ (9 equiv.), ether, –10°C, 1 h.; c) HN(*i*-Pr)$_2$ (2 equiv.), ether, –20°C, 1.5 h.

The phosphorylation of the DMT protected hexaethylene glycol **24** was performed at room temperature. The phosphine was activated with diisopropylammonium tetrazolide **27**. Tetrazolide can in one step be transferred into the better activation agent diisopropylammonium terazolide (Scheme 19).[153] In the activation process one of the two diisopropylammonium groups attached to the phosphorus gets replaced by the terazole. Since the activated phosphorus is prone to be attacked by water, which would reduce the yield drastically, all compounds were dried thoroughly by azeotropic coevaportion with acetonitrile prior to the reaction. Besides working under anhydrous conditions, this reaction also had to be performed under an argon atmosphere to prevent the oxidation of the P(III) to P(V). The obtained phosphoramidite **1** however was less sensitive towards oxidation and therefore could be purified by standard techniques without the need for a protecting gas atmosphere. Nevertheless it was advantageous to use degassed solvents and to work fast. The purified phosphoramidite **1** was stored under argon at –20°C. A reliable method to determine the oxidation stage of the phosphorus is the ^{31}P-NMR spectroscopy. The desired P(III) species produces a characteristic signal in the range of 145 ppm. The signal of the oxidized P(V) species compared to that is shifted to the high-field and is detected at approximately 140 ppm.

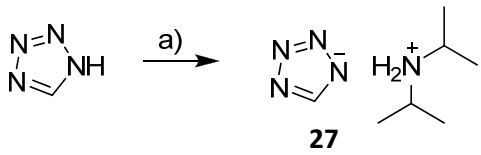

Scheme 19: Synthesis of 27.
a) (i) CH_3CN, 0°C, HN(*i*-Pr)$_2$ (1.8 equiv.); (ii) rt, 1h.

b. Building Blocks for Oligonucleotide Labeling

Both FRET dyes (**28**, **22**) were equipped with activated acid functions in order to couple them to target molecules bearing amino groups via amide bond formation. In our case the target molecules were the oligonucleotides composing the envisaged triple helix. Depending on the position of the amino modification within these sequences different building blocks were considered. For modifying the 3'-end of oligonucleotides the commercially available Amino-ON CPG can be used. A building block for the introduction of amino functionalities at the 5'-end of an oligonucleotide is the 5'-amino-5'-deoxythymidine. For all other locations in between both ends of the oligonucleotide the C5-modified pyrimidine nucleosides are particularly suitable.

Amino-ON CPG

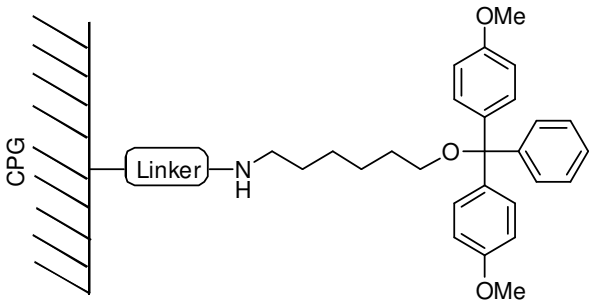

Fig. 34: Amino-ON CPG.

Amino-On CPG is a commercially available building block for modifying synthetic oligonucleotides with amino functionalities at the 3'-end. Its structure, a hexylamino group attached to a CPG solid phase, is depicted in Fig. 34. With an O-DMT group at its end Amino-On CPG can be used similarly to the standard CPG-coupled nucleosides. The DMT group is cleaved in the first step of the synthesis cycle. The free amine is liberated after the synthesis of the oligonucleotide during the cleavage and deprotection step. The aminohexyl-group remains attached to the oligonucleotide. The advantage of this building block is that no changes to the DNA synthesis protocol have to be made. The only difference is that the first 3'-nucleoside is not coupled to CPG itself but must be introduced as phosphoramidite in the first cycle.

5'-Amino-5'-deoxythymidine 29

A common building block for modifying the 5'-end of oligonucleotides with amino functionalities is the 5'-amino-5'-deoxythymidine **29**.[154] It is incorporated in the last cycle of the oligonucleotide synthesis. Starting from thymidine (**30**) this building block was synthesized in just a few steps (Scheme 20). Two different routes to transform the hydroxyl into the amino group are possible.[154, 155] In the first route thymidine (**30**) was transformed into the 5'-azido-5'-deoxythymidine (**31**) and thereafter reduced to the amine **29**. The second method used Mitsunobu conditions to regio-selectively introduce tetrachlorophthalimide (TCP) at the 5'-position of **32**. The TCP was then cleaved with ethylenediamine to yield the desired amino group. The protection of the newly created amino group was achieved simultaneously during cleavage of TCP, while the first synthesis route needed an additional step for protection. In both cases the standard DMT protecting group could not be used because of stability reasons. The stability issue arises due to the higher basicity of the amino group compared to the hydroxyl group, which weakens the bond towards the trityl group.[156] Instead of DMT the more stable monomethoxy trityl group (MMT) was used. The conditions necessary for the cleavage of the group are the same conditions as for the DMT group. It should be noted however, that the color of the MMT cation is pale yellow compared to the intensive orange color of the DMT cation. Especially in automated synthesis this difference causes problems with correctly estimating the coupling efficiency via trityl monitor. In the last step the MMT protected nucleoside **33** was converted into the corresponding phosphoramidite **34**.

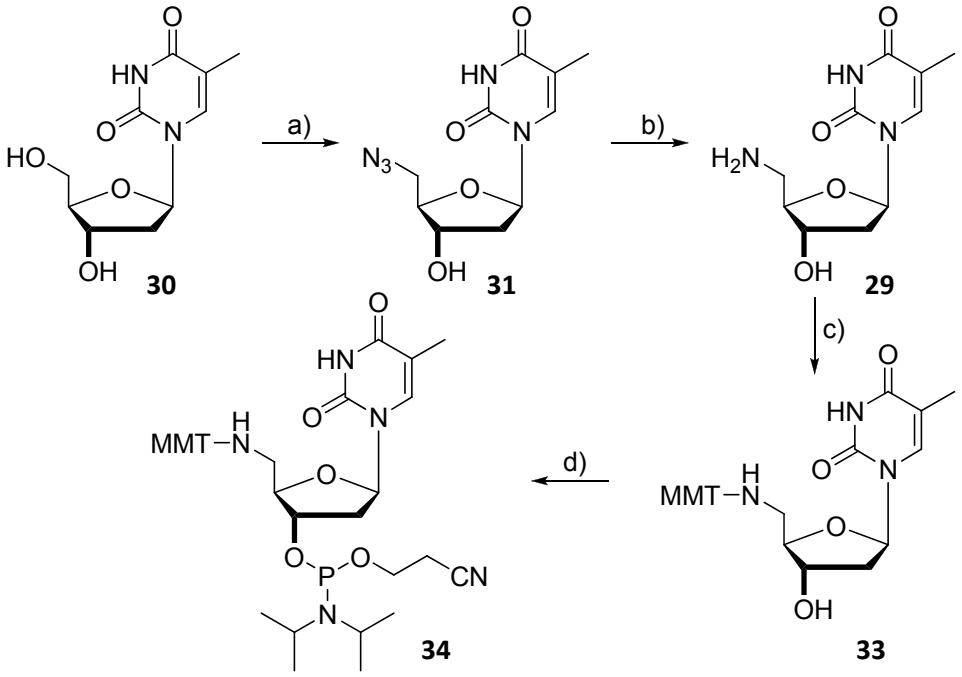

Scheme 20: Synthesis Route for 5'-Amino-5'-deoxythymidine-Phosphoramdite 34.

a) DMF, PPh_3 (1.0 equiv.), NaN_3 (4.7 equiv.), CBr_4 (1.0 equiv.), rt, over night, 77%*; b) H_2 (1 atm.), 10 mol%* Pd/C, EtOH, over night, 92%*; c) MMT-Cl (2.4 equiv.), DMAP (0.5 equiv.), NEt_3 (0.5 equiv.), pyridine, rt, 2 h, 95%*; d) diisopropylammonium tetrazolide (0.5 equiv.), $(i\text{-}Pr_2N)_2\text{-}POCH_2CH_2CN$, (3.0 equiv.), CH_2Cl_2, rt, 2.5 h, 90%*. *Synthesized by Dr. Lilia Clima.[141]

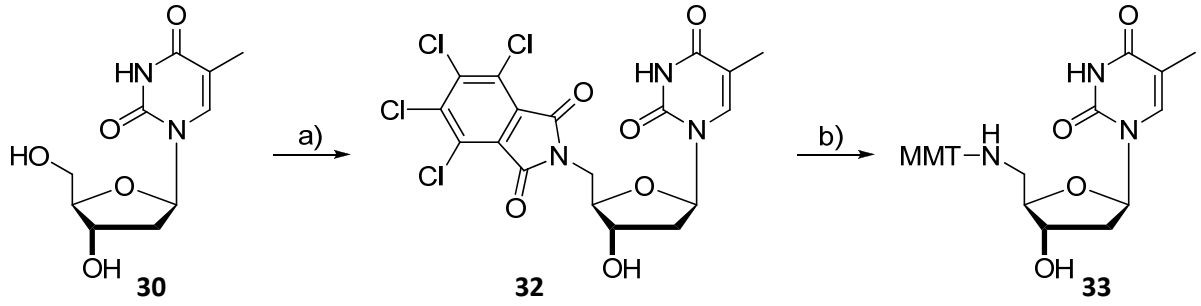

Scheme 21: Alternative Synthesis Route for 5'-Amino-5'-deoxythymidine.

a) Tetrachlorophthalimide (1.3 equiv.), PPh_3 (1.6 equiv.), DIAD (1.6 equiv.), THF, rt, 4 h, 76%*; b) (i) 1,2-ethylenediamine (20 equiv.), THF, 4h; (ii) MMT-Cl (2.4 equiv.), DMAP (0.6 equiv.), NEt_3 (0.6 equiv.), pyridine, rt, 2h, 78%*. *Synthesized by Dr. Lilia Clima.[141]

C5-Modified Pyrimidine Nucleosides

For non-terminal DNA labeling the relative position of the modification within the double helical structure has to be considered. Favorable are those positions which stick into the major or minor groove of DNA and do not disturb the formation of the double helix. The C5-position of pyrimidines as well as the N7-position of purines are known to do just that (Fig. 35). They both extend into the major groove of DNA. Furthermore these positions are adjacent to the hydrogen donating or accepting functionalities. Modifications at these positions therefore do not disturb the base pairing significantly.[157, 158]

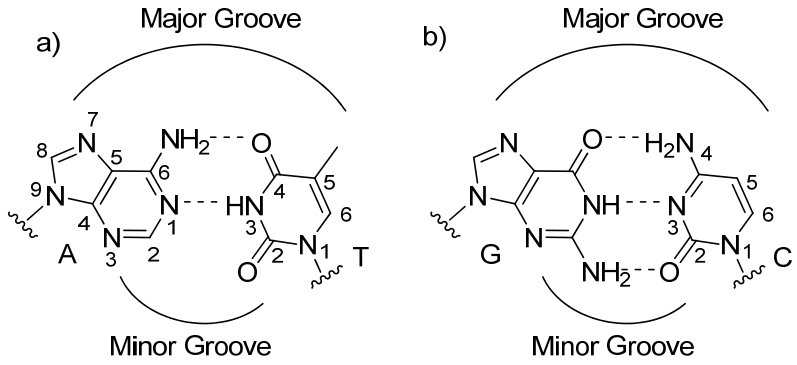

Fig. 35: Watson-Crick Base Pairs A-T and G-C.

We choose to attach the desired amino functionality to the C5-position of thymidine, since these derivatives are well established and are easily accessible starting from commercially available 5-iodo-deoxyuridine (**35**). Besides pyrimidine derivatives are generally more stable towards acids than purine derivatives and additionally, thymine as the base for the modification has no exocyclic amino functionality that needs to be protected. The C5-position can be functionalized by a C-C cross coupling either with aryl or alkine species.[157] Alkines are often favored because of their duplex stabilizing features.[159] A typical C-C coupling reaction for this purpose is the palladium-catalyzed Sonogashira reaction,[160] a variation of the Heck coupling.[161] It was first used on nucleosides by Bergstrom *et al*.[162] The typical catalytic cycle is depicted in Scheme 22. In the first step a Pd(0) species is inserted between the iodo-function and the nucleobase by oxidative addition. Trans-metalation then leads to the replacement of the iodo ligand by a Cu-alkine derivative, which is formed in *situ* by deprotonation of the alkine in the presence of a Cu(I) species. For this stochiometrical amounts of a base are needed, typically NEt_3 is used. Reductive elimination finally forms the new C-C bond and releases the catalyst from the substrate. The advantages of the Sonogashira reaction are the mild conditions and low temperatures (40-50°C) needed for the coupling.

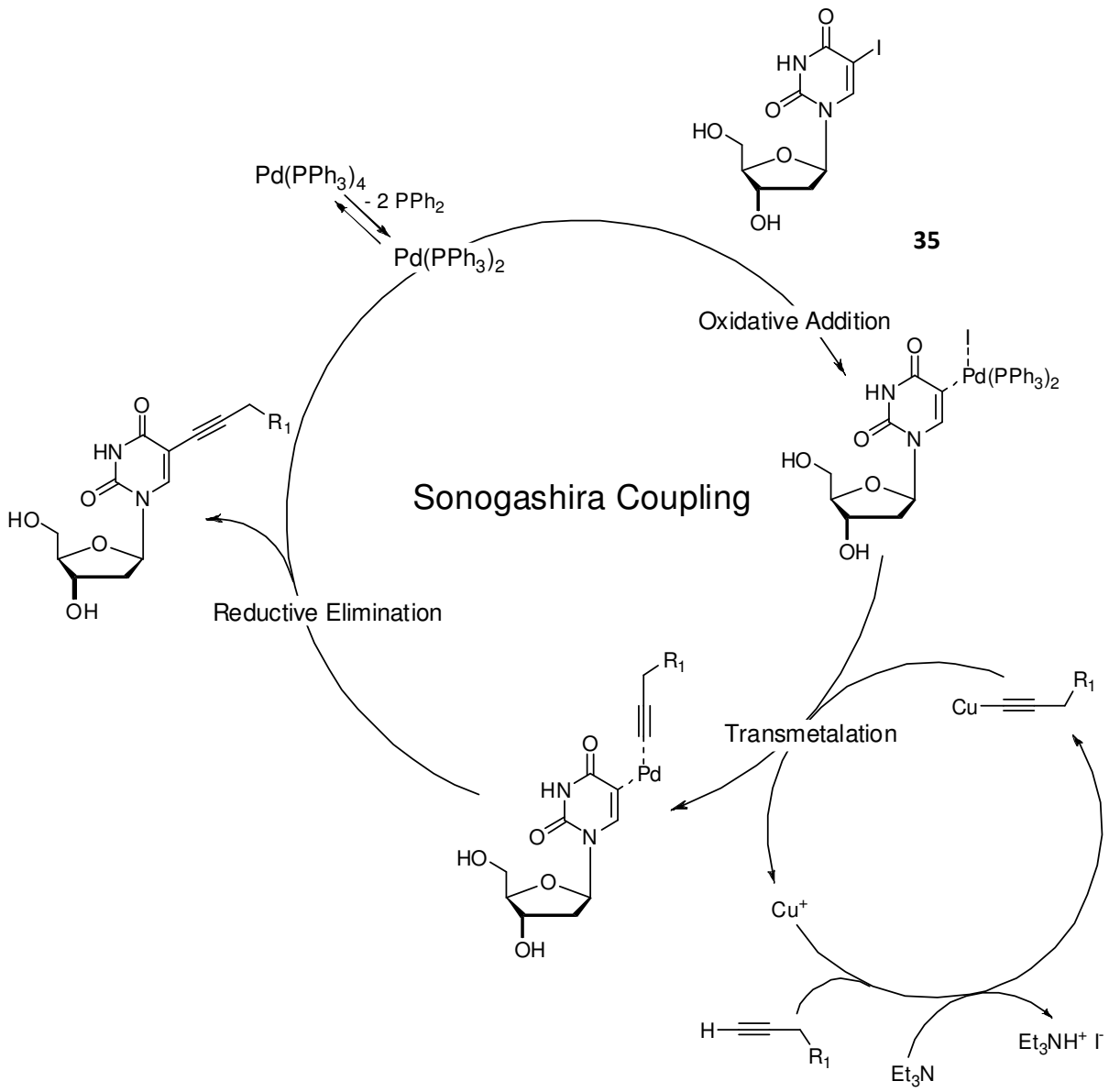

Scheme 22: Catalytic Cycle of the Sonogashira Reaction.

In our case we decided to use propargylamine **36** for the Sonogashira reaction, which is a very prominent functionalization and has often been employed in fluorescence labeling of oligonucleotides. Before coupling it to the nucleobase its amino group had to be protected. The trifluoroacetyl group turned out to be the ideal candidate for this purpose.[163] This protecting group is cleaved under basic conditions but orthogonally to the acidic conditions of the oligonucleotide synthesis cycle. Besides, it can withstand the Sonogashira coupling conditions without cleavage.

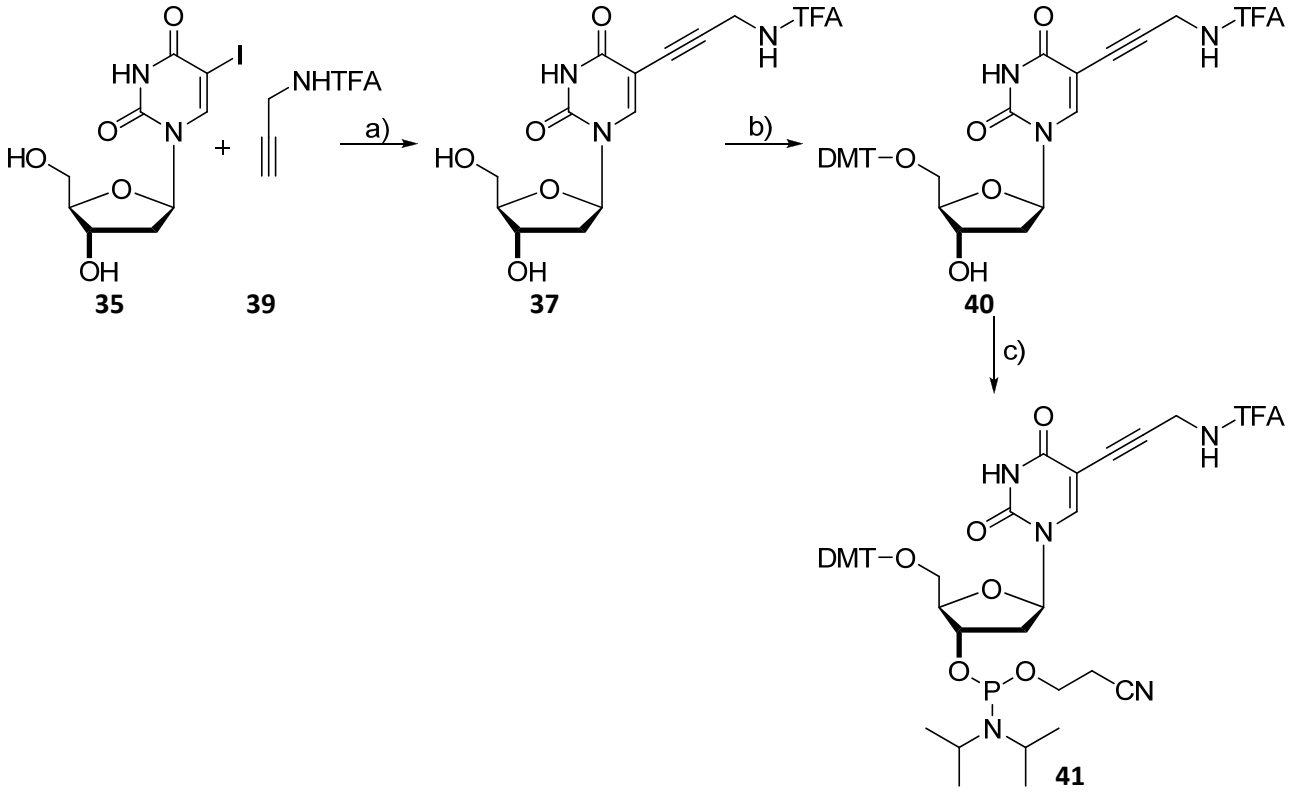

Scheme 23: Synthesis of Aminopropargyl-Modified Thymidine 37 and Corresponding Phosphoramidite 41.
a) See Table 1 for reaction conditions; b) DMAP (0.3 equiv.), NEt_3 (2.0 equiv.), pyridine, DMT-Cl (1.2 equiv.) in pyridine, rt., over night, 44%; c) CH_2Cl_2, diisopropylammonium tetrazolide (0.5 equiv.), (i-$Pr_2N)_2$-$POCH_2CH_2CN$, (2.8 equiv.), rt. 3 h, 83%*. *Synthesized by Dr. Lilia Clima.[141]

Table 1: Reaction Conditions for the Sonogashira Coupling.

Entry	Sonogashira Conditions	Yield of 37	Yield of 38
1	**35**, anhydrous DMF. 10 mol% $Pd(PPh_3)_2Cl_2$, NEt_3 (2.0 equiv.) **39** (2.4 equiv.), 20 mol% CuI, 40°C, 6 h.	18%	Not isolated
2	**35**, anhydrous DMF. 10 mol% $Pd(PPh_3)_4$, NEt_3 (2.0 equiv.) **39** (2.5 equiv.) 20 mol% CuI, 40°C, 6 h.	51%	33%
3	**35** 10% Pd/C (5 mol% Pd), Amberlite, 20 mol% CuI, anhydrous DMF, **39** (2.3 equiv.) in anhydrous DMF, 50°C, 17h.	80%	-

The trifluoroacetyl-protected propargylamine **39** was obtained in high yields and was then subjected to the Sonogashira reaction.[164] The standard conditions (Table 1, entry 1) for this reaction however led to increased formation of side products.[165] The quantity in which they were formed was not negligible. and separation from the desired product **37** was tedious. Especially the presence of triethylammonium hydroiodide as by-product made purification by column chromatography extremely difficult.[166, 167]

In order to improve the yields and to avoid the formation of the triethylammonium hydroiodide by-product, several different reaction conditions were screened (Table 1). A special focus was laid on the choice of catalyst. A good alternative to $Pd(PPh_3)_2Cl_2$ is the tetrakis(triphenylphosphine)palladium $Pd(PPh_3)_4$.[165] Its advantage is the high reactivity, which is caused by the oxidation state of palladium. Being a Pd(0)-species the catalyst can directly participate in the catalytic cycle, whereas the palladium of $Pd(PPh_3)_2Cl_2$ first needs to be reduced in

situ to the catalytical active species. Handling of $Pd(PPh_3)_4$ was a little bit more elaborate and special care had to be taken to avoid air contact. Its application resulted in an increased formation of the desired compound **37**. However, the formation of side-products and the chromatographic workup remained major issues. The main side-product was isolated and later identified by NMR to be the furanopyridine **38**, which is a precursor for potent antiviral agents.[168, 169]

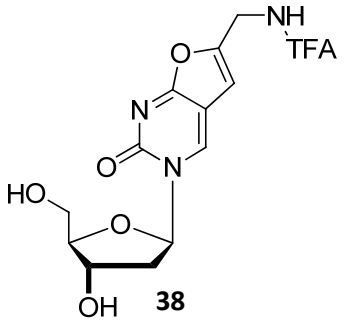

38

Fig. 36: Major Side-Product of the Sonogashira Coupling with $Pd(PPh_3)_4$ as Catalyst.

Because of the poor results obtained with homogenous catalysts we decided to test heterogeneous catalysts instead. Simple palladium on charcoal is reported to be a mild ligand-free catalyst for Heck and Sonogashira reactions.[166] Compared to $Pd(PPh_3)_4$ and $Pd(PPh_3)_2Cl_2$ it is easy to handle and also a lot cheaper. By increasing the reaction temperature from 40°C to 50°C as well as the reaction time from 6 to 17 hours we were able to obtain good conversions using only 10 mol% Pd/C (5 mol% Pd). Even more remarkable is the fact that only traces of side product were found. Additionally to changing the catalyst, we also replaced the base NEt_3, which had caused previously described problems during workup. For it, the basic ion exchange resin Amberlite was used instead. Amberlite effectively neutralized and absorbed the hydroiodide from the reaction mixture and could easily be removed by filtration, after the reaction. This step severely simplified chromatographic workup and made the isolation of the desired product possible. Having finally found the best reaction conditions for the coupling of the TFA protected propargylamine the desired compound **37** was synthesized in yields of up to 80%.

To make this nucleoside compatible with DNA synthesis protocols it was thereafter regio-selectively protected at its 5'-hydroxyl group. For this reaction the standard conditions (DMT-Cl, pyridine, NEt_3) were used. In the last step compound **40** was transformed into the corresponding phosphoramidite **41**. No changes to the standard phosphorylation protocol had to be made. The oxidation state of the phosphorus was determined by ^{31}P-NMR to be that of P(III).

Before DNA building block **41** was used in DNA synthesis it was thoroughly tested for its stability and compatibility towards all applied procedures. Cleavage conditions of the trifluoroacetyl-group (TFA) as well as the stability towards acidic conditions like the ones during the DNA synthesis were tested at the stage of the bare nucleoside **37**. After treating the compound **37** with 3% DCA no deprotection or decomposition was observed. The removal of the TFA group was possible with the same conditions used to deprotect the exocyclic amino functions of oligonucleotides (Scheme 24).

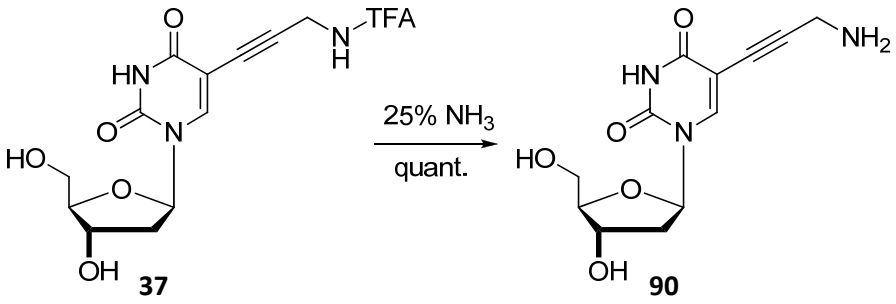

Scheme 24: Deprotection of TFA Protected 37.

The DMT-protected nucleoside **40** was used to determine whether it is possible to selectively remove the TFA in the presence of the trityl group. This would pave the way towards a presynthetic labeling strategy, in which the fluorophore could be coupled to the amino function of the monomeric DNA building block. Therefore compound **40** was subjected to strong basic conditions. As expected, this resulted in the removal of the TFA group, keeping the DMT group untouched. A presynthetic coupling of FRET dyes was thereafter established by Dr. Lilia Clima with the introduction of building block **42** shown in Fig. 37.[141] Building block **42** however did not find its way into this work because oligonucleotide syntheses were already completed by that time. Nevertheless such building blocks provide an interesting alternative route towards our labeled oligonucleotides.

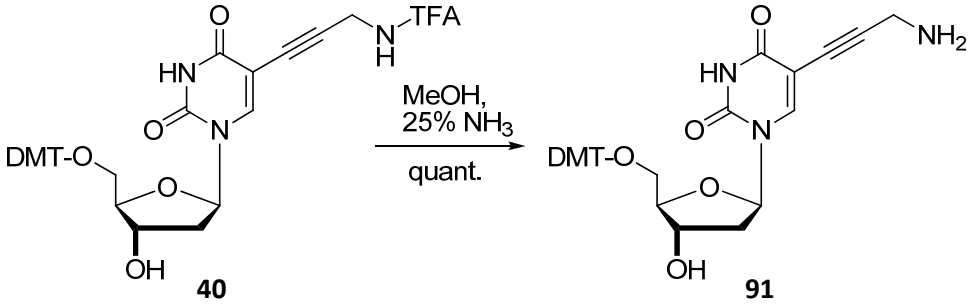

Scheme 25: Deprotection of TFA Protected 40.

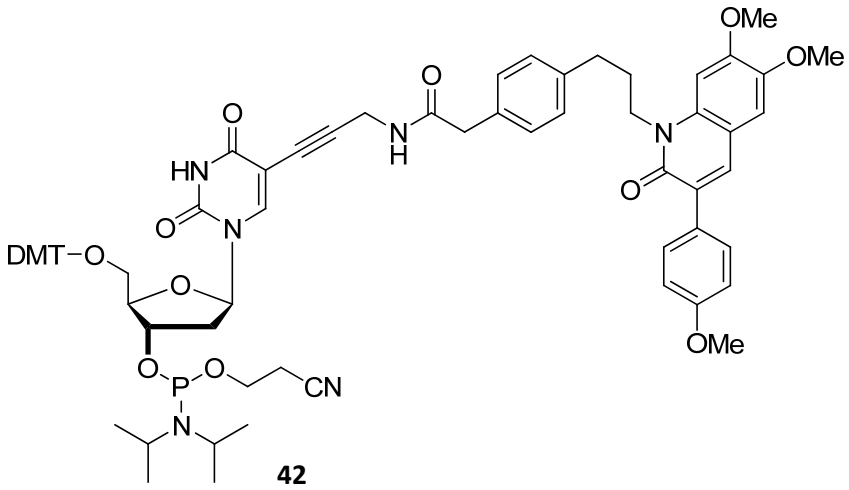

Fig. 37: Building Block 42 for Direct Insertion of Donor 3 into Oligonucleotides.

Besides propargylamino, other linker units for the attachment of our fluorescence labels towards the C5-position of thymidine were also considered. We were especially interested in compound **43**.

In this compound the flexibility of the linker is increased by exchanging the stiff triple bond with a single bond. Nucleoside **43** is accessible via the complete hydrogenation of the triple bond of nucleoside **37** in the presence of PtO_2 (Scheme 26)[170]. However, because of poor reproducibility of the reduction and because this would add an additional step towards our synthesis route the alkyl-linker synthesis was abandoned in favor of the propargyl amino linker.

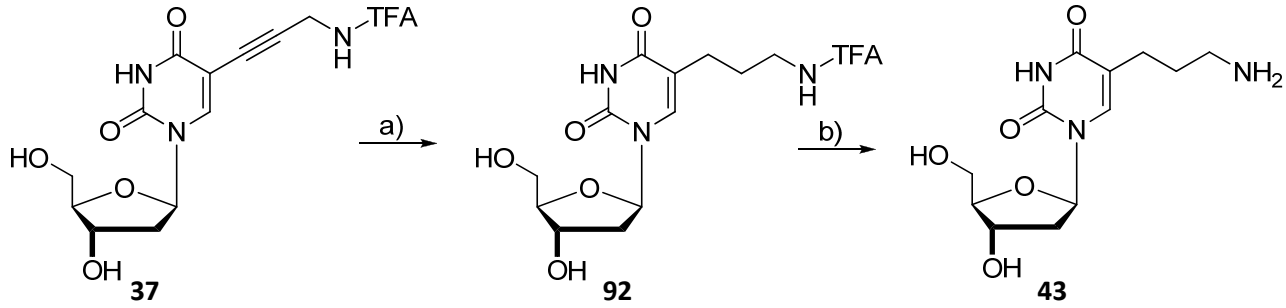

Scheme 26: Reduction of 37.
a) PtO_2 (cat.) H_2 (1 atm.), anhydrous MeOH, rt, 1 h., 70%. b) 25% NH_3, 3 h, rt, quant.

1.5. Oligonucleotide Synthesis

With all necessary building blocks and FRET dyes at hand we focused on the oligonucleotide synthesis for the DNA triple helix. The sequences for the backfolding DNA as well as the short Hoogsteen complementary strand were derived from the iNOS mouse gene and had previously proven to be perfectly suited for our purpose.[136] Different locations for the incorporation of the FRET chromophores were considered. However, in order to minimize interferences of the dyes with the binding of the protein NF-κB or with the triple helix formation only positions outside the essential sequences containing the binding motifs were feasible. For the Hoogsteen complementary oligonucleotide this meant that an amino-modified building block had to be attached either at the 3'- or at the 5'-end of the strand. Depending on this position the backfolding DNA either had to be modified at its open end or at a thymidine position next to the hexaethylene glycol linker to guarantee a close proximity between the two chromophores. The resulting two alternative pairs of backfolding DNA and short Hoogsteen complementary oligonucleotide are depicted in Fig. 38. In both cases the FRET donor was to be coupled to the backfolding DNA and the FRET acceptor to the short third strand. This decision was based on the assumption that the smaller donor molecule attached to the backfolding DNA would less likely effect the binding of the protein then the bulkier acceptor complex.

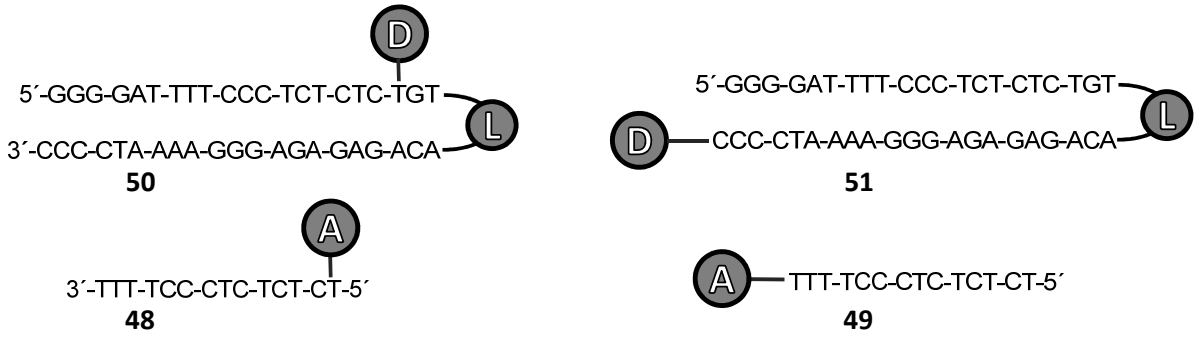

Fig. 38: Possible Positions for the Donor and Acceptor Chromophores.

a. Synthesis of Backfolding DNAs

Two backfolding DNAs differing only in the position of the primary amino-function for the coupling of the dyes were synthesized (Fig. 39). Both syntheses were carried out on an Expedite automated DNA synthesizer. Also hexaethylene glycol building block **1** was incorporated automatically. By increasing the coupling time to 15 minutes and by using a concentration of 0.1 M in anhydrous acetonitrile coupling efficiencies comparable to that of standard nucleotides were possible.

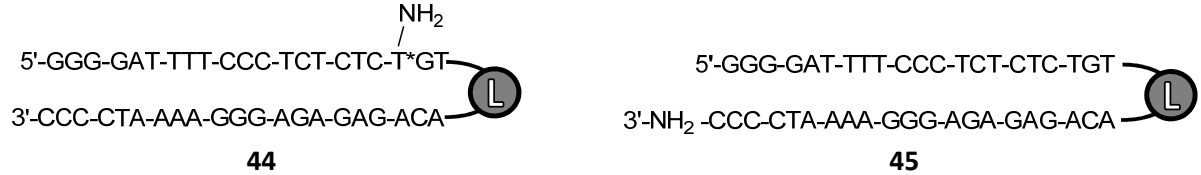

Fig. 39: Amino-Modified Backfolding DNAs 44, 45.

The amino modification in case of backfolding DNA **44** was successfully incorporated at the 3'-end of the homopyrimidine stretch, by using a 68 mM solution of 5-aminopropargyl-2'-deoxy uridine building block **41** in acetonitrile with standard coupling times. The TFA-protected primary amino function was freed at the end of the oligonucleotide synthesis under the same basic conditions

which are applied to oligonucleotides during the cleavage from solid support and deprotection of exocyclic amino groups.

In sequence **45**, the donor binding site was placed at the 3'-end. The synthesis of this oligonucleotide was therefore carried out using Amino-ON CPG as starting material, to which the first nucleotide was then coupled. The following nucleotides were thereafter coupled according to standard protocol. Treatment of the final oligonucleotide with concentrated ammonia resulted in deprotection of exocyclic amino groups and cleavage from solid support giving the free primary amino-function for the coupling.

b. Synthesis of Acceptor Strands 46, 47

The two short Hoogsteen complementary strands **46** and **47** bearing the coupling site for the Ru(II)-bathophenanthroline complex at opposing ends were synthesized using an Expedite automated DNA synthesizer.

46 **47**

Fig. 40: Amino-Modified Hoogsteen Complementary Strands 46, 47.

The 5'-modification of sequence **46** was incorporated manually. Therefore the almost finished but one nucleotide shorter 5'-DMT protected oligonucleotide on CPG was transferred into a frit (the apparatus for the manual coupling is depicted in Fig. 86 (on page 126 in the experimental part). For the coupling 81 µmol of phosphoramidite **34** were activated with 0.7 ml of a 0.3 M BMT solution. The standard coupling times of 3 minutes were used. After oxidation of the phosphorus and capping of failure sequences the MMT-protecting group was removed under acidic conditions. Cleavage of the oligonucleotide from the solid support and deprotection of exocyclic amino-functionalities was performed using concentrated ammonia at room temperature over night.

The synthesis of sequence **47** bearing the amino-modification at its 3'-prime end was straight forward using Amino-ON CPG as solid support, to which the first nucleoside was coupled. The finished oligonucleotide was cleaved from the solid support and its exocyclic amino groups were deprotected under basic conditions, freeing the primary amino group for the labeling.

1.6. Coupling of Dyes

The coupling of the dyes to the primary amino functionalized oligonucleotides by formation of amide bonds was carried out in solution using well established protocols.[141] Previously all oligonucleotides were first treated with KCl in order to replace the NH_4^+ counterion by K^+ and then desalted on NAP 10 columns by means of size exclusion chromatography.

a. Coupling of the Ru(II)-bathophenanthroline Acceptor

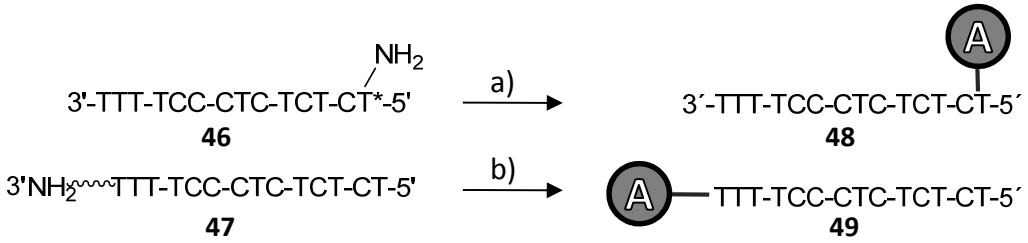

Scheme 27: Coupling of the Ru(II)-bathophenanthroline Acceptor.
a) **46** in DMF/1,4-dioxane/H_2O (1:1:1), *i*-Pr_2EtN (185 equiv.), $Ru(L^1)_2(L^2COOSuc)Cl_2$ **22** (23 equiv.), 25°C, 24 h, 59%; b) **47** in DMF/1,4-dioxane/H_2O (1:1:1), *i*-Pr_2EtN (185 equiv.), $Ru(L^1)_2(L^2COOSuc)Cl_2$ **22** (23 equiv.), 25°C, 24 h, 54%. L^1: **23**, L^2:**18**.

The Ru(II)-bathophenanthroline complex **4** was coupled to the two short acceptor oligonucleotides **46** and **47**. The same reaction conditions were applied in both cases. To ensure a good solubility of the hydrophobic dye and hydrophilic oligonucleotide at the same time a solvent mixture containing DMF, 1,4-dioxane and H_2O in a 1:1:1 volume ratio was used. The Ru(II)-complex was added to the dissolved oligonucleotide in form of the activated hydroxysuccinimide ester **22**. A large excess (approx. 23 equiv.) of the dye was applied to increase the coupling efficiency. Hünig's base was added to quench released protons and the reaction mixture was then incubated at 25°C in the dark for 24 hours. After completion of the reaction the solvents were removed under reduced pressure. Prior to further purifying the labeled oligonucleotides **48** and **49** by HPLC, unreacted acceptor **22** had to be eliminated. By exploiting the low solubility of oligonucleotides in EtOH we were able to extract the remaining Ru(II) complex. The crude oligonucleotide samples were therefore dispensed in ice cold EtOH. After centrifugation the supernatant solvent, which contained dissolved Ru(II) complex, was discarded. The extraction was repeated until the alcoholic solution remained colorless.

b. Coupling of the Donor

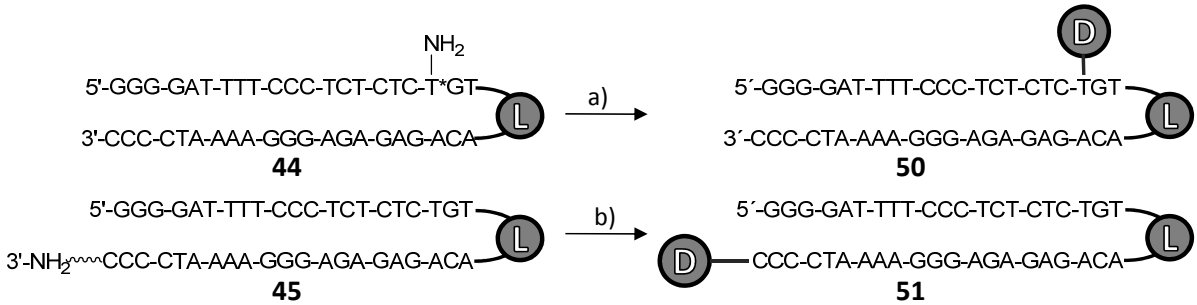

Scheme 28: Coupling of the Donor.
a) **44** in DMF/1,4-dioxane/H_2O (1:1:1), *i*-Pr_2EtN (195 equiv.), donor hydroxysuccinimide ester **28** (23 equiv.), 25°C, 24 h, 11%; b) **45** in DMF/1,4-dioxane/H_2O (1:1:1), *i*-Pr_2EtN (195 equiv.), donor hydroxysuccinimide ester **28** (23 equiv.), 25°C, 24 h, 33%.

For the introduction of the donor into the backfolding DNAs **44** and **45**, conditions similar to those used for the acceptor coupling were applied. Also the carbostyrile donor was coupled in form of the active hydroxysuccinimide ester **28**. To achieve a good solubility of the dye as well as the oligonucleotide a solvent mixture containing DMF, 1,4-dioxane, H_2O in a 1:1:1 volume ratio was

used. Compared to the acceptor the donor displayed a higher solubility in this solvent mixture. Therefore the reaction was performed using less solvent and with it higher concentrations of the reactants. In the presence of Hünig's base 23 equivalents of the donor were added to the oligonucleotide. The reaction mixture was incubated at 25°C in the dark for 24 hours. Thereafter all solvents were removed under reduced pressure and remaining unreacted dye was removed by extracting the crude oligonucleotide several times with ice cold EtOH.

1.7. Purification and Analysis

All labeled oligonucleotides were purified by preparative HPLC. The runs were performed on a reversed phase C18 column of the type EC-125/4-Nucleosil-100-5 on a Merck Hitachi system. The mobile phase consisted of a gradient between an aqueous 0.1 M $Et_3NH(OAc)$ buffer at pH 7.0 and acetonitrile.

For the purification of the donor-modified backfolding DNAs **50** and **51** a gradient of 0-60% acetonitrile within 45 minutes [HPLC method 3 (See chapter: HPLC on page 131)] was used. The HPLC analysis revealed that the desired oligonucleotide **50** was only partially labeled. The employed gradient however allowed an easy separation of the labeled oligonucleotide (t_R = 16 min) from unlabeled oligonucleotides (t_R = 9-11 min). The labeling efficiency of backfolding DNA **51** was a little better.

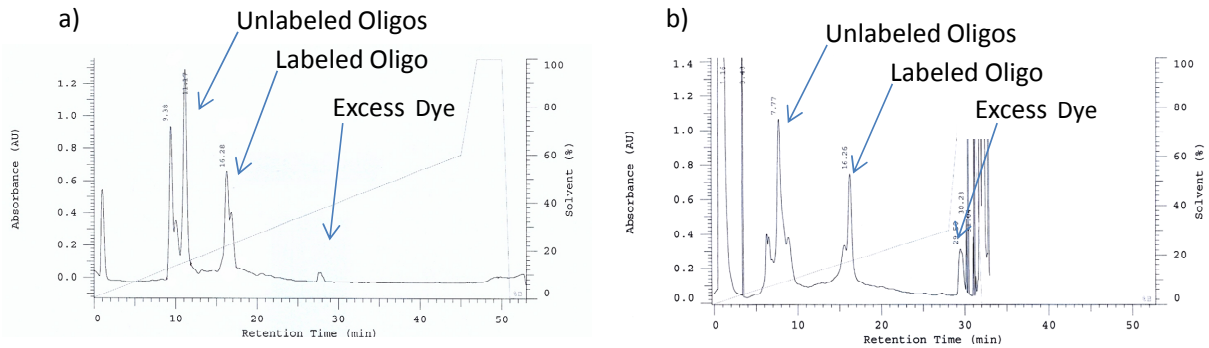

Fig. 41: Preparative HPLC of Donor-Labeled Backfolding DNA a) 50 and b) 51.

For the purification of the accepto-labeled oligonucleotides **48** and **49** a steeper gradient of 0-80% acetonitrile within 30 minutes [HPLC method 4 (See chapter: HPLC on page 131)] was used. It allowed the elution of labeled oligonucleotides in an acceptable time frame while still yielding a good separation of the desired sequence (t_R = 19-21 min) from unlabeled oligonucleotides (t_R = 12 min) and unreacted Ru(II)-complex (t_R = 25-27 min). The labeling protocol for the acceptor proofed to be very effective. Only traces of unlabled oligonucleotide were visible in the HPLC spectra.

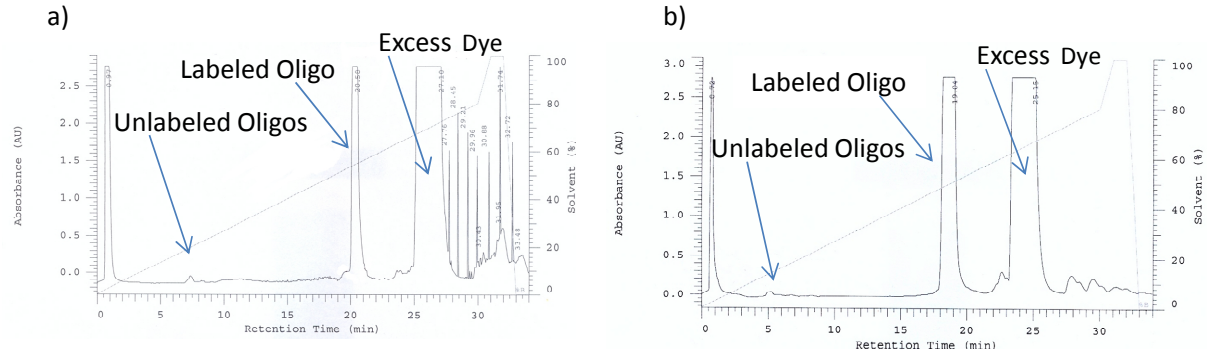

Fig. 42. Preparative HPLC of Acceptor-Labeled Sequences a) 48 and b) 49.

Successful purification of the labeled oligonucleotides by HPLC was verified by analytical polyacrylamide gel electrophoreses (Fig. 43). Fluorescence of the dyes could be detected on the gel

at 366 nm. Staining the gel with StainsAll solution revealed that no unlabeled sequences were present.

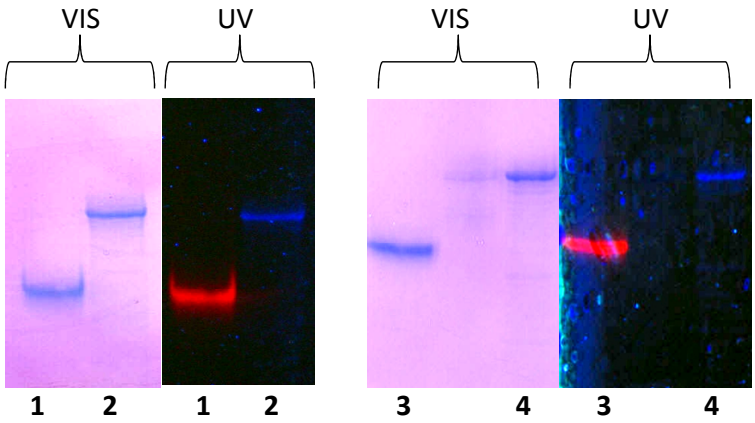

Fig. 43: PAGE of Pure and Labeled Oligonucleotides.
Gel documented under visible light (VIS) and at 366 nm (UV). Lane 1: Acceptor-labeled oligonucleotide **48**; lane 2: Donor-labeled oligonucleotide **50**; lane 3: Acceptor-labeled oligonucleotide **49;** lane 4: Donor-labeled oligonucleotide **51**.

1.8. Fluorescence Measurements

a. Triple Helix FRET Systems

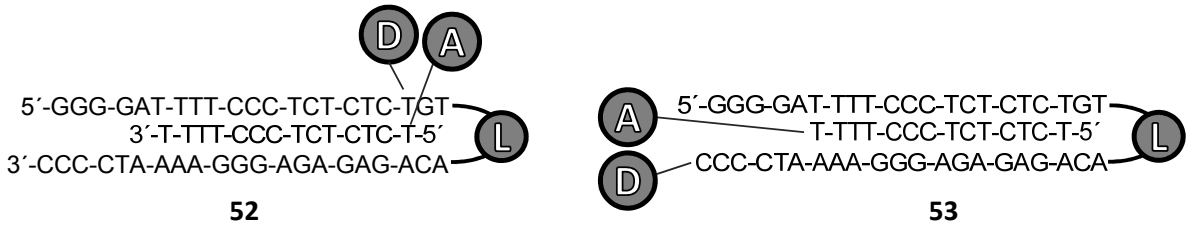

Fig. 44: Triple Helices 52 and 53.
Triple Helix **52**: Hybridization of backfolding DNA **50** with oligonucleotide **48**; Triple Helix **53**: Hybridization of backfolding DNA **51** with oligonucleotide **49**.

After successfully synthesizing and purifying the components of the triple helix we were interested in verifying the quality of the proposed FRET system. The main purpose for these preliminary tests was the evaluation of conditions needed for the detection of NF-κB. For the best possible results during the assay equimolar amounts or even a slight excess of NF κB compared to the triple helix should be used to ensure a complete replacement of the acceptor oligonucleotide by the protein binding. A limiting factor however is obviously the amount of NF-κB which is available. Extraction from cells yields the protein only in pico-mol amounts. We therefore decided to measure the FRET of the two triple helices in the same pico mol range. A possible option to nevertheless maximize the absorption as well as emission intensity of the FRET was to reduce the volume of the sample solution and thereby increase the concentration of its components. A special microcuvette with a sample volume of 20 µl and a light path of 1 cm allowed us to increase the concentration of the triple helix into the mM range without increasing the quantity of the oligonucleotides (Fig. 45).

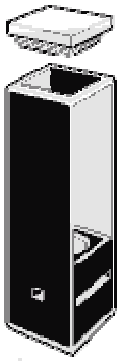

Fig. 45: Fluorescence Cuvette.

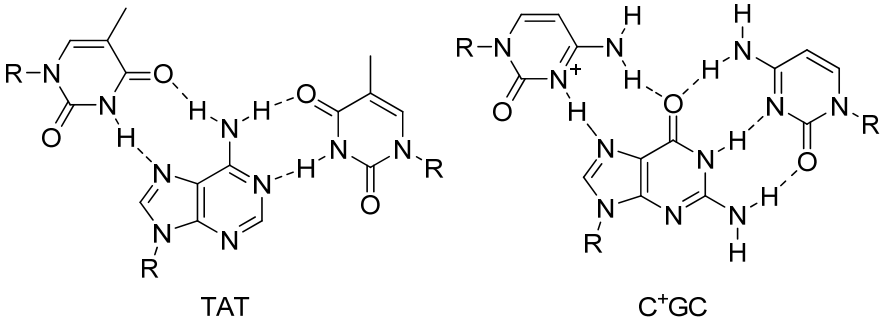

Fig. 46: Hoogsteen Base Triade TAT and C^+GC.

Another vital factor that we needed to address was the stability of the triple helix system. The C^+GC pairs of the Hoogsteen type require slightly acidic conditions to protonate the cytosine (Fig. 46). In the pertinent melting experiments our unlabeled triple helices had proven to be stable at pH 6. A melting temperature around 40°C was obtained. When mixing the two oligonucleotides **50** and **48** at pH 6 the results of the obtained triple helix **52** were not clear cut. This might be attributed to a decreased stability of the triple helix caused by the chromophores, which were attached at the ends of the homopyrimidine stretch. By lowering the pH to 5.5 and by this increasing the triple

helix stability we could indeed observe an acceptor emission at 620 nm after excitation at 360 nm which is indicative for the FRET and was expected after formation of the triple helix.

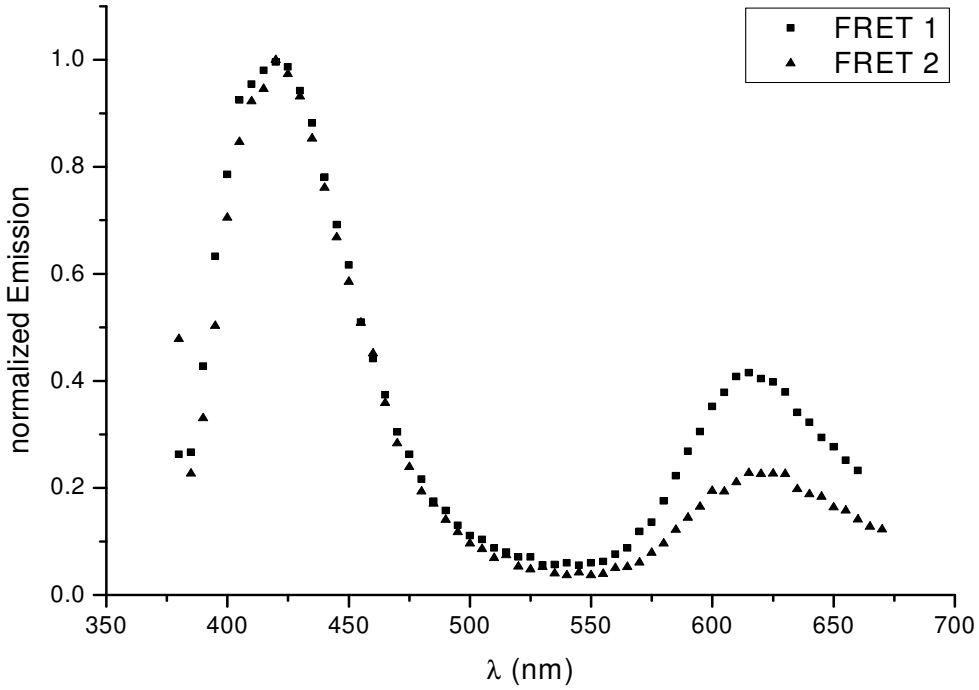

Fig. 47: Emission Spectrum of Triple Helix 52 (■) and 53 (▲).
Excitation at 360 nm, Slit: 10 nm/10 nm, Scan Speed: 100 nm/min, Scan Range: 380-670 nm. Oligonucleotide concentration 0.585 mM in acetate buffer (450 mM, pH 5.5).

The same fluorescence measurements were also performed for the second triple helix **53**. The FRET efficiency of this system was lower than the previous one (Fig. 47). The lower intensity of the acceptor signal is most probably caused by the increased distance between donor and acceptor in triple helix **53**. According to the Förster equation increasing the distance r between both dyes affects the intensity of the FRET to the 6^{th} power.

b. Test System

NF-κB containing protein extracts are usually kept in buffer systems at pH 8. The addition of such a protein extract to the triple helix solution would definitely change the overall pH. Thus a possible influence of the protein buffer on our assay system had to be evaluated by mimicking the assay conditions as realistically as possible.

Based on a protein concentration of 2.6 pmol/µl the decision was made to use 14.7 µl of triple helix solution with a concentration of 0.796 pmol/µl. In the 20 µl measuring cell of the fluorescence cuvette this would leave a capacity of 5.3 µl for the protein containing cell extract. A cell extract sample of this volume and with a concentration of 2.6 pmol/µl contains 13.8 pmol of proteins, enough to allow a small excess of the protein to completely remove the acceptor oligonucleotide from the backfolding DNA.

The triple helix solution was prepared by combining equimolar amounts of the backfolding (1.035 nmol) DNA **50** or **51** and the corresponding acceptor oligonucleotide (1.035 nmol) **48** or **49** in an Eppendorf reaction tube. The solvent was then removed under reduced pressure and the precipitate was dissolved in 1300 µl NaOAc buffer (450 mM, pH 5.5). This gave a final concentration of 0.796 pmol/µl. Hybridization of the oligonucleotides was achieved by heating the solution to 90°C for 2 minutes and afterwards allowing the solution to slowly cool to room temperature.

Test fluorescence measurements using the same concentrations and volumes as outlined above for our assay were performed to evaluate the impact of the previously mentioned pH shift on the stability of the triple helix and hence on the FRET system. In an Eppendorf reaction tube 14.7 µl of the triple helix stock solution (**52** or **53**) were combined with 5.3 µl of Tris buffer (50 mM, pH 8). The solution was immediately transferred into a fluorescence cuvette and the fluorescence spectrum was recorded. (Excitation at 360 nm, Emission recorded between 380-670 nm).

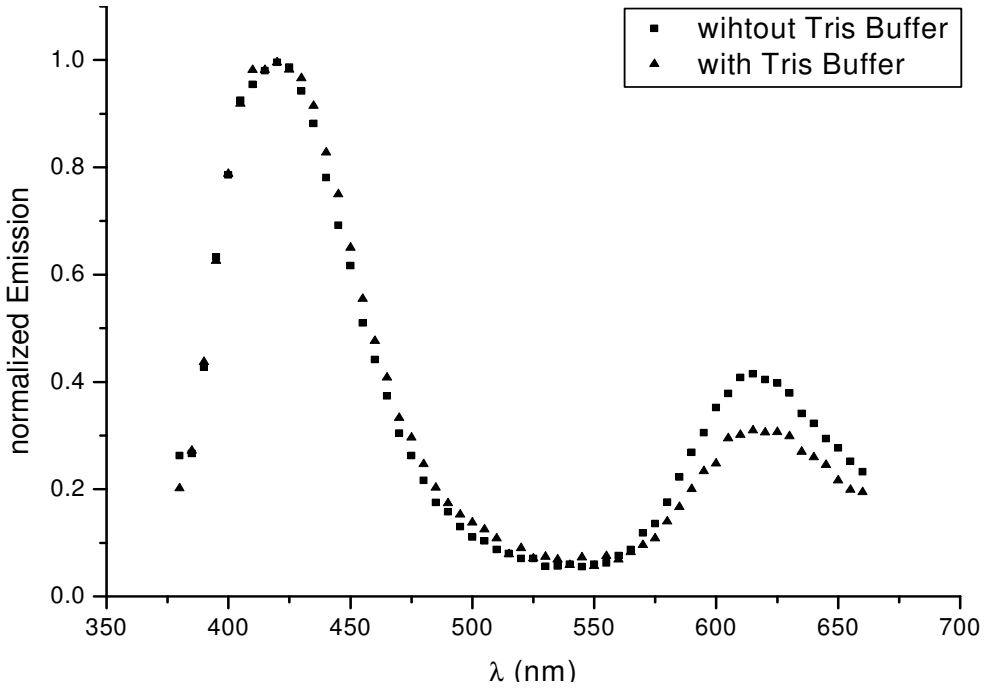

Fig. 48: Effect of Tris-Buffer Addition on Emission Spectrum of Triple Helix 52.

Excitation at 360 nm, Slit: 10 nm/10 nm, Scan Speed: 100 nm/min, Scan Range: 380-670 nm. Oligonucleotide **52** concentration 0.585 mM a) ■ in Acetate Buffer (450 mM, pH 5.5), or b) ▲ in a mixture of Tris-Buffer (13 mM, pH 8) and Acetate Buffer (331 mM, pH 5.5).

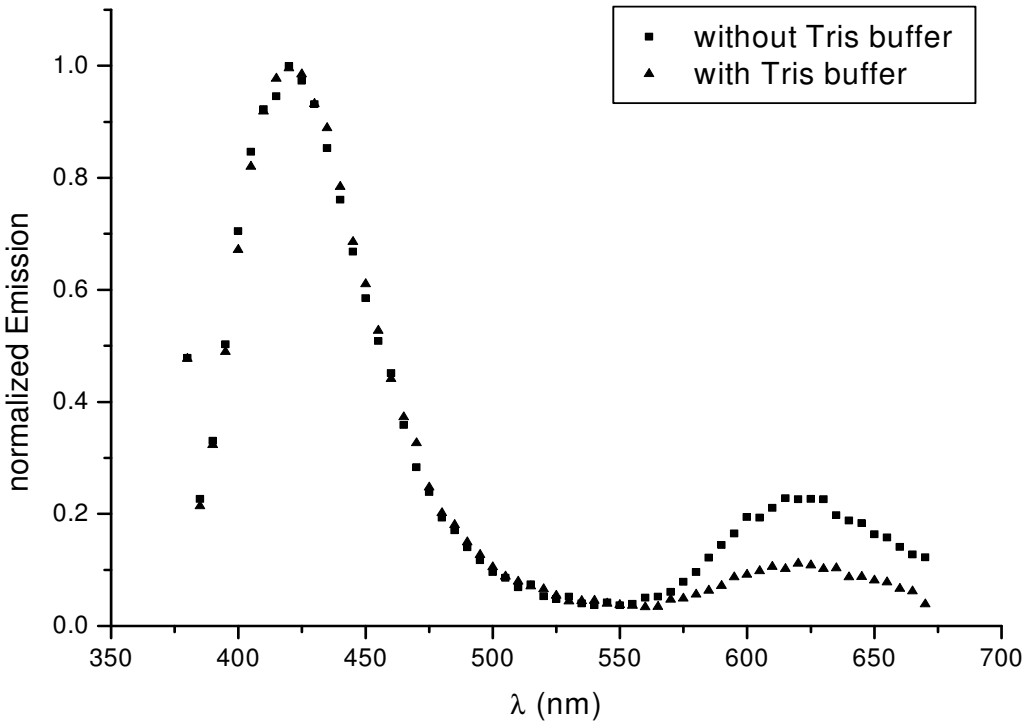

Fig. 49: Effect of Tris-Buffer Addition on Emission Spectrum of Triple Helix 53.
Excitation at 360 nm, Slit: 10 nm/10 nm, Scan Speed: 100 nm/min, Scan Range: 380-670 nm. Oligonucleotide **53** concentration 0.585 mM a) ■ in Acetate Buffer (450 mM, pH 5.5), or b) ▲ in a mixture of Tris-Buffer (13 mM, pH 8) and Acetate Buffer (331 mM, pH 5.5).

In both cases a drop in the acceptor emission was observed due to the pH change. For the triple helix system **52** this drop was only minimal and a strong acceptor signal was still detectable at 620 nm. The already weaker FRET signal of triple helix **53** on the other hand was even further decreased, making the system unattractive for us.

c. Fluorescence Measurements in Presence of NF-κB

Having identified a suitable triple helix (**52**) as well as promising assay conditions for the detection of NF-κB it was now time to measure the effects of the protein on the triple helix **52** and the FRET system. Before applying cell extracts towards our system we planned to establish a proof of principle by using pure recombinant NF-κB. This would give us the opportunity to fine tune the assay conditions (pH, salt concentration) without having to care about other cellular materials still present in cell extracts.

Pure recombinant NF-κB in form of the p50 and p65 monomers is commercially available and was obtained from Biocat (Heidelberg) in the desired concentrations. Annealing of the two monomers to the p65/p50 heterodimer was done by Dr. Andrea Hrenn in the Group of Prof. Dr. Irmgard Merfort at the Pharmaceutical Institute of the University of Freiburg. The success was verified by electrophoretic mobility shift assays (EMSA).

d. EMSA of Recombinant NF-κB

EMSA is a standard method for the detection of DNA-binding proteins.[124] The methodology is based on the size-dependent separation of oligonucleotides in electrophoretic gels. Characteristic is the high sensitivity of this procedure. For the detection, short double-stranded DNA sequences are used which are terminally labeled and contain a specific protein binding motif. Incubation of the double-stranded DNA with protein extracts leads to the formation of DNA-protein complexes. These DNA-protein complexes display a decreased mobility on the gel due to their increased size and are thereby separated from free DNA.

Small sample quantities make it necessary to use radioactive phosphorus for the labeling of the oligonucleotide termini. Usually the γ-phosphate group of [γ-^{32}P]-ATP or [γ-^{33}P]-ATP, is transferred onto DNA by a polynucleotide kinase. Detection is then performed by autoradiography.

A variation of this procedure is the competition assay. It is usually done in parallel to the standard mobility shift in order to identify DNA-protein complex bands. In the competition assay an excess of unlabeled DNA is added to the sample. The result is the weakening or even deletion of the DNA-protein band.

Fig. 50: Commercially Available Promega Sequence for the Detection of NF-κB.
Frame: Binding motif for NF-κB.

Standard DNA sequences for the detection of NF-κB by EMSA are commercially available for example from Promega (Fig. 50). We used those to confirm the binding properties of the recombinant NF-κB by EMSA. Labeling of the DNA was achieved with ^{33}P from [γ-^{33}P]-ATP. The radioactive ^{33}P-isotope is a gamma emitter with a half life of 25.3 days. Its usage was preferred over that of ^{32}P due to safety reasons. The likewise gamma emitter ^{32}P, which has a half life of 14.3 days, displays stronger decay energy than ^{33}P. The decay energy of ^{32}P is 1.711 MeV and that of ^{33}P is 0.249 MeV. The 5'-termini of the control DNA was labeled with ^{33}P by a polynucleotide kinase from bacteriophage T4 (T4-PNK, Promega). The kinase not only has the ability to add ^{33}P to the 5'-termini of oligonucleotides. It can also exchange non-radioactive ^{31}P with radioactive ^{33}P from the [γ-^{33}P]-ATP. Labeled oligonucleotides were purified from excess [γ-^{33}P]-ATP by column chromatography and thereafter incubated with a NF-κB source.

The EMSA results of recombinant NF-κB were compared to those of NF-κB-containing cell extracts. Cell extracts were obtained from Jurkat cells. The cells were stimulated by the addition of immune system messenger TNF-α, which led to the activation of NF-κB by cleaving off its inhibitor IκB. Additionally, competition assays with a 100 fold excess of unlabeled DNA were performed.

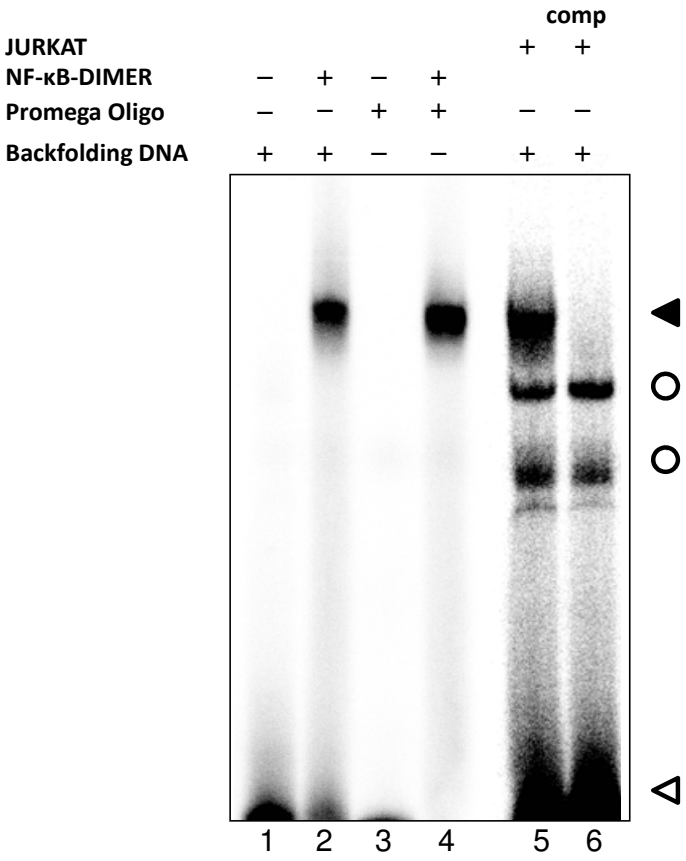

Fig. 51: EMSA of NF-κB Binding to Backfolding DNA and Control Oligonucleotide.

Lane 1: bfDNA **50** wihtout NF-κB; Lane 2: bfDNA **50** with pure NF-κB p65-p50 (900 ng); Lane 3: Promega oligonucleotide without NF-κB; Lane 4: Promega oligonucleotide with pure NF-κB p65-p50 (900 ng); Lane 5 bfDNA **50** with Jurkat cells treated with 200 U/ml TNF-α; Lane 6: competition assay of bfDNA **50** with Jurkat cells treated with 200 U/ml TNF-α. A filled arrowhead indicates the position of NF-κB DNA complexes. The open circle denotes a non-specific activity binding to the probe and the open arrowhead shows unbound oligonucleotide.

EMSA also gave us the ability to verify the affinity of NF-κB towards our donor-labeled backfolding DNA **50**. Both, recombinant NF-κB as well as Jurkat cell extracts were used in this assay. The intensity of the radioactive labels was weaker compared to normal double-stranded DNA, because backfolding DNA **50** possesses only a single 5'-end to which ^{32}P could be coupled.

Analysis of the autoradiographs resulting from the EMSA gels confirmed the desired activity of the pure recombinant NF-κB dimer. A strong band which was attributed to the protein-DNA complex was clearly visible for the Promega sequence (lane 4). Such a band was also observed for the backfolding DNA **50** (lane 2). Both bands had the same height as the one produced by the Jurkat cell extracts (lane 5). Supporting this notion was the fact, that these bands were not visible in control experiments, in which no NF-κB had been added (lane 1 and 2). These results were proofed by the competition assay (lane 6). Here the band attributed to the NFκB-DNA complex disappeared, whereas other bands of lane 5 and 6, caused by non-specific binding activity, remained visible.

e. Proof of Principle

The proof of concept experiments were carried out with the previously described test system (0.796 pmol/µl triple helix **52** in 450 mM NaOAC buffer at pH 5.5). The triple helix **52** was freshly hybridized beforehand. To compensate the slight drop of FRET signal caused by the pH-shift a blank [5.3 ml Tris base (10 mM, pH 8) and 14.7 ml triple helix solution] was recorded and compared to the results obtained by the addition of pure NF-κB (5.3 ml of 2.6 pmol/µl solution in 10 mM Tris buffer, pH 8).

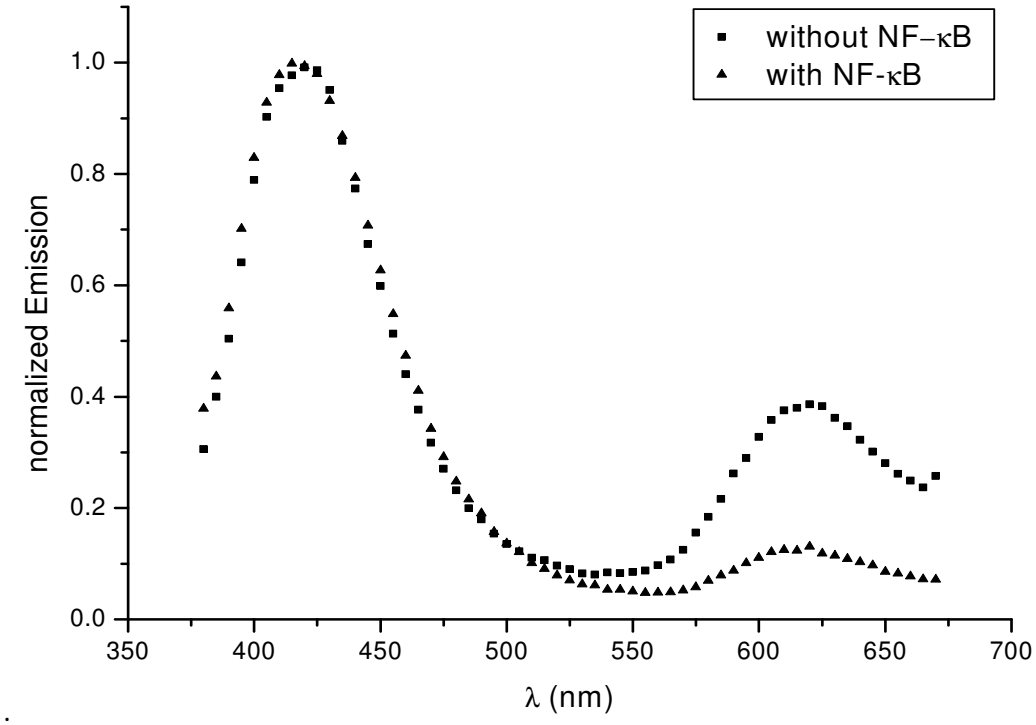

Fig. 52: FRET of Triple Helix 52 before and after Addition of NF-κB.
Excitation at 360 nm, Slit: 10 nm/10 nm, Scan Speed: 100 nm/min, Scan Range: 380-670 nm. Oligonucleotide **52** concentration 0.585 mM in a mixture of Tris-buffer (2.65 mM, pH 8) and acetate buffer (331 mM, pH 5.5). ■ without NF-κB; ▲ with NF-κB (0.689 mM).

Addition of pure heterodimer in small excess led to a substantial decrease of the emission at 620 nm and hence, of the FRET (Fig. 52). The still observable emission at 620 nm can be attributed to direct excitation of the Ru(II)-complex **4**. The almost spontaneous reduction of the acceptor signal prompted us to follow the FRET in a time course experiment (Fig. 53). Spectra were therefore recorded immediately after addition of the protein and after 30, 90 minutes thereafter. Already in the first spectrum the acceptor emission had dropped significantly and only a minimal change was observed within in the next 30 minutes. After that time the signal remained stable.

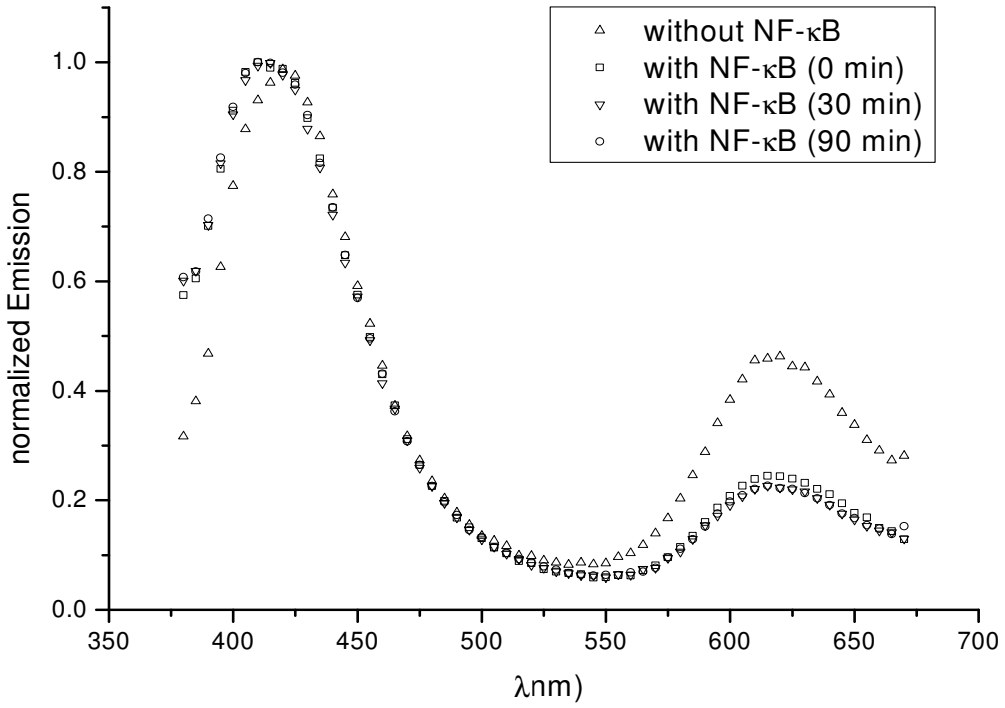

Fig. 53: Time Course after Addition of NF-κB.

Excitation at 360 nm, Slit: 10 nm/10 nm, Scan Speed: 100 nm/min, Scan Range: 380-670 nm. Oligonucleotide **52** concentration 0.585 mM in a mixture of Tris-buffer (2.65 mM, pH 8) and acetate buffer (331 mM, pH 5.5). △ Without NF-κB; □ with NF-κB (0.689 mM) after 0 min; ▽ with NF-κB (0.689 mM) after 30 min; ○ with NF-κB (0.689 mM) after 90 min.

To demonstrate a correlation between the NF-κB concentration and intensity of the FRET acceptor emission, different concentrations of the heterodimer were added to the triple helix solution and the corresponding emission spectra were recorded after an incubation time of 5 minutes. The results are depicted in Fig. 54.

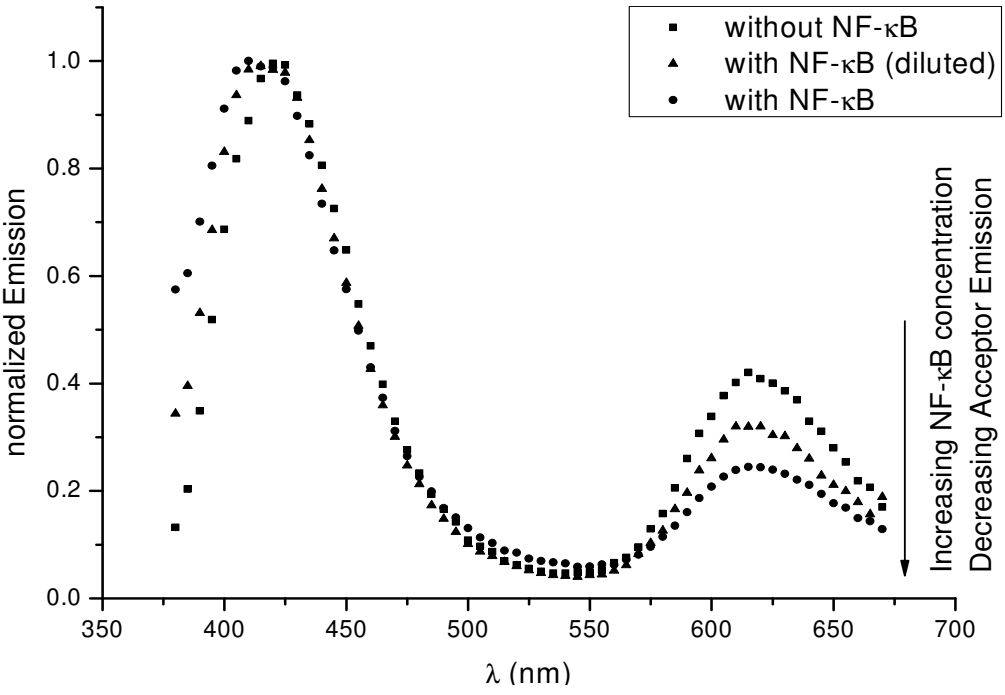

Fig. 54: FRET of Triple Helix with Different Concentrations of NF-κB Heterodimer.

Excitation at 360 nm, Slit: 10 nm/10 nm, Scan Speed: 100 nm/min, Scan Range: 380-670 nm. Oligonucleotide **52** concentration 0.585 mM in a mixture of Tris-buffer (2.65 mM, pH 8) and acetate buffer (331 mM, pH 5.5).

As expected only a relatively small drop of the acceptor emission at 620 nm was recorded for a diluted solution of NF-κB, higher concentrated sample led to an increased drop.

2. Summary and Conclusion

In summary, we have presented a feasibility study for a novel assay for NF-κB. This assay utilizes FRET for the detection of the protein. The sensor is a DNA triple helix derived from the inducible nitric oxide synthetase (iNOS) with a specific binding site for NF-κB. The triple helix is composed of an oligonucleotide bearing the FRET acceptor which is bound by Hoogsteen pairing to a donor-labeled backfolding DNA. An efficient synthesis route towards such triple helices was established. In this context, several building blocks allowing the variable labeling of the oligonucleotides were discussed and their application was demonstrated in the synthesis of the two backfolding DNAs **44**, **45** and the two Hoogsteen complementary oligonucleotides **46** and **47**. Coupling of the dyes **22** and **28** to these oligonucleotides was performed in solution and the obtained labeled oligonucleotides (**50**, **51**, **48**, **49**) were successfully purified by preparative HPLC.

Thermal hybridization led to the corresponding triple helices **52** (**50**·**48**) and **53** (**51**·**49**) differing in the positions of the FRET chromophores. These systems were thoroughly investigated for their chemical and photochemical properties.

The superior triple helix FRET system **52** was thereafter utilized to exemplify the principle of our assay with pure recombinant transcription factor NF-κB heterodimer p50/p65. Binding of NF-κB to the backfolding DNA led to a replacement of the acceptor strand, thus increasing the distance between FRET donor and acceptor. This resulted in a reduced emission of the luminescence at 620 nm due to the diminished FRET.

The advantage of this assay is its avoidance of radioactive markers like in EMSAs and of expensive antibodies like in alternative assays. The new principle might therefore also have implications for assays of other DNA-binding proteins as well. Future experiments will be focused on other heterodimeric combinations of NF-κB and on precise quantification experiments with the new format.

3. DNA-Supported Catalysis

3.1. Principle

DNA-supported catalysis which is sometimes misleadingly referred to as DNA-based catalysis uses the helical structure of double-stranded DNA as a chiral scaffold. The actual catalytic features do not originate from the DNA itself but from added transition metal complexes.[102] Therefore, DNA-supported catalysis can be best compared to the cooperating behavior of enzyme-cofactor complexes, in which the enzyme itself is responsible for the enantiomeric discrimination and the cofactor is responsible for the actual catalysis. The general principle of DNA-supported catalysis is depicted in Scheme 29.

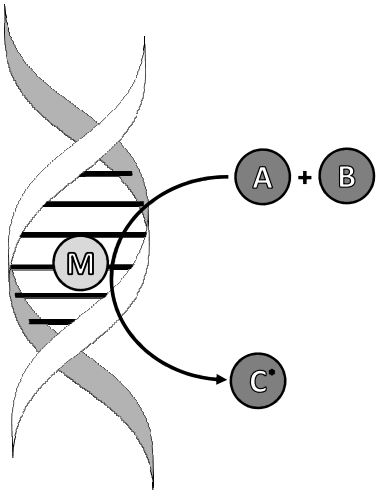

Scheme 29: Principle of DNA-Supported Catalysis.
M: catalyst, A and B: Starting material, C*: chiral product.

The reaction between the starting material A and B is catalyzed by transition-metal complex M. The catalyst interacts in such a fashion with DNA that its double helix can serve as a chiral scaffold for the reaction. Thus, the transition states of the reaction are discriminated, which ultimately can lead to the formation of enantiomeric enriched chiral product C*.

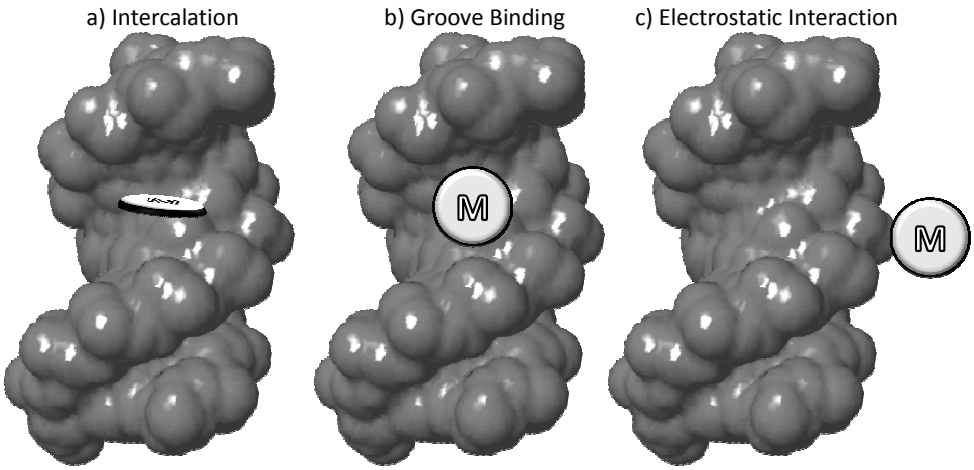

Fig. 55: Possible Interactions with DNA.
Catalyst M binds to DNA by a) intercalation in between the base stacks, b) major groove binding, c) electrostatic interactions with the phosphate backbone.

The common binding mode between DNA and catalyst so far is based on weak interactions, like intercalation, groove binding, or electrostatic interactions with the phosphate backbone (Fig. 55).[102, 103, 105-107, 171] For most ligands it is not known which of these three binding modes is favored, also a combination of them is conceivable.[172] The advantage of using weak interactions lays in the possibility to change the ligand rapidly which makes screening of many different ligand systems easy. However, as pointed out previously, the position of such catalysts within DNA is random, which makes it nearly impossible to investigate aspects of DNA-supported catalysis, like the effect of the base sequence surrounding the catalytical center or the impact of varying the distance between DNA and catalyst.

In the work at hand we aspired to establish a well defined system, in which ligands are covalently attached to double-stranded DNA, thus enabling us to pinpoint the location of the catalytical site within DNA as well as its local chiral environment. To the best of our knowledge only one report towards this endeavor has appeared so far in literature.[173] By attaching the catalytic site to the phosphate on a nicked double-stranded DNA, high enantioselectivities could be observed (Fig. 56). Although the results were remarkable, the fact that the sugar-phosphate entity is located on the outside of double-stranded DNA and due to the flexibility of the linker entity it can only be speculated about the actual location where the catalysis takes place.

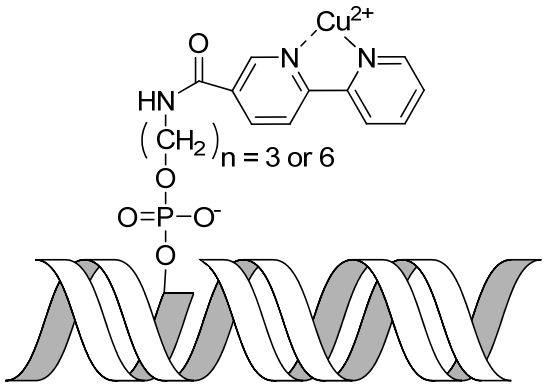

Fig. 56: Catalytic Site Attached to the Phosphate Backbone of a Nicked Double-Stranded DNA.

Our approach to covalently attach ligands for the DNA-supported catalysis differs in this respect that we were aiming at modifying the nucleobase position instead of the phosphate unit thereby keeping the phosphate backbone of the DNA intact.

3.2. Strategy

While designing an appropriate ligand system for the covalent attachment to DNA several considerations regarding its position within DNA and its properties had to be taken into account.

a. Location of the Catalyst within DNA

Within DNA, especially the major groove is known for its sequence dependent interactions as demonstrated by binding restriction enzymes or transcription factors.[174] Another example is the sequence-specific formation of triple helices of the Hoogsteen type.[135] The origin for these interactions with DNA is illustrated in Fig. 57.[175]

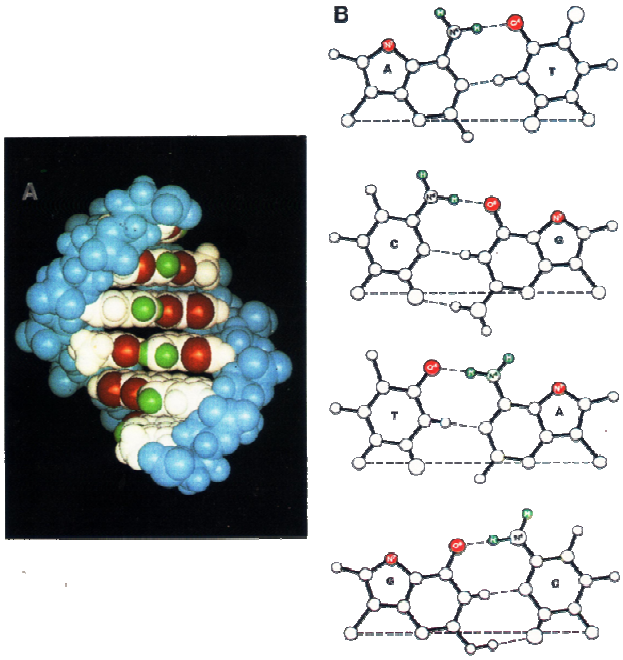

Fig. 57: Model of the Major Groove of a DNA Double Helix.
a) Hetero atoms (red) and hydrogen atoms (green) of nucleobases accessible via the major groove, b) Corresponding base pairs.

It is noticeable that the major groove prominently displays hydrogen atoms (green) as well as hetero atoms (red) of nucleobases, which in their function as hydrogen-bond donor and acceptor provide the identifying feature for the sequence specific binding. It might be possible, that alike interactions could lead to a stabilization of transition states of organic reactions. The major groove, which is close to the helical structure, could in such a scenario be capable to act as enantioselective discriminator. Hence we considered it to be the ideal location for DNA-supported catalysis. Another advantage of this position is its good accessibility for substrates. In order to force the formation of the transition state to take place deep inside the major groove we were aiming at modifying a single nucleobase position of double-stranded synthetic and hence well defined DNA by a ligand. Two different strategies towards this goal were followed.

b. Potential Ligands for DNA-Supported Catalysis

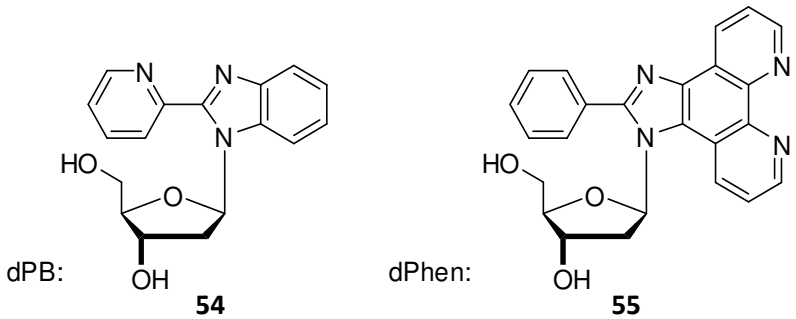

Fig. 58: Envisaged Nucleosides dPB (54) and dPhen (55).

In the initial approach we were aiming at placing the catalytic site directly inside the major groove of DNA by replacing a single nucleobase with a ligand. For this purpose we envisaged the two

nucleosides dPB (**54**) and dPhen (**55**). In both cases the chelator, a bidentate nitrogen ligand, is directly coupled to 2-deoxyribose via a glycosidic bond. The nucleosidic sugar warrants a straightforward conversion to compatible building blocks for DNA synthesis on solid support by the phosphoramidite approach.

With the second strategy we focused on the C5 position of thymidine, a position which we previously had identified to be well suited for the attachment of DNA modifications (Chapter: 5'-Amino-5'-deoxythymidine 29 on page 37). While opposing the hydrogen bonds of base pairing it protrudes into the major groove, making it a great coupling site for a ligand. A general concept of such a nucleoside is depicted in Fig. 59.

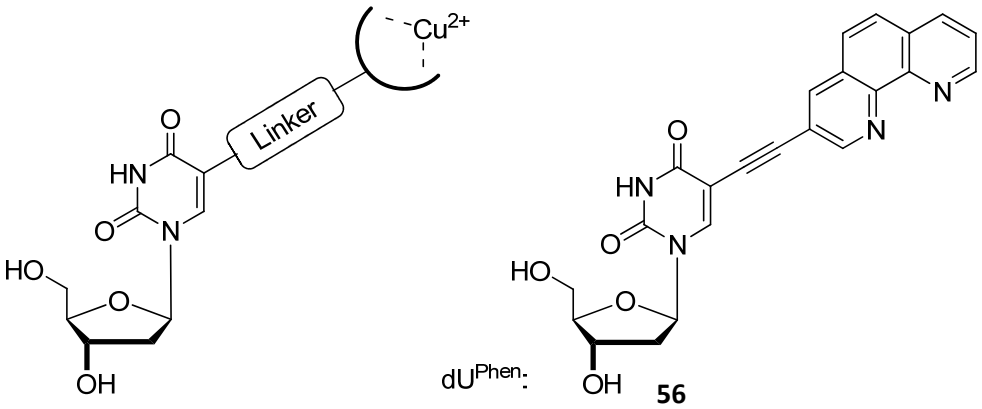

Fig. 59: C5-Modification of Pyrimidines.
Left: General concept for chelator bearing pyrimidines; Right: 1,10-phenanthroline bearing 2'deoxyuridine derivative dU^{Phen} (**56**).

Different linker units would allow varying the distance between ligand and helical structure. The 2'-deoxyuridine derivative dU^{Phen} (**56**) is one example for such a nucleoside. It features 1,10-phenanthroline as bidentate nitrogen ligand, which is coupled via a short alkine linker to the C5 of 2'-deoxyuridine. The 1,10-phenanthroline-containing oligonucleotide was originally applied by Tor *et al.* in fluorescence measurements,[176] but it would also make an interesting ligand system for our purpose.

In order to evaluate the effectiveness of DNA as enantiomeric discriminator one essential criterion for ligands in DNA-supported catalysis is their achiral structure. Only achiral catalysts qualify for the DNA-supported catalysis, since on its own they can produce nothing else than racemic product mixtures. Therefore one can be sure that any enantiomeric excess observed with such catalysts in combination with DNA originates from the chiral scaffold and not from the catalyst itself. The two bidentate nitrogen ligands 1,10-phenanthroline and pyridylbenzimidazole both comply with this criteria. Besides they are great ligands for catalytically active Cu^{2+}-complexes, displaying a good binding affinity towards Cu^{2+}-salts.

3.3. Synthesis of Modified Building Blocks

a. Introduction of Chelators via Glycosylation

Chelator: 2-(2-Pyridyl)benzimdazole

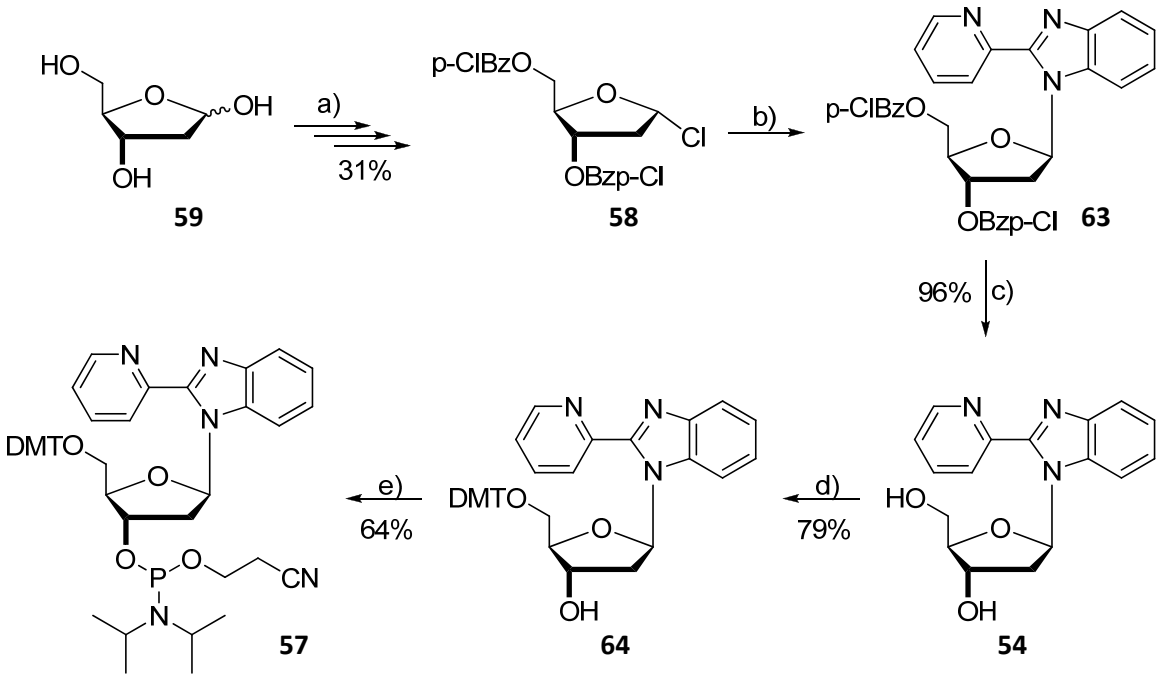

59 58 63 57 64 54

Scheme 30: Synthesis of dPB (54) and Its Corresponding Phosphoramididte 57.

a) See Scheme 31 for details, 31%; b) see Table 2 for reaction conditions; c) NH_3 sat. MeOH, 0°C → rt., 2h, 96%; d) DMAP (0.25 equiv.), pyridine, DMT-Cl (1.5 equiv.) in pyridine, NEt_3 (2.0 equiv), rt, over night, 79%; d) diisopropylammonium tetrazolide (0.75 equiv.), CH_2Cl_2, $(i\text{-}Pr_2N)_2\text{-}POCH_2CH_2CN$ (2.6 equiv.), rt, 2h, 64%; the product (**57**) was stored under argon at –20°C.

The synthetic pathway to nucleoside **54** and its conversion into phosphoramidite **57** is outlined in Scheme 30. In the first part the Hoffer α-chloro sugar like unit **58** was prepared. Such α-chloro sugars are widely used in the synthesis of nucleoside analogs.[177] The synthesis of **58** followed a three step procedure (Scheme 31). In the first step 2-deoxy-α/β-D-ribose (**59**) was treated with a solution of anhydrous HCl (1%) in MeOH to give 1-*O*-methyl-2-deoxy-α/β-D-ribose (**60**). Under these conditions the formation of the desired furanose ring is favored over the pyranose ring.[178] After neutralization with pyridine and evaporation of the solvents, the crude product was repeatedly dried by means of azeotropic coevaporation in order to remove traces of remaining MeOH.

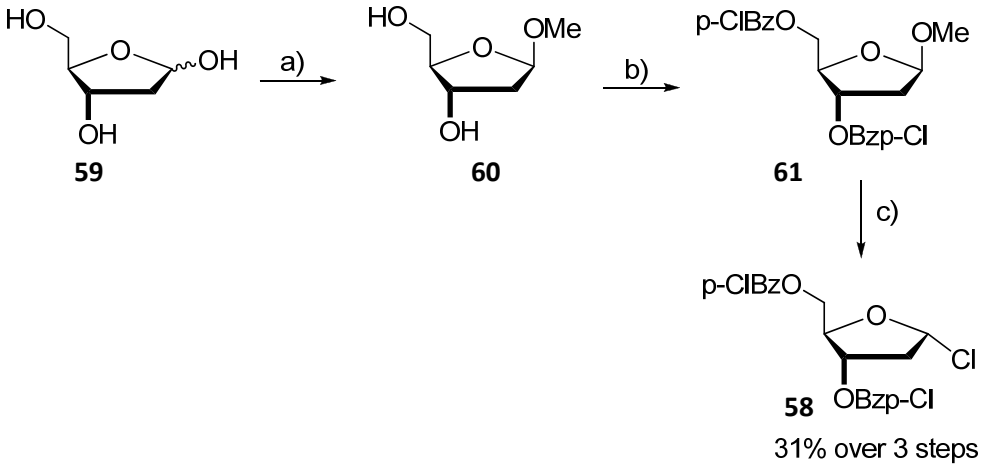

Scheme 31: Synthesis of the α-Chloro Sugar 58.

a) MeOH, 1% HCl in MeOH, rt, 45 min; b) *p*-chlorobenzoyl chloride, pyridine, rt, over night; c) (i) toluene, 0°C; (ii) **61**, conc. HOAc, HCl, 31% over 3 steps.

Without further purification **60** was esterified to **61** using 1.2 equivalents of *p*-chlorobenzoyl chloride per hydroxyl group. In the original Hoffer procedure the reaction was performed using *p*-toluoyl chloride instead.[179] However this protecting group leads to an α-chloro sugar, which is often described as unstable oil.[180] It does not matter that the pure 2-deoxy-3,5-di-*O*-*p*-toluoyl-*α*-D-ribofuranosyl chloride **62** actually is a stable white crystalline solid, because tedious work up procedures are needed to remove *p*-toluonic anhydride which is causing the reported decomposition of **62**.[181] This is not the case when *p*-chlorobenzoyl chloride is used instead.[181] Without purification **61** was converted to the readily crystallizing 2-deoxy-3,5-di-*O*-*p*-chloro-benzoyl-α-D-ribofuranosyl chloride **58** by adding an HCl saturated HOAc solution. The overall yield of the three step synthesis was 31%. Higher yields were only possible by using a slightly altered protocol for the last step in which HCl was continuously bubbled through the solution of **61** in ice cold HOAc. However, due to the fact that concentrated HOAc crystallizes at temperatures below 0°C the route posed an unnecessary safety hazard and was therefore avoided. The pure **58** was stored under vacuum over NaOH and remained stable over the course of time.

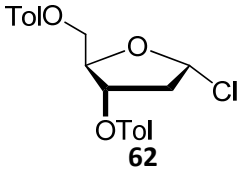

Fig. 60: Hoffer α-Chloro Sugar 62.

Coupling of 2-(2-pyridyl)benzimidazole to 2-deoxy-3,5-di-*O*-(*p*-chlorobenzoyl)-*D*-ribofuranosyl chloride (**58**) via glycosylation led to the desired 2'-deoxyribosyl-pyridylbenzimidazole **54**.[182] The stereogenic outcome of the glycosylation depended strongly on the reaction conditions (Table 1). The β/α-anomeric ratio was determined by ^{1}H-NMR and chiral ADH-HPLC of the crude product.[183] A typical attribute for differentiation of anomers was the ^{1}H-NMR shift of 4'- and the 5' proton. The signals are well separated in the spectrum of the α-anomer [δ = 4.60 (5'-H), 5.01 (4'-H)] but coincide for the β-anomers [δ = 4.52 (4'-H), 4.81 (5'-H)]. Another indication for the stereo configuration was the C-H COSY of **54**, which revealed an additional coupling of the anomeric proton with an aromatic proton of 2-(2-pyridyl)benzimidazole.[184]

Table 2: Reaction Conditions for the Glycosylation.

Entry	Reaction Conditions	Yield[a)]	β/α Ratio[b)]
1	(i) 2-(2-pyridyl)benzimidazole, Bu_4NHSO_4 (0.5 equiv.), CH_2Cl_2, NaOH (50%); (ii) **58** (1.1 equiv.) in CH_2Cl_2, 2 min, shaking.[184]	76%	2:1
3	(i) 2-(2-pyridyl)benzimidazole, DBU (1.2 equiv.), CH_3CN, rt, 20 min; (ii) **58** (1.0 equiv.), 1 h, rt.[185]	47%	1:1.5
2	(i) 2-(2-pyridyl)benzimidazole, NaH (1.5 equiv.), CH_3CN, rt, 9 h; (ii) 0°C, **58** (1.9 equiv.) in CH_2Cl_2, 18 h → rt.[182]	92%	3:1

a) Combined yields of α and β anomers, b) Determined by chiral ADH-HPLC (heptane/EtOH = 2:8) t_R(β-anomer) = 23 min, t_R(α-anomer) = 36-37 min or by ^{1}H-NMR ($CDCl_3$) signal of the 3'-H [δ = 5.01 for 3'-H (α-anomer) and 5.71 for 3'-H (β-anomer)].

Mimicking naturally occurring nucleosides we were only interested in the β-anomers. Best results, regarding anomeric ratio and yield, were achieved by using NaH as base to deprotonate 2-(2-pyridyl)benzimidazole before adding the α-chloro sugar **58** at 0°C. The pure β-anomer **63** was then obtained by selective crystallization in MeOH out of the mixture of the α- and β- isomer. Deprotection of the *p*-ClBz group with NH_3/MeOH yielded nucleoside **54** (dPB).[186] The glycosidic linkage in this compound proofed to be completely stable towards all chemical procedures, applied during synthesis of DNA on solid support by the phosphoramidite approach, including the deprotection with conc. ammonia.[2]

The transformation of dPB (**54**) into the corresponding phosphoramidite **57** was achieved by regioselective protection of the 5´-OH with DMT-Cl yielding compound **64**, followed by phosphinylation at the 3´-position with (2-cyanoethoxy)-bis-(*N,N*-diisopropylamino)phosphine in the presence of diisopropylammonium tetrazolide. The oxidation state of the phosphours group was verified by ^{31}P-NMR to be that of P(III) with a typical shift of δ = 150 ppm in $CDCl_3$. The thus obtained modified DNA building block **57** was stored at –20°C under argon.

Chelator: Phenanthroline

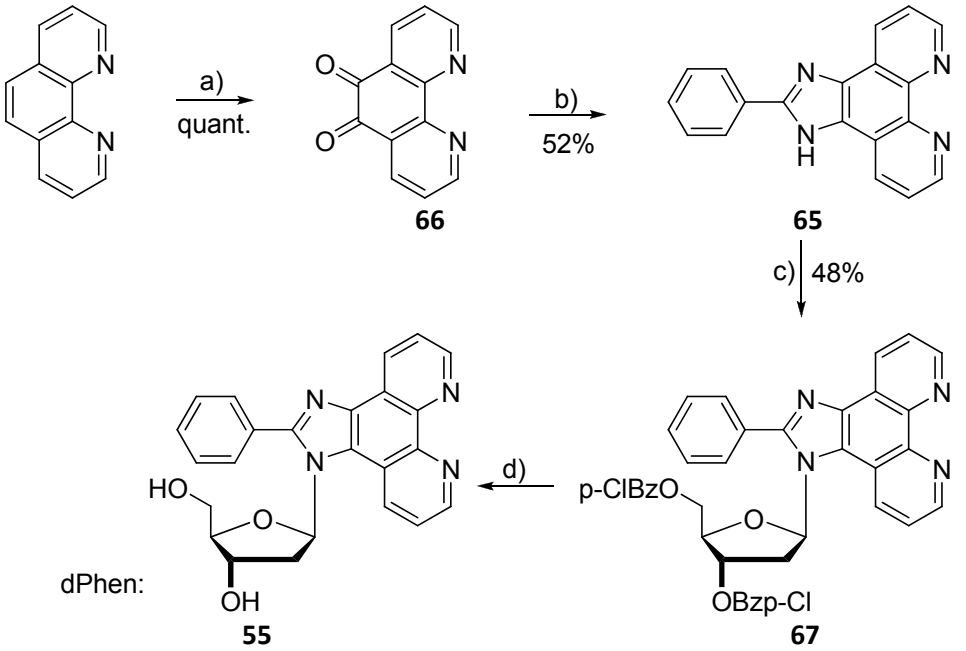

Scheme 32: Synthesis of Nucleoside dPhen (55).

a) 0°C, conc. H_2SO_4, conc. HNO_3, 85°C, 2h, quant; b) (i) HOAc, NH_4OAc (35 equiv.), benzaldehyde (3 equiv.), rt., 2.5 h; (ii) 125°C 3 h, 52%; c) (i) NaH (1.5 equiv.), CH_3CN, rt, 10 h; (ii) 0°C, **58** (1.8 equiv.) in CH_2Cl_2, 22 h → rt, 48%; d) for conditions see Table 3.

A similar synthetic approach was considered for the synthesis of nucleoside **55**. Its ligand **65** was prepared in just two steps starting from 1,10-phenanthroline. First, 1,10-phenanthroline was oxidized to the dione **66** by a 2:1 (v/v) mixture of concentrated sulfuric acid and concentrated nitric acid.[187, 188] During the addition of the acids the reaction mixture had to be cooled by an external ice bath. Especially sulfuric acid had to be added very slowly in order to achieve good yields. The bright yellow dione **66** was then treated with benzaldehyde in the presence of ammonium acetate and acetic acid to form the imidazole **65**. The mechanism of the ring closure is shown in Scheme 33.[189]

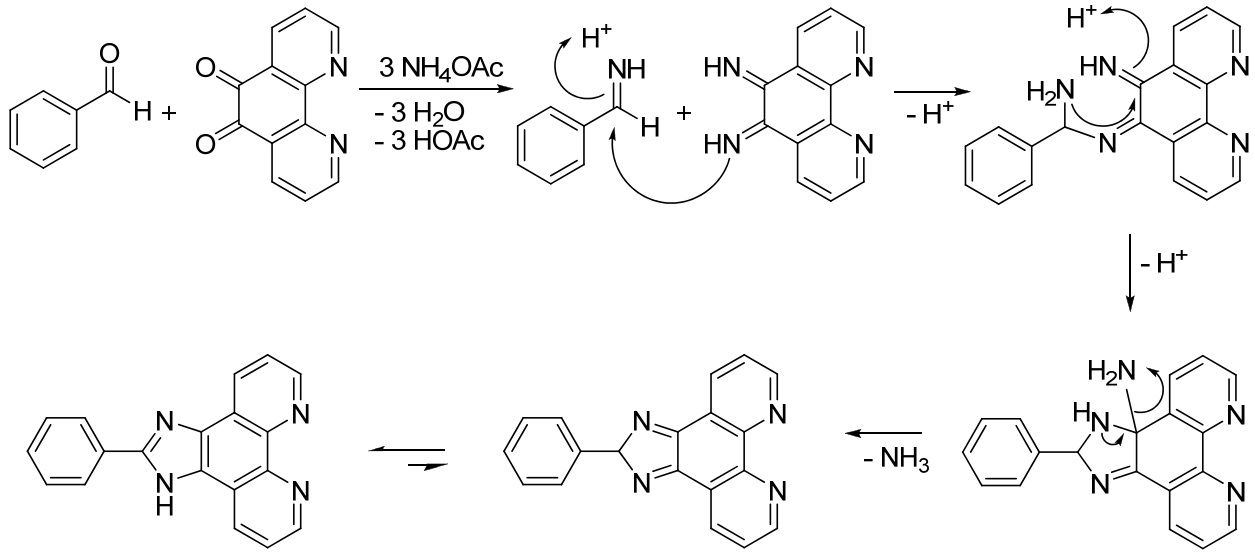

Scheme 33: Mechanism of Imidazole Synthesis.

Ammonium acetate facilitates the conversion of the carbonyl groups into imines. Acid catalyzed, one of the diimine nitrogens can then inter-molecular attack the imine carbonyl resulting in a diimine-amine. In the next step the ring system is closed by an equally acid catalyzed intra-molecular attack of the newly formed amino group at the second imino carbonyl. Cleavage of ammonia leads to a diimine which finally tautomerizes to an imidazole.

Glycosylation of the α-chloro sugar **58** with the 1,10-phenanthroline based ligand **65** was done using the same method that had proven to yield the best conversion and α/β-anomer ratio for 2-(2-pyridyl)benzimidazole.[182] Using imdazole **65** as nucleophile resulted in **67** however with a lower yield of 47.6% and only a 1:1 α/β-anomer ratio. Separation of the anomers by selective crystallization or by column chromatography was not possible. Hoping to solve this problem at a later stage we used the anomeric mixture in the following deprotection step of the 5'- and 3'-hydroxyl groups. To our surprise this step turned out to be crucial since the standard conditions (NH_3 saturated MeOH) resulted in the decomposition of the compound. Many different deprotection protocols were tested (Table 2), most of them failed for the same reason.

Table 3: Deprotection Conditions for 67

Entry	Deprotection Conditions	Result
1	MeOH sat. with NH_3, rt, 2h.[186]	decomposition
2	TMSI (3 equiv.), CH_2Cl_2, –30°C[190]	decomposition
3	K_2CO_3 (2 equiv.), CH_2Cl_2[191]	decomposition
4	NH_3 (2equiv.), MeOH, rt, 4h.	Product formation detected by MS

Only by using exactly one equivalent of NH_3 per protecting group in anhydrous methanol enabled us to isolate small quantities of nucleoside **55** (dPhen), as detected by MS. Anyhow, this material proofed to be fairly unstable and therefore not suited for DNA synthesis. The lability of **55** might be caused by the steric demand of the big 1,10-phenanthroline ring system.

b. Introduction of Chelators at C5 of Pyrimidines

Building block dU^{Phen} (**56**) represents the second category of ligand-bearing nucleosides, which we wanted to apply to DNA-supported catalysis. The ligand in these nucleosides is coupled to a nucleobase instead of replacing it, which enables them to do base pairing.

The synthesis route towards building block **56** is outlined in Scheme 34. The reported procedure starts with the commercially available 5-iodo-2'-deoxyuridine (**35**), to which silyl protected ethylene is coupled via a palladium-catalyzed cross coupling providing 5-ethynyl-2'-deoxyuridine (**68**).[176, 192, 193] The reaction is followed by a second cross coupling with 3-bromo-1,10-phenanthroline.[194-196]

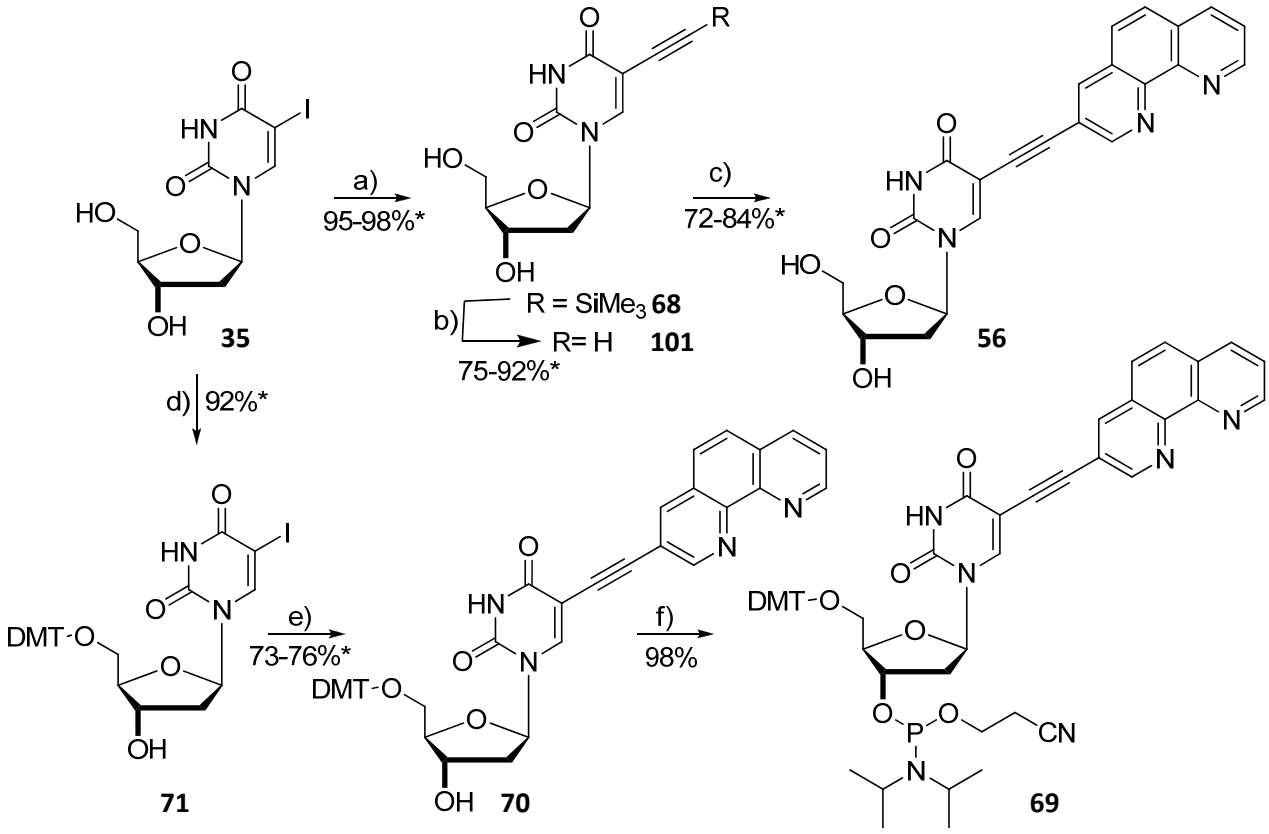

Scheme 34: Synthesis of Nucleoside dU^{Phen} (56) and Its Phosphoramidite 69.
a) (i) $(CF_3CO)_2O$; (ii) $Me_3SiC{\equiv}CH$, $(Ph_3P)_4Pd$, CuI, DMF, Et_3N, 95-98%*; b) K_2CO_3, MeOH, 75-92%*; c) 3-bromo-1,10-phenanthroline, $(dppf)PdCl_2$, CH_2Cl_2, CuI, DMF, Et_3N, 72-84%*; d) 4,4'-dimethoxytrityl chloride (DMT-Cl), DMAP, pyridine, Et_3N, 92%*; e) 3-ethynyl-1,10-phenanthroline (**72**), $(dppf)PdCl_2$, CH_2Cl_2, CuI, DMF, Et_3N, 73-76%*; f) $(i\text{-}Pr_2N)_2\text{-}POCH_2CH_2CN$ (2.6 equiv.), diisopropylammonium tetrazolide (0.75 equiv.), CH_3CN, 98%. *Literature yields.[194]

In order to obtain the corresponding phosphoramidite **69** an alternative synthesis route was advantageous. The original reaction conditions of this synthesis route as published by Tor *et al.*[194] were evaluted by our group member Sandra Barudio; who performed the synthesis of **70**.

Synthesis started by treating 5-iodo-2'-deoxyuridine (**35**) with 4,4'dimethoxytrityl chloride in oyridine in the presence of DMAP which facilitated the regio selective protection of the 5'-hydroxyl group. Cross coupling of the DMT-protected nucleoside **71** to 3-ethynyl-1,10-phenanthroline **72**

than gave **70**, which was phosphinylated with (2-cyanoethoxy)-bis-(*N,N*-diisopropylamino)phosphine in the presence of diisopropylammonium tetrazolide to yield phosphoramidite **69.** The oxidation state of the phosphorus group was verified by ^{31}P-NMR to be that of P(III) with a typical shift of δ = 148 ppm in CD_3CN: The thus obtained modified DNA building block **69** was stored at –20°C under argon.

3.4. DNA-Synthesis

The novel modified DNA building block **57** as well as the modified building block **69** proofed to be fully compatible with standard DNA synthesis, their glycosidic linkage had been tested towards all chemical procedures, applied during DNA synthesis on solid support by the phosphoramidite approach, including the deprotection with concentrated ammonia.[176]

In preliminary experiments the coupling efficiency of both nucleotides was evaluated and building blocks **57** and **69** could be coupled with high efficiency comparable to standard phosphoramidite building blocks. Their application in the automated DNA synthesis was also possible by using stock solution of the phosphoramidites in anhydrous acetonitrile. The best results were obtained with a concentration of 68 mM for **57** and 81 mM for **69** and a standard coupling time of 1.6 minutes. At –20°C and under argon these solutions could be stored for several months without deterioration of quality.

a. Alterations to the DNA-Synthesizer and its Priming Protocol

The Expedite DNA Synthesizer 8909 is a wonderful tool for automation of the repetitive coupling steps in the DNA synthesis cycle. It is capable of running two independent oligonucleotide syntheses simultaneously. Due to this fact and because of its high precision it is able to perform synthesis much faster using less solvent and reagents than it would ever be possible by manual DNA synthesis. Besides, it offers up to five positions for modified DNA building blocks next to the four standard ones. The only real downside originates from the need to purge all lines and valves prior to the synthesis. Especially for the phosphoramidite lines this results in the loss of valuable material, which in our case was not acceptable because of the sheer never ending amounts of oligonucleotides needed for DNA-supported catalysis and the constant scarcity in modified building blocks **57** and **69**. Inspired by a protocol on using minor bases on an Expedite Synthesizer two measures were taken to keep the loss at a minimum level.[197] On the one hand we tweaked the purging protocol and on the other hand we modified a single phosphoramidite position to perfectly suite our needs.

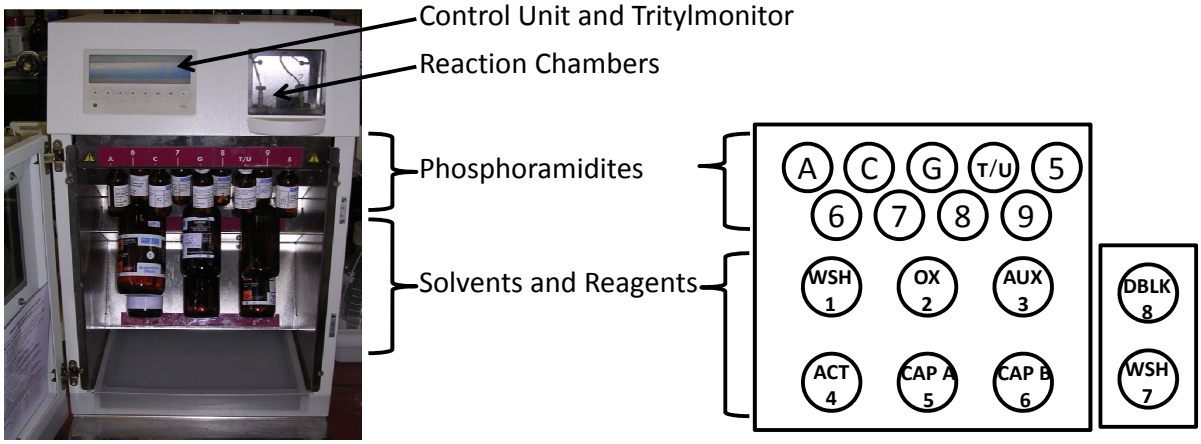

Fig. 61: Expedite 8909 DNA Synthesizer.

Right: Photo of the synthesizer. Left: Layout of vial positions: A, C, G, T/U: standard phosphoramidites, 5-9 modified phosphoramidites (position 5 allows fopr prolonged coupling times of 15 minutes, position 9 was modified to suite 3 ml V-shaped Wheaton vials), WSH1 anhydrous acetonitrile, OX2 oxidation solution, AUX3 empty, ACT4 activation solution, CAPA5 capping solution A, CAPB6 capping solution B, DBLK8 detritylation solution, WSH7 acetonitrile.

The general purging procedure (Prime All) for the Expedite 8909 is accessible via the priming menu. It is designed to deliver 160 µl per priming step irrespective of the solvent or reactant. The priming procedure is usually repeated three times for both reaction columns to dry and fills the lines. Overall this equales to 960 µl of solvent volume for each position. In the original protocol purging of the reactant lines is done utilizing the corresponding phosphoramidite solution, wasting over 8 times the amount needed for one coupling step (Table 4). This is unnecessary, since drying of the tubing can just as well be performed by anhydrous acetonitrile as long as all lines are thereafter filled with the correct phosphoramidite solution. This more elaborate protocol was followed for the modified building blocks after all other lines had been purged using the standard "Prime All" procedure.

At the position of modified building blocks we therefore inserted a vial with 3 ml anhydrous acetonitrile and thoroughly dried the lines by using first the "FLOW" command in "Tools"-"Diagnostic"-"Fluids" mode once and then repeating the "Volume" command until all solvent was used. In order to prevent any dilution of phosphoramidite stock solutions with anhydrous acetonitrile still present in the lines, lines were filled with argon by repeating the "Volume" command three more times with the now empty vial in place. Next, the phosphoramidite solution of the modified building block was inserted and the lines were filled with this solution using the "Prime Individual" mode, which delivers 320 µl solvent in 20 pulses. After 9-10 pulses the reactant line with a previously determined volume of 144 µl, was sufficiently filled and the "Prime Individual" mode was canceled.

Table 4: Expedite 3909 Volume Chart.

Mode	Volume delivered per step	Pulses per step[a)]
Prime All	160 µl	10
Prime Individual	320 µl	20
Amidite Coupling (1 µmol)	112 µl	7
Amidite Coupling (0.2 µmol)	80 µl	5

a) The Expedite 8909 delivers volumes by pulses; one pulse corresponds to approximately 16 µl.

In addition to changing the purging procedure we also modified position 9 of the Expedite 8909 to allow the insertion of 3 ml V-shaped vials (Wheaton V-vial, catalogue no. 986277). First the tubing was twisted and shortened accordingly to fit into the vial. Second, the filter was cut back to the smallest size possible with a razor blade, which minimized the amount of phosphoramidite lost in the frit. Before inserting the 3 ml vial at thus modified position 9 the neighboring vial (vial 8) had to be removed to lower the system wide argon pressure. Otherwise, argon gas flow was too high to allow a spill-free insertion of small vials.

a)

b)

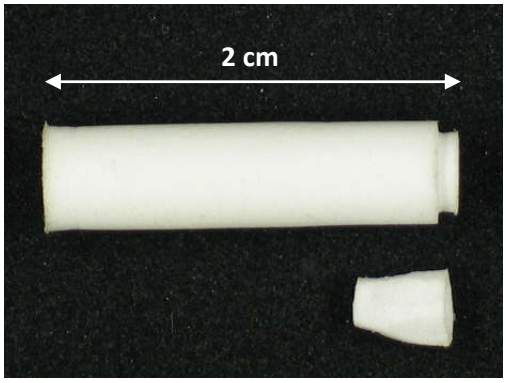

Fig. 62: Alterations to the Expedite 8909 DNA Synthesizer.
a): V-shaped 3ml Wheaton vial for minor bases at position 9; b): Standard filter tip (above), minimized filter tip (below).

By using the above mentioned alterations we were able to yield the maximal number of coupling steps for our modified building blocks **57** and **69**. Oligonucleotide syntheses were carried out until all material was used up, thereby preventing the repetition of the purging procedure.

b. Synthesized Oligonucleotide Sequences

Even though all catalytic reactions were performed on a µl-scale 2-3 DNA syntheses (1 µmol scale each) were needed to afford enough material for the catalytic reactions. Only the above protocols in combination with the high coupling efficiency of the two modified DNA building blocks **57** and **69** allowed us to carry out oligonucleotide syntheses which resulted in the amounts but also in the high quality needed for DNA-supported catalysis.

Compound **57** was used to synthesize the two dPB modified oligonucleotides **73a** (14mer) and **74a** (30mer). Both sequences were chosen in such a fashion as to keep the base sequences surrounding the modification identical. The same sequences were also synthesized using **69** as modification yielding in oligonucleotide **73b** (14mer) and **74b** (30mer). For comparison, the two pertinent unmodified oligonucleotides **73c** (14mer) and **74c** (30mer) with thymine instead of a modified nucleobase were synthesized as well. Together with the two complementary oligonucleotides **75** and **76** this led to the double-stranded constructs **77a,b,c** and **78a,b,c**, respectively (Fig. 63).

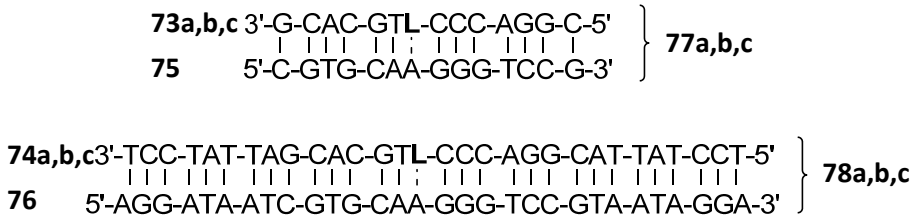

Fig. 63: Formation of the Hybrids 77a,b,c and 78a,b,c Applied to the Investigations.
L = dPB **57** (a), dU^{Phen} **69** (b), Thymidine (c).

The NH_4^+ counterion of all synthesized oligonucleotides was exchanged by K^+ after deprotection with concentrated ammonia. Excess salts were removed by size exclusion chromatography with NAP columns containing a Sephadex G-25 DNA resin as solid phase. Two different types of NAP™ column were used: NAP™10 and NAP™25. The latter can handle an increased sample volume of up to 2.5 ml whereas NAP™10 is applicable for 1.0 ml sample volume with 1 mg/ml DNA. In an effort to increase purification efficiency samples of up to three sequence-identical DNA syntheses were combined, dissolved in 1 ml H_2O (MilliQ) and desalted on NAP™25 columns. However this led to a higher loss in material than purifying the samples separately on NAP™10 columns and was therefore discontinued.

Using these techniques an average yield of 43% for the 14-mer oligonucleotides and 28% for the 30-mer oligonucleotides were achieved.

3.5. Analysis of Synthetic DNA

a. HPLC and PAGE

All synthesized oligonucleotides were obtained in pure form as analyzed by IE-HPLC as well as by analytical polyacrylamide gel electrophoresis (PAGE).

HPLC runs of oligonucleotides were performed on a Merck/Hitachi system, using an ion exchange column type DNAPAc-PA-100 column by Dionex with a diameter of 4 mm and a length 250 mm. The mobile phase was a gradient of A = 20 mM KH_2PO_4 in $CH_3CN:H_2O$ = 1:4 at pH 6.0, B = 1 M KCl, 20 mM KH_2PO_4 in $CH_3CN:H_2O$ = 1:4 at pH 6.0. All solvents were prepared freshly, filtered and degassed prior to applying them on the HPLC. The column was heated to 80°C during HPLC runs. Analysis of the 14mer oligonucleotides (**73a,b,c**, **75**) was done using a gradient of 10-70% solvent B within 35 minutes[HPLC method 1 (See chapter: HPLC on page 131)]

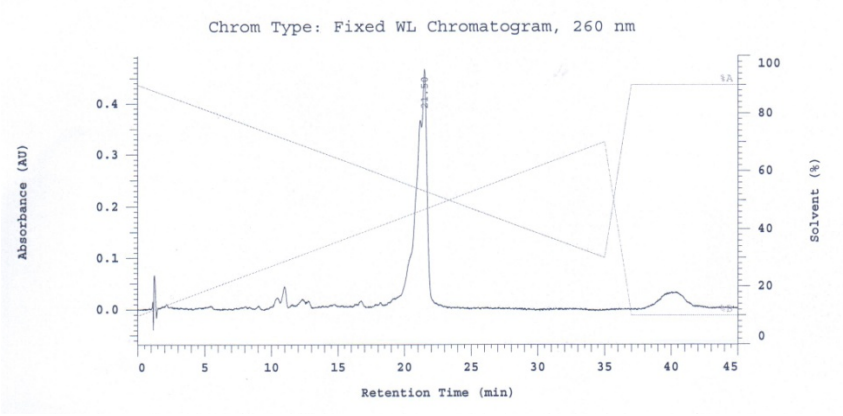

Fig. 64: Analytical HPLC of crude dPB modified 14mer 73a.
t_R (**73a**): 21.5 min

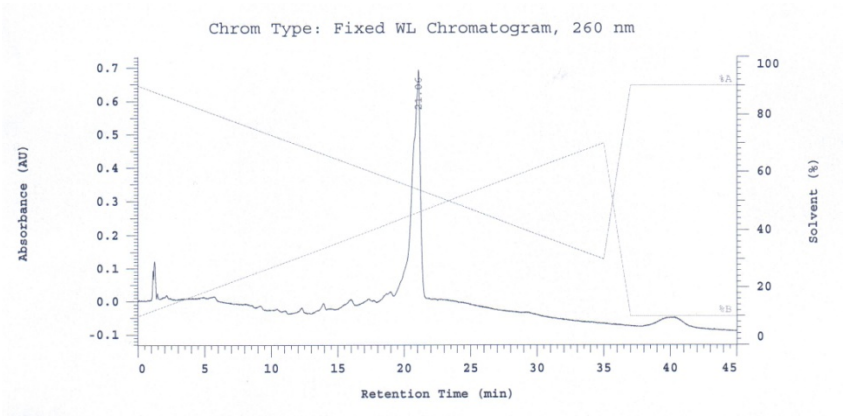

Fig. 65: Analytical HPLC of crude unmodified 14mer 73c.
t_R (**73c**): 21.1 min.

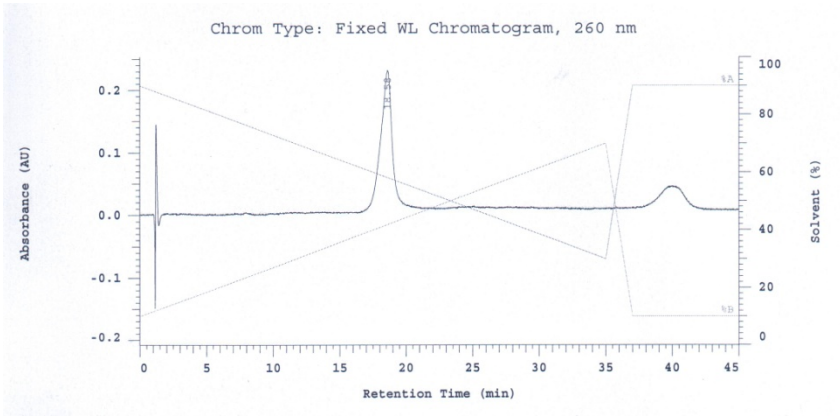

Fig. 66: Analytical HPLC of crude complementary 14mer 75.
t_R (**75**): 18.6 min.

Oligonucleotides **74b** and **73b** bearing the 1,10-phenanthroline modification had to be treated with an excess of Cu^{2+}-salt in order to obtain a distinct HPLC signal. Without the Cu^{2+}-additive no analyzable spectra were possible, probably due to the high affinity of 1,10-phenanthroline to different metal salts, leading to undefined mixtures of complexes.

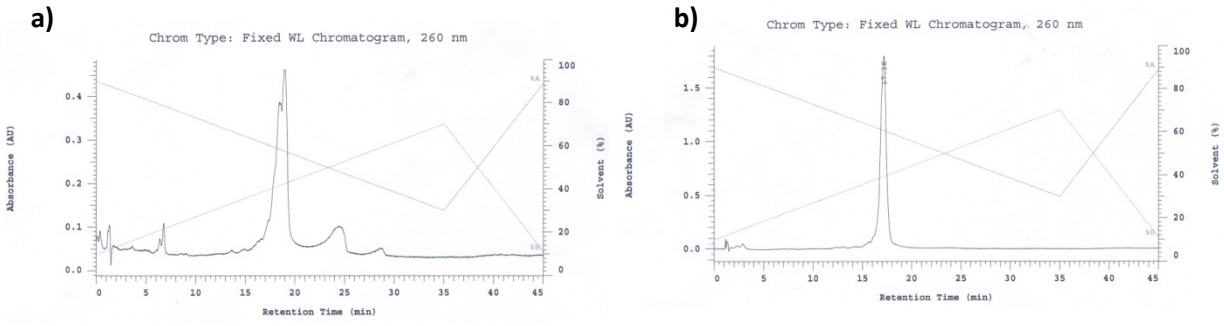

Fig. 67 Analytical HPLC of crude dU^{Phen} modified 14mer 73b.
a) Spectrum of **73b** without Cu^{2+} additive. b) Spectrum of **73b** with Cu^{2+} additive; t_R (**73b**): 17.2 min.

The 30mer oligonucleotides (**74a,b,c**, **76**) were analyzed using a 20-80% gradient of solvent B within 35 minutes [HPLC method 2 (See chapter: HPLC on page 131)].

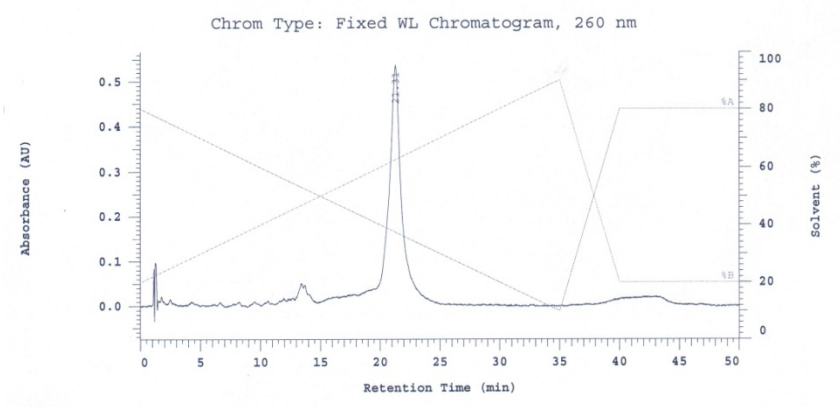

Fig. 68:Analytical HPLC of crude dPB modified 30mer 74a.
t_R (**74a**): 21.3 min.

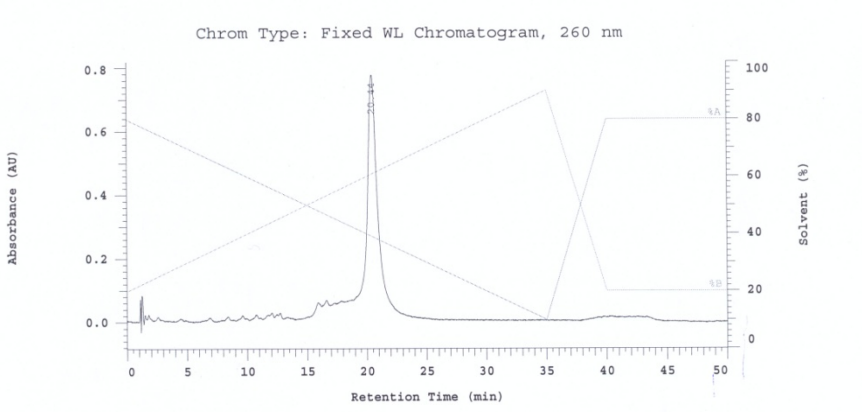

Fig. 69: Analytical HPLC of crude dU^{Phen} modified 30mer 74b.
Spectrum of **74b** with Cu^{2+} additive, t_R (**74b**): 20.4 min.

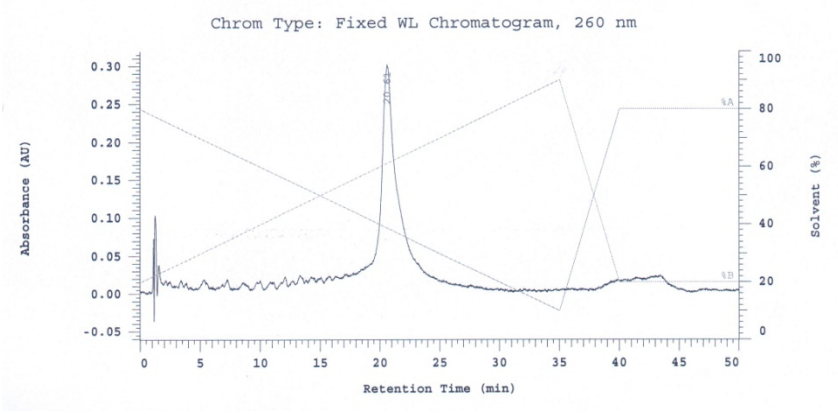

Fig. 70: Analytical HPLC of crude unmodified 30mer 74c.
t_R (**74c**): 20.6 min.

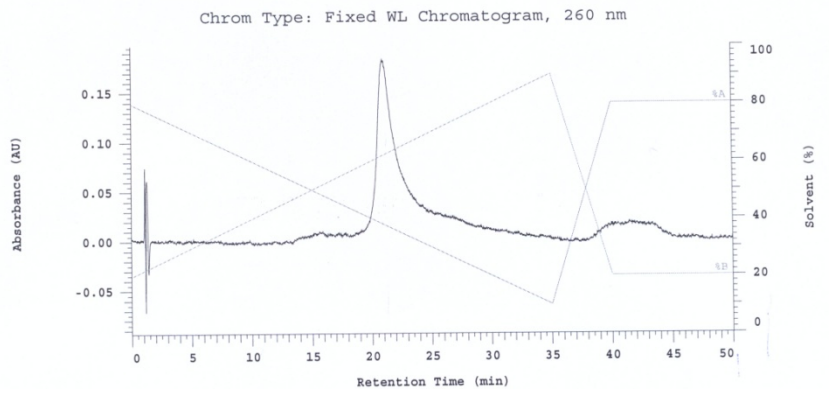

Fig. 71 Analytical HPLC of crude complementary 30mer 76.
t_R (**76**): 21.2 min.

The purity of all synthesized oligonucleotides was verified by analytical polyacrylamide gels.

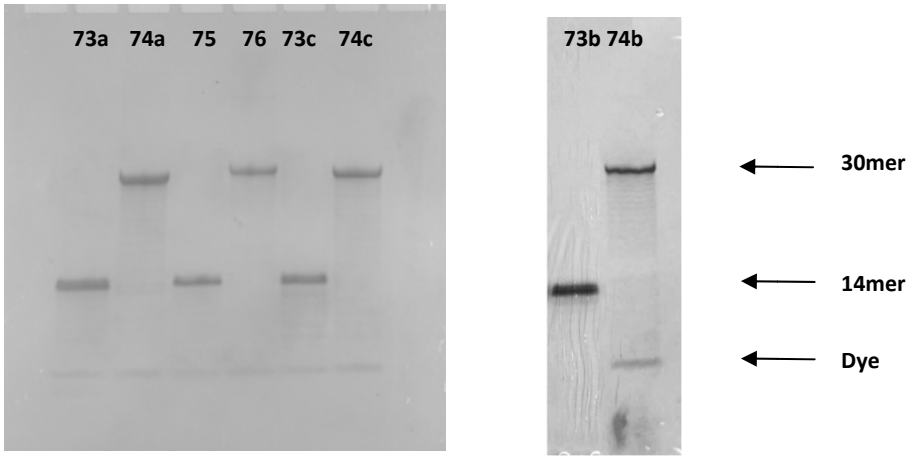

Fig. 72: PAGE of Synthetic Oligonucleotides.

b. Selective Complexation of Cu^{2+}

One essential aspect of our ongoing research in the field of DNA-supported catalysis is the possibility to pinpoint the location of the catalyst within the DNA strand. Therefore we introduced ligands at very specific positions within oligonucleotides, which together with a Cu^{2+}-salt should form catalytical active complexes. DNA however has a multitude of electron donating groups which are known to coordinate metals. Hence their selective complexation at the desired position within the modified DNA had to be verified.

By using UV-spectroscopy we made sure that oligonucleotides having 2-(2-pyridyl)benzimidazole (**73a** and **74a)** or 1,10-phenanthroline (**73b** and **74b**) incorporated lead to specific incorporation of Cu^{2+}. The UV spectrum of the free nucleoside (**54**) displays a prominent absorption band at 287 nm. Upon addition of one equivalent of $Cu(NO_3)_2 \cdot 3H_2O$ this band was shifting to 321 nm. The same shift could also be observed after incorporation of **54** into a DNA strand. To clearly reveal the shift, the predominant absorption of the DNA bases at 260 nm had to be suppressed.[198] Therefore we synthesized the control DNA sequence 3'-d(GCA-CGT-CCC-AGG-C)-5' (**79**) which lacks the nucleoside **54** and subtracted its spectrum from that of ligand-containing DNA **73c**. After addition of 1 equivalent of $Cu(NO_3)_2 \cdot 3H_2O$ the band associated with the bound bidentate ligand was shifting to 320 nm indicating successful complexation of Cu^{2+} (Fig. 73 - Fig. 75)

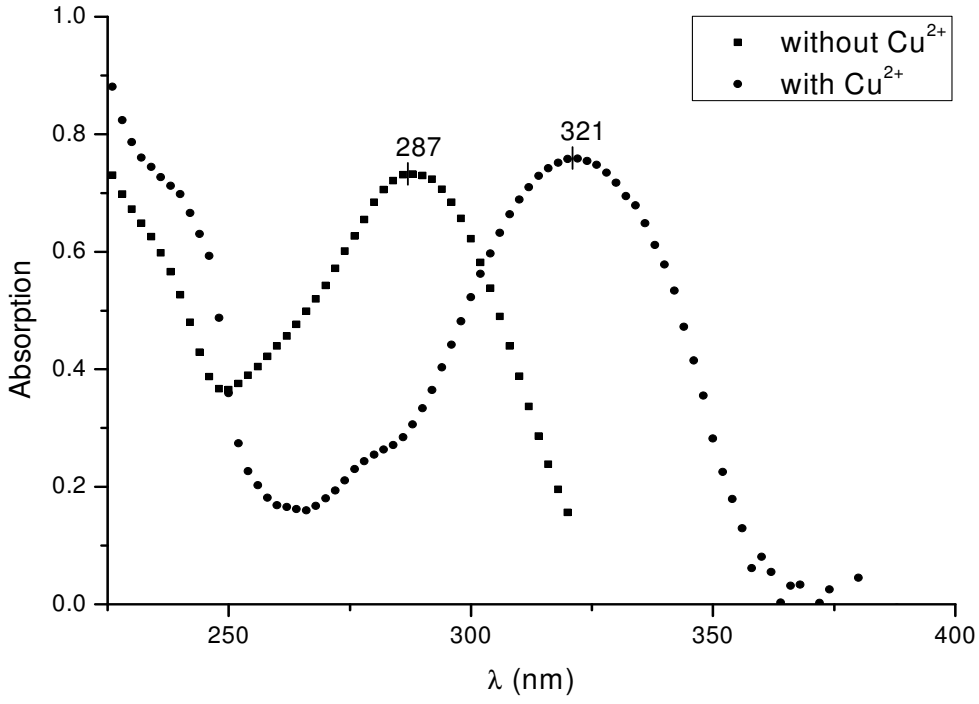

Fig. 73: Absorption Spectra of dPB 54 with and without Cu^{2+}.
■ dPB **54** without Cu^{2+}, • dPB **54** with 1 equivalent of $Cu(NO_3)_2$.

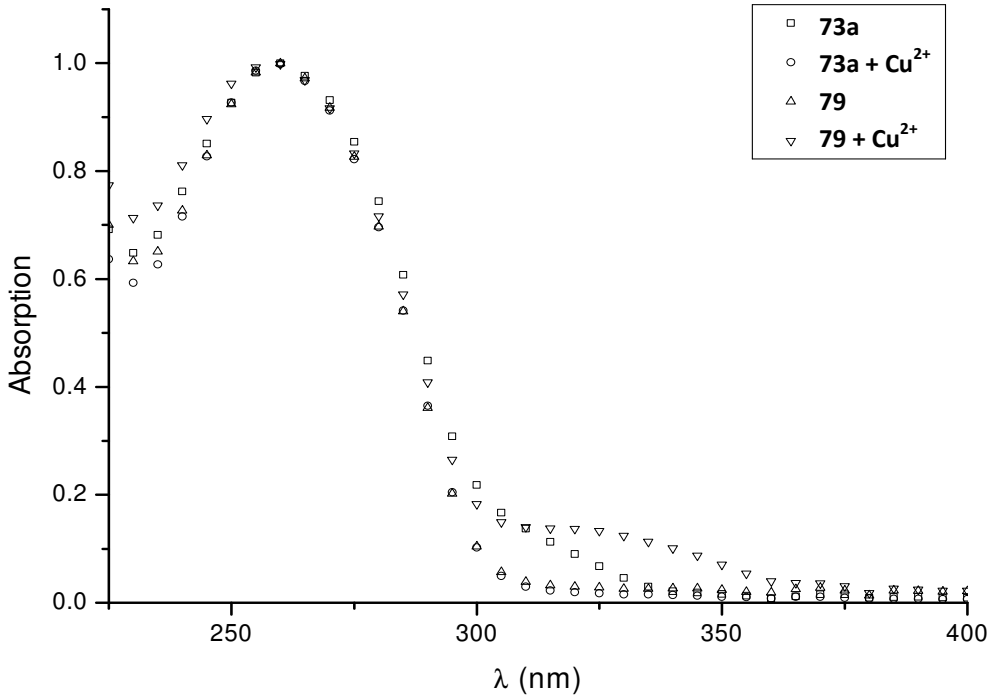

Fig. 74: Absorption Spectra of Oligonucleotides 73a and 79 with and without Cu^{2+}.
☐ **73a** without Cu^{2+}, ○ **73a** with 1 equivalent of $Cu(NO_3)_2$, △ **79** without Cu^{2+}, ▽ **79** with 1 equivalent of $Cu(NO_3)_2$.

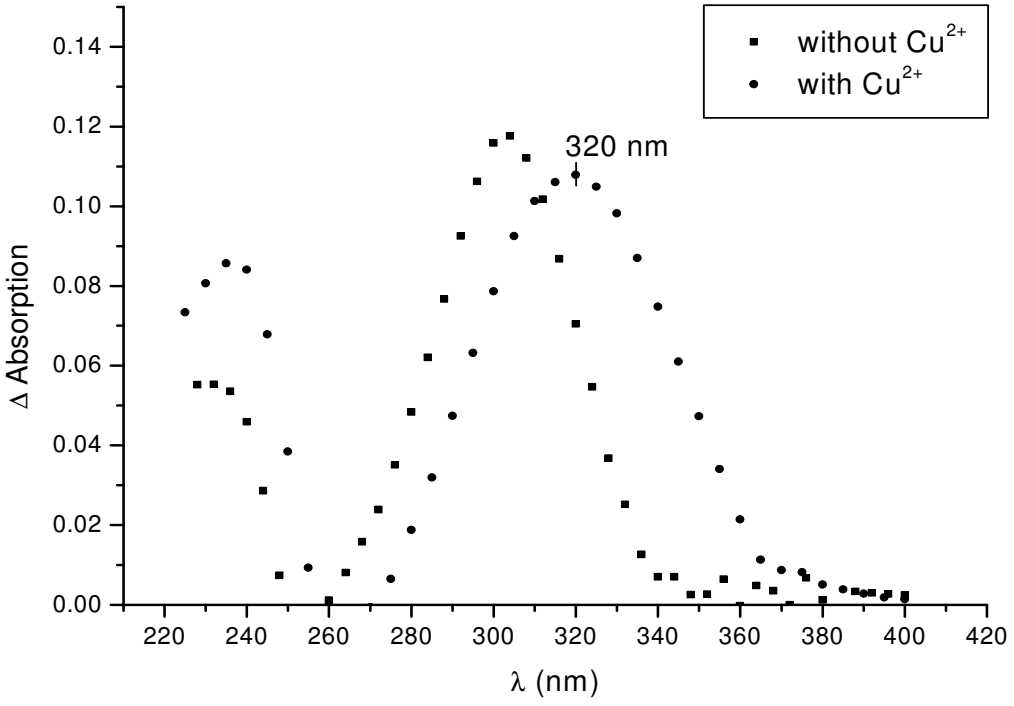

Fig. 75: Absorption Spectra of dPB 54 incorporated in DNA with and without Cu^{2+}.
• dPB **54** in DNA with Cu^{2+}, ■ dPB **54** in DNA without Cu^{2+}.

Homologous spectra were recorded for the 1,10-phenanthroline-containing oligonucleotide **73b** (Fig. 76-Fig. 78). After subtracting from it the spectrum of control sequence **79** the distinct phenathroline maxima at 300 nm and 350 nm became visible. Addition of one equivalent of

$Cu(NO_3)_2 \cdot 3H_2O$ resulted in a shift of the second maximum from 350 nm to 360 nm again indicating successful complexation of Cu^{2+} (Fig. 78).

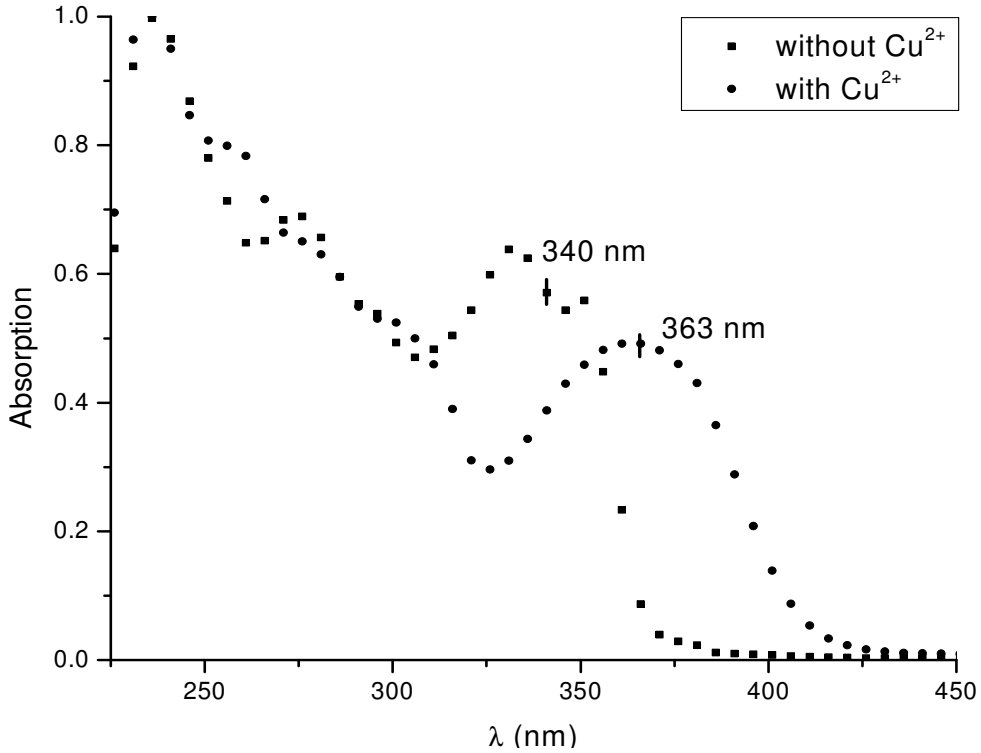

Fig. 76 Absorption Spectra of DMT-dU^{Phen} 70 with and without Cu^{2+}.
■ dPB **70** without Cu^{2+}, • dPB **70** with 1 equivalent of $Cu(NO_3)_2$.

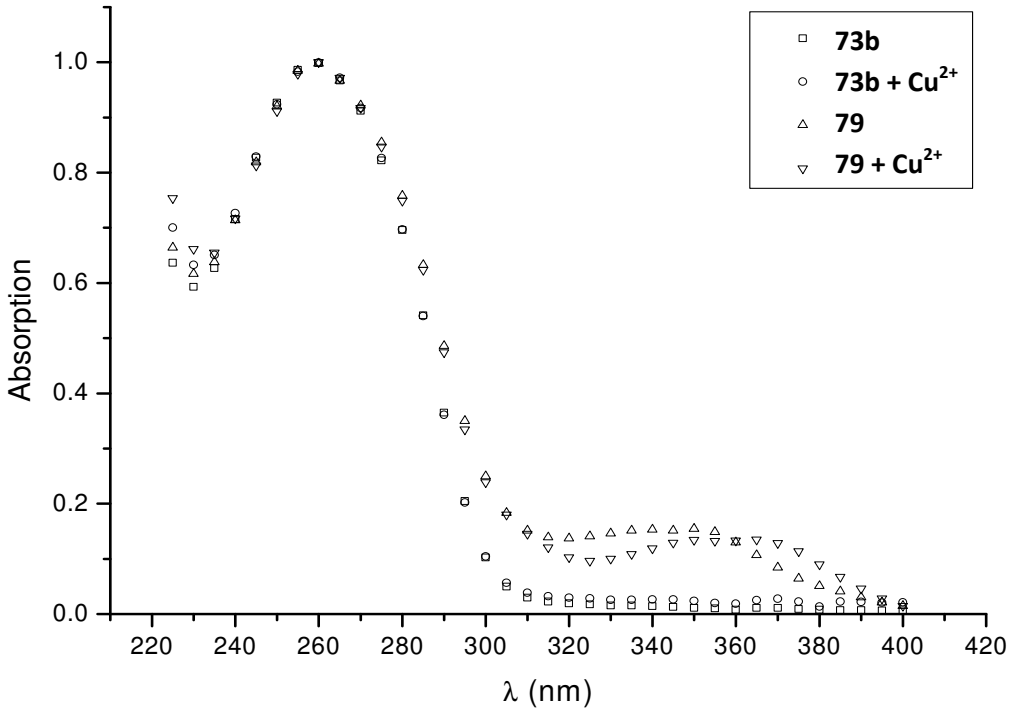

Fig. 77: Absorption Spectra of Oligonucleotides 73b and 79 with and without Cu^{2+}.
□ **73b** without Cu^{2+}, ○ **73b** with 1 equivalent of $Cu(NO_3)_2$, △ **79** without Cu^{2+}, ▽ **79** with 1 equivalent of $Cu(NO_3)_2$.

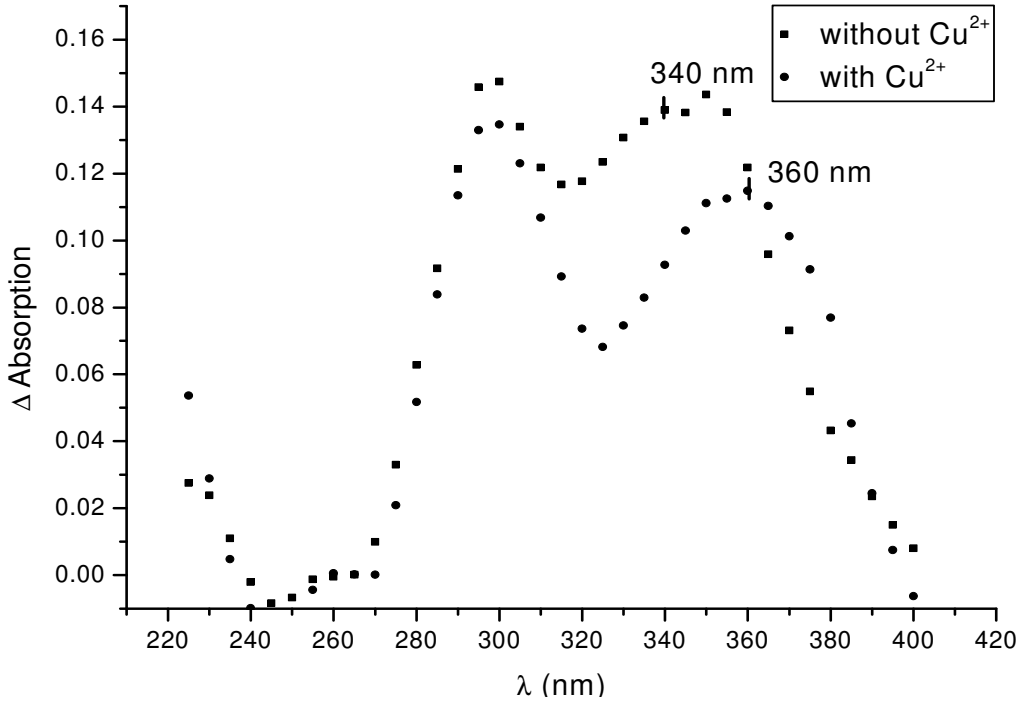

Fig. 78 Absorption Spectra of dU^{Phen} 56 incorporated in DNA with and without Cu^{2+}.
• dU^{Phen} **56** in DNA with Cu^{2+}, ■ dU^{Phen} **56** in DNA without Cu^{2+}.

c. Thermal Denaturation Curves

Thermal denaturation curves were recorded to compare the stability of our modified double-stranded DNAs **77a** and **78a** with the pertinent unmodified duplexes (**77c**, **78c**). These experiments also served to evaluate the effect of Cu^{2+} on the duplex stability.

All melting curves were recorded by Katja Imhof in the group of Prof. Dr. Clemens Richert at the University of Stuttgart. The absorption was measured at 260 nm as function of temperature. Single stranded DNA absorbs light up to 40% better than its double-stranded counterpart. Hence, thermal denaturation of the Watson-Crick base pairs in a restricted temperature range results in a significant change in absorption. The midpoint of this temperature range is defined as melting temperature at which 50% of the duplex is denatured.

Both cooling and heating curves were recorded in a temperature range between 5°C and 85°C with a heating/cooling rate of 1K per minute. The obtained data was then analyzed with TempLab (Software by Perkin Elmer) and the melting temperature was determined (Table 5).

Table 5: Effect of 57 on Melting Temperatures of its DNA Duplexes

Entry	DNA Duplex	Melting Temperature	
		Without Cu^{2+}	With Cu^{2+}
1	**77a** (**73a**·**75**)	53.7 ± 0.84°C	53.7 ± 0.84°C
2	**77c** (**73c**·**75**)	63.3 ± 0.96°C	63.5 ± 0.58°C
3	**78a** (**74a**·**76**)	66.2 ± 0.98°C	66.2 ± 0.43°C
4	**78c** (**74c**·**76**)	85°C	85°C

The unmodified DNA fragments **77c** and **78c** had melting temperatures of 63°C and 85°C, respectively, whereas the fragments **77a** and **78a** revealed lower melting points of 53°C and 66°C indicating a significant destabilization of the double helix as a result of the incorporation of the 2-(2-pyridyl)benzimidazole instead of thymine, which partially results from its inability to form base pairs with adenine.

The 1,10-phenanthroline containing nucleoside **69** on the other hand is able to build hydrogen bridges with adenosine. Its incorporation has only a small detrimental effect on duplex stability, which is caused by its weaker base stacking ability.[176]

3.6. Diels-Alder Reaction

A reaction that had proven to be well suited for DNA-supported catalysis is the Diels-Alder reaction. Bidentate nitrogen ligands, like 1,10-phenthroline and 2-(2-pyridyl)benzimidazole, for catalytically active Cu^{2+}-complexes are often employed in Diels-Alder reactions. Using similar intercalating ligands Feringa *et al.* were able to achieve good conversions with very high enantioselectivities.[103] Due to the outstanding importance of the Diels-Alder reaction in the synthesis of six-membered rings with up to four stereocenters and because of its vast application in organic chemistry, we choose to perform Diels-Alder reaction with our DNA-supported catalysts as well. Besides, using reaction conditions similar to Feringa's would allow comparing the results of the two differing systems, intercalation vs. covalent attachment.

The Diels-Alder reaction is a [4+2]-cycloaddition of a conjugated diene with an alkene or alkyne, which is commonly referred to as dienophile. Products of the Diels-Alder reaction are unsaturated six-membered rings. The mechanism of the reaction is depicted in Scheme 35.

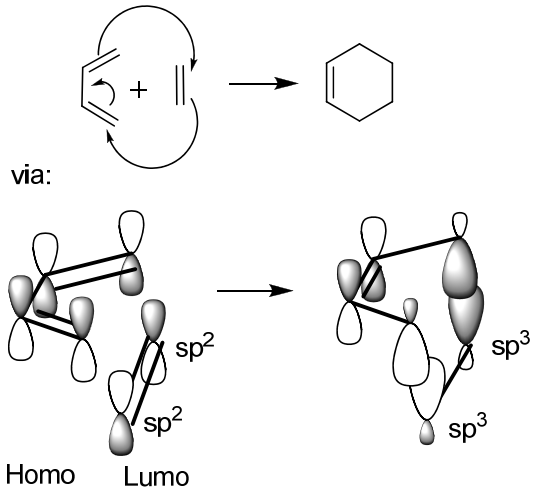

Scheme 35: Mechanism of the Diels-Alder Reaction.

It involves the electrocyclic reaction between 4 π-electrons of the diene and 2 π-electrons of the dienophile. The driving force of the reaction is the conversion of double to single bonds. In the thermally allowed transition state the highest occupied MO (HOMO) of the diene has to overlap with the lowest unoccupied MO (LUMO) of the dienophile. The smaller the energy gap (ΔE)

between these two π-like MOs the higher is the rate constant of the reaction. Typical substrates for the Diels-Alder reaction are therefore dienophiles with electron-withdrawing groups, which will lower the energy of the LUMO. Less typical but also possible are Diels-Alder reaction with an inverse electron demand. Here the HOMO of an electron-rich dienophile overlaps with the LUMO of an electron-poor diene. Our focus however was laid on the normal Diels-Alder reaction, which is why the inverse reaction will not be discussed in more detail.

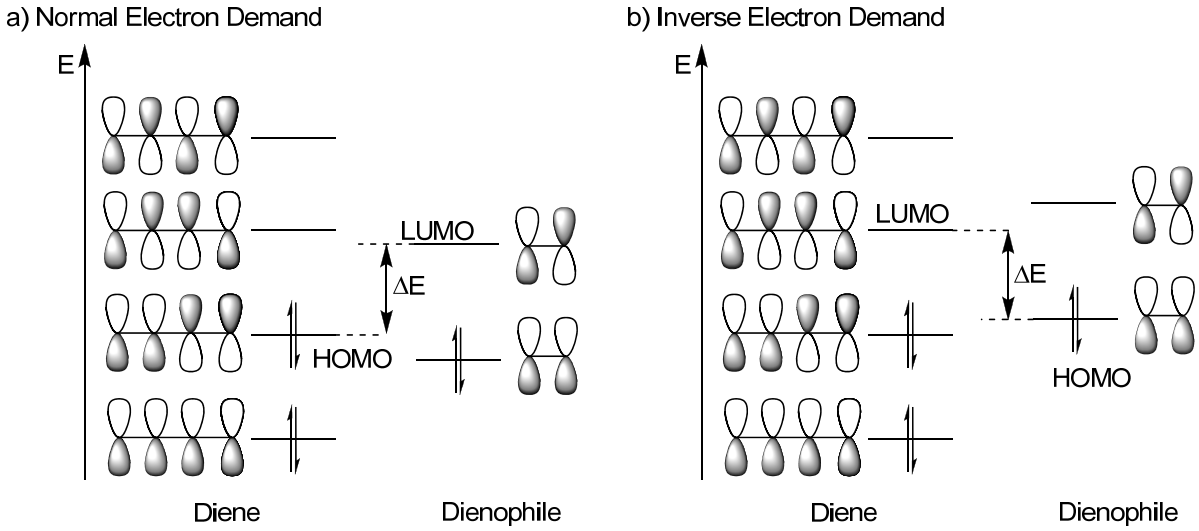

Fig. 79: MO-Energy Diagram.
a) Diels-Alder reaction with normal electron demand; b) Diels-Alder reaction with inverse electron demand.

Typical catalysts for the Diels-Alder reaction are Lewis acids. Their catalytic effect can be explained by their ability to coordinate to the electron-withdrawing groups of the dienophile, thus further decreasing the LUMO. More important than the rate accelerating effect of these catalysts, however is their potential to influence the stereo outcome of the reaction.

Reactions of unsymmetrical dienophiles with cyclic dienes, like cyclopentadien, can lead to four stereo isomeric products (Scheme 36). Usually the endo products are favored over the exo products, due to steric and electronic reasons during the transition state. Lewis acids have a positive effect on this preference.

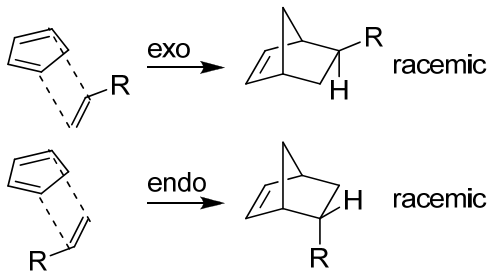

Scheme 36: Stereo-Selectivity of Diels-Alder Reactions.

In order to differentiate the enantiomeric products chiral Lewis acid catalysts have been successfully employed.[199] An important aspect thereby is the coordination of the Lewis acid to the

dienophile. Prerequisite for a good discrimination of enantiomeres is a two point coordination, which inhibits rotation of the substrate.

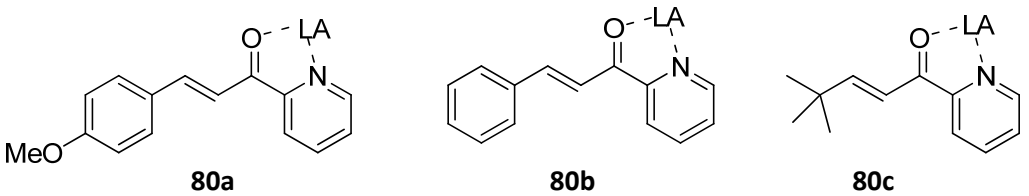

80a **80b** **80c**

Fig. 80: Two Point Coordination of Lewis Acids to Aza-Chalcones 80a, 80b, 80c.

The aza-chalcones **80a**, **80b**, **80c** meet this criteria (Fig. 80). A Lewis acid catalyst can coordinate to the carbonyl-oxygen as well as to the nitrogen of the pyridine thus making them the ideal candidates for our purpose.

a. Synthesis of Azachalcones for Diels-Alder Reactions

All aza-chalcones were synthesized by the aldole condensation of 2-acetylpyridine (**81**) with the corresponding aldehyde **82a**, **82b** and **82c**. The synthesis route is depicted in Scheme 37.

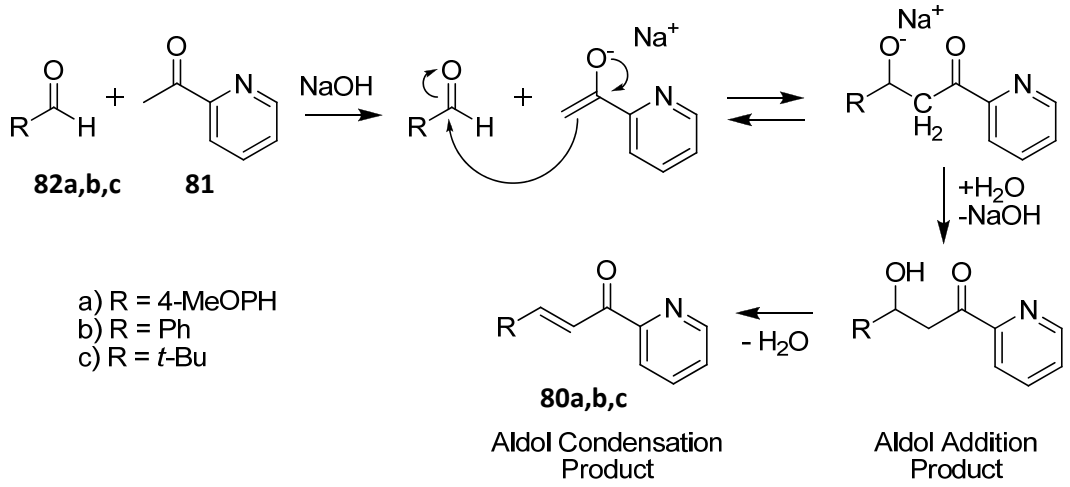

Scheme 37: Aldol Condensation.

Reaction Conditions: (i) For **80a**: H_2O (MilliQ), **82a**, 2-acetylpyridine (1 equiv.), 4°C, 10% NaOH, over night, 26%; (ii) for **80b**: H_2O (MilliQ), **82b**, 2-acetylpyridine (1 equiv.), 4°C, 10% NaOH, over night, 35%; (ii) for **80c**: H_2O (MilliQ), **82c**, 2-acetylpyridine (1 equiv.), 4°C, 10% NaOH, over night, 18%.

Reaction conditions for all three substrates were the same.[200, 201] Equimolar amounts of 2-acetylpyridine (**81**) and the appropriate aldehyde **82a**, **82b** or **82c** were introduced into water. The biphasic system was vigorously shaken to obtain a fine emulsion and then cooled to 4°C. At this temperature NaOH (10%) was added to deprotonate the α-carbonyl position. The reaction mixture was shaken once more and then left overnight undisturbed at 4°C. Stirring was reported to be disadvantageous since it leads to phase separation.[201] Products **80a** and **80b** crystallized over night and where thereafter isolated by filtration. Aza-chalcone **80c** did not crystallize and was isolated as crude oil after evaporation of the solvents. All compounds were purified by column chromatography. Contradicting literature product **80b** should not be purified by crystallization in ethanol, since this would lead to the decomposition of the compound. Even when stored at –20°C

the compound **80b** proofed to be unstable and traces of decomposition became visible in ^{1}H-NMR after a few weeks. The compounds purity was therefore verified on a regular basis and impurities were removed by column chromatography before applying it to Diels-Alder reactions.

3.7. Evaluation of Enantioselectivity Resulting from Double-stranded DNA

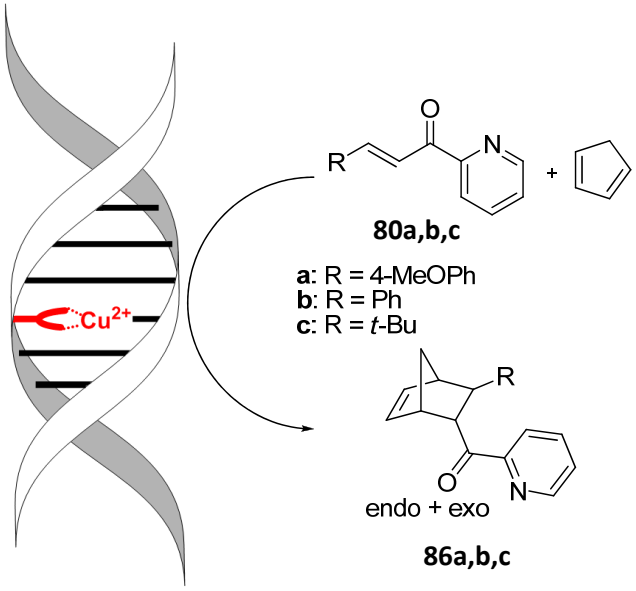

Scheme 38: DNA-Catalyzed Diels-Alder Reaction of Azachalcones 80a,b,c with Cyclopentadiene Leading to the Cycloadducts 86a,b,c.

Our aspired system for the evaluation of enantioselective induction by double-stranded DNA having 2-(2-pyridyl)benzimidazole incorporated is depicted in Scheme 38. It comprises the Diels-Alder reaction between the different aza-chalcones **80a**, **80b** or **80c** and cyclopentadiene in water. Even though aza-chalcones **80a**, **80b** and **80c** are poor dienophiles their Diels-Alder reaction is reported to experience a significant rate acceleration by aqueous solvents, caused by two effects.[202-204] Poor water solubility of the reaction partners forces them into hydrophobic hydration shells. The surface area of the shell which is exposed to water is smallest in the transition state leading to a faster reaction in water as compared to nonaqueous solvents. The second effect is caused by water molecules which can form hydrogen bonds with the electron withdrawing groups of the dienophile thereby lowering the LUMO energy of the dienophile. The rate accelerating effect of water compared to acetonitrile is shown for the Diels-Alder reaction of aza-chalcone **83** with cyclopentadiene in Table 6.

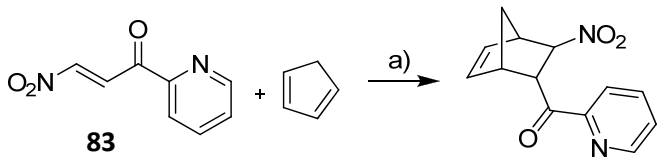

Scheme 39: Diels-Alder Reaction of Aza-Chalcone 83.

Table 6: Second-Order Rate Constants *k*2 for Diels-Alder Reactions of 83 with Cyclopentadiene in Different Solvents:

Entry	Solvent	k_2 (M^{-1} s^{-1})	k_{rel}
1	CH_3CN	1.40×10^{-5}	1
2	EtOH	3.83×10^{-5}	2.7
3	H_2O	4.02×10^{-3}	287
4	$H_2O + Cu(NO_3)_2$	1.11	79 300

Nevertheless, the reaction in water at 25°C is very slow and a good Lewis acid catalyst like $Cu(NO_3)_2$ is needed to increase the reaction rate. Relative to the uncatalyzed reaction in water, $Cu(NO_3)_2$ (10 mM) accelerates the reaction by a factor of 276 and was therefore obvious choice for the complexation with our system.

a. Control Experiments

In order to unambiguously determine the influence of double-stranded DNA on the enantioselectivity of the Diels-Alder reaction a number of control experiments had to be carried out.

Single Stranded DNA + Cu^{2+}

In the first set of experiments we used the single stranded 2-(2-pyridyl)benzimidazole-modified DNA **73a** in combination with $Cu(NO_3)_2$ as catalyst for the above-mentioned Diels-Alder reactions. The reactions were performed on a 1 ml scale in an aqueous buffer system at 5°C. Oligonucleotide **73a** and equimolar amounts of $Cu(NO_3)_2$ were incubated for one hour at rt, before aza-chalcone **80a,** was added at 5 °C. The reaction was then started by the addition of cyclopentadiene. After 3 days at 5°C the reaction was stopped and analyzed by chiral ODH-HPLC.

The detected conversion was less than 4%, which is in the same range as uncatalyzed Diels-Alder reactions. Single stranded oligonucleotides are known to have no rate enhancing effects on Diels-Alder reactions,[104] which possibly is due to the lack of a defined helical structure. The increased flexibility of single stranded oligonucleotides could enable neighboring nucleobases to compete with the azachalcones for binding to Cu^{2+}.

The lack of catalytic activity of single stranded DNA **73a** with Cu^{2+} is, together with the previously proven selective Cu^{2+}complexation, a clear indication that no or only negligible amounts of $Cu(NO_3)_2$ can leach into the reaction mixture. This notion is emphasized by the otherwise high catalytic power of pure $Cu(NO_3)_2$.

Unmodified DNA + Cu^{2+}

Next, the unmodified double-stranded DNAs **77c** and **78c** were used in combination with $Cu(NO_3)_2$ as catalyst for the above-mentioned Diels-Alder reactions. The oligonucleotides were incubated with equimolar amounts of $Cu(NO_3)_2$ for one hour at rt. Thereafter aza-chalcones **80a, 80b, 80c**

were added at 5 °C and the reactions were started by the addition of cyclopentadiene. In both cases the conversions after 3 days were quite high (76-96 %). No enantioselectivity was observed with the shorter oligonucleotide **77c**, however small enantioselectivities of up to 18 % were obtained for the longer oligonucleotide **78c** (Table 1). A possible reason might be the unspecific complexation of Cu^{2+} by the double-helical DNA which should be more pronounced in the longer oligonucleotide **78c**.

Table 7: Results of Unmodified DNAs 77c and 78c with Cu^{2+} but without Ligand.

Entry	Catalyst	Substrate	Conversion (%)[b]	Ee (%)[c]
1	**77c**	**80a**	75.3-76.1	2.1-2.4(-)
2	**77c**	**80b**	86.2-93.6	0.0-1.5(+)
3	**77c**	**80c**	87.5-94.1	6.1-8.3(+)
4	**78c**	**80a**	73.0-74.4	7.0-8.1(+)
5	**78c**	**80b**	89.3-92.0	8.2-9.4(+)
6	**78c**	**80c**	91.9-97.7	17.7-18.0(+)

a) Reaction conditions: 0.3 mM catalyst, 1 mM dienophile and 29 mM cyclopentadiene in MOPS buffer (20 mM, pH 6.5), 3 d, 5°C. b) Determined by chiral ODH-HPLC. c) Determined by chiral ODH-HPLC for the endo isomer.

Catalytical Properties of 84 without DNA

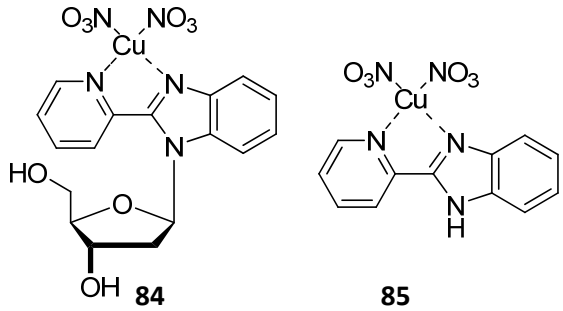

Fig. 81: Nucleoside-Derived Complex 84 and 2-(2-Pyridyl)benzimidazole Complex 85.

For comparison with the actual DNA-supported catalytic reactions, nucleoside-derived complex **84** was employed as catalyst in absence of DNA. The Cu^{2+}-complex **84** was obtained by treating **54** with a minimal deficit of $Cu(NO_3)_2 \cdot 3H_2O$ and was afterwards crystallized from ether. Using a stock solution of it, test reactions of the aza-chalcones **80a, 80b, 80c** with cyclopentadiene were carried out. After 3 d at 5 °C the reactions were stopped and analyzed by chiral ODH-HPLC. The results are summarized in Table 8. Except for substrate **80a** high conversions were observed with an average endo selectivity of >4:1. Most importantly, no enantioselectivities were obtained in the absence of DNA, implying that any enantioselectivity possibly observed with 2-2pyridylbenzimdazole modified double-stranded DNA can only be attributed to the induction by the DNA scaffold.

Table 8: Results Obtained with Nucleoside Cu^{2+}-Complex 84.

Entry	Substrate	Conversion (%)[b]	Ee (%)[c]
1	**80a**	28.3 -42.6	4.2-5.6(-)
2	**80b**	76.3-85.6	0.4-0.6(+)
3	**80c**	97.8-99.6	0.1-0.3(-)

a) Reaction conditions: 0.3 mM catalyst, 1 mM dienophile and 29 mM cyclopentadiene in MOPS buffer (20 mM, pH 6.5), 3 d, 5°C. b) Determined by chiral ODH-HPLC. c) Determined by chiral ODH-HPLC for the endo isomer.

Unmodified Double-Stranded DNA

In an additional set of control experiments, the nucleoside-derived catalyst **84** and the 2-(2-pyridyl)benzimidazole-derived copper complex **85** (Fig. 81) were investigated in the presence of unmodified double-stranded DNA **78c**. This system is very similar to the one reported by Feringa.[103] The flat structure of the bidentate ligand should allow in both cases for intercalations into the double-stranded DNA **78c** and hence, induction of enantioselectivity should be possible as well. For these investigations, double-stranded DNA **78c** was treated with equimolar amounts of **84** or **85,** respectively and incubated for 1 h at rt. Next, aza-chalcones **80a, 80b, 80c** were added at 5°C and the reactions were started by the addition of cyclopentadiene. After 3 days at 5°C the reactions were stopped and analyzed by chiral ODH-HPLC. Both systems proofed to be very active and yielded in high conversions (Table 9). Furthermore, enantioselectivities up to 85 % were achieved.

Table 9: Results for Catalysts 84 and 85 in the Presence of Unmodified DNA 78c.

Entry	Catalyst	Substrate	Conversion (%)[b]	Ee (%)[c]
1	**84**	**80a**	80.2-84.1	75.9-77.3(+)
2	**84**	**80b**	93.5-95.2	68.4-71.4(+)
3	**84**	**80c**	>99	84.0-85.2(+)
4	**85**	**80a**	71.4-72.3	75.4-76.9(+)
5	**85**	**80b**	94.4-96.5	65.5-65.9(+)
6	**85**	**80c**	>99	84.7-84.8(+)

a) Reaction conditions: 0.3 mM catalyst, 0.3 mM dsDNA 12b, 1 mM dienophile and 29 mM cyclopentadiene in MOPS buffer (20 mM, pH 6.5), 3 d, 5°C. b) Determined by chiral ODH-HPLC. c) Determined by chiral ODH-HPLC for the endo isomer.

b. Cu^{2+}-Complex of Modified Double-Stranded DNA 77a and 78a

After having performed various control experiments we turned our interest back to the catalytic activities of the Cu^{2+}-complex of modified double-stranded DNA **77a** and **78a**, respectively. Both duplexes were freshly prepared before every reaction by thermal hybridization of the modified oligonucleotides **73a** or **74a** with 1.1 equivalents of the complementary oligonucleotides **75** and **76** respectively. The resulting duplexes **77a** and **78a** were then incubated with equimolar amounts of $Cu(NO_3)_2 \cdot 3H_2O$ for 1 hour at rt, before the azachalcones **80a, 80b, 80c** and cyclopentadiene were added at 5°C. After 3 days the products **86a, 86b, 86c** were obtained as a mixture of endo and exo isomers, endo being the major product (endo/exo > 5:1). With one exemption (Table 10, entry 4) the conversions were good for both DNA-supported catalysts. Enantioselectivities as analyzed by chiral ODH-HPLC however depended strongly on the catalyst used (Table 10). The 14 base pair long double-stranded DNA **77a** yielded in no notable enantioselectivity (less than 8%). Better results in enantioselectivity were achieved with the 30mer catalyst **78a**, yielding a maximum of 35% ee. Even though these overall ee values were rather mediocre they can undoubtedly be attributed to the influence of the double-stranded DNA since the Cu^{2+}-complex **84** as such had not resulted in any enantioselectivity at all.

Table 10: Results with Modified Double-Stranded DNAs 77a and 78a.

Entry	Catalyst	Substrate	Conversion (%)[b]	Ee (%)[c]
1	**77a**	**80a**	62.3-69.3	3.8-4.4(+)
2	**77a**	**80b**	76.9-86.6	5.8-5.8(+)
3	**77a**	**80c**	84.1-87.1	7.5-8.1(+)
4	**78a**	**80a**	15.9-19.4	26.5-29.5(+)
5	**78a**	**80b**	71.0-75.8	30.1-32.2(+)
6	**78a**	**80c**	91.9-93.7	34.8-35.1(+)

a) Reaction conditions: 0.3 mM catalyst, 1 mM dienophile and 29 mM cyclopentadiene in MOPS buffer (20 mM, pH 6.5), 3 d, 5°C. b) Determined by chiral ODH-HPLC. c) Determined by chiral ODH-HPLC for the endo isomer.

Although the insertion of the modified building block **57** into the DNA had occurred without any problems it resulted in a significant disturbance of the hybridization leading to a decrease of the melting point of about 10 °C. This implies that the helical environment at the position of the ligand is severely disturbed, probably to the extent that it cannot exert its full influence. This is especially true for oligonucleotide **77a**, which in addition is too short to form a complete helical turn around the catalytic center. For this 11.5 base pairs are needed, whereas **77a** only has 7, 6 respectively, surrounding the modified building block **57**.

c. Cu^{2+}-complex of modified double-stranded DNA 78b

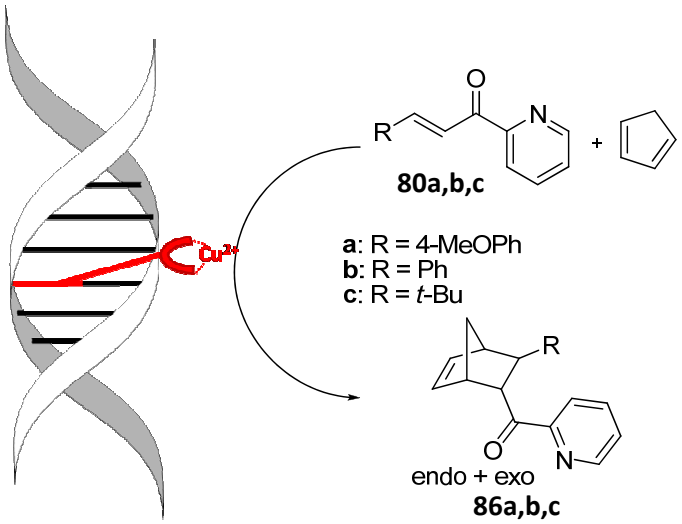

Scheme 40: DNA-catalyzed Diels-Alder Reaction of Azachalcones 82a,b,c with Cyclopentadiene Leading to the Cycloadducts 86a,b,c.

The disturbance of the helical environment as observed with DNA **77a** and **78a** are not exhibited by the 1,10-phenanthroline modified double-stranded DNAs **78b**, due to dU^{Phen} (**55**) ability to do base pairing with adenine. Hence, it is a more robust and as such an even better defined system than its 2-(2-pyridyl)benzimidazole analogous.

The catalytic activities of the Cu^{2+}-complexes of double-stranded **78b** were evaluated using the same conditions for the Diels-Alder reaction. Likewise, DNA duplexes were prepared freshly before every reaction by thermal hybridization of the modified oligonucleotides **74b** with 1.1 equivalents of the complementary oligonucleotides **76** respectively. The resulting duplex **78b** was then

incubated with equimolar amounts of $Cu(NO_3)_2 \cdot 3H_2O$ for 1 hour at rt to form the according complex. To these azachalcones **80a, 80b, 80c** and cyclopentadiene were added at 5°C. After 3 days the cycloadducts **86a, 86b, 86c** were obtained as a mixture of endo and exo isomers, endo being the major product (endo/exo > 5:1). Conversions with both DNA-supported catalysts of the 1,10-phenanthroline type were comparable to the ones achieved with corresponding 2-(2-pyridyl)benzimidazole system, albeit a bit lower.

Table 11: Results with Modified Double-Stranded DNAs 78b.

Entry	Catalyst	Substrate	Conversion (%)[b]	Ee (%)[c]
1	**78b**	**80a**	4.9-5.5	2.4-4.5(+)
2	**78b**	**80b**	55.6-66.8	17.0-24.3(+)
3	**78b**	**80c**	63.0-91.8	7.5-9.3(+)

a) Reaction conditions: 0.3 mM catalyst, 1 mM dienophile and 29 mM cyclopentadiene in MOPS buffer (20 mM, pH 6.5), 3 d, 5°C. b) Determined by chiral ODH-HPLC. c) Determined by chiral ODH-HPLC for the endo isomer.

However, overall enantioselectivities as analyzed by chiral ODH-HPLC dropped drastically. The highest selectivity of 24% ee was obtained with the 30 base pair long double-stranded DNA **78b** and substrate **80b**. The poor enantioselectivities could possibly result from the distance between ligand and DNA template introduced by the alkyne linker, which might be just too large for the DNA to have an explicit effect on the stereo chemical outcome of the reaction. It is also feasible, that the stiffness of the alkyne linker forces the catalytical center into an unfavorable position.

4. Summary and Outlook

We were able to demonstrate that a Cu^{2+}-complexing 2-(2-pyridyl)benzimidazole chelator could be turned into the 2'-β-deoxynucleoside **54,** which was then transferred into the corresponding phosphoramidite **57.** The modified DNA building block was employed with high efficiency in solid phase DNA synthesis by the phosphoramidite technique, to replace one natural nucleobase in the middle of two DNA sequences. The corresponding double-stranded DNA hybrids **77a** and **78a** were incubated with a Cu^{2+} source to create the pertinent Cu^{2+}-complexes.

These DNA-supported catalysts were applied to Diels-Alder reactions of three different aza-chalcones (**80a,b,c**) with cyclopentadiene. High conversions were obtained with an endo/exo selectivity of >5:1. Furthermore, with the pyridylbenzimidazole-based duplexes an enantioselectivity of up to 35 % ee was observed which could be attributed to the induction by the DNA hybrid. Higher ee values were probably prevented by the disturbance of proper hybrid formation due to the insertion of the chelator in place of a natural base.

We then focused on chelators reaching into the major groove from the 5-position of pyrimidines without hampering the hybrid formation of involved DNA strands. Therefore, the literature known dU^{Phen} **56** was synthesized and incorporated in analogues DNA hybrid **78b**. The corresponding Cu^{2+}-complex was applied to the same Diels-Alder reactions resulting in some cases in high conversions and an endo/exo selectivity of >5:1. Compared to the 2-(2-pyridyl)benzimidazole modified duplexes these complexes led to lower enatioselectivities of up to 24% ee.

Even though obtained selectivities are still mediocre they univocally provide proof for the induction by the DNA scaffold. The advantage of our system thereby not only is the possibility to pinpoint the catalyst's position within DNA but also the ability to change the surrounding base sequence at will. We strongly believe that these features will pave the way to a better understanding of the principle of DNA-supported catalysis. The shortcomings in enantioselectivities of our two catalytic systems actually hint at the needed improvements to achieve this goal.

Essential is the stability of the hybrid, future experiments will therefore be focused on modifications of the 5-position of pyrimidines or the 8-position of purine bases with chelators. At these positions the ligands would reach into the major groove without disturbing the hydrogen bond donating and accepting properties of the base. Another interesting location for a ligand would be the 2-position of adenine which reaches into the minor groove and is, unlike in guanine, also not involved in hydrogen-bonding. Two examples for such bidentate chelators are given in Fig. 82. Similar to dPB **54** these proposed ligands do not have a linker unit, which should result in the formation of the catalytical center deep inside the major or minor groove.

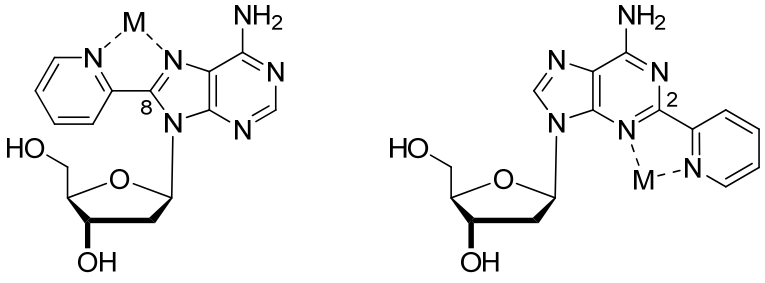

Fig. 82: Adenosine Modified at the 5- and 2-Position.

A further aspect that needs to be addressed in more detail is the linker unit and its role in DNA-supported catalysis. Its length determines the distance between ligand and DNA and thereby directly influences the quality of the interactions between substrate and helical scaffold. Equally important in this regard is the flexibility of the linker. Higher flexibility could be favorable, since it would allow the catalytic site to better adapt to the substrate and its transition state, comparable to the induced fit model of enzymes.[205] The amide resulting from 5-(aminopropane)-2'-deoxyuridine (**43**) and 4-carboxyl-1,10-phenanthroline (**87**) would make a interesting candidate for this purpose (Scheme 41).

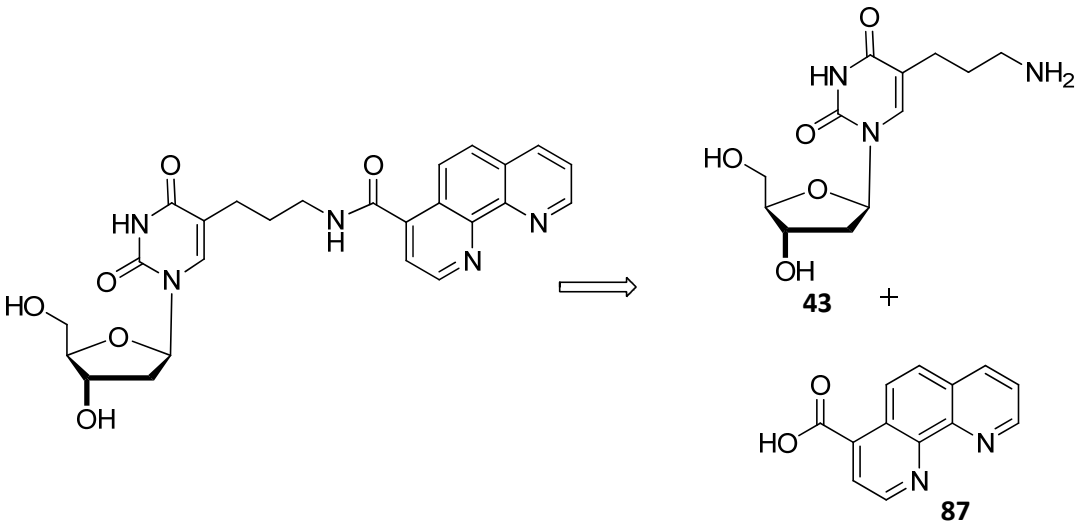

Scheme 41: Proposed 1,10-Phenanthroline-Modified Nucleoside with Flexible Linker.

III. Experimental

1. General Procedures

Reactions with hydrolysis and/or oxygen sensitive educts or products were carried out under argon in well dried glassware.

Reagents and Solvents

Reagents were obtained from ABCR, Acros, Chempur, Merck or Sigma-Aldrich and were used without further purification. All solvents used in the reactions (THF, MeOH, EtOH, CH_2Cl_2, Et_2O, pyridine, CH_3CN) were – unless stated otherwise – purified and dried by means of the common distillation procedures. Solvents for chromatography (CH, EtOAc, CH_2Cl_2, $CHCl_3$, MeOH, EtOH, acetone) were distilled before use on a rotary evaporator.

Chromatography

Thin layer chromatography (TLC) was performed on glass TLC plates with silica gel type 60 F_{254} (Merck). When necessary, chromatograms were treated with molybdato phosphoric acid (4 g in 100 ml EtOH) or conc. H_2SO_4 and developed by heating. All chromatograms were photographed under UV radiation (254 nm, 366 nm).

Column chromatography was carried out manually or on a medium pressure liquid chromatography machine from Büchi (consisting out of: Fraction Collector C660, Pump Module C605, Pump Manager C615, UV Photometer C635) using silicagel from SDS type 60 ACC 35 – 70 µm. Separation conditions are stated in the following order„(a x b cm, c ml, CH/EtOAc = d:e → f:g)“, meaning: a column with a diameter of **a** cm was packed **b** cm high with silica-gel, **c** ml sized fractions were collected; for elution a **d:e** ratio with a gradient to **f:g** of the solvents cyclohexane and ethyl acetate was used.

NMR-Spectroscopy

^1H-, ^{13}C- and ^{31}P-NMR spectra were measured on apparatuses AC 250, AM 400 and DRX 500 from Bruker as well as on a Mercury (type: VX 300) from Varian in deuterated solvents ($CDCl_3$, CD_3CN or dDMSO). All coupling constants *J* are reported in Hertz, all shifts δ in ppm. Unless stated otherwise the solvent was used as standard for ^1H-NMR $CDCl_3$ (7.26 ppm), CD_3CN (1.94 ppm), CD_3OD (3.31 ppm), dDMSO (2.50 ppm) and ^{13}C-NMR $CDCl_3$ (77.2 ppm), CD_3CN (1.3 ppm, 118.3 ppm), CD_3OD (49.0 ppm), dDMSO (39.5 ppm). A spectrometer internal standard was used for ^{31}P-NMR. All signals except those specified as AB-signals, were interpreted as signals of first order. The high field part of AB signals was labeled with A and the low field part with B.

Mass spectrometry

Electron Impact (EI) ionization was done on a mass spectrometer of the type TSQ 700 and MAT 95XL by the company Thermo (ionization energy: 70 eV, source temperature: 200°C). The same spectrometers were used for chemical ionization (CI) (ionization energy: 110eV, source temperature: 200°C, reagent gas: Ammonia or isobutene). High Resolution (HR) mass spectrometry was done on the MAT 95XL using either EI or CI (M/Δ M = 10000). For GC/MS (EI and CI) the TSQ

700 in combination with a Varian 3400 was used. Electrospray Ionization (ESI) and Atmospheric Pressure Chemical Ionization (APCI) were carried out on a LCQ Advantage system by the company Thermo [injection of 2.5 µl sample solution/min. into a flow of 100-200 (200-400) µl/min. Methanol (or acetonitrile) + H_2O; spray-voltage: 4-5 kV (spray-current: 5 µA) ion transfer tube: 250-300°C (150-180°C) vaporizer temp. 250-350°C]. For LC/MS the LCQ Advantage together with a Surveyor LC-system was used.

HPLC

Two systems were available for HPLC. A Merck/Hitachi system with interface module D-6000, pump L-6200A, autosampler AS-2000A, column oven L-5025 and DAD detector L-4500 and an Agilent 1100 system including the following modules: binary pump, autosampler, thermostatted column compartment, diode array detector, controlled by an Agilent ChemStation.

Water Purification System

All bioorganic steps were performed using ultrapure water [H_2O (MilliQ)] from a Millipore Direct Q system with a water resistance of 18.2 MΩ.

UV-Spectroscopy

UV-/VIS-absorptions were measured on a Lambda 35 UV/VIS-spectrometer from PerkinElmer Instruments.

DNA-Synthesis

Unless stated otherwise oligonucleotide synthesis was carried out on an Expedite™ 8909 Nucleic Acid Synthesis System from Perseptive Biosystems on a 1 µmol scale using phosphoramidite chemistry. Standard phosphoramidites as well as nucleosides coupled to CPG solid support were obtained from Proligo/Sigma-Aldrich.

Documentation

For documentation of TLC plates and polyacrylamide gels a system by the DESAGA Sarstedt Group including a digital camera (Canon Powershot G5), a chamber equipped with UV-254, UV-366, Vis Light and a photo printer (Mitsubishi CP 700D) was available.

Centrifuges

Two Eppendorf centrifuges were available: A refrigerated centrifuge (Eppendorf® Centrifuge 5805 R) with 1400 rpm and a vacuum centrifuge (Eppendorf® Concentrator 5301, SpeedVac) for concentration of aqueous and ethanolic media at 30°C, 45°C or 60°C.

Elementary Analysis (C, H, N, S)

Elementary Analysis was performed on a Vario EL system from Elementaranalysesysteme GmbH.

Melting Points

Melting points (Mp) were measured on an IA 9000 system from the company Electrothermal. Obtained values were not corrected.

2. Organic Syntheses

(4', 4''- Dimethoxytrityl)-hexaethylene glycol [145] 24

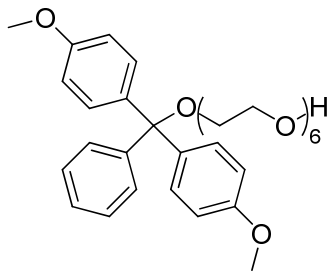

Chemical Formula: $C_{33}H_{44}O_9$
Molecular Weight: 584.70

DMT-Cl (1.27 g, 3.70 mmol) and hexaethylene glycol (5.29 g, 4.70 ml, 18.7 mmol, 5.0 equiv.) were separately dried azeotropically with 5 ml anhydrous pyridine each. Thereafter, hexaethylene glycol was dissolved in 4 ml anhydrous pyridine and DMT-Cl dissolved in 3 ml anhydrous pyridine was slowly added to this solution. The reaction mixture was stirred at rt. overnight whereby the color of the solution slowly turned from orange to pale yellow. The reaction was then quenched by the addition of 12 ml MeOH. The solvent was removed under reduced pressure and the crude product was purified by column chromatography [10 x 4 cm, 50 ml, CH/EE (1% NEt_3) = 1:3 → F9 0:1]. The title compound **24** (0.89 g, 1.5 mmol) was obtained as a colorless oil in 41% yield. Remaining starting material was recovered by rinsing the chromatography column with pure EtOH (4 g hexaethylene glycol).

Spectroscopic data were in accordance with literature data.

^{1}H-NMR (300 MHz. in $CDCl_3$): δ = 3.58 – 3.83 (m, 30H, OCH_3, CH_2), 6.77 – 6.88 (m, 4H, aromat.), 7.13 – 7.50 (m, 9H, aromat.).

(4',4'' -Dimethoxytrityl)-hexaethylene glycol]-β-cyanoethoxy-(diisopropylamino)-phosphine [145] 1

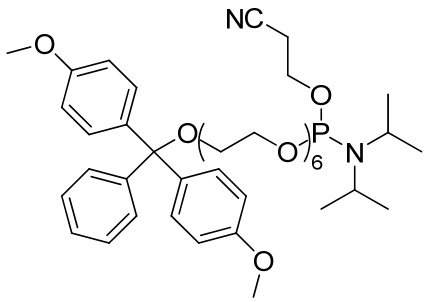

Chemical Formula: $C_{42}H_{61}N_2O_{10}P$
Molecular Weight: 784.91

The DMT protected hexaethylene glycol **24** (700 mg, 1.20 mmol) and diisopropylammoniium tetrazolide (162 mg, 0.946 mmol, 0.8 equiv.), were dried together three times azeotropically with

5 ml anhydrous acetonitrile each. Afterwards, the reactants were dissolved in 12 ml anhydrous CH_2Cl_2. Under an Ar-atmosphere (2-cyanoethoxy)-bis-(*N,N*-diisopropylamino)phosphine (796 mg, 2.60 mmol, 2.2 equiv.) were added drop wise. The reaction mixture was stirred for 18 h at rt. Thereafter, the reaction was quenched by the addition of 50 ml of a sat. $NaHCO_3$ solution. The aqueous phase was extracted three times with 50 ml CH_2Cl_2 each and the combined organic phases were dried over Na_2SO_4. The solvent was removed under reduced pressure. The crude product was purified by column chromatography (10 x 4 cm, 50 ml, CH/EE/NEt_3 = 3:1:1) to give title compound **1** (867 mg, 1.10 mmol) as a pale yellow oil in 92 % yield.

Spectroscopic data were in accordance with literature data.

MS (ESI): m/z (%) = 807 (100) [M+Na^+], 785/786 (6/2) [M^+], 738 (3).

MS (EI): m/z (%) = 481 (7) [M-DMT], 303 (6) [DMT], 121 (23).

^{1}H-NMR (300 MHz, in $CDCl_3$): δ = 1.15 – 1.22 [m, 12H, 2·CH($\underline{CH_3}$)$_2$], 2.64 (q, *J* = 6.0, 2H, CH), 3.22 (t, *J* = 5.2, 2H, CH_2), 3.54 – 3.76 (m, 26H, CH_2), 3.79 (s, 6H, OMe), 6.78 – 6.85 (m, 4H, aromat.), 7.15 – 7.49 (m, 9H, aromat.).

^{13}C-NMR (125 MHz, in $CDCl_3$): δ = 158.5, 145.2, 136.5, 130.2, 128.3, 127.8, 126.8, 113.2, 76.87, 71,4, 71,3, 70.9, 70.9, 70.8, 70.8, 70.7, 70.7, 63.3, 62.8, 62.6, 58.7, 55.3, 43.3, 43.2, 25.8, 25.8, 25.7, 25.7, 25.7.

^{31}P-NMR (120 MHz, in $CDCl_3$): δ = 149.7, 150.3.

5-(3''-Trifluoroacetamidepropargyl)-2'-deoxyuridine 37

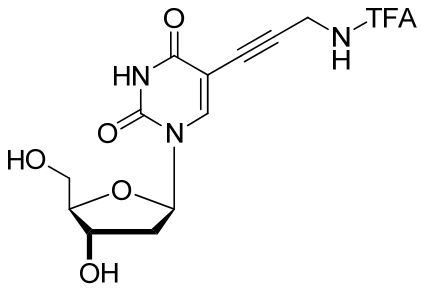

Chemical Formula: $C_{14}H_{14}F_3N_3O_6$
Molecular Weight: 377.27

<u>Method 1 with $PdCl_2(PPh_3)_2$ as catalyst [165]:</u>

In a three-necked flask 2'-deoxy-5'-iodo-uridine (1.0 g, 2.8 mmol) was dissolved in 24 ml of anhydrous DMF. Argon was bubbled through this solution for 10 min. After this $PdCl_2(PPh_3)_2$ (0.20 g, 0.28 mmol, 0.1 equiv.) was added and again argon was bubbled through the solution for another 5 minutes. To the reaction mixture anhydrous NEt_3 (0.57 g, 0.78 ml, 5.6 mmol, 2.0 equiv.) propargyltrifluoroacetamide (1.0 g, 6.8 mmol, 2.4 equiv.) and CuI (0.11 g, 0.56 mmol, 0.2 equiv.) were added. The reaction mixture was stirred in the dark for 6 h at 40°C and was then quenched by addition of 20 ml MeOH/CH_2Cl_2 (1:1) and the ion exchange resin DOWEX (type: HCO_3^-, 4.0 g). After stirring for another 30 min at rt. the reaction mixture was filtered through celite and the solvent

removed under reduced pressure. Remaining DMF was removed by condensation at 40°C and $1 \cdot 10^{-1}$ mbar.

The crude product was purified by column chromatography on a Büchi Sepacore chromatography system (5 x 15 cm, 20 ml, $CHCl_3$/MeOH = 8.25:1.75). However separation from side products even after repeated chromatography was not satisfactory and only small amounts of the pure compound (190 mg, 0.503 mmol, 18%) were isolated.

Method 2 with $Pd(PPh_3)_4$ as catalyst [165]:

In a three necked flask 5'-iodo-uridine (1.0 g, 2.8 mmol) was dissolved in 24 ml of anhydrous DMF. Argon was bubbled through this solution for 10 min. After this $Pd(PPh_3)_4$ (0.33 g, 0.28 mmol, 0.1 equiv.) was added and again argon was bubbled through the solution for another 5 min. To the reaction mixture anhydrous NEt_3 (0.57 g, 0.78 ml, 5.6 mmol, 2.0 equiv.) propargyltrifluoroacetamide (1.1 g, 0.70 ml, 7.1 mmol, 2.5 equiv.) and CuI (0.11 g, 0.56 mmol, 0.2 equiv.) were added. The reaction mixture was stirred in the dark for 6 hours at 40°C and was then quenched by addition of 20 ml MeOH/CH_2Cl_2 (1:1) and the ion exchange resin DOWEX (type: HCO_3^-, 3.7 g). After stirring for another 1 h at rt. the reaction mixture was filtered through celite and the solvent removed under reduced pressure. Remaining DMF was removed by condensation at 40°C and $2.5 \cdot 10^{-2}$ mbar. The crude product was purified by column chromatography on a Büchi Sepacore chromatography system (5 x 15 cm, 20 ml, $CHCl_3$/MeOH = 8.25:1.75). Fractions 12-26 (product; FI) and fractions 43-46 (side-product; FII) were combined separately and the solvent was removed under reduced pressure. The desired product (0.55 g, 1.5 mmol) was obtained as yellow oil in 51% yield. The side product **38** (0.30 g, 0.80 mmol, 33%) was also isolated and identified as **38** by NMR.

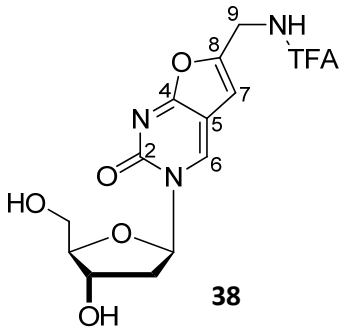

38

Chemical Formula: $C_{14}H_{14}F_3N_3O_6$
Molecular Weight: 377.27

NMR of side product **38**:

^{1}H-NMR (400 MHz, in dDMSO): δ = AB-signal ($\delta_{2'a}$ = 2.04, $\delta_{2'b}$ = 2.4, $J_{A,B}$ = $J_{B,A}$ = 13.5, additional couplings $J_{2'a,3'}$ = $J_{2'a,1'}$ = 6.1, $J_{2'b,1'}$ = 6.2, $J_{2'b,3'}$ = 4.2, 2H, 2'-H), 3.57 – 3.69 (m, 2H, 5'-H), 3.91 (dt, $J_{4',3'}$ = $J_{4',5'a}$ = 3.8, 1H, 4'-H), 4.18 – 4.22 (m, 1H, 3'-H), 4.44 (d, $J_{9,10NH}$ = 5.6, 2H, 9-H), 5.08 (t, $J_{5'OH,5'}$ = 5.3, 1H, 5'-OH), 5.26 (d, $J_{3'OH,3'}$ = 4.3, 1H, 3'-OH), 6.13 (dd, $J_{1',2'b}$ = $J_{1',2'a}$ = 6.1, 1H, 1'-H), 6.64 (s, 1H, 7-H), 8.77 (s, 1H, 6-H), 10.09 (t, $J_{10NH,9}$ = 5.6, 1H, 10-NH).

^{13}C-NMR (100 MHz, in dDMSO): δ = 171.1 (4-C), 156.5 (q, $^{3}J_{11,12F}$ = 36.5, 11-C), 153.7 (2-C), 151.9 (8-C), 138.5 (6-C), 115.8 (q, $J_{6'',6''F}$ = 286.3, 12-C), 105.5 (5-C), 102.6 (7-C), 88.2 (4'-C), 87.6 (1'-C), 69.6 (3'-C), 60.7 (5'-C), 41.2 (2'-C), 36.2 (9'-C).

^{19}F-NMR (235 MHz, in dDMSO): δ = -74.28 (CF_3).

Method 3 with Pd/C as catalyst[166]:

A two necked flask was charged with 5'-iodo-uridine (2.00 g, 5.65 mmol), Pd/C (304 mg, 0.282 mmol), CuI (214 mg, 1.13 mmol, 20 mol%) and Amberlite (5.14 g). The compounds were dried under high vacuum and afterwards kept under argon. Propargyltrifluoroacetamide (1.72 g, 11.3 mmol, 2.3 equiv.) and 56 ml anhydrous DMF were added. Through this suspension anhydrous argon was bubbled for 5 minutes. The apparatus was one more time degassed and flooded with anhydrous argon. The reaction mixture was stirred at 50°C for 17 h, afterwards cooled to rt. and filtered over celite. The celite was washed with 50 ml of CH_2Cl_2/MeOH (5:1). The solvent of the combined organic phases was removed under reduced pressure. Remaining DMF was removed by condensation at 40°C and $4 \cdot 10^{-2}$ mbar. The crude product was purified by column chromatography on a Büchi Sepacore chromatography system (5 x 15 cm, F1-6: 20 ml, F7-30: 10 ml, $CHCl_3$/MeOH = 8.25:1.75). Fractions 7-30 were combined and the solvent was removed under reduced pressure. The desired product (1.71 g, 4.53 mmol) was obtained as brown foam in 80% yield.

Spectroscopic data were in accordance with literature data.

MS (ESI): m/z (%) = 798.7 (13), 777.7 (11), 776.7 (37) [2M+Na^+], 701.9 (14), 550.9 (12), 399.8 (100) [M+Na^+].

^{1}H-NMR (400 MHz, in dDMSO): δ = 2.08 – 2.14 (m, 2H, 2'-H), 3.51 – 3.63 (m, 2H, 5'-H), 3.78 (td, $J_{4',5'}$ = 3.4, $J_{4',3'}$ = 3.6, 1H, 4'-H), 4.20 – 4.22 (m, 3H, NH-$\underline{CH_2}$ + 3'-H), 5.06 (t, $J_{5'OH,5'}$ = 5.1, 1H, 5'-OH), 5.22 (d, $J_{3'OH,3'}$ = 4.3, 1H, 3'-OH), 6.09 (t, $J_{1',2'}$ = 6.7, 1H, 1'-H), 8.17 (s, 1H, 6-H), 10.04 (m_c, 1H, $\underline{NH}$-CH_2), 11.6 (s, 1H, 3-NH).

^{13}C-NMR (100 MHz, in dDMSO): δ = 161.5 (4-C), 156.0 (q, $^{3}J_{5'',6''F}$ = 36.6, 5''-C), 149.4 (2-C), 144.1 (6-C), 115.8 (q, $J_{6'',6''F}$ = 288.1, 6''-C), 97.6 (5-C), 87.6 (4'-C), 87.4 (1''-C), 84.8 (1'-C), 75.4 (2''-C), 70.2 (3'-C), 61.0 (5'-C), 40.2 (2'-C superposed by DMSO signals), 29.4 (3''-C).

5-(Propargylamine)-2'-deoxyuridine [206] 90

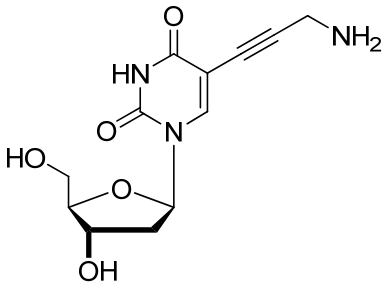

Chemical Formula: $C_{12}H_{15}N_3O_5$
Molecular Weight: 281.26

5-(3''-Trifluoroacetamidepropargyl)-2'-deoxyuridine **37** (234 mg, 0.62 mmol) was dissolved in 10 ml of ammonium hydroxide (25%) and stirred for 2 h at rt. The solvent was removed under reduced pressure. The crude product, a brown oil, was then dissolved in 50 ml H_2O. The aqueous phase was washed four times with 10 ml $CHCl_3$ each. Most of the solvent was removed under reduced pressure the remaining few milliliters of water were removed on a freeze-drier to obtain the desired product (170 mg, 0.60 mmol) quantitatively.

Spectroscopic data were in accordance with literature data.

MS (ESI): m/z (%) = 714.8 (18), 606.8 (19), 584.8 (21) $[2M+Na]^+$, 562.8 (24) $[2\ M]^+$, 322.0 (15), 303.8 (100) $[M+Na^+]$, 298.7 (16) $[M+NH_4]^+$, 281.8 (21) $[M^+]$, 279.1 (18), 263.2 (22).

^{1}H-NMR (300 MHz, in dDMSO): δ = 2.04 – 2.22 (m, 2H, 2'-H), 3.52 – 3.63 (m, 2H, 5'-H), 3.78 – 3.85 (m, 1H, 4'-H), 3.95 (s, 2H, $\underline{CH_2}NH_2$), 4.17 – 4.26 (m, 1H, 3'-H), 5.04 – 5.14 (m, 1H, 5'-OH), 5.20 – 5.30 (m, 1H, 3'-OH), 6.09 (t, $J_{1',2'}$ = 6.6, 1H, 1'-H), 8.19 – 8.44 (m_{br}, 2H, NH_2), 8.23 (s, 1H, 6-H).

(N-TFA)-5-Propargylamino-(2'-deoxy-5'-DMT-O)-uridine 40

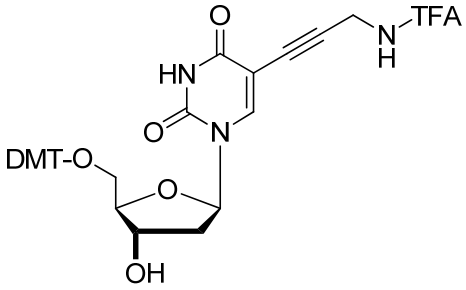

Chemical Formula: $C_{35}H_{32}F_3N_3O_8$
Molecular Weight: 679.64

5-(3''-Trifluoroacetamidepropargyl)-2'-deoxyuridine **37** (1.5 g, 3.9 mmol) was dried three times azeotropically with 10 ml of anhydrous pyridine each. DMAP (122 mg, 1.00 mmol, 0.3 equiv.), NEt_3 (1.1 ml, 7.8 mmol, 2.0 equiv.) were added and everything was dissolved in 30 ml of anhydrous pyridine. A solution of DMT-Cl (1.6 g, 4.8 mmol, 1.2 equiv.) in 10 ml anhydrous pyridine was added. The reaction mixture was then allowed to stir over night at rt. Afterwards, the solvent was

removed under vacuum and the crude product was dissolved in 20 ml CH_2Cl_2 with 1% NEt_3. The organic phase was washed three times with 20 ml of a 1 M $NaHCO_3$ solution each and dried over Na_2SO_4. The solvent was then removed under vacuum. Purification by column chromatography [5 x 15 cm, 18 ml, CH_2Cl_2/MeOH (+ 1% NEt_3) = 98:12 → 95:5]. Fractions 22-35 were combined and the solvent was removed under reduced pressure to give the desired compound (1.2 mg, 1.8 mmol) in 45% yield.

Spectroscopic data were in accordance with literature data.

MS (CI): m/z (%) = 704.0 (6), 703.0 (34), 701.9 (100) [M+Na^+], 440.9 (17), 373.2 (17), 339.3 (5), 304.2 (8), 303.2 (35) [DMT^+], 245.2 (6), 228.3 (5), 226.3 (6), 225.1 (8), 215.4 (15), 202.3 (10), 195.2 (19).

^{1}H-NMR (300 MHz, in dDMSO): δ = 2.12 – 2.33 (m, 2H, 2'-H), AB-signal[**] ($\delta_{5'a}$ = 3.07, $\delta_{5'b}$ = 3.24, $J_{A,B}$ = 10.4, $J_{B,A}$ = 10.3, additional coupling $J_{5'a,4'}$ = 3.1, 2H, 5'-H), 3.73 (s, 6H, OCH_3), 3.87 – 3.94 (m, 1H, 4'-H), 4.04 (d, $J_{3'',3''NH}$ = 4.9, 2H, 3''-H), 4.21 – 4.30 (m, 1H, 3'-H), 5.39 (d, $J_{3'OH,3'}$ = 4.9, 1H, 3'-OH), 6.08 (dd, $J_{1',2'b}$ = $J_{1',2'a}$ = 6.7, 1H, 1'-H), 6.84 – 6.93 (m, 4H, aromat.), 7.17 – 7.42 (m, 9H, aromat.), 7.91 (s, 1H, 6-H), 9.91 – 10.00 (m, 1H, 3''-NH), 11.59 – 11.75 (s_{br}, 1H, 3-NH).

5-Propargylamino-(2'-deoxy-5'-DMT-O)-uridine [206] 91

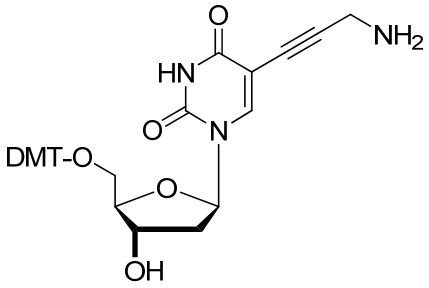

Chemical Formula: $C_{33}H_{33}N_3O_7$
Molecular Weight: 583.63

The TFA protected 5-propargylamino-(2'-deoxy-5'-DMT-O)-uridine **40** (100 mg, 0.147 mmol) was dissolved in 1 ml MeOH and treated with 5 ml of a 25% ammonia-hydroxide solution. The reactions mixture was stirred at rt. for 1 hour. Afterwards, the solvent was removed under vacuum to give the desired compound (85.0 mg, 0.146 mmol) quantitatively.

^{1}H-NMR (400 MHz, in CD_3OD): δ = AB-signal ($\delta_{2'a}$ = 2.34, $\delta_{2'b}$ = 2.4, $J_{A,B}$ = 13.6, $J_{B,A}$ = 13.7, additional couplings $J_{2'a,3'}$ = 6.3, $J_{2'a,1'}$ = 7.2 and $J_{2'b,3'}$ = 3.4, $J_{2'b,1'}$ = 6.1, 2H, 2'-H), 3.12 (m, 2H, $\underline{CH_2}NH_2$), AB-signal[†] ($\delta_{5'a}$ = 3.29, $\delta_{5'b}$ = 3.38, $J_{A,B}$ = 11.0, $J_{B,A}$ = 10.8, additional coupling $J_{5'b,4'}$ = 2.6, 2H, 5'-H), 4.03 (ddd, $J_{4',5'b}$ = 2.7, $J_{4',3'}$ = 3.2, $J_{4',5'a}$ = 3.3, 1H, 4'-H), 3.77 (s, 6H, OCH_3), 4.49 (ddd, $J_{3',4'}$ = 3.2, $J_{3',2'b}$ = 3.1, $J_{3',2'a}$ = 6.1, 1H, 3'-H), 6.24 (dd, $J_{1',2'b}$ = 6.3, $J_{1',2'a}$ = 6.8, 1H, 1'-H), 6.85 – 6.90 (m, 4H, aromat.), 7.20 – 7.24 (m, 1H, aromat.), 7.27 – 7.33 (m, 2H, aromat.), 7.34 – 7.39 (m, 4H, aromat.), 7.45 – 7.50 (m, 2H, aromat.), 8.23 (s, 1H, 6-H).

[*] 5'b Signal partially superposed by traces of H_2O.
[†] 5'a Signal partially superposed by traces of H_2O.

^{13}C-NMR (100 MHz, in CD_3OD): δ = 164.8 (4-C), 160.2 (aromat.), 151.3 (2-C), 146.2 (aromat.), 144.3 (6-C), 137.1 (aromat.), 131.3 (aromat.), 129.3 (aromat.), 129.0 (aromat.), 128.0 (aromat.), 114.4 (aromat.), 100.5 (5-C), 94.5 (Trityl-C), 88.3 (1'-C)*, 88.2 (1''-C)* , 87.3 (4'-C); 74.8 (2''-C), 72.5 (3'-C), 64.7 (5'-C), 55.8 (2·OCH_3), 42.3 (2'-C), 32.0 (3''-C).

5-[(3''-Trifluoroacetamido)propyl]-2'-deoxyuridine [170] 92

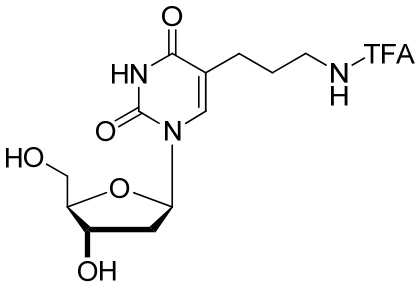

Chemical Formula: $C_{14}H_{18}F_3N_3O_6$
Molecular Weight: 381.30

A two necked flask was charged with 5-(3''-trifluoroacetamidepropargyl)-2'-deoxyuridine **37** (200 mg, 0.530 mmol) and PtO_2 (cat.) The flask was thoroughly flushed with H_2(g) and 50 ml of anhydrous MeOH were added. The reaction mixture was stirred heavily under an H_2 atmosphere (1 atm.) for 1 h. Due to the risk of producing electrostatic sparks, stirring should not be started prior to the addition of solvent! Afterwards, the flask was flushed with air and another 50 ml MeOH were added. The solution was filtered over celite. The celite was washed with an additional 100 ml MeOH and the solvent of the combined organic phases was removed under reduced pressure. The crude product was purified by column chromatography (5 x 6.5 cm, 20 ml, EtOAc/MeOH = 9:1). Fractions 6-9 were combined and the solvent was removed under reduced pressure. The desired product (141 mg, 0.370 mmol) was obtained as pale yellow foam in 70% yield.

Spectroscopic data were in accordance with literature data.

MS (CI): m/z (%) = 399.2 (24) [$M+NH_4^+$], 383.2 (16), 382.2 (100) [M^+], 284.2 (8), 283.2 (67), 282.2 (6), 267.1 (7), 266 (64).

^{1}H-NMR (400 MHz, in dDMSO): δ = 1.63 (q, $J_{2'',3''} = J_{2'',1''}$ = 7.3, 2H, 2''-H), 2.02 – 2.26 (m, 4H, 1''-H + 2'-H), 3.16 (dt, $J_{3'',3''NH} = J_{3'',2''}$ = 6.5, 2H, 3''-H), AB-signal ($\delta_{5'a}$ = 3.53, $\delta_{5'b}$ = 3.58, $J_{A,B}$ = 11.8, $J_{B,A}$ = 11.9, additional couplings $J_{5'a,4'}$ = 3.9, and $J_{5'b,4'}$ = 4.0, 2H, 5'-H), 3.75 (ddd, $J_{4',3'}$ = 3.1, $J_{4',5'a} = J_{4',5'b}$ = 3.8, 1H, 4'-H), 4.23 (ddd, $J_{3',4'}$ = 3.0, $J_{3',2'a}$† = 3.0, $J_{3',2'b}$† = 5.8, 1H, 3'-H), 4.92 – 5.04 (m_{br}, 1H, OH), 5.14 – 5.26 (m_{br}, 1H, OH), 6.15 (dd, $J_{1',2'a}$‡ = 6.3, $J_{1',2'b}$‡ = 7.4, 1H, 1'-H), 7.67 (s, 1H, 6-H), 9.38 (t, $J_{3''NH,3''}$ = 6.0, 1H, 3''-NH), 11.27(s, 1H, 3-NH).

* Signals possibly exchangeable.
† Signals possibly exchangeable.
‡ Signals possibly exchangeable.

^{13}C-NMR (100 MHz, in dDMSO): δ = 163.3 (4-C), 156.1 (q, $^{3}J_{5'',6''F}$ = 35.8, 5''-C), 150.3 (2-C), 136.4 (6-C), 115.9 (q, $J_{6'',6''F}$ = 288.6, 6''-C), 112.6 (5-C), 87.3 (4'-C), 83.9 (1'-C), 70.4 (3'-C), 61.3 (5'-C), 40.2 (2'-C superposed by DMSO signals), 38.7 (1''-C superposed by DMSO signals), 27.1 (2''-C), 23.9 (3''-C).

5-[3''-(Amino)-propyl]-2'-deoxyuridine 43

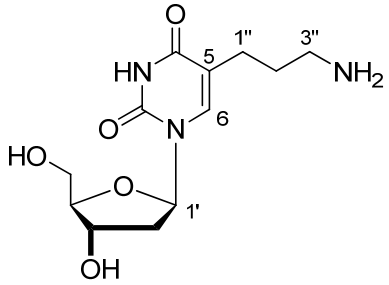

Chemical Formula: $C_{12}H_{19}N_3O_5$
Molecular Weight: 285.30

5-[(3''-Trifluoroacetamido)propyl]-2'-deoxyuridine **92** (292 mg, 0.766 mmol) was dissolved in 10 ml of ammonium hydroxide (25%) and stirred for 3 h at rt. The solvent was removed under reduced pressure. The crude product, a brown oil, was dissolved in 5 ml of H_2O and dried in a freeze-drier to obtain the desired product (214 mg, 0.750 mmol) quantitatively.

MS (CI): m/z (%) = 286.2 (41) [M^+], 172.1 (12), 171.1 (9), 170.1 (100), 129.1 (5), 127.1 (6).

^{1}H-NMR (300 MHz, in dDMSO): δ = 1.70 (dd, $J_{2'',3''}$ = 7.3, $J_{2'',1''}$ = 7.8, 2H, 2''-H), 2.09 (dd, $J_{2',3'}$ = 4.7, $J_{2',1'}$ = 6.7, 2H, 2'-H), 2.26 (t, $J_{3'',2''}$ = 7.3, 2H, 3''-H), 2.76 (t, $J_{1'',2''}$ = 7.6, 2H, 1''-H), AB-signal ($\delta_{5'a}$ = 3.54, $\delta_{5'b}$ = 3.60, $J_{A,B}$ = 11.8, $J_{B,A}$ = 11.9, additional couplings $J_{5'a,4'}$ = 4.0, $J_{5'b,4'}$ = 3.8, 2H, 5'-H), 3.77 ($J_{4',3'}$ = 3.2, $J_{4',5'a}$ = $J_{4',5'b}$ = 3.5, 1H, 4'-H), 4.20 – 4.28 (m, 1H, 3'-H), 5.23 (m_c, 1H, OH), 6.16 (t, $J_{1',2'}$ = 6.9, 1H, 1'-H), 7.71 (s, 1H, 6-H).

Diisoprapylammonium-tetrazolide 27

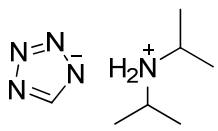

Chemical Formula: $C_7H_{17}N_5$
Molecular Weight: 171.24

Anhydrous diisopropylamine (11.6 ml, 81.8 mmol, 1.8 equiv.) was slowly added at 0°C to 100 ml of a 0.45 M solution of tetrazole (45 mmol) in anhydrous CH_3CN. Thereby the colorless product crystallized. The reaction mixture was allowed to stir 1 h at rt, before the product was filtered and washed with CH_3CN and Et_2O. The product was then dried in a desiccator.

2-Deoxy-3,5-di-O-(p-chlorobenzoyl)-D-ribofuranosyl chloride [180] 58

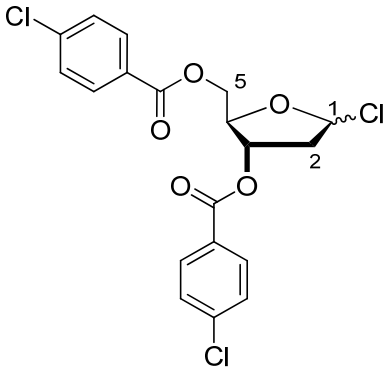

Chemical Formula: $C_{19}H_{15}Cl_3O_5$
Molecular Weight: 429.68

Step 1

Deoxy-*D*-ribose (8.4 g, 62 mmol) was dissolved in 160 ml anhydrous MeOH and treated with 8.4 ml of 1% HCl in anhydrous MeOH. The reaction mixture was stirred at rt. for 45 min. Afterwards 45 ml anhydrous pyridine were added to neutralize the reaction solution. The solvents were removed under reduced pressure. The residue was co-evaporated with 20 ml of anhydrous pyridine to remove traces of MeOH.

Step2

The oily sugar was than dissolved in 50 ml of anhydrous pyridine and cooled to 0°C. At this temperature 20.0 ml of *p*-chlorobenzoyl chloride (27 g, 0.16 mol, 2.5 equiv.) were added. The internal temperature did not exceed 30°C. A colorless precipitate crystallized. The reaction mixture was stirred at rt. over night. The precipitate was filtered and dissolved in 200 ml CH_2Cl_2. 125 ml water were added to hydrolyze excess *p*-chlorobenzoyl-chloride. The aqueous phase was extracted with 60 ml CH_2Cl_2. The combined organic phases were than washed twice with 120 ml of each: cold sat. $NaHCO_3$ solution, water, cold 3 N H_2SO_4 and again with water. The organic phase was dried over Na_2SO_4. The solution was filtered and the solvent was removed under reduced pressure. The oily residue was dried under high vacuum.

Step 3

Traces of water from the crude product of Step 2 were removed azeotropically with 30 ml anhydrous toluene. The residue was than dissolved in 36 ml anhydrous toluene and cooled at 0°C for 1 hour. The precipitate was filtered and washed with anhydrous toluene. The combined filtrates were concentrated under reduced pressure and the residue was dissolved in 48 ml concentrated acetic acid. Under careful cooling 90 ml of ice cold concentrated acetic acid saturated with anhydrous HCl were added. The crystallization of the desired compound completed within 20 min whereupon it was filtered and washed with Et_2O until the wash solution remained neutral. The colorless crystals of **58** (8.30 g, 19.4 mmol) were dried under high vacuum and stored over KOH at reduced pressure (< 1 mbar). The yield over 3 steps was 31%.

Spectroscopic data were in accordance with literature data.

MS (CI): m/z (%) = 450.1 (9), 449.2 (5), 448.1 (26), 447.2 (6), 446.2 (25) $[m+NH_4]^+$, 412.1 (8), 410.1 (12), 397.1 (6), 396.1 (7), 395.1(32), 394.1 (10), 393.1 (47), 140.9 (12), 138.9 (37), 98.0 (10), 80.9 (100).

^{1}H-NMR (400 MHz, in $CDCl_3$)*: δ = AB-signal (δ_{2a} = 2.75, δ_{2b} = 2.85, $J_{A,B}$ = 15.0, $J_{B,A}$ = 15.2, additional couplings for $J_{2a,3}$ = 1.2 and $J_{2b,1'}$ = 5.1, $J_{2b,3}$ = 7.4, 2H, 2-H), AB-signal (δ_{5a} = 4.60, δ_{5b} = 4.68, $J_{A,B}$ = 12.0, $J_{B,A}$ = 12.0, additional couplings for $J_{5a,4}$ = 4.6 and $J_{5b,4}$ = 3.5, 2H, 5-H), 4.84 (ddd, $J_{4,3}$ = 2.9, $J_{4,5b}$ = 3.5, $J_{4,5a}$ = 4.6, 1H, 4-H), 5.54 (ddd, $J_{3,2a}$ = 1.2, $J_{3,4}$ = 3.0, $J_{3,2b}$ = 7.4, 1H, 3-H), 6.47 (d, $J_{1,2b}$ = 5.0, 1H, 1-H), 7.37 – 7.47 (m, 4H, aromat.), 7.92 – 8.05 (m, 4H, aromat).

^{13}C-NMR (100 MHz, in $CDCl_3$)*: δ = 165.6 (carboxylic C), 165.3 (carboxylic C), 140.2 (quaternary aromat.), 140.0 (quaternary aromat.), 131.3 (aromat.), 131.1 (aromat.), 129.0 (aromat.), 129.0 (aromat.), 128.0 (quaternary aromat.), 127.9 (quaternary aromat.), 95.1 (1-C), 84.5 (4-C), 74.0 (3-C), 63.9 (5-C), 44.5 (2-C).

Anal. Calcd for $C_{19}H_{15}Cl_3O_5$: C, 53.11; H, 3.52. Found: C, 52.51; H, 3.64.

[1,10]-Phenanthroline-5,6-dione [187, 188] 66

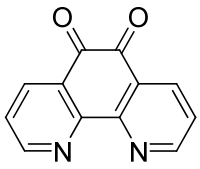

Chemical Formula: $C_{12}H_6N_2O_2$
Molecular Weight: 210.19

[1,10]-Phenanthrolinium hydrochloride monohydrate (1.17 g, 5.04 mmol) and KBr (5.95 g, 50.0 mmol, 10 equiv.) were provided in a 500 ml flask. Under heavy stirring and cooling in an ice bath 20 ml concentrated H_2SO_4 were carefully added, by allowing the acid to slowly run down the inner glass wall of the flask. 10 ml of concentrated HNO_3 were added. The reaction mixture was than heated to 85°C and stirred for 2 h. Afterwards the solution was cooled to rt. and then poured into 400 ml water. The yellow solution was neutralized with $NaHCO_3$ and 4 times extracted with 100 ml CH_2Cl_2 each. The combined organic phases were dried over Na_2SO_4 and the solvent was removed under reduced pressure to give the crude product (636 mg, 3.02 mmol) in 60% yield.

For analysis the crude product was re-crystallized in MeOH.

Spectroscopic data were in accordance with literature data.

* Signals of the major isomer.

MS (CI): m/z (%) = 228.1 (25), 212.1 (13), 211.1 (100) [M^+], 199.1 (6), 183.1 (6), 182.1 (15).

^{1}H-NMR (400 MHz, in $CDCl_3$): δ = 7.52 (dd, $J_{3,2} = J_{8,9}$ = 4.7, $J_{3,4} = J_{8,7}$ = 7.9, 2H, 3-H + 8-H), 8.44 (dd, $^4J_{4,2} = {}^4J_{7,9}$ = 1.9, $J_{4,3} = J_{7,8}$ = 7.9, 2H, 4-H + 7-H), 9.06 (dd, $^4J_{2,4} = {}^4J_{9,7}$ = 1.8, $J_{2,3} = J_{9,8}$ = 4.7, 2H, 2-H + 9-H).

^{13}C-NMR (100 MHz, in $CDCl_3$): δ = 178.8 (2C, carboxylic C), 156.5 (2C, 2-C + 9-C), 153.0 (2C, quaternary aromat.), 137.4 (2C, 4-C + 7-C), 128.2 (2C, quaternary aromat.), 125.7 (2C, 3-C + 8-C).

[1,10]-Phenanthrolino-[5,6-d]-2'-phenyl-imidazole 65

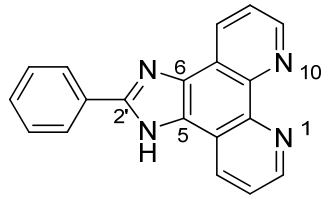

Chemical Formula: $C_{19}H_{12}N_4$
Molecular Weight: 296.33

[1,10]-Phenanthroline-5,6-dione **66** (586 mg, 2.79 mmol) was dissolved in 80 ml of AcOH together with NH_4OAc (12.6 g, 164 mmol, 59 equiv.). Benzaldehyde (888 mg, 0.850 ml, 8.37 mmol, 3.0 equiv.) was added and the solution was stirred for 2.5 h at rt, followed by 3 h of refluxing at 125°C. The yellow solution was cooled to rt. and poured into 80 ml of water. The solution was than neutralized with a 25% solution of NH_3 in water. The yellow precipitate was filtered, washed with cold water and dried under high vacuum to give the desired product (428 mg, 1.45 mmol) in 52% yield.

MS (EI): m/z (%) = 297.0 (21), 296.0 (100) [M^+], 295.0 (8), 193.0 (6), 165.9 (6), 164.9 (5), 148.0 (9).

^{1}H-NMR (400 MHz, in dDMSO): δ = 7.51 (m, 1H, 4''-H), 7.61 (m, 2H, 3''-H + 5''-H), 7.83 (dd, $J_{3,2} = J_{8,9}$ = 4.3, $J_{3,4} = J_{8,7}$ = 8.1, 2H, 3-H + 8-H), 8.30 (m, 2H, 2''-H + 6''-H), 8.94 (dd, $^4J_{4,2} = {}^4J_{7,9}$ = 1.8, $J_{4,3} = J_{7,8}$ = 8.1, 2H, 4-H + 7-H), 9.03 (dd, $^4J_{2,4} = {}^4J_{9,7}$ = 1.8, $J_{2,3} = J_{9,8}$ = 4.3, 2H, 2-H + 9-H).

^{13}C-NMR (100 MHz, in dDMSO): δ = 172.4 (quaternary aromat.), 150.7 (quaternary aromat.), 147.7 (2C, 2-C, 9-C), 143.6 (quaternary aromat.), 130.2 (quaternary aromat.), 129.6 (2C, 4-C + 7-C), 129.5 (1C, 4''-C), 129.0 (2C, 3''-C + 5''-C), 126.2 (2C, 2''-C + 6''-C), 123.3 (2C, 3-C + 8-C).

[1'',10'']-Phenanthrolino-[4,5-f]-1-(2'-deoxy-3',5'-di-O-[p-chlorobenzoyl]-D-ribofuranos-1'-yl)-2-phenyl-imidazole 88

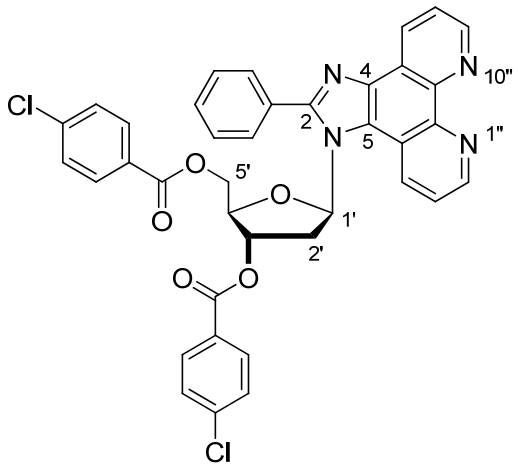

Chemical Formula: $C_{38}H_{26}Cl_2N_4O_5$
Molecular Weight: 689.54

To a 100 ml Schlenk flask equipped with [1,10]-phenanthrolino-[5,6-d]-imidazole **65** (296 mg, 1.00 mmol) and NaH (60% dispersion in mineral oil, 60.0 mg, 1.50 mmol, 1.5 equiv.) 10 ml of anhydrous acetonitrile was added. The yellow suspension was stirred at rt. for 10 h. The suspension was than cooled to 0°C and treated with an ice cold solution of 2-deoxy-3,5-di-*O*-(*p*-chlorobenzoyl)-*D*-ribofuranosyl chloride **58** (azeotropically dried with anhydrous acetonitrile, 773 mg, 1.80 mmol , 1.8 equiv.) in 12 ml anhydrous CH_2Cl_2.The reaction mixture was stirred for 22 h allowing the temperature to slowly rise to rt. Afterwards the solvent was removed at reduced pressure and the crude product was purified by column chromatography [6 x 4.5 cm, 18 ml, CH_2Cl_2/MeOH (0.1% NEt_3) 99:1 → 97:3]. Fractions 30-46 were combined and the solvent removed under reduced pressure to give the desired product (328 mg, 0.476 mmol) in 48% yield.

The α-/β- anomeric ratio was 1:1 as determined by ^{1}H-NMR.

MS (ESI): m/z (%) = 693.1 (15), 692.1 (24), 691.1 (66), 690.1 (39), 689.0 (100) [M^+], 519.1 (18), 297.4(55), 280.2 (15), 279.2 (87).

^{1}H-NMR (400 MHz, in CD_3CN)*: δ = AB-signal [$\delta_{2'a(\beta)}$ = 2.33, $\delta_{2'b(\beta)}$ = 2.82, $J_{A,B}$ = 14.7, $J_{B,A}$ = 14.7, additional couplings for $J_{2'a(\beta),1'(\beta)}$ = 6.4, $J_{2'a(\beta),3'(\beta)}$ = 2.7, and $J_{2'b(\beta),1'(\beta)}$ = 9.2, $J_{2'b(\beta),3'(\beta)}$ = 8.7, 2H, 2'-H(β-anomere)], AB-signal [$\delta_{2'a(\alpha)}$ = 2.70, $\delta_{2'b(\alpha)}$ = 2.82, $J_{A,B}$ = 14.4, additional couplings for $J_{2'a(\alpha),3'(\alpha)}$ = 5.4, $J_{2'a(\alpha),1'(\alpha)}$ = 8.9, 2H, 2'-H(α-anomere)]†, 4.61 [ddd, $J_{4'(\beta),3'(\beta)}$ = $J_{4'(\beta),5'b(\beta)}$ = 4.9, $J_{4'(\beta),5'a(\beta)}$ = 6.1, 1H, 4'-H(β-anomere)], 4.68 [d, $J_{5'(\alpha),4'(\alpha)}$ = 3.6, 2H, 5'-H(α-anomere)], AB-signal [$\delta_{5'a(\beta)}$ = 4.79, $\delta_{5'b(\beta)}$ = 4.99, $J_{A,B}$ = 12.0, $J_{B,A}$ = 12.1, additional couplings for $J_{5'a(\beta),4'(\beta)}$ = 6.0, $J_{5'b(\beta),4'(\beta)}$ = 4.6, 2H, 5'-H(β-anomere)], 5.01 [dt, $J_{4'(\alpha),3'(\alpha)}$ = 2.8, $J_{4'(\alpha),5'(\alpha)}$ = 3.6, 1H, 4'H(α-anomere)], 5.51 [ddd, $J_{3'(\beta),2'a(\beta)}$ = 2.9, $J_{3'(\beta),4'(\beta)}$ = 5.3, $J_{3'(\beta),2'b(\beta)}$ = 8.3, 1H, 3'-H (β-anomere)], 5.57 [ddd, $J_{3'(\alpha),4'(\alpha)}$ = 2.9, $J_{3'(\alpha),2'a(\alpha)}$ = 5.4, $J_{3'(\alpha),2'b(\alpha)}$ = 8.3, 1H, 3'-H (α-anomere)], 6.59 (dd, $J_{1'(\beta),2'a(\beta)}$ = 6.3, $J_{1'(\beta),2'b(\beta)}$ = 9.4, 1H, 1'-H(β-anomere)], 6.73 (dd, $J_{1'(\alpha),2'b(\alpha)}$ = 6.5, $J_{1'(\alpha),2'a(\alpha)}$ = 8.9, 1H, 1'H(α-anomere)], 7.26 – 7.62 (m, 8H, aromat.), 7.71 – 7.80 (m, 2H, aromat.), 7.84 – 7.98 (m, 5H, aromat.), 8.88 – 9.03 (m, 3H, aromat.), 9.05 – 9.09 (m, 1H, aromat.).

* Assignment of anomers possibly exchangeable.
† Couplings for 2'b-H with 1'-H and 3-H' could not be resolved.

^{13}C-NMR (100 MHz, in CD_3CN)*: δ = 166.2 (carboxylic C_α + C_β), 166.0 (carboxylic C_α), 165.8 (carboxylic C_β), 156.4 (aromat.), 156.1 (aromat.), 149.9 (aromat.), 148.6 (aromat.), 145.6 (aromat.), 145.6 (aromat.), 140.4 (aromat.), 140.3 (aromat.), 140.2 (aromat.), 140.0 (aromat.), 138.6 (aromat.), 138.1 (aromat.), 133.2 (aromat.), 132.1 (aromat.), 132.0 (aromat.), 131.9 (aromat.), 131.7 (aromat.), 131.2 (aromat.), 130.9 (aromat.), 130.7 (aromat.), 130.5 (aromat.), 129.9 (aromat.), 129.8 (aromat.), 129.6 (aromat.), 129.5 (aromat.), 129.3 (aromat.), 129.2 (aromat.), 129.1 (aromat.), 127.6 (aromat.), 127.3 (aromat.), 124.7 (aromat.), 124.5 (aromat.), 123.5 (aromat.), 121.6 (aromat.), 121.3 (aromat.), 89.0 (1'-C_α), 87.2 (1'-C_β), 82.6 (4'-C_α), 81.2 (4'-C_β), 76.4 (3'-C_α), 74.4 (3'-C_β), 65.5 (5'-C_α), 64.2 (5'-C_β), 37.6 (2'-C_α), 36.9 (2'-C_β).

Mp: 95-100°C (Decomposition).

[1'',10'']-Phenanthrolino-[4,5-f]-1-(2'-deoxy-D-ribofuranos-1'-yl)-2-phenyl-imidazole 55

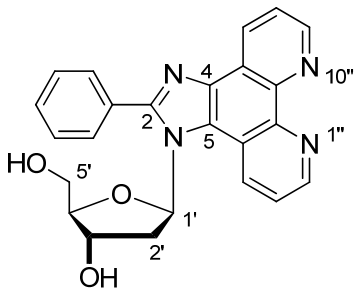

Chemical Formula: $C_{24}H_{20}N_4O_3$
Molecular Weight: 412.44

[1'',10'']-Phenanthrolino-[4,5-f]-1-(2'-deoxy-3',5'-di-*O*-[*p*-chlorobenzoyl]-*D*-ribofuranos-1'-yl)-2-phenyl-imidazole (**88**) (50 mg, 0.07 mmol) was first cooled to 0°C in an ice bath. A 0.1 M solution of NH_3(g) in MeOH (1.5 ml, 0.15 mmol, 2 equiv.) also cooled to 0°C, was added to the protected nucleoside **88** and the reaction mixture was stirred overnight with gradual warming to rt. Reaction progress was monitored by TLC (CH_2Cl_2/CH_3OH = 80:20). The solvent was evaporated and the crude material was subjected to azeotropic evaporation with acetonitrile to remove the cleaved protecting groups. The desired product was isolated as an orange oil (28 mg, 0.07 mmol) in 97% yield.

MS (ESI): m/z (%) = 985.1 (6), 848.1 (11), 847.1 (21), 553.1 (7), 552.1 (6), 551.1 (20), 414.1 (26), 413 (100) [M^+], 298 (7), 297 (34).

1-[2'-Deoxy-3',5'-di-O-(p-chlorobenzoyl)-D-ribofuranos-1'-yl]-2-(pyridine-2-yl)-benzo[d]imidazole 63

Method 1 with NaOH as base in a biphasic system:

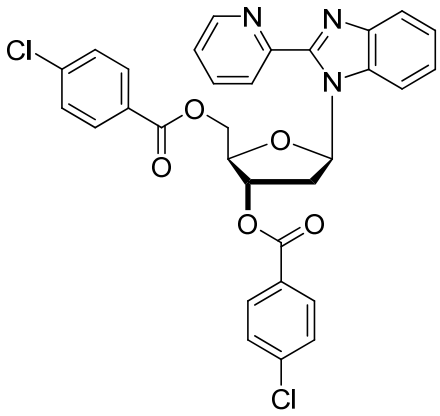

Chemical Formula: $C_{31}H_{23}Cl_2N_3O_5$
Molecular Weight: 588.44

A suspension of 2-(2-pyridyl)benzimidazole (0.33 g, 1.7 mmol) and Bu_4NHSO_4 (61 mg, 0.80 mmol, 0.5 equiv.) in 10 ml CH_2Cl_2 and 10 ml of an aqueous solution of NaOH (50%) was treated with a solution of 2-deoxy-3,5-di-*O*-(*p*-chlorobenzoyl)-*D*-ribofuranosyl chloride **58** (0.87 g, 1.9 mmol, 1.1 equiv.) in 8 ml anhydrous CH_2Cl_2. The biphasic reaction was heavily shaken for 2 min after which the organic layer was isolated. The aqueous layer was extracted three times with 50 ml CH_2Cl_2 each. The combined organic phases were dried over Na_2SO_4 and the solvent was removed under reduced pressure. A sample of the crude product was analyzed by ^{1}H-NMR to determine the anomeric ratio of β/α = 2:1. The remaining crude product was purified by column chromatography (5 x 4 cm, 20 ml, CH/acetone = 8:2). Fractions 8-20 were combined and the solvent was removed under reduced pressure to give the desired compound (762 mg, 1.30 mmol) in 76% yield.

The pure β-anomer was isolated by means of re-crystallization from MeOH. However several cycles of re-crystallization were needed.

Method 2 with DBU as base:

A suspension of 2-(2-pyridyl)benzimidazole (351 mg, 1.80 mmol) and DBU (335 mg, 2.20 mmol, 1.2 equiv.) in 20 ml anhydrous CH_3CN was stirred at rt. for 20 min. Thereafter, 2-deoxy-3,5-di-*O*-(*p*-chlorobenzoyl)-*D*-ribofuranosylchloride **58** (773 mg, 1.80 mmol, 1.0 equiv.) was added stepwise (0.60 mmol each) to the suspension. The brown reaction mixture was stirred for 1 h at rt. Afterwards the solvent was removed under reduced pressure. A sample of the crude product was analyzed by ADH-HPLC (*n*-heptane/EtOH = 2:8) to determine the anomeric ratio of β (23 min) : α (37 min) = 1:1.5. The remaining crude product was purified by column chromatography (6 x 5 cm, 20 ml, CH/acetone = 8:2). The combined solutions of fractions 10-15 were reduced under vacuum to remove acetone from the solvent. The solution was then allowed to rest over night during which the product crystallized. The colorless crystals were isolated and dried. A second fraction of crystals

was obtained by further concentrating the mother solution, giving a total yield of 47% (506 mg, 0.860 mmol).

Method 3 with NaH as base:

A suspension of 2-(2-pyridyl)benzimidazole (200 mg, 1.02 mmol) and NaH (60% w/w dispersion in mineral oil, 60 mg, 1.5 mmol, 1.5 equiv.) in 10 ml anhydrous CH_3CN was stirred at rt. for 9 h. The suspension was then cooled to 0°C and treated with an ice cold solution of 2-deoxy-3,5-di-*O*-(*p*-chlorobenzoyl)-*D*-ribofuranosylchloride **58** (800 mg, 1.86 mmol, 1.9 equiv.) in 12 ml anhydrous CH_2Cl_2. The reaction was stirred for 18 h while the temperature was allowed to slowly rise to rt. Afterwards, the solvent was removed under reduced pressure. A sample of the crude product was analyzed by ADH-HPLC (*n*-heptane/EtOH = 2:8) to determine the anomeric ratio of β (22 min) : α (36 min) = 3:1. The remaining crude product was purified by column chromatography (6 x 5 cm, 20 ml, CH/acetone = 8:2). The combined solutions of fractions 6-11 were reduced under vacuum to remove acetone from the solvent. The solution was then allowed to rest over night during which the product crystallized. The colorless crystals were isolated and dried. A second fraction of crystals was obtained by further concentrating the mother solution, giving **63** (554 mg, 0.942 mmol) in a total yield of 92%.

Mp: 105-108°C.

^{1}H-NMR (400 MHz, in $CDCl_3$): δ = AB-signal [$\delta_{2'a(\alpha)}$ = 2.74, $\delta_{2'b(\alpha)}$ = 3.35, $J_{A,B}$ = 14.7, $J_{B,A}$ = 15.1, additional couplings for $J_{2'a(\alpha),1'(\alpha)}$ = 5.5, $J_{2'a(\alpha),3'(\alpha)}$ = 3.4, and $J_{2'b(\alpha),1'(\alpha)}$ = 7.5, $J_{2'b(\alpha),3'(\alpha)}$ = 7.5, 2H, 2'-H(α-anomere)], AB-signal [$\delta_{2'a(\beta)}$ = 2.83, $\delta_{2'b(\beta)}$ = 3.06, $J_{A,B}$ = 14.3, $J_{B,A}$ = 14.3, additional couplings for $J_{2'a(\beta),1'(\beta)}$ = 5.9, $J_{2'a(\beta),3'(\beta)}$ = 2.3, and $J_{2'b(\beta),1'(\beta)}$ = 9.0, $J_{2'b(\beta),3'(\beta)}$ = 7.8, 2H, 2'-H(β-anomere)], 4.52 [ddd, $J_{4'(\beta),5'b(\beta)}$ = 3.4, $J_{4'(\beta),5'a(\beta)}$ = 3.9, $J_{4'(\beta),3'(\beta)}$ = 4.0, 1H, 4'H(β-anomere)], AB-signal [$\delta_{5'a(\alpha)}$ = 4.60, $\delta_{5'b(\alpha)}$ = 4.68, $J_{A,B}$ = $J_{B,A}$ = 11.9, additional couplings for $J_{5'a(\alpha),4'(\alpha)}$ = 4.2, and $J_{5'b(\alpha),4'(\alpha)}$ = 4.4, 2H, 5'-H(α-anomere)], AB-signal [$\delta_{5'a(\beta)}$ = 4.81, $\delta_{5'b(\beta)}$ = 4.86, $J_{A,B}$ = $J_{B,A}$ = 12.2, additional couplings for $J_{5'a(\beta),4'(\beta)}$ = 3.9, and $J_{5'b(\beta),4'(\beta)}$ = 3.3, 2H, 5'-H(β-anomere)], 5.01 [ddd, $J_{4'(\alpha),3'(\alpha)}$ = 2.2, $J_{4'(\alpha),5'b(\alpha)}$ = $J_{4'(\alpha),5'a(\alpha)}$ = 4.2, 1H, 4'H(α-anomere)], 5.01 [ddd, $J_{3'(\alpha),4'(\alpha)}$ = 2.2, $J_{3'(\alpha),2'a(\alpha)}$ = 3.4, $J_{3'(\alpha),2'b(\alpha)}$ = 7.6, 1H, 3'-H (α-anomere)], 5.71 [ddd, $J_{3'(\beta),2'a(\beta)}$ = 2.3, $J_{3'(\beta),4'(\beta)}$ = 4.0, $J_{3'(\beta),2'b(\beta)}$ = 7.6, 1H, 3'-H (β-anomere)], 6.97 – 7.01 [m, 1H (β-anomere), aromat.], 7.27 – 7.50 [m, 6H (β-anomere) + 7H (α-anomere), aromat.], 7.71 [dd, $J_{1'(\beta),2'a(\beta)}$ = 5.8, $J_{1'(\beta),2'b(\beta)}$ = 9.0, 1H, 1'-H (β-anomere)], 7.71 – 8.09 [m, 7H (β-anomere) + 7H (α-anomere), aromat. + 1'-H (α-anomere)], 8.39 – 8.53 [m, 1H (β-anomere) + 2H (α-anomere), aromat.], 8.65 – 8.69 [m, 1H (β-anomere), aromat.].

^{13}C-NMR (100 MHz, in $CDCl_3$): δ = 165.5 (carboxylic C), 165.3 + 165.2 (carboxylic C), 149.9 (aromat.), 149.8 (aromat.), 148.6 (aromat.), 148.6 (aromat.), 140.3 (aromat.), 140.2 (aromat.), 140.1 (aromat.), 140.0 (aromat.), 137.3 (aromat.), 133.6 (aromat.), 131.2 (aromat.), 131.2 (aromat.), 131.1 (aromat.), 129.1 (aromat.), 129.0 (aromat.), 129.0 (aromat.), 128.1 (aromat.), 128.0 (aromat.), 127.9 (aromat.), 127.5 (aromat.), 125.8 (aromat.), 125.7 (aromat.), 124.4 (aromat.), 124.1 (aromat.), 123.9 (aromat.), 123.5 (aromat.), 120.5 (aromat.), 113.9 (aromat.), 113.5 (aromat.), 89.1 + 86.5 (1'-C), 83.3 + 81.2 (4'-C), 75.6 + 74.4 (3'-C), 65.5 + 64.2 (5'-C), 39.6 + 37.1 (2'-C).

The pure β-anomer was isolated by means of re-crystallization from MeOH. However several cycles of re-crystallization were needed.

LC-MS (Nucleosil-C18AB, ESI): m/z (%) = 591.78 (12), 590.8 (20), 589.8 (61) [M^+], 588.8 (26), 587.7 (100), 196.2 (28).

^{1}H-NMR (300 MHz, in $CDCl_3$): δ = AB-signal ($\delta_{2'a}$ = 2.84, $\delta_{2'b}$ = 3.07, $J_{A,B}$ = 14.2, $J_{B,A}$ = 14.3, additional couplings for $J_{2'a,1'}$ = 5.7, $J_{2'a,3'}$ = 2.3, and $J_{2'b,3'}$ = 7.9, $J_{2'b,1'}$ = 8.8, 2H, 2'-H), 4.52 (ddd, $J_{4',5'b}$ = 3.6, $J_{4',3'}$ = 3.8, $J_{4',5'a}$ = 3.9, 1H, 4'H), AB-signal ($\delta_{5'a}$ = 4.81, $\delta_{5'b}$ = 4.87, $J_{A,B}$ = 12.3, $J_{B,A}$ = 12.2, additional couplings for $J_{5'a,4'}$ = 3.9, $J_{5'b,4'}$ = 3.5, 2H, 5'-H), 5.76 – 5.82 (m, 1H, 3'-H), 6.96 – 7.03 (m, 1H, aromat.), 7.27 – 7.33 (m, 1H, aromat.), 7.38 – 7.51 (m, 5H, aromat.), 7.71 (dd, $J_{1',2'a}$ = 5.8, $J_{1',2'b}$ = 8.8, 1H, 1'-H), 7.77 – 7.94 (m, 3H, aromat.), 8.00 – 8.09 (m, 4H, aromat.), 8.40 – 8.46 (m, 1H, aromat.), 8.65 – 8.69 (m, 1H, aromat.).

Anal. Calcd for $C_{31}H_{23}Cl_2N_3O_5$: C, 63.28; H, 3.94; N, 7.14. Found: C, 63.46; H, 4.22; N, 6.80.

1-(2'-Deoxy-ribofuranos-1'-yl)-2-(pyridine-2-yl)-benzo[d]imidazole 54

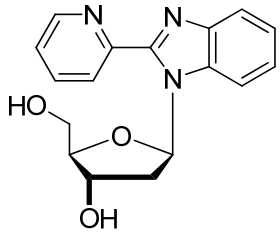

Chemical Formula: $C_{17}H_{17}N_3O_3$
Molecular Weight: 311.34

1-[2'-Deoxy-3',5'-di-*O*-(*p*-chlorobenzoyl)-*D*-ribofuranos-1'-yl]-2-(pyridine-2-yl)-benzo[*d*]imidazole **63** (303 mg, 0.515 mmol) was suspended in 100 ml of anhydrous MeOH. The suspension was cooled to 0°C and gaseous NH_3 was bubbled through this solution for 10 minutes. The suspension was then stirred for further two hours. During this time the temperature was allowed to rise to rt. and the compound slowly dissolved. The solvent was removed in vacuum and the residue was suspended in Et_2O. Filtration of the colorless solid gave the desired compound (153 mg, 0.493 mmol) in 96% yield.

HPLC: (ChiralPak ADH, *n*-heptan/EtOH = 8:2; 0.8 ml/min): α (14.5 min) 1%, β (16.4 min) 99%.

Mp: 156-158°C.

MS (ESI): m/z (%) = 685.1 (8), 312.9 (18), 311.9 (100) [M^+], 197.3 (10) 196.3 (86).

^{1}H-NMR (400 MHz, in dDMSO): δ = AB-signal ($\delta_{2'a}$ = 2.23, $\delta_{2'b}$ = 2.60, $J_{A,B}$ = $J_{B,A}$ = 13.3, additional couplings for 2'a *J* = 6.1, *J* = 2.5 and 2'b *J* = 8.8, *J* = 7.5, 2H, 2'-H), AB-signal ($\delta_{5'a}$ = 3.69, $\delta_{5'b}$ = 3.74, $J_{A,B}$ = 11.8, $J_{B,A}$ = 11.7, additional couplings for $J_{5'a,4'}$ = 4.2, $J_{5'a,5'OH}$ = 5.3 and $J_{5'b,4'}$ = 3.6, $J_{5'b,5'OH}$ = 5.1, 2H, 5'-H), 3.79 (ddd, $J_{4',5'b}$ = 3.6, $J_{4',5'a}$ = 4.1, $J_{4',3'}$ = 4.0, 1H, 4'-H), 4.40 – 4.45 (m, 1H, 3'-H), 5.04 (t, $J_{5'OH,5'}$ = 5.1, 1H, 5'OH), 5.29 (d, $J_{3'OH,3'}$ = 4.3, 1H, 3'OH), 7.23 – 7.31 (m, 3H, 2·aromat. + 1'-H), 7.54 – 7.58 (m, 1H, aromat.), 7.71 – 7.76 (m, 1H, aromat.), 7.98 – 8.06 (m, 2H, aromat.), 8.19 – 8.23 (m, 1H, aromat.), 8.75 – 8.78 (m, 1H, aromat.).

^{13}C-NMR (100 MHz, in dDMSO): δ = 149.9 (aromat.), 149.8 (aromat.), 148.9 (aromat.), 142.7 (aromat.), 137.5 (aromat.), 133.6 (aromat.), 125.2 (aromat.), 124.5 (aromat.), 123.1 (aromat.), 122.5 (aromat.), 119.7 (aromat.), 114.5 (aromat.), 86.9 (4'-C), 85.6 (1'-C), 70.0 (3'-C), 61.2 (5'-C), 40.2 – 38.9 (2'-C superposed by DMSO signals).

Anal. Calcd for $C_{17}H_{17}N_3O_3$: C, 65.58; H, 5.50; N, 13.50. Found: C, 65.37; H, 5.55; N, 13.33.

1-(2'-Deoxy-5'-DMT-O-ribofuranos-1'-yl)-2-(pyridine-2-yl)-benzo[d]imidazole 64

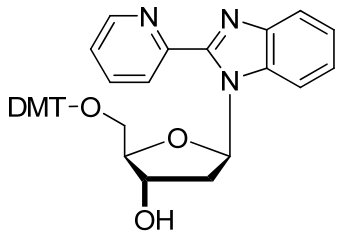

Chemical Formula: $C_{38}H_{35}N_3O_5$
Molecular Weight: 613.70

1-(2'-Deoxy-ribofuranos-1'-yl)-2-(pyridine-2-yl)-benzo[*d*]imidazole **54** (412 mg, 1.32 mmol) was dried three times azeoptropically with 3 ml of anhydrous pyridine each. Under argon, DMAP (41 mg, 0.34 mmol, 0.25 equiv.) was added and dissolved in 4.4 ml anhydrous pyridine. To this solution DMT-Cl (685 mg, 2.02 mmol, 1.5 equiv.) dissolved in 4 ml anhydrous pyridine was added. The reaction mixture was then treated with anhydrous NEt_3 (373 µL, 272 mg, 2.70 mmol, 2.0 equiv.). After stirring at rt. over night the solvent was removed under reduced pressure. The residue was dissolved in 10 ml CH_2Cl_2 (+ 1% NEt_3) and washed three times with 10 ml of a saturated $NaHCO_3$ solution each. The organic phase was dried over Na_2SO_4 and the solvent was removed under reduced pressure. The crude product was purified by column chromatography [5.5 x 3.5 cm, 18 ml, CH_2Cl_2/MeOH (+ 0.1% NEt_3) = 100:0 → 98:2]. Fractions 39-60 were combined and the solvent was removed under reduced pressure to give the desired compound (657 mg, 1.07 mmol) in 79% yield.

MS (ESI): m/z (%) = 1289.0 (6), 638.1 (8), 637.1 (36), 636.1 (100) [M+Na^+], 304.2 (20), 303.2 (90), 289.2 (5), 288.1 (10), 260.2 (7), 259.2 (10), 245.2 (9), 196.2 (8).

^{1}H-NMR (400 MHz, in $CDCl_3$): δ = 2.21 (d, $J_{3'OH,3'}$ = 3.8, 1H, 3'-OH), AB-signal ($\delta_{2'a}$ = 2.51, $\delta_{2'b}$ = 2.85, $J_{A,B}$ = 14.0, $J_{B,A}$ = 13.8, additional couplings for 2'a *J* = 6.7, *J* = 3.3, and for 2'b *J* = 8.2, *J* = 8.3, 2H, 2'-H), AB-signal ($\delta_{5'a}$ = 3.54, $\delta_{5'b}$ = 3.57, $J_{A,B}$ = $J_{B,A}$ = 10.3, additional couplings $J_{5'a,4'}$ = 4.2, $J_{5'b,4'}$ = 4.1, 2H, 5'-H), 3.78 (s, 6H, OMe), 4.00 (ddd, $J_{4',5'a}$ = $J_{4',5'b}$ = 4.1, $J_{4',3'}$ = 4.9, 1H, 4'-H), 4.75 – 4.80 (m, 1H, 3'-H), 6.78 – 6.85 (m, 4H, aromat.), 6.88 – 6.92 (m, 1H, aromat.), 7.20 – 7.25 (m, 2H, aromat.), 7.26 – 7.40 (m, 7H, aromat.), 7.44 – 7.51 (m, 3H, 1'-H + 2·aromat.), 7.77 – 7.87 (m, 3H, aromat.), 8.26 – 8.30 (m, 1H, aromat.), 8.67 – 8.70 (m, 1H, aromat.).

^{13}C-NMR (100 MHz, in $CDCl_3$): δ = 158.6 (aromat.), 150.4 (aromat.), 150.3 (aromat.), 148.8 (aromat.), 144.6 (aromat.), 143.2 (aromat.), 136.9 (aromat.), 135.8 (aromat.), 135.7 (aromat.), 133.8 (aromat.), 130.2 (aromat.), 130.2 (aromat.), 128.3 (aromat.), 127.9 (aromat.), 127.0 (aromat.), 125.3 (aromat.), 123.9 (aromat.), 123.4 (aromat.), 122.9 (aromat.), 120.2 (aromat.), 114.1 (aromat.), 113.2 (aromat.), 86.8 (Trityl-C), 85.8 (1'-C), 84.6 (4'-C), 72.0 (3'-C), 63.1 (5'-C), 55.2 (MeO), 39.7 (2'-C).

Phosphoramidite 57

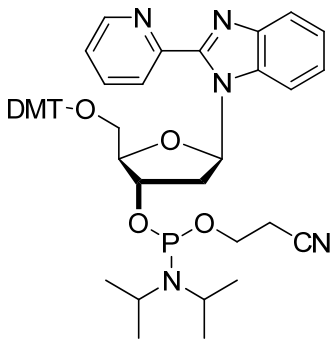

Chemical Formula: $C_{47}H_{52}N_5O_6P$
Molecular Weight: 813.92

1-(2'-Deoxy-5'-DMT-O-ribofuranos-1'-yl)-2-(pyridine-2-yl)-benzo[*d*]imidazole **64** (614 mg, 1.00 mmol) was dried three times azeotropically with 5 ml anhydrous acetonitrile each. Under argon, diisopropylammonium tetrazolide (238 mg, 0.750 mmol, 0.75 equiv.) and 10 ml anhydrous CH_2Cl_2 were added. The solution was treated with (2-cyanoethoxy)-bis-(*N,N*-diisopropylamino)phosphine (784 mg, 2.60 mmol, 2.6 equiv.) and stirred at rt. for two hours. The reaction was monitored by TLC (CH/EtOAc + 1% NEt_3 = 4.2:5.8) and upon completion quenched with 10 ml of a degassed saturated $NaHCO_3$ solution. The aqueous phase was extracted three times with 10 ml degassed CH_2Cl_2 each. The combined organic phases were dried over Na_2SO_4 and the solvent was removed under reduced pressure. The crude product was purified by column chromatography on a Büchi Sepacore chromatography system [4 x 15 cm, 18 ml, degassed CH/EtOAc (+ 1% NEt_3) = 1:1, 30 ml/min, threshold: 4%, sensitivity: 3]. Fractions 8-30 were combined and the solvent was removed under reduced pressure to give the desired compound (512 mg, 0.640 mmol) in 64% yield. The product was stored under argon at –20°C.

MS (ESI): m/z (%) = 1025.1 (5), 838.2 (11), 837.2 (47), 836.2(100) [M+Na^+], 525.3 (5), 524.3 (20), 303.2 (21).

^{1}H-NMR (400 MHz, in CD_3CN): δ = 1.03 – 1.23 [m, 12H, 2·CH($\underline{CH_3}$)$_2$], 2.46 – 2.62 (m, 3H, 2'a-H + CH_2CN), 2.76 – 2.86 (m, 1H, 2'b-H), 3.41 – 3.49 (m, 2H, 5'-H), 3.52 – 3.83 (m, 4H, OCH_2 + 2·*i*-Pr-CH), 3.74 (s, 6H, 2·OCH_3), 4.06 – 4.14 (m, 1H, 4'-H), 4.77 – 4.93 (m, 1H, 3'-H), 6.78 – 6.87 (m, 5H, aromat.), 7.18 – 7.32 (m, 4H, aromat.), 7.32 – 7.41 (m, 4H, aromat.), 7.41 – 7.53 (m, 4H, 1'-H + 3·aromat.), 7.67 – 7.73 (m, 1H, aromat.), 7.87 – 7.98 (m, 2H, aromat.), 8.21 – 8.27 (m, 1H, aromat.), 8.65 – 8.70 (m, 1H, aromat.).

^{13}C-NMR (100 MHz, in CD_3CN): δ = 159.7, 159.7, 151.4, 151.3, 151.3, 149.7, 146.0, 146.0, 144.3, 138.2, 136.8, 136.7, 136.7, 136.7, 134.9, 134.9, 131.2, 131.2, 131.2, 129.2, 129.1, 128.9, 127.9, 127.9, 126.2, 126.2, 125.2, 125.2, 124.1, 124.1, 123.7, 120.9, 119.5, 119.3, 115.6, 115.5, 114.1, 114.1, 87.4 + 87.0 (1'-C), 85.4 + 85.4 + 85.2 + 85.2 (4'-C), 74.2 + 74.0 + 73.6 + 73.4 (3'-C), 63.8 + 63.6 (5'-C), 59.6 + 59.5 + 59.4 + 59.3(O<u>C</u>H$_2$), 55.9 + 55.9 (MeO), 44.1 + 44.0 (*i*-Pr-<u>C</u>H), 39.4 + 39.4 (2'-C), 25.0 + 24.9 + 24.9 + 24.8 + 24.8 (*i*-Pr-<u>C</u>H$_3$), 21.1 + 21.0 + 20.9 (<u>C</u>H$_2$CN).

^{31}P-NMR (121 MHz, in $CDCl_3$): δ = 151.1, 149.9.

^{31}P-NMR (121 MHz, in CD_3CN): δ = 148.6, 148.1.

Phosphoramadite dU$^{Phen\ [194]}$ 69

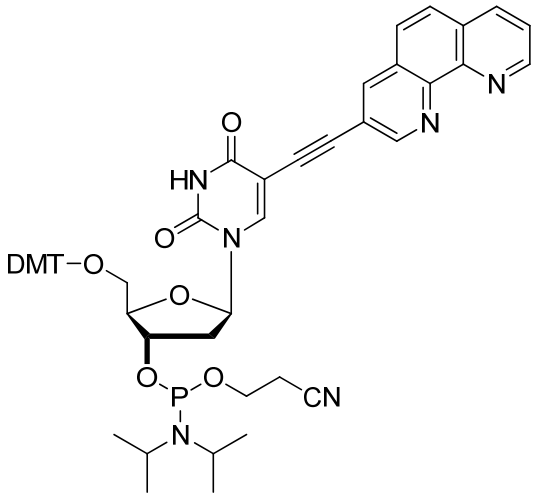

Chemical Formula: $C_{53}H_{53}N_6O_8P$
Molecular Weight: 933.00

5-[Propargyl-3''-(1''-10''-*N*,*N*-phenanthrolino)]-(2'-deoxy-5'-DMT-*O*)-uridine (90 mg, 0.12 mmol) and diisopropylammonium tetrazolide (16 mg, 0.09 mmol, 0.75 equiv.) were dried three times azeotropically with 4 ml anhydrous acetonitrile each. The remainder was then dissolved in 5 ml anhydrous CH_2Cl_2 treated with (2-cyanoethoxy)-bis-(*N,N*-diisopropylamino)phosphine (0.10 ml, 96 mg, 0.32 mmol, 2.6 equiv.). The reaction mixture was stirred for 3 h at rt and was then quenched by the addition of 15 ml degassed CH_2Cl_2 and 30 ml of a degassed saturated $NaHCO_3$ solution. All following work up steps were done under a protecting atmosphere of argon. The aqueous phase was extracted three times with 20 ml degassed CH_2Cl_2 each. The combined organic phases were dried over Na_2SO_4 and the solvent was removed under reduced pressure. The crude product was purified by column chromatography on a Büchi Sepacore chromatography system [1.5 x 15 cm, 18 ml, degassed CH_2Cl_2/MeOH (+ 0.1% NEt_3) = 98:2, 20 ml/min, threshold: 4%, sensitivity: 3]. Fractions 8-22 were combined and the solvent was removed under reduced pressure to give the desired compound (0.12 g, 0.12 mmol) quantitatively. The product was stored under argon at –20°C.

Spectroscopic data were in accordance with literature data.

^{1}H-NMR (400 MHz, in CD_3CN): δ = 1.02 – 1.27 [m, 12H, 2·CH($\underline{CH_3}$)$_2$], 2.46 – 2.66 (m, 4H, 2'-H + CH_2CN), 3.25 – 3.85 (m, 12H, 5'-H + OCH_2 + 2·*i*-Pr-CH + 2·OCH_3), 4.11 – 4.19 (m, 1H, 4'-H), 4.64 – 4.74 (m, 1H, 3'-H), 6.18 – 6.25 (m, 1H, 1'-H), 6.75 – 6.81 (m, 4H, aromat.), 7.10 – 7.16 (m, 1H, aromat.), 7.24 – 7.29 (m, 2H, aromat.), 7.36 – 7.42 (m, 4H, aromat.), 7.49 – 7.54 (m, 2H, aromat.), 7.56 – 7.61 (m, 2H, aromat.), 7.66 – 7.70 (m, 1H, aromat.), 7.86 – 7.88 (m, 1H, aromat.), 8.33 – 8.36 (m, 1H, aromat.), 8.41 and 8.43 [2·s, 1H, 6-H(both diastereomers)], 8.61 – 8.62 (m, 1H, aromat.), 9.09 – 9.10 (m, 1H, aromat.).

^{13}C-NMR (100 MHz, in CD_3CN): δ = 162.2 (2-C), 159.1 (aromat.), 151.9 (aromat.), 151.3 (aromat.), 150.3 (4-C), 146.7 (aromat.), 145.8 (aromat.), 145.5 (aromat.), 144.8 (6-c), 144.8 (aromat.), 138.9 (aromat.), 137.1 (aromat.), 136.8 (aromat.), 136.8 (aromat.), 136.8 (aromat.), 131.0 (aromat.), 131.0 (aromat.), 130.1 (aromat.), 129.1 (aromat.), 129.1 (aromat.), 129.0 (aromat.), 128.6 (aromat.), 128.4 (aromat.), 128.0 (aromat.), 127.1 (aromat.), 124.4 (aromat.), 119.7 (aromat.), 119.7 (aromat.), 114.3 (aromat.), 114.2 (aromat.), 99.7 + 99.6 (5-C), 87.8 (alkine), 86.8 (1'-C), 86.7 (alkine), 86.6 + 86.5 (4'-C), 73.9 + 73.8 + 73.4 + 73.2 (3'-C), 63.9 + 63.6 (5'-C), 59.6 + 59.4(O$\underline{C}H_2$), 55.8 (MeO), 44.1 + 44.0 (*i*-Pr-$\underline{C}$H), 41.4 + 41.1 (2'-C), 24.9 + 24.8 (*i*-Pr-$\underline{C}H_3$), 21.1 + 21.0 + 20.9 ($\underline{C}H_2CN$).

^{31}P-NMR (121 MHz, CD_3CN): δ = 148.1, 148.0.

3-(4''-Methoxyphenyl)-1-(2'-pyridyl)-2-propen-1-one [201] 80a

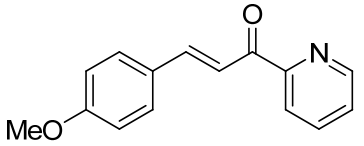

Chemical Formula: $C_{15}H_{13}NO_2$
Molecular Weight: 239.27

To 100 ml H_2O (MilliQ) anisaldehyde (2.0 ml, 2.3 g, 17 mmol) and 2-acetylpyridine (1.9 ml, 2.1 g, 17 mmol, 1 equiv.) were added. The mixture was shaken vigorously and then cooled to 4°C. At this temperature 10 ml of an 10% aqueous solution of NaOH was added. The reaction mixture was again shaken vigorously and then allowed to rest over night at 4°C without any stirring. During this time the crude product crystallized and could easily be obtained by filtration. Traces of water were removed by repeated co-evaporation with CH_3CN. The crude product was purified by column chromatography (5 x 5 cm, 18 ml, CH/EtOAc = 9:1). Fractions 18-41 were combined and the solvent was removed under reduced pressure to give the desired product as yellow solid (1.1 g, 4.6 mmol) in 26% yield.

Spectroscopic data were in accordance with literature data.

MS (EI): m/z (%) = 240.2 (17), 239.2 (100) [M^+], 224.1 (10), 211.2 (10), 210.1 (60), 196.1 (6), 167.1 (7), 161.1 (34), 133.1 (15), 132.1 (17).

^{1}H-NMR (400 MHz, in $CDCl_3$): δ = 3.86 (s, 3H, OCH_3), 6.94 (d, $J_{3'',2''}$ = $J_{5'',6''}$ = 8.8, 2H, 3''-H + 5''-H), 7.48 (ddd, $^{4}J_{5',3'}$ = 1.3, $J_{5',6'}$ = 4.8, $J_{5',4'}$ = 7.6, 1H, 5'-H), 7.70 (d, $J_{2'',3''}$ = $J_{6'',5''}$ = 8.6, 2H, 2''-H + 6''-H), 7.88 (ddd, $^{4}J_{4',6'}$ = 1.8, $J_{4',5'}$ = 7.6, $J_{4',3'}$ = 7.8, 1H, 4'-H), 7.92 (d, $J_{3,2}$ = 15.9, 1H, 3-H), 8.18 (d, $J_{2,3}$ = 16.0, 1H, 2-H), 8.19 (ddd, $^{5}J_{3',6'}$ = 1.1, $^{4}J_{3',5'}$ = 1.1, $J_{3',4'}$ = 7.8, 1H, 3'-H), 8.74 (ddd, $^{5}J_{6',3'}$ = 0.9, $^{4}J_{6',4'}$ = 1.7, $J_{6',5'}$ = 4.8, 1H, 6'-H).

^{13}C-NMR (100 MHz, in $CDCl_3$): δ = 189.3 (1-C), 161.8 (4''-C), 154.5 (2'-C), 148.7 (6'-C), 144.8 (3-C), 137.1 (4'-C), 130.7 (2''-C + 6''-C), 128.0 (4''-C), 126.7 (5'-C), 122.9 (3'-C), 118.6 (2-C)114.4 (3''-C + 5''-C) 55.4 (OCH_3).

3-Phenyl-1-(2'-pyridyl)-2-propen-1-one [201] 80b

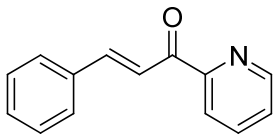

Chemical Formula: $C_{14}H_{11}NO$
Molecular Weight: 209.24

To 100 ml H_2O (MilliQ) benzaldehyde (1.7 ml, 1.8 g, 17 mmol) and 2-acetylpyridine (1.9 ml, 2.1 g, 17 mmol, 1 equiv.) were added. The mixture was shaken vigorously and then cooled to 4°C. At this temperature 10 ml of a 10% aqueous solution of NaOH was added. The reaction mixture was again shaken vigorously and then allowed to rest over night at 4°C without any stirring. During this time the crude product crystallized and could easily be obtained by filtration. Traces of water were removed by repeated co-evaporation with CH_3CN. The crude product was purified by column chromatography (5 x 6 cm, 20 ml, CH/EtOAc = 95:5) to give the desired product as yellow solid (1.2 g, 5.9 mmol) in 35% yield.

Spectroscopic data were in accordance with literature data.

MS (EI): m/z (%) = 210.0 (7), 209.0 (42) [M^+], 181.0 (18), 180.0 (100), 130.9 (11), 102.9 (12), 102 (10), 76.9 (6).

^{1}H-NMR (400 MHz, in $CDCl_3$): δ = 7.39 – 7.44 (m, 3H, Benzyl), 7.50 (ddd, $^{4}J_{5',3'}$ = 1.3, $J_{5',6'}$ = 4.8, $J_{5',4'}$ = 7.5, 1H, 5'-H), 7.69 – 7.77 (m, 2H, benzyl), 7.89 (ddd, $^{4}J_{4',6'}$ = 1.8, $J_{4',5'}$ = 7.6, $J_{4',3'}$ = 7.8, 1H, 4'-H), 7.95 (d, $J_{3,2}$ = 16.1, 1H, 3-H), 8.20 (ddd, $^{5}J_{3',6'}$ = 1.1, $^{4}J_{3',5'}$ = 1.1, $J_{3',4'}$ = 7.8, 1H, 3'-H), 8.32 (d, $J_{2,3}$ = 16.0, 1H, 2-H), 8.75 (ddd, $^{5}J_{6',3'}$ = 0.9, $^{4}J_{6',4'}$ = 1.8, $J_{6',5'}$ = 4.8, 1H, 6'-H).

^{13}C-NMR (100 MHz, in $CDCl_3$): δ = 189.2 (1-C), 154.0 (2'-C), 148.7 (6'-C), 145.0 (3-C), 137.3 (4'-C), 135.2 (phenyl-C_q), 130.6 (phenyl-C), 128.9 (phenyl-C), 128.9 (phenyl-C), 127.0 (5'-C), 123.1 (3'-C), 120.9 (2-C).

4,4-Dimethyl-1-(2'pyridyl)-2-penten-1-one [103] 80c

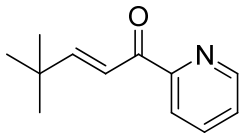

Chemical Formula: $C_{12}H_{15}NO$
Molecular Weight: 189.25

To 100 ml H_2O (MilliQ) pivaldehyde (1.8 ml, 1.4 g, 17 mmol) and 2-acetylpyridine (1.9 ml, 2.1 g, 17 mmol, 1 equiv.) were added. The mixture was shaken vigorously and then cooled to 4°C. At this temperature 10 ml of an 10% aqueous solution of NaOH was added. The reaction mixture was again shaken vigorously and then allowed to rest over night at 4°C without any stirring. The reaction mixture was then concentrated under reduced pressure. The crude product was dissolved in 10 ml of a saturated NH_4Cl solution and extracted four times with 10 ml CH_2Cl_2 each. The combined organic layers were dried over Na_2SO_4 and the solvent was removed under reduced pressure. The crude product was purified by column chromatography (5 x 5 cm, 18 ml, CH/EtOAc = 9:1). Fractions 5-9 were combined and the solvent was removed under reduced pressure to give the desired product as colorless oil (0.53 g, 3.0 mmol) in 18% yield.

Spectroscopic data were in accordance with literature data.

MS (CI): m/z (%) = 191.2 (9), 190.1 (71) [M^+], 174.1 (15), 146.1 (11), 134.1 (8), 133.0 (75), 132.0 (100), 106.0 (5), 78.1 (6).

^{1}H-NMR (400 MHz, in $CDCl_3$): δ = 1.18 (s, 9H, *t*-Bu), 7.25 (d, $J_{3,2}$ = 15.8, 1H, 3-H), 7.48 (ddd, $^4J_{5',3'}$ = 1.3, $J_{5',6'}$ = 4.8, $J_{5',4'}$ = 7.6, 1H, 5'-H), 7.55 (d, $J_{2,3}$ = 15.8, 1H, 2-H), 7.87 (ddd, $^4J_{4',6'}$ = 1.8, $J_{4',5'}$ = 7.8, $J_{4',3'}$ = 7.7, 1H, 4'-H), 8.13 (ddd, $^5J_{3',6'}$ = 1.1, $^4J_{3',5'}$ = 1.1, $J_{3',4'}$ = 7.9, 1H, 3'-H), 8.73 (ddd, $^5J_{6',3'}$ = 0.9, $^4J_{6',4'}$ = 1.8, $J_{6',5'}$ = 4.8, 1H, 6'-H).

^{13}C-NMR (100 MHz, in $CDCl_3$): δ = 189.9 (1-C), 160.2 (3-C), 154.1 (2'-C), 148.6 (6'-C), 137.2 (4'-C), 126.8 (5'-C), 123.0 (3'-C), 119.5 (2-C),34.4 (*t*-Bu-C_q) 28.8 (*t*-Bu-C_p).

rac. ((1S,2R,3R,4R)-3-(4''-Methoxyphenyl)bicyclo[2.2.1]hept-5-en-2-yl)(pyridin-2'-yl)methanone[201] 86a

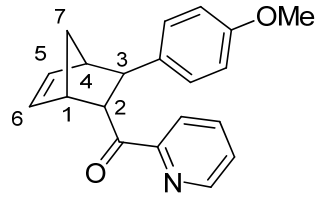

Chemical Formula: $C_{20}H_{19}NO_2$
Molecular Weight: 305.37

3-(4''-Methoxyphenyl)-1-(2'-pyridinyl)-2-propen-1-one **80a** (157 mg, 0.655 mmol) was added to a solution of $Cu(NO_3)_2 \cdot 3H_2O$ (791 mg, 3.28 mmol, 5.0 equiv.) in 330 ml H_2O. The yellow suspension was stirred 30 min at rt. before freshly cracked and distilled cyclopentadiene (162 µl, 130 mg, 1.97 mmol, 3.0 equiv.) was added. The reaction mixture was stirred at rt. for 5 d, after which it was quenched by the addition of 50 ml Et_2O. The aqueous phase was extracted twice with 50 ml Et_2O each. The combined organic phases were dried over $MgSO_4$ and the solvent was removed under reduced pressure. The crude product was purified by column chromatography (5 x 6.5 cm, 18 ml, CH/EtOAc = 5:1). Fractions 6-11 were combined and the solvent was removed under reduced pressure to give the desired product (136 mg, 0.447 mmol) as racemic mixture in 68% yield.

Spectroscopic data were in accordance with literature data.

MS (CI): m/z (%) = 307.2 (18), 306.1 (92) [M^+], 241.1 (14), 240.0 (100), 239.0 (57), 210.0 (9), 160.9 (5).

NMR-spectra of the endo isomeres:

^{1}H-NMR (400 MHz, in $CDCl_3$): δ = AB-signal (δ_{7a} = 1.60, δ_{7b} = 2.06, $J_{A,B}$ = 8.5, $J_{B,A}$ = 8.4, additional coupling for $^4J_{7a,2}$ = 1.7, 2H, 7-H)*, 3.01 – 3.04 (m, 1H, 1-H), 3.38 (dd, $^4J_{2,7a}$ = 1.6, $J_{2,3}$ = 5.1, 1H, 2-H), 3.51 – 3.54 (m, 1H, 4-H), 3.77 (s, 3H, OCH_3), 4.49 (dd, $J_{3,4}$ = 1.6, $J_{3,2}$ = 5.2, 1H, 3-H), 5.81 (dd, $J_{5,4}$ = 2.8, $J_{5,6}$ = 5.6, 1H, 5-H), 6.48 (dd, $J_{6,1}$ = 1.6, $J_{6,5}$ = 5.6, 1H, 6-H), 6.82 (d, $J_{3'',2''}$ = $J_{5'',6''}$ = 8.8, 2H, 3''-H + 5''-H), 7.23 (d, $J_{2'',3''}$ = $J_{6'',5''}$ = 8.9, 2H, 2''-H + 6''-H), 7.45 (ddd, $^4J_{5',3'}$ = 1.3, $J_{5',6'}$ = 4.8, $J_{5',4'}$ = 7.6, 1H, 5'-H), 7.81 (ddd, $^4J_{4',6'}$ = 1.8, $J_{4',5'}$ = 7.7, $J_{4',3'}$ = 7.7, 1H, 4'-H), 8.00 (ddd, $^5J_{3',6'}$ = 1.1, $^4J_{3',5'}$ = 1.1, $J_{3',4'}$ = 7.9, 1H, 3'-H), 8.68 (ddd, $^5J_{6',3'}$ = 0.9, $^4J_{6',4'}$ = 1.7, $J_{6',5'}$ = 4.8, 1H, 6'-H).

^{13}C-NMR (100 MHz, in $CDCl_3$): δ = 201.2 (carbonylic-C), 157.8 (4''-C), 153.7 (2'-C), 148.9 (6'-C), 139.5 (6-C), 136.8 (1''-C), 136.7 (4'-C), 132.8 (5-C), 128.6 (2''-C, 6''-C), 126.9 (5'-C), 122.2 (3'-C), 113.8 (3''-C, 5''-C), 55.3 (OCH_3), 54.3 (3-C), 49.7 (1-C), 48.7 (4-C), 48.2 (7-C), 44.9 (2-C).

HPLC conditions:

Daicel chiracel-ODH, *n*-heptane/*i*-PrOH = 98:2, 0.5 ml/min. Retention times (min): 8.7 + 9.5 (exo-products), 10.6 + 14.7 (endo-products), 19.0 (starting material).

* Couplings with 1-H and 4-H could not be resolved.

rac. ((1S,2R,3R,4R)-3-(tert-Butyl)bicyclo[2.2.1]hept-5-en-2-yl)(pyridin-2'-yl)methanone[201] 86b

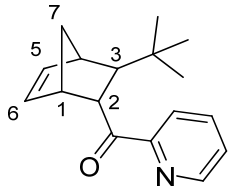

Chemical Formula: $C_{17}H_{21}NO$
Molecular Weight: 255.35

4,4-Dimethyl-1-(2'-pyridinyl)-2penten-1-one **80c** (86.6 mg, 0.665 mmol) was added to a solution of $Cu(NO_3)_2 \cdot 3H_2O$ (791 mg, 3.28 mmol, 5.0 equiv.) in 330 ml H_2O. The yellow suspension was stirred 30 min at rt. before freshly cracked and distilled cyclopentadiene (108 µl, 80.6 mg, 1.33 mmol, 2.0 equiv.) was added. The reaction mixture was stirred at rt. for 5 d, after which it was quenched by the addition of 50 ml Et_2O. The aqueous phase was extracted twice with 50 ml Et_2O each. The combined organic phases were dried over $MgSO_4$ and the solvent was removed under reduced pressure. The crude product was purified by column chromatography on a Büchi Sepacore chromatography system (5 x 15 cm, 20 ml, *n*-heptane/*i*-PrOH = 99:1). The desired fractions were combined and the solvent was removed under reduced pressure. The product (90 mg, 0.35 mmol) was obtained as racemic mixture in 53% yield.

Spectroscopic data were in accordance with literature data.

^{1}H-NMR (400 MHz, in $CDCl_3$): δ = 0.79 (s, 9H, *t*-Bu_{exo}), 0.91 (s, 9H, *t*-Bu_{endo}), AB-signal (δ_{7a} = 1.32, δ_{7b} = 1.73, $J_{A,B}$ = 8.2, $J_{B,A}$ = 8.3, additional coupling for $^4J_{7a,3}$ = 1.5, 2H, 7-H_{exo})*, AB-signal (δ_{7a} = 1.40, δ_{7b} = 1.81, $J_{A,B}$ = 8.4, $J_{B,A}$ = 8.3, additional coupling for $^4J_{7a,2}$ = 1.7, 2H, 7-H_{endo})*, 1.92 (dd, $^4J_{2,7a}$ = 1.7, $J_{2,3}$ = 6.2, 1H, 2-H_{endo}), 2.70 (dd, $^4J_{2,1}$ = 3.2, $J_{2,3}$ = 6.3, 1H, 2-H_{exo}), 2.77 – 2.81 (m, 1H, 1-H_{endo} + 1-H_{exo}), 2.97 – 3.01 (m, 1H, 4-H_{exo}), 3.23 – 3.27 (m, 1H, 4-H_{endo}), 3.81 (dd, $J_{3,7a}$ = 1.4, $J_{3,2}$ = 6.3, 1H, 3-H_{exo}), 4.28 (dd, $J_{3,4}$ = 3.2, $J_{3,2}$ = 6.2, 1H, 3-H_{endo}), 5.71 (dd, $J_{5,4}$ = 2.8, $J_{5,6}$ = 5.6, 1H, 5-H_{endo}), 6.20 (dd, $J_{5,4}$ = 2.9, $J_{5,6}$ = 5.5, 1H, 5-H_{exo}), 6.27 (dd, $J_{6,1}$ = 3.2, $J_{6,5}$ = 5.6, 1H, 6-H_{exo}), 6.45 (dd, $J_{6,1}$ = 3.3, $J_{6,5}$ = 5.6, 1H, 6-H_{endo}), 7.45 (ddd, $^4J_{5',3'}$ = 1.3, $J_{5',6'}$ = 4.8, $J_{5',4'}$ = 7.5, 1H, 5'-H_{exo}), 7.46 (ddd, $^4J_{5',3'}$ = 1.3, $J_{5',6'}$ = 4.8, $J_{5',4'}$ = 7.5, 1H, 5'-H_{endo}), 7.81 (ddd, $^4J_{4',6'}$ = 1.8, $J_{4',5'}$ = 7.6, $J_{4',3'}$ = 7.8, 1H, 4'-H_{endo}), 7.82 (ddd, $^4J_{4',6'}$ = 1.8, $J_{4',5'}$ = 7.6, $J_{4',3'}$ = 7.8, 1H, 4'-H_{exo}), 7.99 (ddd, $^5J_{3',6'}$ = 1.0, $^4J_{3',5'}$ = 1.2, $J_{3',4'}$ = 7.9, 1H, 3'-H_{endo}), 8.07 (ddd, $^5J_{3',6'}$ = 1.0, $^4J_{3',5'}$ = 1.2, $J_{3',4'}$ = 7.9, 1H, 3'-H_{exo}), 8.71 (ddd, $^5J_{6',3'}$ = 0.9, $^4J_{6',4'}$ = 1.8, $J_{6',5'}$ = 4.7, 1H, 6'-H_{exo}), 8.73 (ddd, $^5J_{6',3'}$ = 1.0, $^4J_{6',4'}$ = 1.8, $J_{6',5'}$ = 4.8, 1H, 6'-H_{endo}).

^{13}C-NMR (100 MHz, in $CDCl_3$): δ = 203.4 (carbonylic-C_{exo}), 202.4 (carbonylic-C_{endo}), 153.8 (2'-C_{endo} + 2'-C_{exo}), 149.1 (6'-C_{exo}) 149.0 (6'-C_{endo}), 140.9 (4'-C_{endo}), 137.1 (4'-C_{exo}), 136.9 (6-C_{endo}), 136.8 (6-C_{exo}), 135.1 (5-C_{exo}), 131.8 (5-C_{endo}), 126.8 (5'-C_{endo}), 126.8 (5'-C_{exo}), 122.5 (3'-C_{exo}), 122.3 (3'-C_{endo}), 54.3 (3-C_{exo}), 53.4 (3-C_{endo}), 49.2 (1-C_{exo}), 48.6 (1-C_{endo}), 48.4 (4-C_{exo}), 48.1 (4-C_{endo}), 47.1 (7-C_{exo}), 46.7 (7-C_{endo}), 45.2 (2-C_{exo}) 44.6 (2-C_{endo}), 32.8 [C($\underline{C}H_3$) $_{exo}$], 32.7 [$\underline{C}(CH_3)$ $_{endo}$]., 29.4 [C($\underline{C}H_3$) $_{exo}$], 29.0 [C($\underline{C}H_3$) $_{endo}$].

* Couplings with 1-H and 4-H could not be resolved.

HPLC conditions:

Daicel chiracel-ODH, *n*-heptane/*i*-PrOH = 99.75:0.25, 0.5 ml/min. Retention times (min): 6.5 + 6.7 (exo-products), 8.2 + 10.4 (endo-products), 9.7 (starting material).

rac. ((1S,2R,3R,4R)-3-(Phenyl)bicyclo[2.2.1]hept-5-en-2-yl)(pyridin-2'-yl)methanone 86c[201]

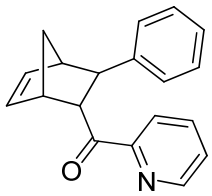

Chemical Formula: $C_{19}H_{17}NO$
Molecular Weight: 275.34

3-Phenyl-1-(2'-pyridinyl)-2-propen-1-one **80b** (80.6 mg, 0.656 mmol) was added to a solution of $Cu(NO_3)_2 \cdot 3H_2O$ (791 mg, 3.28 mmol, 5.0 equiv.) in 330 ml H_2O. The yellow suspension was stirred 30 min at rt. before freshly cracked and distilled cyclopentadiene (108 µl, 86.6 mg, 1.33 mmol, 2.0 equiv.) was added. The reaction mixture was stirred at rt. for 5 days, after which it was quenched by the addition of 50 ml Et_2O. The aqueous phase was extracted twice with 50 ml Et_2O each. The combined organic phases were dried over $MgSO_4$ and the solvent was removed under reduced pressure. The crude product was purified by column chromatography (5 x 6 cm, 20 ml, CH/EtOAc = 5:1). The desired fractions were combined and the solvent was removed under reduced pressure. The product (102 mg, 0.370 mmol) was obtained as racemic mixture in 56% yield.

Spectroscopic data were in accordance with literature data.

NMR-spectra of the endo isomeres:

^{1}H-NMR (400 MHz, in $CDCl_3$): δ = AB-signal (δ_{7a} = 1.62, δ_{7b} = 2.09, $J_{A,B}$ = 8.5, $J_{B,A}$ = 8.4, additional coupling for $^4J_{7a,2}$ = 1.8, 2H, 7-H)*, 3.07 – 3.10 (m, 1H, 1-H), 3.45 (dd, $^4J_{2,7a}$ = 1.6, $J_{2,3}$ = 5.1, 1H, 2-H), 3.53 – 3.57 (m, 1H, 4-H), 4.56 (dd, $J_{3,4}$ = 3.4, $J_{3,2}$ = 5.2, 1H, 3-H), 5.82 (dd, $J_{5,4}$ = 2.8, $J_{5,6}$ = 5.6, 1H, 5-H), 6.50 (dd, $J_{6,1}$ = 3.2, $J_{6,5}$ = 5.6, 1H, 6-H), 7.13 – 7.35 (m, 5H, aromat.), 7.49 (ddd, $^4J_{5',3'}$ = 1.3, $J_{5',6'}$ = 4.8, $J_{5',4'}$ = 7.6, 1H, 5'-H), 7.86 (ddd, $^4J_{4',6'}$ = 1.8, $J_{4',5'}$ = 7.7, $J_{4',3'}$ = 7.7, 1H, 4'-H), 8.03 (ddd, $^5J_{3',6'}$ = 1.1, $^4J_{3',5'}$ = 1.1, $J_{3',4'}$ = 7.9, 1H, 3'-H), 8.71 (ddd, $^5J_{6',3'}$ = 0.9, $^4J_{6',4'}$ = 1.7, $J_{6',5'}$ = 4.8, 1H, 3'-H).

^{13}C-NMR (100 MHz, in $CDCl_3$): δ = 200.5 (carbonylic-C), 153.0 (2'-C), 148.4 (6'-C), 144.5 (1''-C), 139.6 (6-C), 137.5 (4'-C), 132.8 (5-C), 128.4 (3''-C, 5''-C)†, 127.7 (2''-C, 6''-C)†, 127.1 (5'-C), 122.5 (4''-C), 122.5 (3'-C), 54.3 (3-C), 49.5 (1-C), 48.8 (4-C), 48.2 (7-C), 45.7 (2-C).

* Couplings with 1-H and 4-H could not be resolved.
† Signals possibly exchangeable.

HPLC conditions:

Daicel chiracel-ODH, *n*-heptane/*i*-PrOH = 98:2, 0.5 ml/min. Retention times (min): 7.4 + 8.2 (exo-products), 8.9 + 11.3 (endo-products), 12.7 (starting material).

1,10-Phenanthroline-4-carbaldehyde [207, 208] 89

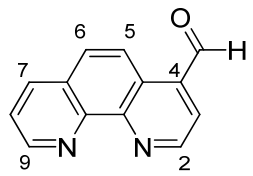

Chemical Formula: $C_{13}H_8N_2O$
Molecular Weight: 208.22

To 4-methyl-1,10-phenanthroline (1.0 g, 5.1 mmol) in 16 ml dioxane and 0.7 ml H_2O (MilliQ), SeO_2 (1.4 g, 13 mmol, 2.5 equiv.) was added. The reaction mixture was stirred under reflux for 3 hours. The hot solution was then filtered through celite and washed with plenty of EtOH. The solvent was removed under reduced pressure and the residue was dissolved in H_2O (MilliQ). After adjusting the pH to pH = 7 by addition of $NaHCO_3$ the solution was extracted three times with $CHCl_3$. The combined organic phases were dried over Na_2SO_4. After filtration the solvent was removed under reduced pressure to give the desired product as yellow crystals (700 mg, 3.36 mmol) in 66% yield.

Spectroscopic data were in accordance with literature data.

^{1}H-NMR (300 MHz, in $CDCl_3$): δ = 7.73 (dd, $J_{8,9}$ = 4.4, $J_{8,7}$ = 8.2, 1H, 8-H), 8.01 (d, $J_{3,2}$ = 9.3, 1H, 3-H), 8.03 (d, $J_{5,6}$ = 4.35, 1H, 5-H), 8.34 (d, $J_{7,8}$ = 8.2, 1H, 7-H), 9.04 (d, $J_{2,3}$ = 9.2, 1H, 2-H), 9.28 (d, $J_{9,8}$ = 4.4, 1H, 9-H), 9.49 (d, $J_{6,5}$ = 4.3, 1H, 6-H) 10.60 (s, 1H, CHO).

4-Carboxyl-[1,10]-phenanthroline [209] 87

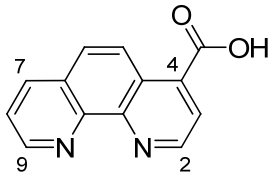

Chemical Formula: $C_{13}H_8N_2O_2$
Molecular Weight: 224.21

[1,10]-Phenanthroline-4-carbaldehyde **89** (298 mg, 1.43 mmol) was dissolved in 5 ml HNO_3 (80%) and stirred under reflux at 80°C for 3 h. The solution was then poured onto ice. The yellow precipitate was filtered and dried under high vacuum. After further concentrating the filtrate to give a second batch of crystals, the desired compound (186 mg, 0.830 mmol) was obtained in a combined yield of 58%.

Spectroscopic data were in accordance with literature data.

MS (CI): m/z (%) = 226.1 (16), 225.1 (100) [M^+], 224.1 (10), 211.1 (7), 209.1 (24), 181.1 (6).

^{1}H-NMR (300 MHz, in $CDCl_3$): δ = 8.33 (d, $J_{3,2}$ = 9.5, 1H, 3-H), 8.37 (dd, $J_{8,9}$ = 6.0, $J_{8,7}$ = 7.8, 1H, 8-H), 8.48 (d, $J_{5,6}$ = 4.6, 1H, 5-H), 9.18 (d, $J_{2,3}$ = 9.5, 1H, 2-H), 9.29 (d, $J_{9,8}$ = 7.7, 1H, 9-H), 9.29 (d, $J_{7,8}$ = 6.0, 1H, 7-H), 9.36 (d, $J_{6,5}$ = 4.3, 1H, 6-H).

^{13}C-NMR (100 MHz, in $CDCl_3$): δ = 167.6 (COOH), 151.9 (6-C), 147.1 (9-C), 145.4 (7-C), 141.0 (C_q), 139.2 (C_q), 138.4 (C_q), 131.1 (C_q), 128.9 (C_q), 128.4 (2-C), 128.0 (5-C), 127.9 (3-C), 126.5 (6-C).

[Cu(2-(2-Pyridyl)benzimidazole)$(NO_3)_2$·H_2O] [103] 85

A solution of 2-(2-pyridyl)benzimidazole (75 mg, 0.38 mmol) in 4 ml ethyl acetate was added to a solution of $Cu(NO_3)_2$·$3H_2O$ (97 mg, 0.39 mmol) in a mixture of acetone (4 ml) and ethanol (0.3 ml). The dark green solution was filtered and the vial was closed with a cotton plug to allow for slow evaporation of acetone. After 6 h green crystals were isolated and washed with a few ml of ice cold ethyl acetate. The desired compound (129 mg, 0.37 mmol) was yielded 85 %.

Spectroscopic data were in accordance with literature data.

[Cu(1-(2'-Deoxy-ribofuranos-1'-yl)-2-(pyridine-2-yl)-benzo[d]imidazole) $(NO_3)_2$·H_2O] 84

Nucleoside **54** (59.2 mg, 0.19 mmol) was dissolved in 2 ml EtOH and treated with a solution of $Cu(NO_3)_2$·$3H_2O$ (47 mg, 0.20 mmol, 1.1 equiv.) in 2 ml EtOH. The corresponding Cu^{2+}-complex of **54** with its characteristic green color was then crystallized by overlaying the ethanol solution with Et_2O. The thus obtained crystals were isolated, washed with ice cold EtOAc and dried under vacuum. The desired compound (86 mg, 0.17 mmol) was obtained in 88% yield.

Anal. Calcd for $C_{12}H_{19}CuN_5O_{10}$: C, 39.50; H, 3.70; N, 13.55. Found: C, 40.39; H, 3.68; N, 13.44. (Contained traces of Cu^{2+} free ligand).

Nucleoside-Based Catalyst 93

A 1.8 mM stock solution of Cu(II)-complex **84** in H_2O was prepared. To 166 µl of this stock solution 166 µl MOPS buffer (120 mM, pH 6.5) were added to give a final catalyst concentration of 0.9 mM.

DNA-Supported Catalyst (Covalent Attachment of Ligand)

Oligonucleotide **73c, 73a, 73b, 74c, 74a or 74b** (0.3 µmol, 0.1 OD/µl in H_2O) were combined with the corresponding complementary sequence **75** or **76** (0.33 µmol, 0.1 OD/µl in H_2O, 1.1 equiv.). The solvent was removed in vacuum and the precipitate dissolved in 166 µl MOPS buffer (120 mM, pH

6.5). Thermal hybridization was performed by heating the sample to 95°C for 2 minutes and then cooling the sample slowly to rt. At this temperature 166 µl of $Cu(NO_3)_2 \cdot 3H_2O$ (1.8 mM in H_2O) were added to give a final catalyst concentration of 0.9 mM.

DNA-Supported Catalyst (Interchalating Ligands)

Oligonucleotide **73c** or **74c** (0.3 µmol, 0.1 OD/µl in H_2O) were combined with the corresponding complementary sequence **75** or **76** (0.33 µmol, 0.1 OD/µl in H_2O, 1.1 equiv.). The solvent was removed in vacuum and the precipitate dissolved in 166 µl MOPS buffer (120 mM, pH 6.5). Thermal hybridization was performed by heating the sample to 95°C for 2 minutes and then cooling the sample slowly to rt. At this temperature 166 µl of a 1.8 mM stock solution of **84** or **85** in H_2O were added to give a final catalyst concentration of 0.9 mM.

General Procedure for Diels Alder Reactions

In an Eppendorf reaction tube 332 µl of the corresponding catalyst (0.9 mM) in MOPS buffer (60 mM, pH 6.5) were diluted with 647 µl of water and then cooled to 5°C. At this temperature 20 µl of the dienophile (0.05 M in CH_3CN) and 2.4 µl of freshly cracked and distilled cyclopentadiene were added. The reaction mixture was shaken with 700 rpm at 5°C for 3 days using a thermomixer. After this time the reaction mixture was extracted with Et_2O. The organic phases were combined and the solvent was removed under reduced pressure. The crude product was analyzed by chiral HPLC (Daicel chiracel-ODH column).

HPLC Conditions:

86a: Daicel chiracel-ODH, *n*-heptane/*i*-PrOH = 98:2, 0.5 ml/min. Retention times (min): 8.7 + 9.5 (exo-products), 10.6 + 14.7 (endo-products), 19.0 (starting material).

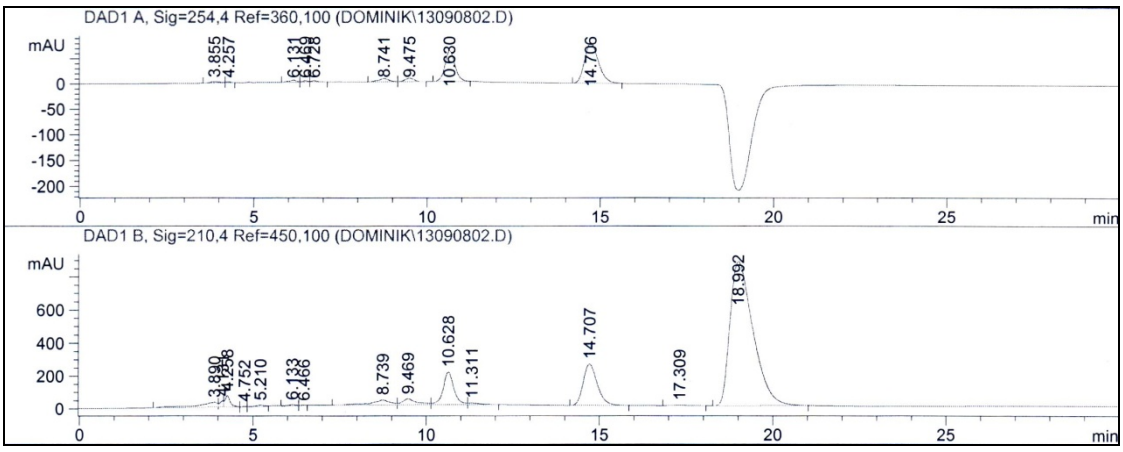

Fig. 83: Exemplary HPLC of 86a.

86c: Daicel chiracel-ODH, *n*-heptane/*i*-PrOH = 98:2, 0.5 ml/min. Retention times (min): 7.4 + 8.2 (exo-products), 8.9 + 11.3 (endo-products), 12.7 (starting material).

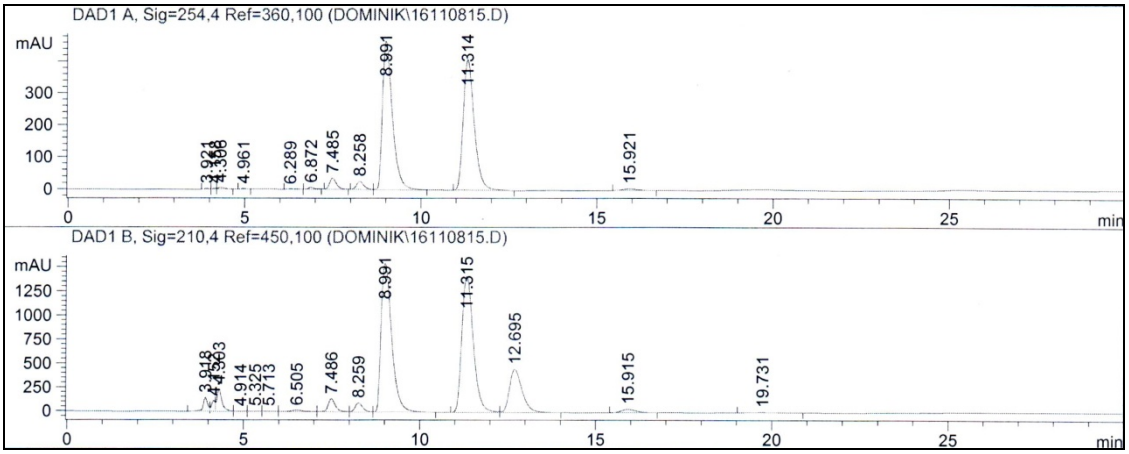

Fig. 84: Exemplary HPLC of 86c.

86b: Daicel chiracel-ODH, *n*-heptane/*i*-PrOH = 99.75:0.25, 0.5 ml/min. Retention times (min): 6.5 + 6.7 (exo-products), 8.2 + 10.4 (endo-products), 9.7 (starting material).

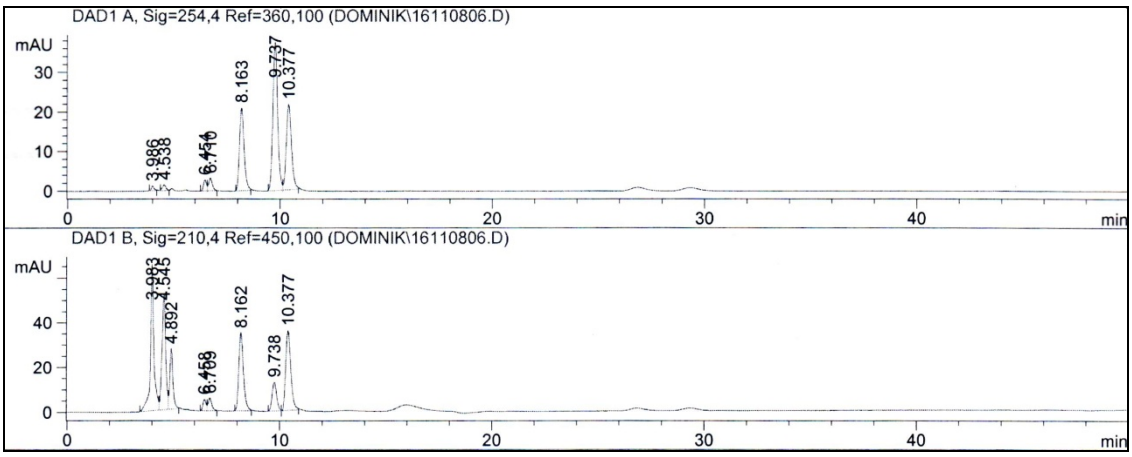

Fig. 85: Exemplary HPLC of 86b.

3. Bioorganic Methods

a. Solvents and Buffers

10 x TBE-Buffer	60.5 g Tris base, 30.9 g boric acid and 3.7 g Na-EDTA were dissolved in 1000 ml H_2O (MilliQ). The solution was stored at 4°C.
20% Sol. of Acrylamide	To 90 g acrylamide, 10 g bisacrylamide and 420 g urea 100 ml of the 10 x TBE-buffer were added and the solution was filled up to 1000 ml with H_2O (MilliQ). The solution was stored at 4°C.
PAGE Buffer	100 ml of 10 x TBE-buffer were diluted with 900 ml H_2O (MilliQ) to give the final buffer concentration.
Gel-Dye	6 g of urea and 10 ml H_2O (MilliQ) were added to 1 ml of bromophenol blue – xylenecyanol solution (Fluka).
Stains-All Stock Solution	100 mg Stains-All (Fluka) was added to 100 ml formamide and 100 ml H_2O (MilliQ). The stock solution was stored in the dark at 4°C.
Stains-All Staining Solution	25 ml Stains-All stock solution were diluted with 75 ml formamide and 100 ml H_2O (MilliQ). The staining solution was stored in the dark at 4°C. The solution was used to stain several gels.
Anhydrous Acetonitrile	DNA Grade Acteonitrile [≤ 0.003% water (Karl Fischer)] was bought at Sigma-Aldrich and was stored over 3Å molsieve.
BMT-Solution	875 mg anhydrous BMT was dissolved in 15 ml anhydrous acetonitrile. The solution was stored over 3Å molsieve.
3% DCA	30 ml dichloroacetic acid (DCA) was diluted with 970 ml 1,2-dichloroethane.
4% DCA	40 ml dichloroacetic acid (DCA) was diluted with 960 ml 1,2-dichloroethane.
Capping A	A 6% solution of DMAP in acetonitrile (6 g DMAP dissolved in 100 ml acetonitrile). The solution was filtered prior usage.
Capping B	50 ml acetonitrile and 20 ml acetic acid anhydride were added to 30 ml collidine. The solution was stirred strongly and afterwards filtered.
Oxidation Solution (0.01 M)	1.03 g iodine were dissolved in 260 ml acetonitrile. Once the idodine was dissolved completely 24 ml collidine and 120 ml H_2O (MilliQ) were added.
Oxidation Solution (0.02 M)	2.06 g iodine were dissolved in 260 ml acetonitrile. Once the idodine was dissolved completely 24 ml collidine and 120 ml H_2O (MilliQ) were added.

Na-Acetate Buffer (100 mM) The pH-value of a 0.1 M solution of NaOAc [13.6 g NaOAc in 1 l H_2O (MilliQ)] was adjusted to the desired value with 0.1 M acetic acid.

b. DNA Synthesis

Manual DNA Synthesis

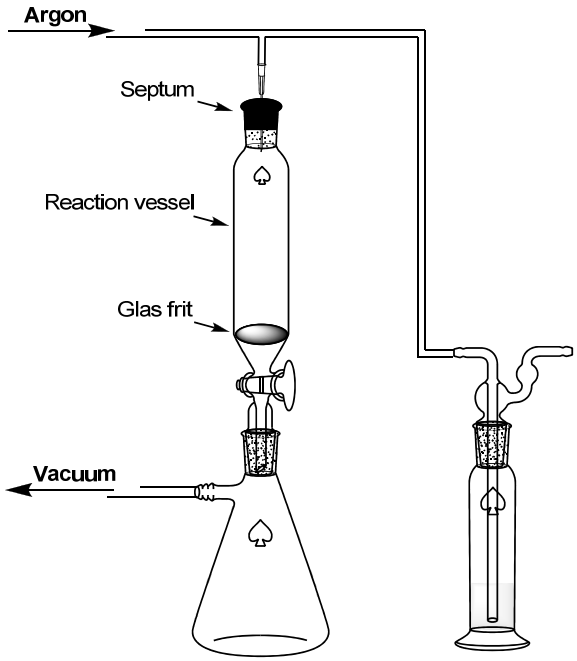

Fig. 86: Apparatus for Manual DNA Synthesis.

For every coupling step 55 mg of the corresponding phosphoramidite (dT, dC^{bz}, dA^{bz} or dG^{ib}) was transferred into a small vial which was then closed with a septum-cap. A hollow needle was stuck through this septum. The vials together with sufficient BMT, 1 ml syringes and long hollow needles were then placed in a desiccator and dried over $CaCl_2$ over night. On the next day the condensation mix was prepared. For this all phosphoramidites were dissolved in 0.7 ml BMT solution (875 mg anhydrous BMT in 15 ml anhydrous acetonitrile). The manual DNA synthesis was then carried out on a small glas frit, which was previously silylated with 5 ml dichloro-dimethylsilane and washed with ethanol. 1 µmol of the first building block (3'-end) coupled to CPG [500 Å CPG solid support loaded with dT, dC^{bz}, dA^{bz} or dG^{ib} (Sigma-Aldrich)] was loaded on the frit. For each coupling all steps of the DNA-synthesis cycle were followed.

Table 12: Manual DNA Synthesis Protocol:

Entry	Step	Solution	Amount in ml	Time in min	Remark
1	Washing	Acetonitrile	3 x 1.5	1.5	
2	Detritylation	3% DCA sol.	4 x 1.5	2.0	
3	Washing	Anhydrous acetonitrile	4 x 1.5	2.0	Under Argon
4	Coupling	Condensation mix	1 x 0.7	3.0	Under Argon
5	Capping	Capping A + Capping B	1 x (0.5 + 1)	2.0	
6	Washing	Acetonitrile	2 x 1.5	1.0	
7	Oxidation	0.01 M Iodo sol.	1 x 1.5	2.0	

For documentation and evaluation of the coupling success the detritylation solution during step 2 was collected in a reaction tube. The solid support bound oligonucleotide was washed with acetonitrile and ether at the end of the syntheses. The CPG material was then transferred into an Eppendorf reaction tube for deprotection and cleavage from the solid support.

Automated DNA Synthesis

Single stranded oligonucleotides were synthesized in a 1 µmol scale on an Expedite™ Nucleic Acid Synthesis System (Model 8909). The system uses the phosphoramidite method for DNA synthesis.

Before a DNA synthesis could be started the synthesizer had to be prepared accordingly. The argon pressure was adjusted to 5 bar and all solvents and reagents with the exemption of the phosphoramidites were loaded at the corresponding port. Empty vials were inserted at the phosphoramidite positions. Afterwards all solvent and reagent lines were purged three times. By this procedure all lines were filled with the corresponding solvent or reagent and the phosphoramidite lines were dried and filled with argon. Prior to loading the phosphoramidites (0.05 M in anhydrous acetonitrile over 3 Å molsieve, stored at –20°C) they had to be adjusted to rt. The insertion of the phosphoramidites was done quickly to avoid any contamination with air and moisture. Once installed all phosphoramidite lines were purged three more times. The synthesizer was now ready for synthesis of the programmed DNA sequence. For this 1 µmol of the corresponding nucleoside on solid support [500 Å CPG functionalized with dT, dC^{bz}, dA^{bz} or dG^{ib} (Sigma-Aldirch)] was loaded in a small reactor and tightly sealed. For each coupling all steps of the DNA-synthesis cycle were followed:

1. Deprotection (DCA solution)
2. Coupling (activation with BMT solution)
3. Capping (Capping A + B solution)
4. Oxidation (0.02 M iodine solution)
5. Capping (Capping A + B solution)

Reagents and side products were removed in between these steps by rinsing the reactor with acetonitrile. Standard coupling time was 1.6 minutes. This time could be extended to 15 minutes when needed. The coupling efficiency was monitored in real time via an integrated trityl monitor. After completion of the synthesis all phosphoramidites were removed from the synthesizer and stored at –20°C under argon. The lines were thoroughly purged with acetonitrile to prevent any clocking.

c. Deprotection of Oligonucleotides and their Cleavage from the Solid Support

The CPG material bearing the synthesized oligonucleotides was transferred into Eppendorf® reaction tubes with screw on caps. The cleavage of the oligonucleotide from the solid support and its deprotection was done under basic conditions by adding 500 µl of a 25% ammonia solution and either heating to 70°C for 2 h or at rt. over night. The ammonia solution was cooled, diluted with

200 µl H_2O (MilliQ) and separated from the solid support: The solid support was extracted two times with 200 µl H_2O (MilliQ). The combined aqueous phases were concentrated in a vacuum centrifuge (SpeedVac) at 60°C. The resulting pellet was dissolved in 250 µl H_2O (MilliQ) for purification and analysis.

d. Oligonucleotide Purification and Analysis

Salt Exchange

After deprotection and cleavage from the solid support the oligonucleotide was obtained in form of the ammonium salt. The exchange of the salt with K^+ was achieved by adding KCl (10 mg based on 1 µmol DNA synthesis scale) to the oligonucleotide and dissolving everything in 200 µl H_2O (MilliQ). The water was then removed at 60°C in a SpeedVac. The remaining sample was two more times dissolved in 200 µl H_2O (MilliQ) and concentrated. Afterwards the remaining salt excess was removed by size exclusion chromatography.

Desalting

Desalting of the oligonucleotides by means of size exclusion chromatography was usually done after salt exchange, preparative PAGE and preparative HPLC. For this NAP™ columns of the types 10 and 25 obtained from GE Healthcare were used. The column matrix consisted out of DNA grade Sephadex G-25. The column was prepared by allowing the supernatant solvent to completely flow through the column. This was followed by the equilibration of the column with three column volumes of H_2O (MilliQ). After equilibrating, the oligonucleotide sample dissolved in water (for volumes please refer to Table 13) was applied to the column. The sample was allowed to enter the gel bed completely before the elution solvent was added. For elution of the purified sample two fractions of H_2O (MilliQ) were added one after another. The first fraction was discarded, the second, which was containing the desired sample, was collected in Eppendorf® reaction tubes and concentrated.

Table 13: NAP™ Column Volumes:

Column Type	Sample Volume (ml)	Elution Volume Fraction 1	Fraction 2
NAP™-10	0.3	0.7	1.5
NAP™-25	1.0	1.5	2.5

It was possible to reuse the NAP™ columns several times after rinsing them with at least 200 ml H_2O (MilliQ). For storage the columns were covered with H_2O (MilliQ) to keep them from running dry.

UV/VIS Absorption

Oligonucleotide concentrations and yields were determined by UV/VIS absorption measurements. Values are stated in OD_{260}. Whereas one OD_{260} equals the amount of DNA which, dissolved in 1 ml of water and measured in a cuvette with a light path of 1 cm, gives an absorption value at 260nm of 1. For the determination of the OD_{260} 1% of the sample was diluted with water (MilliQ) to 700 µl and transferred into a cuvette with a 1 cm light path. The absorption was then measured with a Lambda UV/VIS Spectrometer (PerkinElmer) with the following settings:

Range:	300 – 200 nm
Data Interval:	1.0 nm
Scan speed:	240 nm/min
Smooth:	2 nm
Slit:	2 nm
Lampchange:	326 nm

The absorption at 260 nm (A_{260}) was then converted into the OD_{260} by multiplication with a factor of 70:

$$\mathrm{OD}_{260} = \mathrm{A}_{260} \cdot \mathrm{f}_d \cdot \frac{x\,\mu l}{1000\,\mu l}$$

Equation 2: Equation for Calculating the OD_{260} from Absorption.
A_{260}: Absorption at 260 nm in a cuvette with 1 cm light path, f_d: Dilution factor, x: Sample volume in µl.

With the so obtained OD_{260} value it possible to calculate the molecular amount of DNA using formula 2.

$$Amount\,(nMOL) = \frac{OD_{260} \cdot 1000}{16 \cdot A + 12 \cdot G + 7 \cdot C + 9.6 \cdot T + z \cdot L}$$

Equation 3: Molecular Oligonucleotide Amounts.
A: Number of adenines, G: Number of guanines, C: Number of cytosines, T: Number of thymines, L: Number of modifications, z = Extinction coefficient of modification divided by factor 1000.

A rough estimate is possible with empirical Equation 4:

$$1\,OD_{260} \approx 20 - 35 \mu g\ DNA$$

Equation 4: Rule of Thumb.

Polyacryl Gel Electrophoreses:

Analytical PAGE

Two glass plates (18 x 16 cm) were silylated using a 5% dichloro-dimethylsilane solution in CCl_4 and afterwards washed with EtOH. This procedure minimized the absorption of DNA on the glass and

simplified the removal of the gel after electrophoreses. The two glass plates were put on each other and firmly affixed with clamps. At the bottom and on both sides the two glass plates were separated with Teflon-spacers of 0.4 mm thickness.

To 10 ml of a 20% acrylamide solution in a beaker 500 µl of a 10% ammonia peroxodisulfate solution were added. After the addition of 4 µl TEMED the solution was casted speedily between the glass plates, avoiding the formation of bubbles. Then the comb (8-10 pockets) was inserted at the top and adjusted with two clamps. The buffer chambers of the electrophoreses machine were filled with 800 ml PAGE buffer After complete polymerization of the gel the bottom spacer was removed and the gel was inserted in the electrophoreses chamber. All air bubbles at the bottom of the gel were removed using a syringe. The comb was then carefully removed and all pockets were washed with the TBE buffer.

Pre-electrophoreses was performed using a voltage of 500 V until the current dropped below 7 mA. In the meantime the samples were prepared: For each pocket 1 µl of the oligonucleotide in water (0.1 OD/µl) was combined with 2 µl gel-dye. The samples were then denatured by heating them at 90°C for 2 min and afterwards cooling them rapidly to 0°C. Once pre-electrophoreses was finished, the gel pockets were once more washed with the PAGE buffer in order to remove any air bubbles The samples were loaded into the pockets and electrophoreses was started with a voltage of 500 V.

Electrophoreses was finished when the lower dye-band (bromophenol blue) almost reached the bottom of the gel (usually within 2 hours). The speed of bromophenol blue on the gel is comparable to an 8mer oligo whereas the speed of xylenecyanol resembles that of a 28mer oligo. The gel was then carefully removed from the glass plates and stained with Stains-All solution for 15 minutes under the exclusion of light. The stained gel was afterwards photographed for documentation with our DESAGA documentation system.

Preparative PAGE

Two glass plates (34 x 16 cm) were silylated using a 5% dichloro-dimethylsilane solution in CCl_4 and afterwards washed with EtOH. This procedure minimized the absorption of DNA on the glass and simplified the removal of the gel after electrophoreses. The two glass plates were put on each other and firmly affixed with clamps. At the bottom and on both sides the two glass plates were separated with Teflon-spacers of 3 mm thickness.

First only the bottom part of the gel was filled to avoid leakages. For this 500 µl of a 10% ammonia peroxodisulfate solution were added to 10 ml of a 20% acrylamide solution in a beaker. After the addition of 4 µl TEMED the solution was poured speedily between the glass plates, avoiding the formation of bubbles. The remaining part of the gel was filled after the gel base had polymerized. Therefore 130 ml of a 20% acrylamide solution were mixed with 2500 µl 10 % ammonia peroxodisulfate and 10 ml TEMED. The solution was cast between the glass plates. Then the comb (12 pockets) was inserted at the top and adjusted with two clamps. When needed, the gel solution was refilled because the gel was shrinking during polymerization.

The buffer chambers of the electrophoreses machine were filled with 1000 ml PAGE buffer. After complete polymerization of the gel the bottom spacer was removed and the gel was inserted in the

electrophoreses machine. All air bubbles at the bottom of the gel were removed using a syringe. The comb was then carefully removed and all pockets were washed with PAGE buffer.

Pre-electrophoreses was performed using a voltage of 400 V until the current dropped below 20 mA. Once pre-electrophoreses was finished, the gel pockets were once more washed with the PAGE buffer in order to remove any air bubbles. Thereafter, the samples were prepared: For each pocket not more than 5 ODs of the oligonucleotide in water (0.1 OD/µl) were combined with the same volume of gel-dye. The samples were then denatured by heating them at 90°C for 2 min and afterwards cooling them rapidly to 0°C. The samples were loaded into the pockets and electrophoreses was started with a voltage of 500 V.

Electrophoreses was finished when the lower dye-band (bromophenol blue) almost reached the bottom of the gel (usually within 12 hours). The speed of bromophenol blue on the gel is comparable to an 8mer oligo whereas the speed of xylenecyanol resembles that of a 28mer oligo. The gel was then carefully removed from the glass plates. The oligonucleotide bands were detected on a UV-fluorescening plate at 254 nm. The desired spots were cut out of the gel and extracted with water.

Extraction of DNA from Polyacrylamide Gels

The spots containing the desired DNA were cut out of the gel and transferred into plastic tubes. There the gel was chopped into small pieces and then suspended in H_2O (MilliQ). After 12 hours the aqueous phase was isolated. The remaining gel pieces were extracted two more times using the same procedure. The combined aqueous phases were concentrated at 60°C in a SpeedVac. The resulting DNA pellet was dissolved in 1-2 ml H_2O (MilliQ), depending on the salt concentration and afterwards desalted.

HPLC

HPLC runs were performed on a Merck/Hitachi system. For reversed phase either a SP-250/10-Nucleosil-100-5-C18 (preparative) or an EC-125/4-Nucleosil-100-5-C18 (analytical) column was used. The mobile phase was a gradient of solvent A = 0.1 M $Et_3NH(OAc)$ buffer at pH 7.0 and solvent B = CH_3CN. Ion exchange HPLC was done on a 250/4 Dionex DNAPAc-PA-100 column. Here the mobile phase consisted of a gradient from solvent A = 20 mM KH_2PO_4 in CH_3CN/H_2O 1:4 at pH 6.0 and solvent B = 1 M KCl, 20 mM KH_2PO_4 in CH_3CN/H_2O 1:4 at pH 6.0. The following methods were used:

Table 14: HPLC Methods for Oligonucleotides:

Method 1 (IE-HPLC)

Time (min)	A (%)	B (%)
0.0	90.0	10.0
2.0	90.0	10.0
35.0	40.0	60.0
38.0	0.0	100.0
41.0	0.0	100.0
44.0	90.0	10.0
46.0	90.0	10.0

Method 2 (IE-HPLC)

Time (min)	A (%)	B (%)
0.0	100.0	0.0
45.0	40.0	60.0
47.0	0.0	100.0
50.0	0.0	100.0
51.0	100.0	0.0
53.0	100.0	0.0

Method 3 (RP-HPLC)

Time (min)	A (%)	B (%)
0.0	100.0	0.0
5.0	100.0	0.0
45.0	11.0	89.0
46.0	0.0	100.0
48.0	0.0	100.0
51.0	100.0	0.0
55.0	100.0	0.0

Method 4 (RP-HPLC)

Time (min)	A (%)	B (%)
0.0	100.0	0.0
10.0	100.0	0.0
55.0	0.0	100.0
62.0	0.0	100.0
66.0	100.0	0.0
70.0	100.0	0.0

3.1. Synthesized Oligonucleotides

a. Oligonucleotides for NF-κB Assay

Oligonucleotide **2**

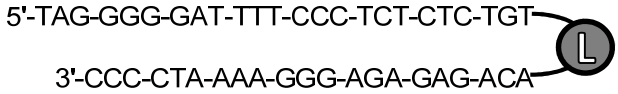

The synthesis of **2** was carried out on a 1 μmol scale following the general protocol for DNA synthesis. Modified building block (4',4''-dimethoxytrityl)-hexaethylene glycol]-β-cyanoethoxy-(diisopropylamino)-phosphine (0.1 M in CH_3CN) was incorporated automatically using an increased coupling time of 15 minutes. In the last cycle, the DMT-protecting group at the 5'-end was cleaved off. Cleavage from solid support was performed with 25% aq. NH_3 at rt over night. The crude oligos were purified by preparative PAGE and afterwards desalted on NAP^{TM}-10 columns. After purification **2** was analyzed by analytical PAGE.

Oligonucleotides **94** - **96**

3'-TTT-TCC-CTC-T-5'	3'-TTT-TCC-CTC-TCT-5'	3'-TTT-TCC-CTC-TCT-CT-5'
94	**95**	**96**

The synthesis of sequences **94**-**96** was carried out on a 1 μmol scale following the general protocol for DNA synthesis. In the last cycle, the DMT protecting group at the 5'-end was cleaved off. Cleavage from solid support was performed with 25% aq. NH_3 at rt. over night. The crude oligos were purified by preparative PAGE and afterwards desalted on NAP^{TM}-10 columns. After purification **94**-**96** were analyzed by analytical PAGE.

*Oligonucleotide **50***

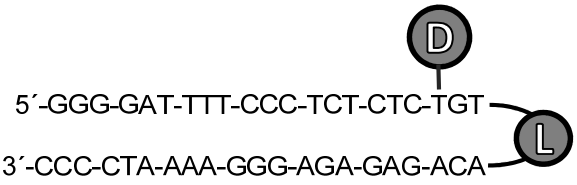

The synthesis of **50** was carried out on a 1 μmol scale following the general protocol for DNA synthesis. Modified building block (4',4''-dimethoxytrityl)-hexaethyleneglycol]-β-cyanoethoxy-(diisopropylamino)-phosphine **1** (0.1 M in CH_3CN) was incorporated automatically using an increased coupling time of 15 minutes. Aminopropargyl-2'-deoxy uridine **41** (68 mM in CH_3CN) was incorporated automatically at the specific site, by using standard coupling times. In the last cycle,

the DMT-protecting group at the 5'-end was cleaved off. Cleavage from solid support was performed with 25% aq. NH_3 at rt. over night. After replacement of NH_4^+ with K^+ the oligo was desalted with a NAP^{TM}-10 column. Coupling of the donor was carried out in solution. To a soln. of the oligo (50 OD, 113 nmol) in DMF/1,4-dioxane/H_2O 1:1:1 (339 µl), *i*-Pr_2EtN (3.5 µl, 22 µmol) and the hydroxysuccinimide ester of donor **28** (1.5 mg, 2.6 µmol) were added. The mixture was incubated at 25°C in the dark for 24 h. After removal of the solvents, residue was washed three times with cold EtOH (3 x 500 µl) to remove the excesses of the donor. The crude **50** was purified by preparative reversed phase HPLC [HPLC method 3 (Table 14 on page 132): EC-125/4-Nucleosil-100-5-C18 column, 0-60% B in 45 min; t_R = 16.28 min] and desalted on NAP-10 columns. After purification 7.9 OD of **50** (12.4 nmol) were obtained and analyzed by analytical PAGE.

*Oligonucleotide **51***

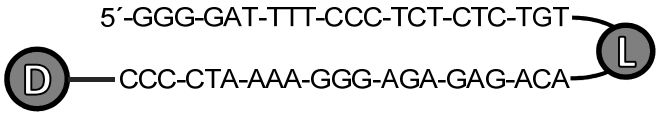

The synthesis of **51** was carried out on a 1 µmol scale following the general protocol for DNA synthesis. Starting material was Amino-On CPG. Modified building block (4',4''-dimethoxytrityl)-hexaethyleneglycol]-β-cyanoethoxy-(diisopropylamino)-phosphine **1** (0.1 M in CH_3CN) was incorporated automatically using an increased coupling time of 15 minutes. In the last cycle, the DMT-protecting group at the 5'-end was cleaved off. Cleavage from solid support was performed with 25% aq. NH_3 at rt. over night. After replacement of NH_4^+ with K^+ the oligo was desalted with a NAP-10 column. Coupling of the donor was carried out in solution. To a soln. of the oligo (50 OD, 113 nmol) in DMF/1,4-dioxane/H_2O 1:1:1 (339 µl), *i*-Pr_2EtN (3.5 µl, 22 µmol) and the hydroxysuccinimide ester of donor **28** (1.5 mg, 2.6 µmol) were added. The mixture was incubated at 25°C in the dark for 24 h. After removal of the solvents, residue was washed three times with cold EtOH (3 x 500 µl) to remove the excesses of the donor. The crude **51** was purified by preparative reversed phase HPLC [HPLC method 3 (Table 14 on page 132): EC-125/4-Nucleosil-100-5-C18 column, 0-60% B in 45 min; t_R = 16.26 min] and desalted on NAP^{TM}-10 columns. After purification 17.5 OD of **51** (37.6 nmol) were obtained and analyzed by analytical PAGE.

*Oligonucleotide **48***

The synthesis of **48** was carried out on a 1 µmol scale following the general protocol for DNA synthesis. Modified building block 5'-deoxy-5'-$§[(4-methoxyphenyl)diphenylmethyl]amino}thymidine-3'-[cyanoethoxy-diisopropylamino)-phosphine]

34 (60 mg) was incorporated manually in the last cycle by using 0.7 ml of 0.3 M BMT as activation reagent. The (MeO)Tr-protecting group at the 5'-end was cleaved off. Cleavage from solid support was performed with 25% aq. NH_3 at rt over night. Coupling of the acceptor was carried out in solution. To a soln. of the oligo (23 OD, 179 nmol) in DMF/1,4-dioxane/H_2O 1:1:1 (536 µl), *i*-Pr_2EtN (6.10 µl, 35.8 µmol) and (bathophenanthroline)ruthenium(II) complex hydroxysuccinimide ester **22** (6.1 mg, 4.5 µmol) were added. The mixture was incubated at 25°C in the dark for 24 h. After removal of the solvents, the residue was washed three times with cold EtOH (3 x 500 µl) to remove excesses of acceptor. The crude **48** was purified by preparative reversed phase HPLC [HPLC method 4 (Table 14 on page 132): EC-125/4-Nucleosil-100-5-C18 column, 0-80% B in 30 min; t_R = 20.58 min] and afterwards desalted by NAP^{TM}-10 column. After purification 12.45 OD of **48** (105 nmol) were obtained and analyzed by analytical PAGE.

*Oligonucleotide **49***

The synthesis of **49** was carried out on a 1 µmol scale following the general protocol for DNA synthesis. Starting material was Amino-On CPG. Cleavage from solid support was performed with 25% aq. NH_3 at rt over night. Coupling of the acceptor was carried out in solution. To a soln. of the oligo (23 OD, 194 nmol) in DMF/1,4-dioxane/H_2O 1:1:1 (536 µl), *i*-Pr_2EtN (6.10 µl, 35.8 µmol) and (bathophenanthroline)ruthenium(II) complex hydroxysuccinimide ester **22** (6.1 mg, 4.5 µmol) were added. The mixture was incubated at 25°C in the dark for 24 h. After removal of the solvents, the residue was washed three times with cold EtOH (3 x 500 µl) to remove excesses of acceptor. The crude **49** was purified by preparative reversed phase HPLC [HPLC method 3 (Table 14 on page 132): EC-125/4-Nucleosil-100-5-C18 column, 0-80% B in 30 min; t_R = 19.04 min] and afterwards desalted by NAP^{TM}-10 column. After purification 12.45 OD of **49** (104.8 nmol) were obtained and analyzed by analytical PAGE.

General Procedure for the Formation of Triple Helices

Table 15: Oligonucleotide Triple Helices:

Entry	Conditions	Triple Helix
1	Equimolar **2** + **94**	**97**
2	Equimolar **2** + **95**	**98**
3	Equimolar **2** + **96**	**99**
4	Equimolar **50** + **48**	**52**
5	Equimolar **51** + **49**	**53**

Equimolar amounts of the backfolding DNA (1.035 nmol) and the third oligonucleotide (1.035 nmol) were combined in an Eppendorf reaction tube. The solvent was removed under vacuum and the precipitate was dissolved in 1300 µl NaOAc buffer (450 mM, pH 5.5) to give a final concentration of 0.796 pmol/µL. The solution was heated to 90°C for 2 minutes and afterwards slowly cooled to rt.

b. Oligonucleotides for DNA-Supported Catalysis

Table 16: Oligonucleotide Sequences for DNA-Supported Catalysis:

Oligo	Sequence	Modified Building Block L
73c	3'-G-CAC-GT**L**-CCC-AGG-C-5'	Thymidine
73a		dPB
73b		dU^{Phen}
74c	3'-TCC-TAT-TAG-CAC-GT**L**-CCC-AGG-CAT-TAT-CCT-5'	Thymidine
74a		dPB
74b		dU^{Phen}
75	5'-C-GTG-CA**L**-GGG-TCC-G-3'	dA
76	5'-AGG-ATA-ATC-GTG-CAA-GGG-TCC-GTA-ATA-GGA-3'	
79	3'-GCA-CGT-CCC-AGG-C-5'	

Oligonucleotides *73a* and *74a*

The synthesis of sequences **73a**, **74a** were carried out on a 1 µmol scale following the general protocol for DNA synthesis. The modified building block phosphoramidite **57** (68 mM in CH_3CN) was incorporated automatically. In the last cycle, the DMT protecting group at the 5'-end was cleaved off. Cleavage from solid support was performed with 25% aq. NH_3 at rt. over night. The crude oligonucleotides were desalted on NAP-10™ columns. After purification **73a**, **74a** were analyzed by analytical PAGE and IE-HPLC (250/4 Dionex DNAPAc-PA-100 column).

Oligonucleotides 73b and 74b

The synthesis of sequences **73b** and **74b** were carried out on a 1 µmol scale following the general protocol for DNA synthesis. The modified building block phosphoramidite **69** (81 mM in CH_3CN) was incorporated automatically. In the last cycle, the DMT protecting group at the 5'-end was cleaved off. Cleavage from solid support was performed with 25% aq. NH_3 at rt. over night. The crude oligonucleotides were desalted on NAP™-10 columns. After purification **73b** and **74b** were analyzed by analytical PAGE and IE-HPLC (250/4 Dionex DNAPAc-PA-100 column).

Oligonucleotides 73c, 74c, 75, 76 and 79

The synthesis of sequences **73c**, **74c**, **75**, **76** and **79** were carried out on a 1 µmol scale following the general protocol for DNA synthesis. In the last cycle, the DMT protecting group at the 5'-end was cleaved off. Cleavage from solid support was performed with 25% aq. NH_3 at rt. over night. The crude oligonucleotides were desalted on NAP™-10 columns. After purification **73c**, **74c**, **75**, **76** and **79** were analyzed by analytical PAGE and IE-HPLC (250/4 Dionex DNAPAc-PA-100 column).

c. Thermal Hybridization Studies

Triple Helices 97, 98, 99

All samples were arranged to yield in an absorption between A_{260} = 0.2 und A_{260} = 0.4 at 260 nm. For this 100 µl of triple helices **97**, **98**, **99** were diluted with 600 µl of the corresponding acetate buffer (100 mM, pH 6 and pH 7). Melting curves were recorded in Karlsruhe by Dr. Carolin Ahlborn (AK Prof. Richert). Different NaCl concentrations (no salt, 150 mM, 450 mM, 1 M) were used. The absorption was measured at 260 nm on a Perkin-Elmer Lambda 10 spectrophotometer using a cuvette with the pure buffer solution as a blank. Both cooling and heating curves were recorded in a temperature range between 5°C and 85°C. The heating/cooling rate was 1°C per minute. For analysis however only data obtained from the heating phases was used. The curves were computer supported smoothened and the first derivative was calculated. In most cases two maxima were visible, the first one resembling the melting temperature for the Hoogsteen pairing (triple helix) and the second one resembling the melting temperature of the Watson-Crick pairing (double helix). In most cases the second melting temperature was not visible indicating a melting temperature of the Watson-Crick base pair above 85°C.

Table 17: pH Dependency of Melting Points for Hoogsteen Base Pairs:

Entry	Triple Helix	Mp at pH 6	Mp at pH 7
1	**97**	16.2°C	not stable at rt.
2	**98**	30.6°C	not stable at rt.
3	**99**	43.6°C	16°C

Table 18: Salt Concentration Dependency of Melting Points for Hoogsteen Base Pairs:

Entry	Salt concentration	Mp of 99
1	No salt	40.1°C
2	150 mM	40.6°C
3	450 mM	43.6°C
4	1000 mM	48.5°C

DNA Metal Complexes

*Double Helix **77c** (with Cu^{2+})*

Two samples of equimolar amounts of oligonucleotide **73c** (2.8 µl, 2.0 pmol, 0.28 OD_{260}) and oligonucleotide **75** (3.0 µl, 2.0 pmol, 0.30 OD_{260}) were combined in an Eppendorf® reaction tube each. One sample was treated with an aqueous solution of $Cu(NO_3)_2 \cdot 3H_2O$ (20 µM, 100 µl). The solvents of both samples were removed under reduced pressure at 60°C in a SpeedVac and the resulting pellets were dissolved in 1000 µl NaOAc buffer (300 mM, pH 7.7) each.

*Double Helix **77a** (with Cu^{2+})*

Two samples of equimolar amounts of oligonucleotide **73a** (2.8 µl, 2.0 pmol, 0.28 OD_{260}) and oligonucleotide **75** (3.0 µl, 2.0 pmol, 0.30 OD_{260}) were combined in an Eppendorf® reaction tube each. One sample was treated with an aqueous solution of $Cu(NO_3)_2 \cdot 3H_2O$ (20 µM, 100 µl). The

solvents of both samples were removed under reduced pressure at 60°C in a SpeedVac and the resulting pellets were dissolved in 1000 µl NaOAc buffer (300 mM, pH 7.7) each.

*Double Helix **78a** (with Cu^{2+})*

Two samples of equimolar amounts of oligonucleotide **74a** (3.1 µl, 1.0 pmol, 0.31 OD_{260}) and oligonucleotide **76** (3.7 µl, 1.0 pmol, 0.37 OD_{260}) were combined in an Eppendorf® reaction tube each. One sample was treated with an aqueous solution of $Cu(NO_3)_2 \cdot 3H_2O$ (20 µM, 50 µl). The solvents of both samples were removed under reduced pressure at 60°C in a SpeedVac and the resulting pallets were dissolved in 1000 µl NaOAc buffer (300 mM, pH 7.7) each.

*Double Helix **78c** (with Cu^{2+})*

Two samples of equimolar amounts of oligonucleotide **74c** (3.1 µl, 1.0 pmol, 0.31 OD_{260}) and oligonucleotide **76** (3.7 µl, 1.0 pmol, 0.37 OD_{260}) were combined in an Eppendorf® reaction tube each. One sample was treated with an aqueous solution of $Cu(NO_3)_2 \cdot 3H_2O$ (20 µM, 50 µl). The solvents of both samples were removed under reduced pressure at 60°C in a SpeedVac and the resulting pellets were dissolved in 1000 µl NaOAc buffer (300 mM, pH 7.7) each.

Melting curves of double helices (**77a**, **77c**, **78a**, **78c**) were recorded in Stuttgart by Katja Imhof (AK Prof. Richert). The absorption was measured at 260 nm on a Perkin-Elmer Lambda 10 spectrophotometer using a cuvette with the pure NaOAc buffer solution (300 mM, pH 7.7) as a blank. Both cooling and heating curves were recorded in a temperature range between 5°C and 85°C. The heating/cooling rate was 1°C per minute. The data was then analyzed with TempLab (Software by Perkin Elmer).

Table 19: Effect of 57 on Melting Temperatures of its DNA Duplexes:

Entry	DNA Duplex	Melting Temperature	
		Without Cu^{2+}	With Cu^{2+}
1	**77a** (**73a·75**)	53.7 ± 0.84°C	53.7 ± 0.84°C
2	**77c** (**73c·75**)	63.3 ± 0.96°C	63.5 ± 0.58°C
3	**78a** (**74a·76**)	66.2 ± 0.98°C	66.2 ± 0.43°C
4	**78c** (**74c·76**)	85°C	85°C

d. Electrophoretic Mobility Shift Assays (EMSAs)

The following experiments for the evaluation of the binding conditions for NF-κB with our DNA triple helices was carried out by Dr. Andrea Hrenn in the group of Prof. Dr. Irmgard Merfort at the Pharmaceutical Institute of the Albert-Ludwigs-Universität Freiburg. Procedures including radioactive materials were taking place solely in a special equipped isotope laboratory under strict safety measures.

Solutions and Buffers

10 x Annealing Buffer	20 mM Tris/HCl (pH 7.6), 10 mM $MgCl_2$, 50 mM NaCl, 1 mM DTT.
Buffer F	20% Ficoll 400, 100 mM HEPES (pH 7.9), 300 mM KCl, 10 mM DTT, 0.1% PMSF.
Buffer D+	20 mM HEPES (pH 7.9), 20% glycerol, 100 mM KCl, 0.5 mM EDTA, 0.25% NP-40, 2 mM DTT, 0.1% PMSF dissolved in 1 ml EtOH.
5 x TBE	108 g TRIS, 55 g boric acid, 40 ml 0.5 M Na-EDTA (pH 8.3), 1960 ml H_2O (MilliQ).
Gel-Dye	6 g of urea and 10 ml H_2O (MilliQ) were added to 1 ml of bromophenol blue-xylenecyanol solution (Fluka).

Sample Preparation

Backfolding DNAs **2**, **50** and **51** (~5 nmol) were transferred into sterile save-lock reaction tubes. The solvent was removed at 60°C in a SpeedVac. Afterwards 10 µl of the 10 x Annealing buffer and 100 µl H_2O (MilliQ) were added to the sample. The samples were incubated for 5 min at 95°C and afterwards slowly cooled to room temperature. The samples were then diluted with H_2O (MilliQ) to give a concentration of 25 ng/µl and stored at –20°C.

Radioactive Labeling

To 1 µl of the DNA samples (25 ng/µl) 5 µl [γ-^{33}P]-ATP, 5 µl 10 x Kinase buffer (Promega), 1.5 µl T4-PNK and 37 µl H_2O (MilliQ) were added. The reaction mixture was incubated at 37°c for 1 hour. The samples were then purified from excess [γ-^{33}P]-ATP by chromatography, following the protocol for Nuc Trap® Probe Purification columns (Stratagene). The so obtained 50 µl of almost pure DNA probe were stored at 4°C.

Polyacrylamide Gel for EMSA

The glass plates were wiped clean with ethanol and the cover plate with Gel Slick Solution. Thereafter the spacers were inserted and the plates were assembled. The gel solution was prepared in a beaker with stirring magnet by mixing 7.0 ml 5 x TBE, 10.0 ml 30% acryl amide solution, 10.0 µl TEMED and 400 µl APS. The solution was then cast between the glass plates, avoiding any air bubbles. And the comb was inserted. Once polymerization had completed the comb as well as the lower space were removed. The glass plates were fixed into an electrophoreses chamber and the buffer reservoirs were filled with 0.5 x TBE buffer. All gas bubble sitting at the lower end of the gel were removed using a syringe filled 0.5 x TBE buffer.

EMSA Mix

The EMSA mix was fabricated according to Table 20 using the previously prepared radioactively labeled DNA probe.

Table 20: EMSA-Mix:

Entry	Substance	µl/Sample	Annotation
1	H_2O (MilliQ)	4	
2	BSA (10 µg/µl)	2	
3	DIDc (1 µg/µl)	2	
4	Buffer F	4	
5	Buffer D+	2	
6	Radioactively labeled probe (25 ng/µl)	1	Added in isotope lab

For each gel pocket an Eppendorf® reaction tube was filled with 14 µl of the EMSA mix and 5 µl of NF-κB containing sample. Along 4 protein extracts listed in Table 21 also pure recombinannt NF-κB was used as source for the NF-κB hetero dimer. All samples were centrifuged and incubated at rt. for 30 min.

Table 21: Protein Extracts:

Entry	Labeling	Cell Type	NF-κB
1	H+	Hepatozyten	stimulated
2	H-	Hepatozyten	not stimulated
3	J+	Jurkat	stimulated
4	J-	Jurkat	not stimulated

EMSA Mix for the Competition Assay

Competition assays were carried out following the same procedures described in chapter: EMSA Mix on page 140. However, 1 µl unlabelled oligonucleotide (25 ng/µl) was added to the EMSA mix prior to incubating it with NF-κB.

Electrophoreses

Pre-electrophoreses was carried out at 200 V (22-14 mA) for 25 min. This was usually done during incubation times of the samples. Before loading the sample on to the gel, the gel was disconnected from the electric circuit. The first pocket was filled with three drops of gel dye. The remaining pockets were filled with 14 µl sample solution. Electrophoreses was then carried out at 200 V for approx. 1.5 h. Documentation and analysis of the gel was done at a PhosphoImager model FLA-3000 from FujiFilm.

IV. Reference

1 J. D. Watson, F. H. C. Crick, *Nature* **1953**, *171*, 737-738.
2 W. Bannwarth, *Chimia* **1987**, *41*, 302-317.
3 S. L. Beaucage, R. P. Iyer, *Tetrahedron* **1992**, *48*, 2223-2311.
4 A. M. Michelson, A. R. Todd, *J. Chem. Soc.* **1955**, 2632-2638.
5 R. H. Hall, A. Todd, R. F. Webb, *J. Chem. Soc.* **1957**, 3291-3296.
6 P. J. Garegg, T. Regberg, J. Stawinski, R. Strömberg, *Chem. Scr.* **1985**, *25*, 280-282.
7 B. C. Froehler, M. D. Matteucci, *Tetrahedron Lett.* **1986**, *27*, 469-472.
8 R. M. Siegel, E. M. Callaway, *PLoS Biology* **2004**, *2*, e419.
9 H. G. Khorana, *Pure Appl. Chem.* **1968**, *17*, 349-381.
10 H. G. Khorana, *Biochem. J.* **1968**, *109*, 709-725.
11 H. G. Khorana, *Science* **1979**, *203*, 614-625.
12 K. L. Agarwal, A. Yamazaki, P. J. Cashion, H. G. Khorana, *Angew. Chem. Int. Ed.* **1972**, *11*, 451-459.
13 R. L. Letsinger, F. J. L., G. A. Heavner, W. B. Lunsford, *J. Am. Chem. Soc.* **1975**, *97*, 3278-3279.
14 R. L. Letsinger, W. B. Lunsford, *J. Am. Chem. Soc.* **1976**, *98*, 3655-3661.
15 L. J. McBride, M. H. Caruthers, *Tetrahedron Lett.* **1983**, *24*, 245-248.
16 S. P. Adams, K. S. Kavka, E. J. Wykes, S. B. Holder, G. R. Galluppi, *J. Am. Chem. Soc.* **1983**, *105*, 661-663.
17 S. L. Beaucage, M. H. Caruthers, *Tetrahedron Lett.* **1981**, *22*, 1859-1862.
18 M. D. Matteucci, M. H. Caruthers, *J. Am. Chem. Soc.* **1981**, *103*, 3185-3191.
19 G. Alvaredo-Urbina, G. M. Sathe, W.-C. Liu, M. F. Gillen, P. D. Duck, R. Bender, K. K. Ogilvie, *Science* **1981**, *214*, 270-274.
20 S. L. Beaucage, R. P. Iyer, *Tetrahedron* **1993**, *49*, 1925-1963.
21 S. L. Beaucage, R. P. Iyer, *Tetrahedron* **1993**, *49*, 6123-6194.
22 N. Venkatesan, S. J. Kim, B. H. Kim, *Curr. Med. Chem.* **2003**, *10*, 1973-1991.
23 C. Beller, W. Bannwarth, *Helv. Chim. Acta* **2005**, *88*, 171-179.
24 S. Altmann, A. M. Labhardt, D. Bur, C. Lehmann, W. Bannwarth, M. Billeter, K. Wüthrich, W. Leupin, *Nucleic Acids Res.* **1995**, *23*, 4827-4835.
25 M. Y.-X. Ma, L. S. Reid, S. C. Climie, W. C. Lin, R. Kuperman, M. Sumner-Smith, R. W. Barnett, *Biochemistry* **1993**, *32*, 1751-1175.
26 C. Meier, T. Huynh-Dinh, *Bioorg. Med. Chem. Lett.* **1991**, *1*, 527-530.
27 A. V. Kabanov, S. V. Vinogradov, A. V. Ovcharenko, A. V. Krivonos, N. S. Melik-Nubarov, V. I. Kiselev, E. S. Severin, *FEBS Lett.* **1990**, *259*, 327-330.
28 N. Tomita, R. Morishita, Y. Kaneda, J. Higaki, T. Ogihara, *Drug News Perspect.* **2000**, *13*, 206-212.
29 K.-H. Altmann, D. Fabbro, T. Geiger, in *Advances in DNA Sequence-Specific Agents*, JAI Press Inc: London, **1998**; Vol. 3, pp 227-266.
30 R. G. Schultz, S. M. Gryaznov, *Tetrahedron Lett.* **2000**, *41*, 1895-1899.
31 S. M. Hecht, *J. Am. Chem. Soc.* **2009**, *131*, 3791-3793.
32 R. B. Merrifield, *Fed. Proc.* **1962**, *21*, 412.
33 R. B. Merrifield, *J. Am. Chem. Soc.* **1963**, *85*, 2149-2154.
34 R. B. Merrifield, *Science* **1965**, *150*, 178-185.
35 V. A. Efimov, S. V. Reverdatto, O. B. Chakhmakcheva, *Nucleic Acids Res.* **1982**, 6675-6694.
36 C. Wojczewski, K. Stolze, J. W. Engels, *Synlett* **1999**, *10*, 1667-1678.
37 T. Förster, *Ann. Phys.* **1948**, *437*, 55-75.
38 L. Stryer, *Ann. Rev. of Biochem.* **1978**, *47*, 819-846.
39 P. R. Selvin, *Methods Enzymol.* **1995**, *246*, 300-334.
40 R. M. Clegg, *Methods Enzymol.* **1992**, *211*, 353-388.

41 J. R. Lakowicz, *Principles of Fluorescence Spectroscopy* 2ed.; Springer: Heidelberg, **1999**; p 725.
42 B. Valeur, *Molecular Fluorescence: Principles and Applications*. 1 ed.; Wiley-VCH: Weinheim **2001**; p 250.
43 P. Tinnefeld, M. Sauer, *Angew. Chem. Int. Ed.* **2005**, *44*, 2642-2671.
44 X. S. Xie, J. K. Trautman, *Ann. Rev. Phys. Chem.* **1998**, *49*, 441-480.
45 W. H. Tan, K. M. Wang, T. J. Drake, *Curr. Opin. Chem. Biol.* **2004**, *8*, 547-553.
46 L. Tan, Y. Li, T. J. Drake, L. Moroz, K. M. Wang, J. Li, A. Montean, C. Y. J. Yang, K. Martinez, W. H. Tan, *Analyst* **2005**, 1002-1005.
47 Webpage: http://www.invitrogen.com/site/us/en/home/References/Molecular-Probes-The-Handbook.html
48 J. E. Berlier, A. Rothe, G. Buller, J. Bradford, D. R. Gray, i. B. J. Filanosk, W. G. Telford, S. Yue, J. Liu, C. Y. Cheung, W. Chang, J. D. Hirsch, J. M. Beechem, R. P. Haugland, *J. Histochem. Cytochem.* **2003**, *12*, 1699-1712.
49 P. S. Dittrich, P. Schwille, *Appl. Phys. B* **2001**, *73*, 829-837.
50 J.-C. G. Bünzli, C. Piguet, *Chem. Soc. Rev.* **2005**, *34*, 1048-1077.
51 R. T. Wegh, H. Donker, K. D. Oskam, A. Meijerink, *Science* **1999**, *283*, 663-666.
52 M. Li, P. R. Selvin, *J. Am. Chem. Soc.* **1995**, *117*, 8132-8138.
53 M. Li, P. R. Selvin, *Bioconjugate Chem.* **1997**, *8*, 127-132.
54 J.-C. G. Bünzli, in *Rare Earths*, eds. R. S. Puche, P. Caro, Madrid, **1998**; pp 223-259.
55 M. D. Ward, *Ann. Rep. Prog. Chem. Sect. A* **2006**, *102*, 584-614.
56 W. Bannwarth, D. Schmidt, R. L. Stallard, C. Hornung, R. Knorr, F. Müller, *Helv. Chim. Acta* **1988**, *71*, 2085-2099.
57 D. García-Fresnadillo, G. Orellana, *Helv. Chim. Acta* **2001**, *84*, 2708-2730.
58 E. K. Kainmüller, E. P. Ollé, W. Bannwarth, *Chem. Commun.* **2005**, *43*, 5459-5461.
59 R. A. Kramer, L. Rumi, W. Bannwarth, *Helv. Chim. Acta* **2009**, *92*, 267-272.
60 R. A. Kramer, E. K. Kainmüller, R. Flehr, M. U. Kumke, W. Bannwarth, *Org. Biomol. Chem.* **2008**, *6*, 2355-2360.
61 L. Clima, W. Bannwarth, *Helv. Chim. Acta* **2008**, *91*, 165-175.
62 R. A. Cardullo, S. Agrawal, C. Flores, P. C. Zamecnik, D. E. Wolf, *Proc. Natl. Acad. Sci. USA* **1988**, *85*, 8790-8794.
63 E. Lopez-Crapez, H. Bazin, E. Andre, J. Noletti, J. Grenier, G. Mathis, *Nucleic Acids Res.* **2001**, *29*, e70.
64 S. Sueda, J. Yuan, K. Matsumoto, *Bioconjugate Chem.* **2002**, *13*, 200-204.
65 L. Clima, C. Hirtz-Haag, A. Kienzler, W. Bannwarth, *Helv. Chim. Acta* **2007**, *90*, 1082-1098.
66 S. Tyagi, D. P. Bratu, F. R. Kramer, *Nat. Biotech.* **1998**, *16*, 49-53.
67 T. Matsuo, *Biochim. Biophys. Acta* **1998**, *1379*, 178-184.
68 P. Zhang, T. Beck, W. Tan, *Angew. Chem. Int. Ed.* **2001**, *40*, 402-405.
69 K. J. Livak, *Gen. Anal. Biomol. Eng.* **1999**, *14*, 143-149.
70 D. Whitcombe, J. Theaker, S. P. Guy, T. Brown, A. Little, *Nat. Biotech.* **1999**, *17*, 804-807.
71 L. M. Smith, J. Z. Sanders, R. J. Kaiser, P. Hughes, C. Dodd, C. R. Connell, C. Heiner, S. B. H. Kent, L. E. Hood, *Nature* **1986**, *321*, 674-679.
72 S. Hardin, X. Gao, J. Briggs, R. Willson, S.-C. Tu, Patent: 11/007,797, *Visigen Biotechnologies, Inc.* (**2004**).
73 S. M. Roberts, *Pure Appl. Chem.* **1992**, *64*, 1933-1937.
74 Webpage: http://www.ch.ic.ac.uk/ectoc/papers/04/1-Contents.html
75 C. Chan, P. B. Cox, S. M. Roberts, *J. Chem. Soc., Chem. Commun.* **1988**, 971-972.
76 C. Chan, P. B. Cox, S. M. Roberts, *Biocatalysis* **1990** *3*, 111-118.
77 A. D. Borthwick, S. Butt, K. Biggadike, A. M. Exall, S. M. Roberts, P. M. Youds, B. E. Kirk, B. R. Booth, J. M. Cameron, S. W. Cox, C. L. P. Marr, M. D. Shill, *J. Chem. Soc., Chem. Commun.* **1988**, 656-658.

78 A. D. Borthwick, D. N. Evans, A. M. Exall, B. E. Kirk, K. Biggadike, P. M. Youds, S. M. Roberts, D. J. Knight, J. A. V. Coates, *J. Med. Chem.* **1990**, *33*, 179-186.

79 C. Evans, R. McCague, S. M. Roberts, A. G. Sutherland, *J. Chem. Soc., Perkin Trans. 1* **1991**, 656-657.

80 J. Crosby, J. Moilliet, J. S. Parratt, N. J. Turner, *J. Chem. Soc., Perkin Trans 1* **1994**, 1679-1687.

81 C. A. Pittol, S. M. Roberts, P. W. Sutton, J. O. Williams, *J. Chem. Soc., Chem. Commun.* **1994**, 803−804.

82 I. C. Cotterill, R. Jaouhari, G. Dorman, S. M. Roberts, F. Scheinmann, B. J. Wakefield, *J. Chem. Soc., Perkin Trans. 1* **1991**, 2505-2512.

83 G. R. Hobbs, M. D. Lilly, N. J. Turner, J. M. Ward, A. J. Willetts, J. M. Woodley, *J. Chem. Soc., Perkin Trans 1* **1993**, *2*, 165-166.

84 T. R. Cech, *Proc. Natl. Acad. Sci. USA* **1986**, *83*, 4360-4363.

85 C. Carola, F. Eckstein, *Curr. Opin. Chem. Biol.* **1999**, *3*, 274-283.

86 T. R. Cech, A. J. Zaug, P. J. Grabowski, *Cell* **1981**, *27*, 487-496.

87 C. Guerrier-Takada, K. Gardiner, T. Marsh, N. Pace, S. Altman, *Cell* **1983**, *35*, 849-857.

88 C. Guerrier-Takada, S. Altman, *Science* **1984**, *223*, 285-286.

89 K. Kruger, P. J. Grabowski, A. J. Zaug, J. Sands, D. E. Gottschling, T. R. Cech, *Cell* **1982**, *31*, 147-157.

90 D. P. Bartel, P. J. Unrau, *Science* **1999**, *24*, M9-M13.

91 A. Jäschke, B. Seelig, *Curr. Opin. Chem. Biol.* **2000**, *4*, 257-262.

92 B. Seelig, A. Jäschke, *Chem. Biol.* **1999**, *6*, 167-176.

93 C. Höbartner, S. K. Silverman, *Biopolymers* **2007**, *87*, 279-292.

94 R. R. Breaker, G. F. Joyce, *Chem. Biol.* **1994**, *1*, 223-229.

95 W. E. Purtha, R. L. Coppins, M. K. Smalley, S. K. Silverman, *J. Am. Chem. Soc.* **2005**, *127*, 13124-13125.

96 A. Flynn-Charlebois, Y. Wang, T. K. Prior, I. Rashid, K. A. Hoadley, R. L. Coppins, A. C. Wolf, S. K. Silverman, *J. Am. Chem. Soc.* **2003**, *125*, 2444-2454.

97 S. W. Santoro, G. F. Joyce, *Proc. Natl. Acad. Sci. USA* **1997**, *94*, 4262-4266.

98 R. P. G. Cruz, J. B. Withers, Y. Li, *Chem. Biol.* **2004**, *11*, 57-67.

99 J. Liu, A. K. Brown, X. Meng, D. M. Cropek, J. D. Istok, D. B. Watson, Y. Lu, *Proc. Natl. Acad. Sci. USA* **2007**, *104*, 2056-2061.

100 Y. Wang, S. K. Silverman, *Biochemistry* **2005**, *44*, 3017-3023.

101 W. E. Purtha, R. L. Coppins, M. K. Smalley, S. K. Silverman, *J. Am. Chem. Soc.* **2005**, *127*, 13124-13125.

102 G. Roelfes, B. L. Feringa, *Angew. Chem. Int. Ed.* **2005**, *44*, 3230-3232.

103 G. Roelfes, A. J. Boersma, B. L. Feringa, *Chem. Commun.* **2006**, *6*, 635-637.

104 A. J. Boersma, J. E. Klijn, B. L. Feringa, G. Roelfes, *J. Am. Chem. Soc.* **2008**, *130*, 11783-11790.

105 D. Coquière, B. L. Feringa, G. Roelfes, *Angew. Chem. Int. Ed.* **2007**, *46*, 9308-9311.

106 N. Shibata, H. Yasui, S. Nakamura, T. Toru, *Synlett* **2007**, *7*, 1153-1157.

107 A. J. Boersma, B. L. Feringa, G. Roelfes, *Angew. Chem. Int. Ed.* **2009**, *48*, 3346-3348.

108 M. Karin, Y. Yamamoto, Q. M. Wang, *Nat. Rev. Drug Discov.* **2004**, *3*, 17-26.

109 S. Ghosh, M. J. May, E. B. Kopp, *Ann. Rev. Immunol* **1998**, *16*, 225-260.

110 M. S. Hayden, A. P. West, S. Ghosh, *Oncogene*, *25*, 6758-6780.

111 F. E. Chen, D.-B. Huang, Y.-Q. Chen, G. Ghosh, *Nature* **1998**, *391*, 410-413.

112 B. B. Aggarwal, Y. Takada, S. Shishodia, A. M. Gutierrez, O. V. Oommen, H. Ichikawa, Y. Baba, A. Kumar, *Indian J. Exp. Bio.* **2004**, *42*, 341-353.

113 P. J. Barnes, M. Karin, *N. Engl. J. Med.* **1997**, *336*, 1066-1071.

114 M. F. Neurath, I. Fuss, G. Schurmann, *Ann. NY Acad. Sci.* **1998**, *859*, 149-159.

115 C. L. Curran, T. S. Blackwell, J. W. Christman, *Expert Opinion on Therapeutic Targets* **2001**, *5*, 197-204.

116 S. Olivier, P. Robe, V. Bours, *Biochemical Pharmacology* **2006**, *72*, 1054-1068.
117 T. D. Gilmore, M. Herscovitch, *Oncogene*, *25*, 6887-6899.
118 B. Haefner, *Prog Med Chem.* **2005**, *43*, 137-188.
119 I. Merfort, *Expert Opinion on Therapeutic Patents* **2006**, *16*, 797-810.
120 V. Pande, M. J. Ramos, *Curr. Med. Chem.* **2005**, *12*, 357-374.
121 S. W. Tas, P. H. J. Remans, K. A. Reedquist, P. P. Tak, *Curr. Pharm. Des.* **2005**, *11*, 581-611.
122 M.-J. Yin, Y. Yamamoto, R. B. Gaynor, *Nature* **1998**, *396*, 77-80.
123 F. D'Acquisto, M. J. May, S. Ghosh, *Molecular Interventions* **2002**, *2*, 22-35.
124 M. Fried, D. M. Crothers, *Nucleic Acids Res.* **1981**, *9*, 6505-6525.
125 A. K. Kiemer, *Immunol. Akt.* **2002**, *3*, 107-111.
126 D. J. Galas, A. Schmitz, *Nucleic Acids Res.* **1978**, *5*, 3157-3170.
127 D. Shalloway, T. Kleinberger, D. M. Livingston, *Cell* **1980**, *20*, 411-422.
128 J. L. Li, H. Chen, M. Li, D. Hua, Z. Lu, J. Wang, *Colloids Surf. B Biointerfaces* **2007**, *55*, 31-37.
129 M. T. Lindenmeyer, A. J. García-Piñeres, V. Castro, I. Merfort, *Analytical Biochemistry* **2004**, *328*, 147-154.
130 J. Wang, T. Li, X. Guo, Z. Lu, *Nucleic Acids Res.* **2005**, *33*, e23.
131 V. V. Didenko, *Biotechniques* **2001**, *31*, 1106-1121.
132 D. A. De Angelis, *Physiological Genomics* **1999**, *1*, 93-99.
133 W. S. Furey, C. M. Joyce, M. A. Osborne, D. Klenerman, J. A. Peliska, S. Balasubramanian, *Biochemistry* **1998**, *37*, 2979-2990.
134 L. Wang, S. Zou, A. K. Gaigalas, A. Zhou, T.-N. Zhu, R. Pires, H.-J. He, *BioTechniques* **2007**, *43*, 93-98.
135 G. Felsenfeld, D. R. Davies, A. Rich, *J. Am. Chem. Soc.* **1957**, *79*, 2023-2024.
136 D. Altevogt, Diploma Thesis, *Albert-Ludwigs Universität*, Freiburg **2005**.
137 E. K. Kainmüller, W. Bannwarth, *Helv. Chim. Acta* **2006**, *89*, 3056-3070.
138 E. P. Ollé, Diploma Thesis, *Albert-Ludwigs Universität*, Freiburg **2001**.
139 R. Knorr, A. Trzeciak, W. Bannwarth, D. Gillessen, *Tetrahedron Lett.* **1989**, *30*, 1927-1930.
140 M. Á. Alonso, M. d. M. Blanco, C. Avendaño, J. C. Menèndez, *Heterocycles* **1993**, *36*, 2315-2325.
141 L. Clima, PhD Thesis, *Albert-Ludwigs Universität*, Freiburg **2007**.
142 W. Bannwarth, R. Knorr, F. Mueller, D. Schmidt, Patent: EP19890107439 *Hoffmann, LA. Roche (CH)* (**1989**).
143 W. Bannwarth, F. Mueller, Patent: EP19910100343 *Hoffmann, LA. Roche (CH)* (**1991**).
144 B. P. Sullivan, D. J. Salmon, T. J. Meyer, *Inorg. Chem.* **1978**, *17*, 3334-3341.
145 A. Müller, PhD Thesis, *Albert-Ludwigs Universität*, Freiburg **2005**.
146 W. Bannwarth, PhD Thesis, *Universität Konstanz*, Konstanz **1977**.
147 S. Honda, K.-i. Urakami, K. Koura, K. Terada, Y. Sato, K. Kohno, M. Sekine, T. Hata, *Tetrahedron* **1984**, *40*, 153-163.
148 B. Reese, *Colloq. Int. Cent. Natl. Rech. Sci.* **1970**, 319-328.
149 N. D. Sinha, J. Biernat, H. Köster, *Tetrahedron Lett.* **1983**, *24*, 5843-5846.
150 W. Bannwarth, A. Trzeciak, *Helv. Chim. Acta* **1987**, *70*, 175-186.
151 N. D. Sinha, J. Biernat, J. McManus, H. Köster, *Nucleic Acids Res.* **1984**, *12*, 4539-4557.
152 C. Le Bec, T. Huynh-Dinh, *Tetrahedron Lett.* **1991**, *32*, 6553-6556.
153 D. S. Pedersen, C. Rosenbohm, T. Koch, *Synthesis* **2002**, *2002*, 0802-0808.
154 W. Bannwarth, *Helv. Chim. Acta* **1988**, *71*, 1517-1527.
155 C. N. Tetzlaff, I. Schwope, C. F. Bleczinski, J. A. Steinberg, C. Richert, *Tetrahedron Lett.* **1998**, *39*, 4215-4218.
156 B. A. Connolly, *Nucleic Acids Res.* **1987**, *15*, 3131-3139.
157 U. Asseline, N. T. Thuong, C. Helene, *New J. Chem.* **1997**, *21*, 5-17.
158 G. G. G. Rasched, PhD Thesis, *Rheinische Friedrich-Wilhelms-Universität*, Bonn **2007**.
159 J. L. He, F. Seela, *Nucleic Acids Res.* **2002**, *30*, 5485-5496.
160 K. Sonogashira, Y. Tohda, N. Hagihara, *Tetrahedron Lett.* **1975**, *50*, 4467-4470.

161 H. A. Dieck, R. F. Heck, *J. Am. Chem. Soc.* **1974**, *96*, 1133-1136.
162 D. E. Bergstrom, J. L. Ruth, *J. Am. Chem. Soc.* **1976**, *98*, 1587-1589.
163 S. Jager, G. Rasched, H. Kornreich-Leshem, M. Engeser, O. Thum, M. Famulok, *J. Am. Chem. Soc.* **2005**, *127*, 15071-15082.
164 K. A. Cruickshank, D. L. Stockwell, *Tetrahedron Lett.* **1988**, *29*, 5221-5224.
165 T. R. Battersby, D. N. Ang, P. Burgstaller, S. C. Jurczyk, M. T. Bowser, D. D. Buchanan, R. T. Kennedy, S. A. Benner, *J. Am. Chem. Soc.* **1999**, *121*, 9781-9789.
166 N. K. Garg, C. C. Woodroofe, C. J. Lacenere, S. R. Quake, B. M. Stoltz, *Chem. Commun.* **2005**, 4551-4553.
167 L. Yin, J. Liebscher, *Chemical Reviews* **2007**, *107*, 133-173.
168 T. S. Mansour, C. A. Evans, M. Charron, B. E. Korba, *Bioorg. Med. Chem. Lett* **1997**, *7*, 303-308.
169 A. Carangio, C. McGuigan, G. Andrei, R. Snoeck, E. D. Clercq, J. Balzarini, *Antiviral Chem. Chemother* **2001**, *12*, 187-197.
170 S. E. Lee, A. Sidorov, T. Gourlain, N. Mignet, S. J. Thorpe, J. A. Brazier, M. J. Dickman, D. P. Hornby, J. A. Grasby, D. M. Williams, *Nucleic Acids Res.* **2001**, *29*, 1565-1573.
171 A. J. Boersma, B. L. Feringa, G. Roelfes, *Org. Lett.* **2007**, *9*, 3647-3650.
172 N. K. Modukuru, K. J. Snow, B. S. Perrin, J. Thota, C. V. Kumar, *J. Phys. Chem. B* **2005**, *109*, 11810-11818.
173 N. S. Oltra, G. Roelfes, *Chem. Commun.* **2008**, *45*, 6039-6041.
174 A. A. Travers, in *DNA-protein interactions* Springer: **1993**; Vol. Reprint, pp 52-86.
175 Picture, in, Cell.
176 D. J. Hurley, S. E. Seaman, J. C. Mazura, Y. Tor, *Org. Lett.* **2002**, *4*, 2305-2308.
177 V. H. Vorbrüggen, C. Ruh-Pohlenz, *Handbook of nucleoside synthesis*. Wiley: **2001**; p 631.
178 R. E. Deriaz, W. G. Overend, M. Stacey, L. F. Wiggins, *J. Chem. Soc.* **1949**, 2836-2841.
179 M. Hoffer, *Chem. Ber.* **1960**, *93*, 2777-2781.
180 K. Eger, M. Jalalian, M. Schmidt, *Tetrahedron* **1994**, *50*, 8371-8380.
181 I. Dhimitruka, J. J. SantaLucia, *Synlett* **2004**, 335-337.
182 M. Zhong, I. Nowak, M. J. Robins, *J. Org. Chem.* **2006**, *71*, 7773-7779.
183 P. Nuhn, A. Zschunke, D. Heller, G. Wagner, *Tetrahedron* **1969**, *25*, 2139-2144.
184 F. Seela, H. Steker, *Helv. Chim. Acta* **1985**, *68*, 563-570.
185 J. Lehbauer, W. Pfleiderer, *Helv. Chim. Acta* **2001**, *84*, 2330-2342.
186 K. Eger, M. Jalalian, M. Schmidt, *J. Heterocycl. Chem.* **1995**, *32*, 211-218.
187 M. Yamada, Y. Tanaka, Y. Yoshimoto, S. Kuroda, I. Shimao, *Bull. Chem. Soc. Jpn.* **1992**, *65*, 1006-1011.
188 J. E. Dickeson, L. A. Summers, *Aust. J. Chem.* **1970**, *23*, 1023-1027.
189 D. T. Davies, *Basistexte Chemie: Aromatische Heterocyclen*. 1 ed.; Wiley-VCH: Weinheim, **1995**.
190 T. Tatsuoka, K. Imao, K. Suzuki, *Heterocycles* **1986**, *24*, 2133-2136
191 T. Kawate, C. R. Allerson, J. L. Wolfe, *Org. Lett.* **2005**, *7*, 3865-3868.
192 M. J. Robins, P. J. Barr, *J. Org. Chem.* **1983**, *48*, 1854-1862.
193 H. Hashimoto, M. H. Nelson, C. Switzer, *J. Am. Chem. Soc.* **1993**, *115*, 7128-7138.
194 P. J. J. Connors, D. Tzalis, A. L. Dunnick, Y. Tor, *Inorg. Chem.* **1998**, *37*, 1121-1123.
195 D. Tzalis, Y. Tor, *Tetrahedron Lett.* **1995**, *36*, 6017-6020.
196 D. Tzalis, Y. Tor, S. Failla, J. S. Siegel, *Tetrahedron Lett.* **1995**, *36*, 3489-3490.
197 Webpage: http://www.glenresearch.com//Technical/ExpeditePriming.html
198 H. Weizman, Y. Tor, *J. Am. Chem. Soc.* **2001**, *123*, 3375-3376.
199 K. Narasaki, *Synthesis* **1991**, *01*, 1-11.
200 C. S. Marvel, L. E. Coleman, G. P. Scott, *J. Org. Chem.* **1955**, *20*, 1785-1792.
201 S. Otto, F. Bertoncin, J. B. F. N. Engberts, *J. Am. Chem. Soc.* **1996**, *118*, 7702-7707.
202 W. Blokzijl, M. J. Blandamer, J. B. F. N. Engberts, *J. Am. Chem. Soc.* **1991**, *113*, 4241-4246.
203 S. Otto, W. Blokzijl, J. B. F. N. Engberts, *J. Org. Chem.* **1994**, *59*, 5372-5376.

204 J. B. F. N. Engberts, *Pure Appl. Chem.* **1995**, *67*, 823-828.
205 D. E. Koshland, *Proc. Natl. Acad. Sci. USA* **1958**, *44*, 98-104.
206 J. A. Brazier, T. Shibata, J. Townsley, B. F. Taylor, E. Frary, N. H. Williams, D. M. Williams, *Nucleic Acids Res.* **2005**, *33*, 1362-1371.
207 R. H. Terbrueggen, T. W. Johann, J. K. Barton, *Inorg. Chem.* **1998**, *37*, 6874-6883.
208 C. J. Chandler, L. W. Deady, J. A. Reiss, *J. Heterocycl. Chem.* **1981**, *18*, 599-601.
209 P. Kus, G. Knerr, L. Czuchajowski, *J. Heterocycl. Chem.* **1991**, *28*, 7-11.